

# **Application of Structural Electricity Models**

From Parameter Estimation and Parameter Risk to an  
Implied Hedging Framework

Dissertation

zur Erlangung des Doktorgrades

Dr. rer. nat.

der Fakultät für Mathematik  
der Universität Duisburg-Essen

vorgelegt von  
Cord Harms, M.Sc.

Essen, im März 2017

Amtierender Dekan: Prof. Dr. Gerhard Starke

1. Gutachter: Prof. Dr. Rüdiger Kiesel

2. Gutachter: Prof. Dr. Alfred Müller

Datum der Disputation: 20. Juni 2017

# Acknowledgements

I am very grateful to my supervisor Prof. Dr. Rüdiger Kiesel for his helpful and continuous guidance throughout my studies. I am especially thankful for his flexibility and his motivating support under the circumstances of an additional part-time agreement with my employer Ernst & Young GmbH. From my point of view, we have found an interesting trade-off between acting in the theoretical field of financial mathematics and delivering applicable results for practitioners at the same time.

During my research, I have worked on structural electricity models. I am pleased that Prof. Dr. Alfred Müller has agreed to act as second examiner. Amongst others, he has investigated structural approaches on how to incorporate the impact of temperature and oil prices into a gas price model. Furthermore, he has analyzed different approaches on how to forecast medium-term electricity demand. Both topics deliver interesting connections and I am very grateful for his willingness to read my thesis.

I was working part-time for Ernst & Young GmbH during my research. I express gratitude to my director Bernd Georgi for being a reliable support throughout my research.

Last but not least, I am deeply grateful to my wife Cornelia for her support during those busy times.



# Abstract

This thesis provides a mathematical analysis of structural electricity spot models and their applicability for dynamic hedging in practice. The analysis requires the application of stochastic analysis, computational finance and asymptotic statistics.

Due to the complexity to store electricity, it usually has to be consumed immediately after its production. Consequently, seasonalities in electricity wholesale prices are not only observed between different months (due to weather conditions) or between different weekdays (due to industry and retail demand) but also between different hours of a day (i.e. due to retail demand and the photovoltaic power production). In detail, they are caused by fundamentals, i.e. expected demand, expected marginal<sup>1</sup> power plants and expected weather conditions (i.e. intensity of the sun, or expected wind conditions). As soon as fundamentals behave unexpectedly, the electricity (equilibrium) price has to change in order that demand and production volumes can rematch.

The close relation between electricity prices and fundamental information has been the basic idea to investigate so-called structural electricity models. These models integrate fundamental knowledge of the price setting mechanism into an electricity spot model. However, they still ensure close-form formulas for at least forward contracts. Though structural models are well investigated in terms of derivatives pricing, there is still a lack of applicability in practice, i.e. how those models can be used for hedging and how model parameters are estimated respectively.

The basic idea of our research is that a structural electricity spot model implies an electricity forward model (between fuels and electricity) being close to a model with cointegrated forwards. The dynamic is directly implied by the merit order of the market. Furthermore, electricity forwards become risk-neutral  $\mathbb{Q}$ -martingales under certain conditions. With this knowledge, we can use a structural electricity model for hedging in practice. By switching the model into a risk-neutral measure, we even receive implied information about the expected risk-neutral demand. In detail, the demand is implied by the fuels' and power forward prices. As power forward contracts are not always liquid, we construct an alternative hedging strategy where fuels are used to hedge power based on the marginal fuel according to the merit order of the market.

Based on those results, we investigate how to estimate the set of model parameters from histor-

---

<sup>1</sup>The most expensive power plant in the grid which is necessary to serve the demand sets the overall wholesale price.

ical data. We derive historical estimators for the model parameters (i.e. mean-reversion speeds and volatilities). We prove that the estimators are asymptotically normally distributed. Afterwards, we use the asymptotic covariance matrix to quantify the risk of using those estimators for derivative pricing and hedging. We find that the incorporation of the merit order can cause significant uncertainty in the present value of a contingent claim.

Furthermore, the model results in high electricity spot volatility for deliveries later than 6 months, at least for hours with high demand. The volatility is mainly caused by the steepness of the bid stack for hours with high demand. To cope with that volatility, we generalize the common known Kirk formula to a structural electricity model. We find that the approach can compete in terms of numerical performance with a Monte Carlo method.

Different numerical approaches can be used to calculate hedging strategies. However, these approaches have not been investigated for structural electricity models so far. Therefore, we compare different approaches to calculate the Greeks of a contingent claim (i.e. delta, gamma, vega). In detail, we compare the difference quotient method to the likelihood ratio method and pathwise derivative method.

Finally, we use the model to calculate delta hedging strategies for a virtual power plant.

# Zusammenfassung

Diese Arbeit analysiert die Anwendung von dynamischen Sicherungsstrategien für sogenannte strukturelle Strompreismodelle. Die Analyse erfordert die Anwendung mathematischer Methoden der stochastischen Analysis, Finanznumerik und asymptotischen Statistik.

Aufgrund von eingeschränkten Möglichkeiten zur Speicherung von Strom wird dieser grundsätzlich unmittelbar nach Produktion verbraucht. Der unmittelbare Verbrauch hat monatliche, wöchentliche als auch stündliche Saisonalitäten zur Folge. Darüber hinaus wirken sich Änderungen in den Vorhersagen von Fundamentaldaten (z. B. erwartete Nachfrage, erwartete Kraftwerksleistungen, erwartete Wetterbedingungen) direkt auf den erwarteten Börsen-Strompreis aus.

Der enge Zusammenhang zwischen Saisonalitäten und Fundamentaldaten hat dazu geführt, dass sogenannte strukturelle Modelle erforscht wurden. Diese Art von Modell versucht zum einen, Fundamentalzusammenhänge in ein stochastisches Modell einzubauen, zum anderen sollen weiterhin geschlossene Formeln für zumindest Terminverträge hergeleitet werden. Strukturelle Modelle wurden zwar ausgiebig im Zusammenhang mit der Bewertung von Derivaten erforscht, in der praktischen Anwendung besteht jedoch noch Forschungsbedarf. Mit dieser Arbeit wollen wir eine weitere Lücke bei der praktischen Anwendung schließen.

Als zentrale Idee verwenden wir den theoretischen Zusammenhang zwischen Spot- und Terminmarktmodellen, um ausgehend von einem strukturellen Strompreismodell ein näherungsweise kointegriertes Terminmarktmodell abzuleiten. Die dem Prinzip der Kointegration nahe Dynamik wird direkt durch die Merit Order des Energiemarktes impliziert. Wir zeigen, dass Strom-Terminmarktverträge unter bestimmten Bedingungen Martingale unter der risikoneutralen Erwartung  $\mathbb{Q}$  sind. Das Ergebnis bildet die Basis dafür, strukturelle Strompreismodelle für die Berechnung von Sicherungsstrategien anzuwenden. Über den Wechsel in ein risikoneutrales Maß erhalten wir darüber hinaus implizite Informationen über die erwartete (risikoneutrale) Stromnachfrage in der Zukunft (basierend auf den Terminpreisen von Strom und Brennstoffen). Insgesamt analysieren wir mit Hilfe eines strukturellen Strompreismodells zwei unterschiedliche Sicherungsstrategien. Sofern Strom-Terminkontrakte als liquide gehandelt angenommen werden, werden diese in die Berechnung der Sicherungsstrategie einbezogen. Sofern diese als nicht-liquide gehandelt angenommen werden, werden Strompreisänderungen mittels Derivate auf Brennstoffe (z. B. Kohle oder Gas) abgesichert. Es verbleibt jedoch die Unsicherheit in der

Nachfrage als nicht unmittelbar handelbare Größe (unvollständiger Markt).

Auf Basis dieser Ergebnisse erforschen wir die Schätzung der Modellparameter in einem strukturellen Strompreismodell. Wir berechnen asymptotisch normalverteilte Schätzer für die Modelldynamiken. Außerdem schätzen wir den Bid Stack anhand historischer Daten. In der Anwendung lässt sich darüber die Parameterunsicherheit quantifizieren. Wir zeigen, dass die Parameterunsicherheit in der Modellierung der Merit Order gerade für Stunden mit hoher Nachfrage einen signifikanten Anteil bei der Bewertung von Strom-Derivaten einnimmt.

Weiterhin stellen wir für Stunden mit hoher Nachfrage eine hohe modellimplizierte Volatilität ab Lieferzeiten von 6 Monaten fest. Die Volatilität ergibt sich durch die starke Steigung des Bid Stacks für Stunden mit hoher Stromnachfrage. Aus diesem Grund verallgemeinern wir die Kirk-Formel zur Verwendung bei strukturellen Modellen. Basierend auf den historisch geschätzten Modellparametern ergibt sich zwar eine feste Bewertungsgenauigkeit, diese wird jedoch in unserem Berechnungsbeispiel anhand realistischer Marktdaten numerisch schneller mit der Kirk-Formel als mit einer Monte Carlo Methode erreicht.

Weiterführend vergleichen wir verschiedene Methoden zur Berechnung ausgewählter *Griechen* (delta, gamma, vega). Im letzten Kapitel verwenden wir die Ergebnisse zur Berechnung einer Sicherungsstrategie für virtuelle Kraftwerke in der Praxis.



# Contents

<b>1</b>	<b>Introduction</b>	<b>1</b>
1.1	Electricity Markets . . . . .	1
1.2	Energy Trading / Quantitative Risk Management . . . . .	4
1.2.1	Importance of Electricity Price Forward Curves . . . . .	4
1.2.2	Structural Models: Fundamentals and Tractability . . . . .	5
1.2.3	Hedging Strategies . . . . .	8
1.2.4	Virtual Power Plants . . . . .	10
1.2.5	Model Risk and Parameter Risk . . . . .	12
1.3	Contribution of the Thesis . . . . .	13
1.4	Structure of the Thesis . . . . .	15
1.5	Publications . . . . .	16
1.6	Implementation . . . . .	16
<b>2</b>	<b>Market Setting</b>	<b>17</b>
2.1	A Structural Model for Electricity Markets . . . . .	17
2.2	The Dynamics for Fuels and Demand and a Risk-Neutral Measure . . . . .	19
2.3	From Market Data to an Hourly Price Forward Curve . . . . .	21
<b>3</b>	<b>The Idea - Hedging with Structural Models</b>	<b>25</b>
3.1	Forward Dynamics . . . . .	25
3.2	Link to Cointegration . . . . .	27
3.3	Replication Portfolio . . . . .	29
3.4	Practical Interpretations . . . . .	32
3.4.1	Liquidity . . . . .	32
3.4.2	Volatility . . . . .	33
3.5	From Forward Deltas to Futures Deltas . . . . .	34
<b>4</b>	<b>Historical Estimators and Parameter Risk</b>	<b>39</b>
4.1	The Approach to Quantify Parameter Risk . . . . .	39
4.2	Historical Estimators . . . . .	41

4.2.1	Fuels' Dynamics . . . . .	41
4.2.2	Bid Stack Parameters . . . . .	50
4.2.3	Demand Dynamic . . . . .	59
4.3	Numerical Results for Parameter Risk . . . . .	62
4.3.1	Uncertainty in Price Forward Curves and Monte Carlo Risk . . . . .	63
4.3.2	Fuels Dynamics . . . . .	65
4.3.3	Bid Stack Parameters . . . . .	67
4.3.4	Demand Dynamic . . . . .	68
4.4	An Extension - Bid Stack Estimation and Parameter Risk for Several Days . . . .	69
4.5	Derivation of the Density Function implied by an Exponential Bid Stack . . . .	72
4.5.1	Bid Stack Parameters for Negative Demand . . . . .	72
4.5.2	Bid Stack Parameters for Price Spikes . . . . .	72
4.6	Additional Analysis: Maximum Likelihood to Estimate the Bid Stack . . . . .	73
<b>5</b>	<b>A Generalization of the Kirk Formula for Structural Electricity Models</b>	<b>75</b>
5.1	Additional Models . . . . .	75
5.1.1	A simple Bid Stack . . . . .	75
5.1.2	Geometric Brownian Motions for Fuels and Demand . . . . .	79
5.2	From the Idea to the Algorithm . . . . .	80
5.3	Numerical Results . . . . .	81
5.4	Derivation of the European Call Option Formula . . . . .	84
5.4.1	Proof: Derivation for a fix Demand; Low Demand . . . . .	96
5.4.2	Proof: Derivation for a fix Demand; High Demand . . . . .	102
5.4.3	Proof: Derivation for a fix Demand; Spikes and Negative Prices . . . .	107
5.4.4	Proof: Exemplary Derivation for truncated normal distributed Demand; Low Case . . . . .	110
<b>6</b>	<b>Numerical Greek Calculation</b>	<b>113</b>
6.1	Numerical Techniques - An Overview . . . . .	114
6.2	Difference Quotient Method . . . . .	116
6.3	Likelihood Ratio Method . . . . .	117
6.3.1	Forward Deltas in a Framework with Historical Volatilities . . . . .	119
6.3.2	Forward Gamma in a Framework with Historical Volatilities . . . . .	123
6.3.3	Vega Calculation . . . . .	125
6.3.4	Sensitivity in Mean-Reversion . . . . .	128
6.4	Pathwise Derivative Method . . . . .	128
6.4.1	Power Forward Delta in a Framework with Historical Volatilities . . . .	129

6.4.2	Fuel Forward Delta in a Framework with Historical Volatilities . . . . .	130
6.5	Numerical Comparison of Different Greek Calculation Methods . . . . .	132
6.6	Additional Lemma: Likelihood Ratio Method . . . . .	140
6.7	Additional Simplifications: Pathwise Derivative Method . . . . .	142
<b>7</b>	<b>Delta Hedging - A Practical Analysis for a Virtual Power Plant</b>	<b>145</b>
7.1	An Example based on Realistic Price Forward Curves . . . . .	145
7.2	Illustrations in case of an Illiquid Power Futures Market . . . . .	150
<b>8</b>	<b>Conclusion</b>	<b>153</b>
<b>9</b>	<b>Outlook</b>	<b>155</b>
	<b>Appendices</b>	<b>159</b>
<b>A</b>	<b>Additional Results for the Structural Model</b>	<b>159</b>
A.1	Spot Price Formula . . . . .	159
A.2	Forward Price Formula . . . . .	161
A.3	Extension of the Forward Price Formula to Price Thresholds . . . . .	163
<b>B</b>	<b>Additional Insights on Calibration and Parameter Risk</b>	<b>165</b>
B.1	Selective Results from Asymptotic Statistics . . . . .	165
B.2	Selective Results from Multiple Time Series Analysis . . . . .	165
B.3	Choice of Model Volatility for Expected Demand . . . . .	167
B.4	Additional Visualizations . . . . .	168
B.4.1	Daily VPP Sensitivities . . . . .	168
B.4.2	Daily VPP Parameter Risk . . . . .	173
<b>C</b>	<b>Additional Insights regarding Greek Calculation</b>	<b>177</b>
C.1	Interchange of Integration and Differentiation . . . . .	177
C.2	Additional Numerical Evaluations and Figures . . . . .	177
	<b>Bibliography</b>	<b>180</b>
	<b>List of Propositions and Definitions</b>	<b>184</b>
	<b>List of Figures</b>	<b>186</b>
	<b>List of Tables</b>	<b>190</b>



# List of Abbreviations

$\mathbb{R}$	denotes the ordinary real line $(-\infty, \infty)$
$\mathbb{R}^+$	denotes the positive real line $(0, \infty)$ without 0
$\mathbf{s} \in \mathbb{R}^{n \times m}$	bold letters are used to depict vectors and matrices, $n > 1$ and $m \geq 1$
$\mathbb{E}^{\mathbb{Q}}$	denotes the expectation of a random variable under a measure $\mathbb{Q}$ on $(\Omega, \mathcal{F})$
$\mathbb{V}^{\mathbb{Q}}$	denotes the variance of a random variable under a measure $\mathbb{Q}$ on $(\Omega, \mathcal{F})$
$\mathbb{Q}$	denotes a risk-neutral probability measure on $(\Omega, \mathcal{F})$
$\mathbb{I}_A(a)$	indicator function, delivers for a set $A$ : 1 if $a \in A$ and 0 otherwise
$\mathcal{N}(\mu, \sigma^2)$	Normal Distribution with mean $\mu$ and variance $\sigma^2$
$\phi^{\mu, \Sigma}$	Normal density function with mean $\mu$ and covariance matrix $\Sigma$
$\Phi^{\mu, \Sigma}$	Normal distribution function with mean $\mu$ and covariance matrix $\Sigma$
$F_{t,T}^i$	denotes a forward contract price at $t > 0$ which delivers one unit of a fuel $i = 1, \dots, n$ or power $i = P$ in $T > t$ .
$F_t^i(t^a, t^b)$	denotes a futures contract price at $t > 0$ which delivers a fuel $i = 1, \dots, n$ or power $i = P$ during $t^a < t^b$ on an hourly/daily basis.
$\mathcal{L}^1(\mathbb{P})$	denotes the space of integrable functions under $\mathbb{P}$
$\mathcal{L}^1(\mathbb{R})$	denotes the space of Lebesgue-integrable functions



## CHAPTER 1.

# Introduction

## 1.1 Electricity Markets

Once the deregulation of electricity markets started in Western Europe in the early 1990s, energy trading has not only led to new ways of profit but has also forced energy companies to rethink their management of market and volume risks. Especially, the difficulty to store electricity is still one of the main complexities to producers (and consumers) as they are - in general - forced to sell (or consume) electricity immediately after its production (delivery). Due to these circumstances, the market faces an increase in electricity spot price volatility whenever electricity demand and production volumes behave unexpected during a day. The volatility may even lead prices to become negative (production volumes higher than demand volumes) being one stylized fact of electricity. Other stylized facts of the electricity spot price are seasonalities (monthly, weekly, daily, hourly), mean-reversion and spikes. A summary can be found in [Burger et al., 2014].

Therefore, the electricity spot price, demand and supply are closely related. Consequently, the relation leads market participants to face the risk of unexpected price changes due to changes in fundamental information. Naturally, they are seeking to mitigate that risk by (i) taking effort to forecast the main price drivers of electricity like demand and renewables production as well as (ii) acting in the electricity exchange in order to switch the spot exposure (i.e. from its power plants) to a tradable exposure in futures positions. By trading derivatives on electricity, market participants can therefore individually decide on how much electricity spot exposure they want to deal with.

The most common derivative on electricity is a futures contract. An electricity futures contract is a typically cash-settled product which refers to the price of a certain amount of electricity during a certain time window. Due to its delivery time window instead of one single point-in-time delivery, power futures contracts are referred to as electricity swaps as well. The non-exchange traded version of a futures contract is a forward contract. Forward contracts are non-standardized alternatives to futures contracts. They mainly differ in its exposed credit risk: whereas futures contracts are typically settled on a daily basis (daily margining) with a central

counterparty (i.e. London Clearing House), forward contracts typically face counterparty default risk. Indeed, risk is often mitigated by bilateral clearing (due to regulatory constraints, i.e. EMIR), however, there are still open risks due to a default of the counterparty (i.e. margin period of risk). Counterparty credit risk is treated by various authors in recent years, i.e. [Burger et al., 2014], [Fiorenzani et al., 2012] for energy markets or [Brigo et al., 2013] for financial markets in general.

In this thesis, we will mainly deal with hourly forwards. Hourly forwards deliver a certain amount of a good in a specified hour in the future. In order to have a straight distinction between futures and forward contracts throughout the thesis, we directly give the Definitions.

**Definition 1.1 (Futures Data)** Let  $F_{t_0}^i(t^a, t^b)$  denote the price of a futures contract as of  $t_0$  delivering a commodity  $i \in I := \{1, \dots, n\}$  during the time window  $[t^a, t^b]$ . We define a range of futures contracts by

$$F_{t_0}^i(t_1^a, t_1^b), \dots, F_{t_0}^i(t_{n_i}^a, t_{n_i}^b) \in \mathbb{R}^+, \forall i \in I, t_0 < t_j^a \leq t_j^b \forall j = 1, \dots, n_i (\in \mathbb{N}),$$

$$F_{t_0}^P(t_1^a, t_1^b), \dots, F_{t_0}^P(t_{n_P}^a, t_{n_P}^b) \in \mathbb{R}, t_0 < t_j^a \leq t_j^b \forall j = 1, \dots, n_P (\in \mathbb{N}).$$

**Definition 1.2 (Forwards Data)** For  $F_{t_0, t}^i := F_{t_0}^i(t, t)$  ( $t > t_0$ ) and  $m \in \mathbb{N}$ , we define hourly forward prices

$$F_{t_0, t_1}^i, \dots, F_{t_0, t_m}^i \in \mathbb{R}^+, \forall i \in I,$$

$$F_{t_0, t_1}^P, \dots, F_{t_0, t_m}^P \in \mathbb{R},$$

$$\mathbf{F} := (F_{t_0, t_1}^1, \dots, F_{t_0, t_m}^1, \dots, F_{t_0, t_1}^n, \dots, F_{t_0, t_m}^n, F_{t_0, t_1}^P, \dots, F_{t_0, t_m}^P).$$

We define  $\mathcal{T} := \{t_i\}_{i=1, \dots, m} \subset (t_0, \infty)$  and choose  $t_i - t_{i-1} = \frac{1}{24 \cdot 365}$  for  $i = 1, \dots, m$ . We assume there is no arbitrage between futures contracts in Definition 1.1 and forwards data ( $t_{n_i}^b < \frac{m}{24 \cdot 365}$  for  $i \in I \cup \{P\}$ ):

$$F_{t_0}^i(t_j^a, t_j^b) = \frac{1}{|k \in \mathbb{N} : t_k \in (t_j^a, t_j^b)|} \sum_{k \in \mathbb{N} : t_k \in (t_j^a, t_j^b)} F_{t_0, t_k}^i, \forall i \in I \cup \{P\}, j = 1, \dots, n_i.$$

At the European Electricity Exchange<sup>1</sup> (EEX) weekly, monthly, quarterly and yearly electricity futures are quoted. The cascading principle is typical for the market: a futures contract will cascade into a portfolio of next smaller futures contracts as soon as the delivery period starts (i.e a yearly futures contract for 2016 will cascade after the last trading day in 2015 into: three monthly futures for January, February and March 2016 and three quarterly futures). Besides futures contracts, EEX offers more complex derivatives like options on electricity. In detail, call

---

<sup>1</sup>www.eex.com



and put options on futures contracts as well as spread options between interconnected markets (i.e. French-Spain, Germany-French, etc.) are quoted.

Due to the difficulty to store electricity, a pure spot market for electricity does not exist. However, it was established a platform to trade electricity short term with maturities of and below one day. The short term trading is offered by EPEX Spot for certain Western European markets<sup>2</sup> and has the purpose to deal as the spot market for electricity. At EPEX Spot a day ahead auction is offered on a daily basis for each hour of the next day. The auction takes place at 12pm. Within those auctions producers and consumers bid for electricity: producers offer part of their capacity for a certain price and consumers bid part of their demand for a certain price. Market participants can offer (bid) electricity for single hours or blocks of several hours. As soon as the auction closes, the market clearing price - which is the price where demand and production volume match - is determined for each hour of the day. Demand and offer curves are published by EPEX Spot. An example of a typical pair of curves for a certain hour of the day is depicted in Figure 1.1.

After the release of the day ahead auction for hourly deliveries more and more trading opportunities were added at EPEX Spot. In the meantime, i. e. a day ahead auction for quarterly spot contracts was introduced. The auction takes place at 3pm each day. After the results (market clearing volumes and clearing prices) of the quarterly auction have been published, a continuous trading of quarterly contracts is offered in the intraday market of EPEX Spot until one hour before delivery.

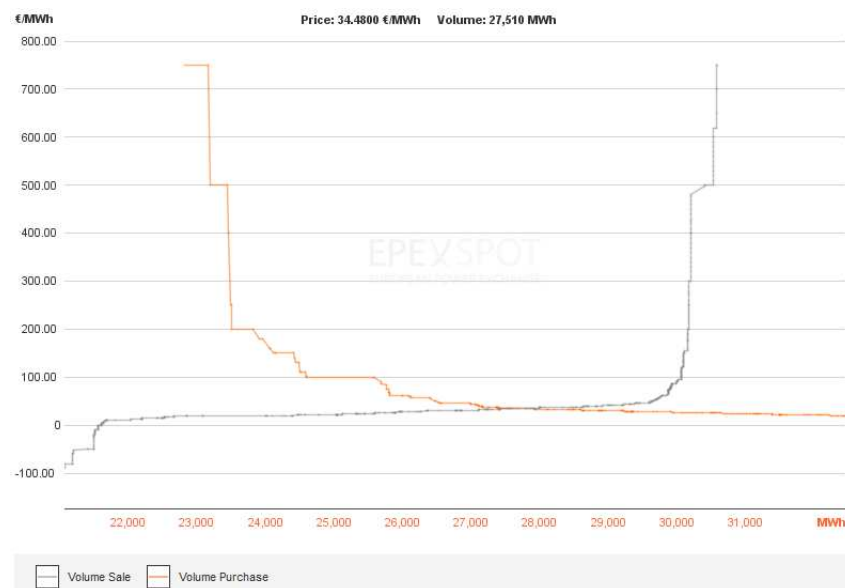


Figure 1.1: Typical Demand and Offer curve for a certain hour of a certain day at EPEX Spot (source: [www.epexspot.com](http://www.epexspot.com))

<sup>2</sup>Germany, France, Austria, Switzerland and Luxembourg.

## 1.2 Energy Trading / Quantitative Risk Management

The literature concerning mathematical aspects of energy trading is manifold. One of the basic textbooks are [Clewlow and Strickland, 2000] and [Eydeland and Wolyniec, 2003]. A more recent textbook is [Burger et al., 2014]. It gives insights on how energy risk management has been adapted in recent years.

One of the most important aspect from a hedger's point of view (or a market maker respectively) is - independently of any asset class - that a model does not offer arbitrage opportunities between liquidly traded products. However, liquidity already sets the electricity market apart from i.e. interest rate markets. Whereas, an interest rate model - due to high liquidity - has to price i.e. interest rate swaps, swaptions, caps/floors and forward rate agreements without any arbitrage (cf. [Brigo and Mercurio, 2006]), arbitrage conditions are difficult to deal with in the case of electricity. Options - at least for the German market - are rather traded OTC than at an exchange making public information sparse (cf. [Fiorenzani et al., 2012]).

To stress this aspect further, a practitioner is forced to price not only futures contracts but the whole range of single-hour forward contracts for at least the next year (cf. Chapter 1.2.1). However, arbitrage opportunities for hourly prices are difficult to realize as they are typically not traded in the market.

### 1.2.1 Importance of Electricity Price Forward Curves

The prior Section indicated that market participants in energy markets are forced to build price forecasts of hourly forward prices up to several years in the future. Additionally, the average of all hourly prices of a month should equal the price of a liquidly traded monthly futures contract (no-arbitrage condition). We present an algorithm on how to derive an hourly price forward curve for electricity in Chapter 2.3.

The reasons for the need of such an hourly price forward curve are manifold, i.e.:

- An electricity producer has to operate his power plants on a daily basis. In general, they are not gaining profit 24 hours a day due to the hourly shape of the electricity spot price. In order to hedge the future exposure (market risk in i.e. coal and electricity prices), the operator is forced to decide how much *future volume* he intends to hedge today. Therefore, he has to have an idea how many hours his plant will produce electricity based on the today's futures prices.
- An industry company may have a special demand profile for each day of the week. I. e. a company may always need electricity in the night, where electricity is cheaper than the

average price of a day. The customer may ask the energy producer to give an individual price for that guaranteed demand profile.

- (De-) Investment decisions may be driven by the hourly shape of electricity prices. However, the hourly shape is changing over time, i. e. due to the increasing role of renewables power production capacity. An energy producer must have an opinion how this hourly shape changes over years.

### 1.2.2 Structural Models: Fundamentals and Tractability

As soon as non-linear derivatives on electricity are traded, stochastic models are commonly used to derive a present value of the contingent claim using a risk-neutral measure. If the derivative depends merely on an electricity futures price, a forward model like Black 76 may be used (cf. [Clewlow and Strickland, 2000]). The electricity futures price is then exogenously linked to stochastic factors.

In this thesis however, we want to deal with derivatives which are directly linked to the electricity spot price instead of a traded futures price. In this case, it arises the complexity to build a bridge from hedging instruments (futures) to spot instruments which are not able to be used as hedging instruments due to the obstacles to store electricity effectively. Therefore, we either use a stochastic model for the forward price  $F_{t,T}$  and use the theoretical relation  $S_t = \lim_{T \rightarrow t} F_{t,T}$  to price the spot price dependent claim. Or we directly start with a spot model and use the risk-neutral expectation  $F_{t,T} = \mathbb{E}^{\mathbb{Q}}[S_T | \mathcal{F}_t]$  to link the model to forward prices.

So-called structural electricity spot models have been investigated in recent years to incorporate fundamental information into a spot model. Therefore, structural models set itself apart from ordinary *reduced-form models* which directly link a futures contract or the spot price to state variables (exogenous approach). The electricity spot price is instead endogenously given by a function of fundamentals.

A structural model typically offers close form formulas to calculate electricity forward prices. Consequently, the model can be calibrated rather fast against an hourly price forward curve. The trade-off between the incorporation of fundamentals and keeping the model tractable at the same time is the main feature of structural models.

Typical fundamentals to be included are the so-called merit order of an energy market.

**Definition 1.3 (Bid Stack, Merit Order and Marginal Fuel)** *As explained in the prior Chapter, the day ahead spot price is for Western European markets determined by an auction where the main output is clearing price and clearing volume. The auction is constructed such that the clearing price is always set by the most expensive power plant necessary to serve the electricity*

demand in the market. In case of a thermal power plant, the according fuel is called to be the marginal fuel.

The merit order defines the ascending order of marginal fuels which are available for power generation (renewables, nuclear, coal, gas, etc.) on a certain market (cf. Figure 1.2). The resulting function of the power price over electricity demand is called the bid stack.

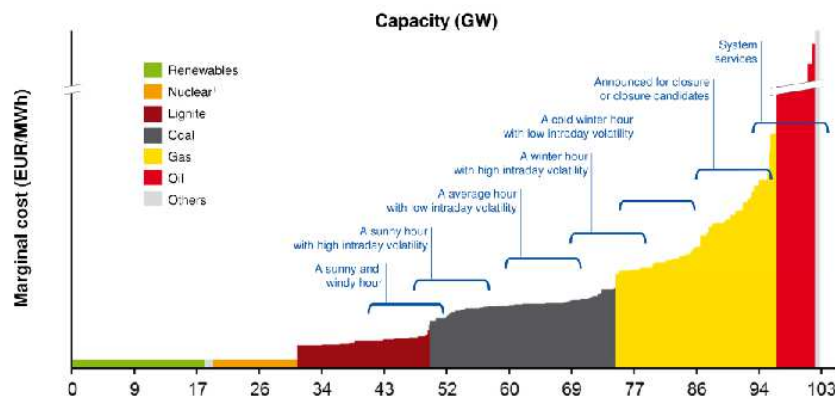


Figure 1.2: Merit order in the German Electricity as of 2015;  
source: [RWE Supply & Trading GmbH, 2015]

Beyond demand and supply, the individual capacities of different power plants as well as renewables are other fundamental factors of the electricity spot price. Because renewables are - due to the so called feed-in tariffs - treated with priority in Western European markets, they shift the merit order to the right (high production by renewables) and to the left (low production by renewables) but do not affect the slope of the bid stack. Due to its rather inflexible dispatching of nuclear plants, nuclear power plants have a similar impact on the bid stack. Altogether, nuclear and renewables are commonly defined to belong to the so called must-run stack (cf. [Coulon et al., 2014]) indicating that those power plants produce electricity independently of the power price. In order to analyze the shape of the bid stack, the must-run stack is often subtracted from the demand. This enables to have a clear view on the slope of the bid stack after highly volatile renewables production. The resulting excess demand is called residual demand and may become negative in case renewables production is higher than electricity demand.

A detailed survey about how structural electricity models have been designed in recent research is given in [Carmona and Coulon, 2014]. In the following, we introduce five basic approaches.

### The first structural model

The first article on a stochastic model which incorporates demand and supply curves into a derivatives pricing model is [Barlow, 2002]. Based on an increasing supply function  $u_t(x)$  and

a decreasing demand function  $d_t(x)$  ( $x$ =price of electricity; cf. Figure 1.1), the resulting power price  $S_t^P$  is uniquely giving by calculating the intersection

$$u_t(S_t^P) = d_t(S_t^P).$$

The author assumes the demand to be inelastic  $d_t(S_t^P) \equiv D_t$ . Consequently, the power price is given by

$$S_t^P = u_t^{-1}(D_t).$$

Afterwards,  $u_t$  is assumed to have the form

$$u_t(x) = \xi - b_0 x^\alpha$$

for  $\alpha < 0$  and  $\xi, b_0 > 0$ . It leads the power price to become

$$S_t^P = \left( \frac{\xi - D_t}{b_0} \right)^{1/\alpha}$$

as long as the demand is lower than the maximum market capacity  $\xi$ . We define  $D_t := -\alpha b_0 Y_t + \xi - b_0$  for a stochastic process  $Y_t$  and get

$$S_t^P = \begin{cases} (1 + \alpha Y_t)^{1/\alpha} & \alpha \neq 0, Y_t \in \mathbb{R} \setminus \{-1/\alpha\} \\ \exp(Y_t) & \alpha = 0. \end{cases}$$

The model is the basis for more realistic structural models where certain parts of the bid stack belong to certain marginal fuels.

### A Bid Stack with Static Merit Order but Stochastic Capacities

The bid stack was introduced in [Aïd et al., 2013]. The authors assume  $n$  different fuels  $(S_t^{(1)}, \dots, S_t^{(n)})$  with individual heat rates  $h_1, \dots, h_n$  and capacities  $C_t^{(1)}, \dots, C_t^{(n)}$ . The authors define  $\bar{C}_t^{(j)} := \sum_{i=1}^j C_t^{(i)}$  and end up with the following parts of the bid stack:

$$I_t^{(1)} := (-\infty, \bar{C}_t^{(1)}) \quad I_t^{(i)} := [\bar{C}_t^{(i-1)}, \bar{C}_t^{(i)}) \quad (i = 2, \dots, n-1) \quad I_t^{(n)} := [\bar{C}_t^{(n)}, \infty)$$

The power price is then defined by

$$S_t^{(i)} = g\left(C_t^{(n)} - D_t\right) \sum_{i=1}^n h_i S_t^{(i)} \mathbb{I}_{D_t \in I_t^{(i)}}$$

where

$$g(x) = \min\left(M, \frac{\gamma}{x^\nu}\right) \mathbb{I}_{x>0} + M \mathbb{I}_{x \leq 0}$$

and constant parameters  $M, \nu, \gamma > 0$ .

### An Exponential Bid Stack

We decided to use the structural model in [Carmona et al., 2013] as a basis for our research. Based on exponential bid stack functions for each relevant fuel  $i = 1, \dots, n$

$$b_i(D_t, S_t^{(i)}) := S_t^{(i)} e^{k_i + m_i D_t} \quad (k_i \in \mathbb{R}, m_i > 0),$$

the overall bid stack function is derived by finding the market clearing price for each possible demand such that the electricity demand is met. The model is introduced in detail in Chapter 2.1 (i. e. (2.3)). The model enables dynamic changes in the merit order, i.e. the order from cheapest to most expensive fuel changes over time depending on fuel prices and demand. Capacities are assumed to be constant over time. The model provides close form formulas for forward prices as well as spread option prices and was already analyzed for the application in the German Electricity market (cf. [Coulon et al., 2014]). Amongst others, we derive the according close form formula for European call options under that structural model in this thesis (Chapter 5.4).

### Incorporation of Emission Prices

In [Carmona et al., 2012] the exponential bid stack is extended to capture emission certificate prices  $E_t$ :

$$b_i(D_t, S_t^{(i)}, E_t) := S_t^{(i)} e^{k_i + m_i D_t} + E_t e^{a_i + m_i D_t} \quad (k_i, a_i \in \mathbb{R}, m_i > 0),$$

The authors find that a forward backward differential equation has to be solved in order to calculate power prices in the model. The reason is that  $E_t$  is merely known at the end of the first compliance period  $T$ .

### Interconnected Markets

In [Füss et al., 2015], the exponential bid stack with one marginal fuel is used as a starting point to model the interconnection between two different markets (i. e. Germany and France). Interconnectivity of two power prices  $S_{1,t}^P, S_{2,t}^P$  is modeled by a function  $-K < J(t) < K > 0$  such that

$$\begin{aligned} S_{1,t}^P &= \alpha_1 \cdot (S_{1,t}^F)^{\delta_1} \cdot \exp(\beta_1 D_{1,t} - \gamma_1 J(t)) \\ S_{2,t}^P &= \alpha_2 \cdot (S_{2,t}^F)^{\delta_2} \cdot \exp(\beta_2 D_{2,t} + \gamma_2 J(t)), \end{aligned}$$

for  $\alpha_1, \alpha_2, \beta_1, \beta_2, \gamma_1, \gamma_2, \delta_1, \delta_2 > 0$ . Close form formulas for power forwards are derived.

### 1.2.3 Hedging Strategies

For the purpose of our thesis we derive the definition of hedging naturally from the idea of replicating a certain payoff structure in the future: if a practitioner agrees to deliver electricity

at a certain future date (short forward contract), he might hedge the risk by buying an according amount of coal and emission certificates today to run his power plant at the delivery date to deliver electricity. Thus, the practitioner *replicates* an electricity forward by buying an outright of emissions and coal.

In [Fries, 2007], the idea of replication was used to define hedging as follows.

**Definition 1.4 (Hedging)** *A replication portfolio (almost) replicating a derivative product and thus, if considered together with the derivative product neutralizing (reducing) the total risk, is called a (partial or incomplete) hedge. The corresponding trading strategy is called hedging.*

As soon as volume risk or restrictions on a real asset (cf. Chapter 1.2.4) are included into a derivatives contract (i.e. virtual power plants), the valuation as well as the calculation of a hedging strategy leads to an optimization procedure in order to identify the optimal hedging volumes. A practical introduction in the context of gas contracts with volume optionality (swing contracts) is given in [Breslin et al., 2008]. The derivation of optimal volumes can be derived either on an intrinsic, rolling intrinsic, or extrinsic basis.

The intrinsic approach assumes the hourly/daily forward curves to be available without any uncertainty. Based on that a assumption optimal volumes can be derived by solving a deterministic optimization problem. The intrinsic approach assumes the hedge to be established directly at initiation of the contract. The hedge remains static until maturity of the contract.

A more realistic approach is the rolling intrinsic approach. This approach considers that a practitioner might adjust the portfolio over time by rebalancing the intrinsic hedge based on changed market conditions in the future. Consequently, a Monte Carlo method is used to simulate i.e. monthly price changes. On each simulated date the intrinsic hedge is rebalanced. The present value of an intrinsic strategy is always lower than a present value a rolling intrinsic strategy. The reason is that the portfolio would only be adjusted in case the value of the hedge can be increased.

The extrinsic approach can for instance be based on an option basket approach, a Least-Square Monte Carlo method or tree methods. In all approaches forward prices become stochastic leading deterministic optimization methods to be inapplicable. In that case the optimization procedure becomes stochastic. Delta hedging is a common method to derive a hedging strategy under this model assumption (cf. [Fries, 2007]). We will derive this approach for structural models in Chapter 3. Besides delta hedging, gamma and vega hedging is often applied in practice as well. According definitions are i.e. given in [Fries, 2007]:

**Definition 1.5 (delta)** *The first-order partial derivative of the price of a derivative product with respect to the underlyings is called delta. It is the first-order sensitivity of the derivative product to price changes of the market-traded assets (or market quotes).*



**Definition 1.6 (gamma)** *The second-order partial derivative of the price of a derivative product with respect to the underlyings is called gamma. It is the second-order sensitivity of the derivative product to price changes of the market-traded assets (or market quotes).*

**Definition 1.7 (vega)** *The first-order partial derivative of the price of a derivative product with respect to the underlyings log-volatility is called vega. It is the first-order sensitivity of the derivative product to log-volatility changes of the market-traded European options.*

### 1.2.4 Virtual Power Plants

A typical representative of electricity spot price dependent claims is a virtual power plant. Virtual power plants are financial simplifications of real power plants where the power plant is modeled by a portfolio of spread options: in case production costs to produce one unit of electricity (i.e. in order to buy the fuel) are cheaper than the electricity price, the producer will decide to switch on his plant. In this thesis, we will assume each of the spread options for different maturities to be independent of other options, i.e. we will not treat the optionality in production volumes. Related to the prior Chapter, we use a spread option approach to value a VPP. However, we do not need to perform any optimization procedure due to the missing interconnection of payoff functions.

Consequently, the present value of a virtual power plant under a financial market<sup>3</sup>

$$(\Omega, \mathcal{F}, \mathbb{P}, (S_t^c, S_t^g, S_t^p)_{t \geq 0}, \mathbb{Q})$$

at  $t_0 > 0$  is given by

$$PV_{\mathcal{T}}^{VPP}(h_R, K) := \sum_{t \in \mathcal{T}} e^{-r(t-t_0)} \mathbb{E}^{\mathbb{Q}} \left[ (S_t^p - h_R \cdot S_t^{(c)} - K)^+ \middle| \mathcal{F}_{t_0} \right], \quad (1.1)$$

where the parameters can be interpreted as follows:

- $S_t^p$ : electricity spot price at  $t > t_0$ ,
- $S_t^{(c)}$ : coal spot price at  $t > t_0$ ,
- $\mathcal{T}$ : the time horizon for the VPP; as we intend to analyze a VPP on an hourly basis, the set of forward prices in Definition 1.2 and the time horizon of the VPP will match throughout this thesis in general (both are denoted by  $\mathcal{T}$ ),
- $h_R > 0$ : determines the volume of fuel which is needed to produce one unit of electricity (heat rate),

---

<sup>3</sup>  $(\Omega, \mathcal{F}, \mathbb{P})$  denotes a filtered measurable space.



- $K > 0$ : determines additional costs like starting costs, emission costs, or other fuels like heating oil which may be needed additionally to the main fuel; for the purpose of this thesis, we decided not to include emission costs separately. The reason is that a structural model gets quite complex in that case leading to non-tractable forward price formulas in general (i.e. [Carmona et al., 2012]),
- $r > 0$ : constant interest rate; we will use  $r = 0$  for the purpose of this thesis,
- $t_0$ : value date; we will use year-end 2015 for our evaluations.

In practice, the spread on gas is called spark spread and the spread on coal is called dark spread. In case emission costs are included as a separate variable, the spread is called *clean*. Otherwise the spread is called *dirty*. The spread option approach in equation (1.1) is defined without emission costs which means we typically refer to a portfolio of dirty spread options throughout the thesis.

The importance of smart hedging strategies for virtual power plants is given by narrowing margins i.e. due to the increasing share of renewables in the market. In order to see that we depict the historical clean spark spread of a gas power plant in Figure 1.3. It can be seen that the exchange traded peak<sup>4</sup> power price in Germany and France causes the spreads to be negative for a large amount of data points. In practice, a producer would additionally face fix costs in terms of a positive strike which is likely to cause the majority of peak spreads to become negative as a whole. Consequently, a gas power plant is obliged to generate profit from only a few hours where the power plant is in the money.

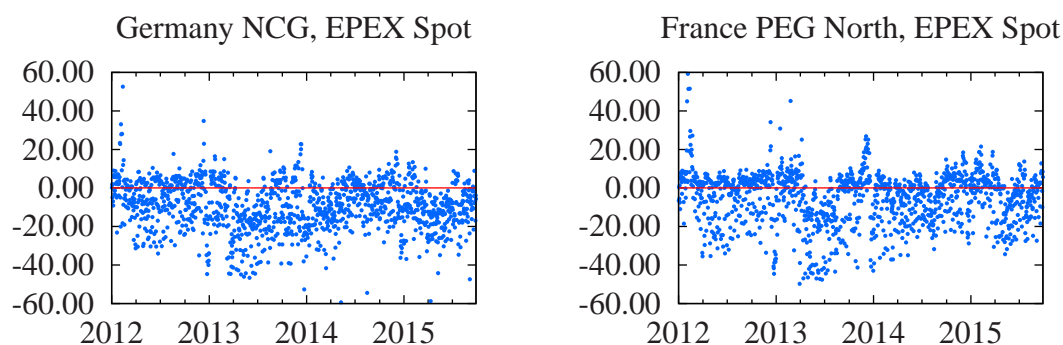


Figure 1.3: Peak clean spark spread (blue dots) in Germany (left) and France (right) from 2012 until September 2015 in EUR/MWh (effectiveness was assumed to be 50% and CO<sub>2</sub>-conversion factor 0.4; data source: Bloomberg).

Similar results can be derived when analyzing the clean spark spread for gas and power futures. We will call this spread the *intrinsic* spread. Due to negative spreads, a simple (rolling) intrinsic

<sup>4</sup>Peak hours are defined to be the daily time range from 8.00h am until 8.00h pm.

hedge of a gas power plant will hardly result in remarkable profit for the power plant as a whole. This is the reason why we concentrate on delta hedging in this thesis. Using delta hedging we may even trade negative spreads in order to make profit from volatility in the market. In case we end up with positive spreads, the power plant is switched on to earn the payoff. In the end, the power plant may have created a certain profit even though it has not produced electricity.

### 1.2.5 Model Risk and Parameter Risk

Whenever markets are non-transparent (i.e. prices cannot be observed on a daily basis), uncertainty about the value of goods will naturally grow. This is especially true for power markets where implied volatility is rather traded non-transparently over the counter than at an exchange (cf. [Fiorenzani et al., 2012]). At the same time practitioners' assets bear volume optionalities and non-linear constraints such that they became an integral part in energy contracts (i.e. virtual gas storages, virtual power plants). Consequently, a fair value of those contracts will naturally face uncertainty. Under those circumstances, model risk can deal as a suitable instrument to quantify fair value uncertainty.

In detail, the lack of observable electricity futures option prices i.e. in the German electricity market (cf. [Fiorenzani et al., 2012]) naturally leads to higher uncertainty in the parameter estimation of stochastic electricity models. The reason is amongst others given by the consequence that volatility estimators for electricity may not be derived completely from observable option prices but historical estimators are required instead. This leads to parameter uncertainty. However, we might already question the choice of electricity model in general: are reduced form models able to explain all of the stylized facts of electricity (model risk)?

Based on the terminology of [Knight, 1921], *model risk* measures the risk in model choice and is clearly distinguished from *parameter risk* being defined as the risk in parameter estimation for a given model. The measures to quantify model and parameter risk are manifold, i.e. stress testing methods ([Rebonato, 2010]), worst-case scenarios ([Cont, 2006]) or methods from asymptotic statistics ([Bannör and Scherer, 2013]). Model risk is also considered in the context of model validation, calibration and hedging ([Morini, 2011]) which further extends the broad relevance of model risk in general.

In terms of commodity markets, recent progress regarding model risk was for instance achieved in [Cartea et al., 2012]. The authors defined a class of stochastic differential equations which are typical for commodity derivatives pricing. Based on that class, they introduced a penalty for being *far away* from a reference model inside the class. An example of a quantification of parameter risk is for instance given by the authors of [Bannör et al., 2013]. The authors derive historical estimators for a jump-diffusion model and calculated parameter risk in terms of the average value-at-risk using results of asymptotic statistics. The approach was introduced for a

general financial market in [Bannör and Scherer, 2013].

We will apply the approach of [Bannör and Scherer, 2013] within this thesis to quantify parameter risk of a structural electricity model with retrospectively derived bid stack and model parameters using historical data. The authors define model uncertainty, parameter uncertainty and model risk as follows.

Let  $(\Omega, \mathcal{F}, \mathbb{P})$  be a filtered measurable space and let  $(\mathbf{S}_t)_{t \geq 0}$  denote a  $n$ -dimensional  $\mathbb{P}$ -adapted stochastic process modeling the basic instruments  $\mathbf{S}_t = (S_t^{(1)}, \dots, S_t^{(n)})$ .

**Definition 1.8 (Model Uncertainty)** Let  $\mathcal{Q}$  be a family of probability measures on  $(\Omega, \mathcal{F})$  such that all stochastic processes modelling discounted basic instruments  $(S_t^{(i)})_{t \geq 0}$   $i = 1, \dots, n$  are  $\mathbb{Q}$ -martingales for all  $\mathbb{Q} \in \mathcal{Q}$ . The financial market model  $(\Omega, \mathcal{F}, \mathbb{P}, (\mathbf{S}_t)_{t \geq 0}, \mathcal{Q})$  faces model uncertainty if  $|\mathcal{Q}| > 1$ , where  $|\mathcal{Q}|$  denotes the cardinality of  $\mathcal{Q}$ .

**Definition 1.9 (Parameter Uncertainty)** Let  $(\mathbb{Q}_\theta)_{\theta \in \Theta}$  be a family of pairwise different probability measures on  $(\Omega, \mathcal{F})$  such that the models  $(\Omega, \mathcal{F}, \mathbb{P}, (\mathbf{S}_t)_{t \geq 0}, \mathbb{Q}_\theta)$  are arbitrage-free for all  $\theta \in \Theta$ . The model faces parameter uncertainty if  $|\Theta| > 1$ .

**Definition 1.10 (Model Risk)** Let  $(\Omega, \mathcal{F}, \mathbb{P}, (\mathbf{S}_t)_{t \geq 0}, \mathcal{Q})$  be a financial market model exhibiting model uncertainty, i.e.  $|\mathcal{Q}| > 1$ . If there is a  $\sigma$ -algebra  $\mathcal{F}^\mathcal{Q}$  on  $\mathcal{Q}$  and a probability measure  $R : \mathcal{F}^\mathcal{Q} \rightarrow [0, 1]$  assigning a "likelihood of validity" to the models in doubt, the financial market model exhibits model risk.

**Definition 1.11 (Parameter Risk)** We will call model risk synonymously to be parameter risk whenever  $\mathcal{Q}$  is given by different parametrizations  $\Theta$  of a certain model:  $\mathcal{Q} := \{\mathbb{Q}_\theta\}_{\theta \in \Theta}$ .

## 1.3 Contribution of the Thesis

This thesis conducts a mathematical analysis how structural electricity models can be used in practice to hedge electricity spot price dependent claims (i.e. virtual power plants). The analysis comprises (i) the inclusion of hedging instruments into a structural model, (ii) the mathematical evidence that structural models can under certain restrictions be used to build replication portfolios, (iii) the derivation of historical estimators for model parameters including a quantification of implied parameter risk and (iv) how hedging strategies can be calculated numerically.

Based on our knowledge comparable analyzes of structural electricity models in the context of hedging are uncommon until now (i.e. [Aïd et al., 2013]). The focus of recent years was rather to analyze different approaches to include fundamental information into a structural model and whether its fundamental input factors should be considered stochastically or deterministically

(cf. [Carmona and Coulon, 2014] for an overview). In our research however, we go beyond the construction of structural models and propose a framework on how to prepare a certain structural model for practice.

As been stated, the first step is to identify the universe of hedging instruments. Mathematically, we have to ensure that a model prizes all hedging instruments without any arbitrage opportunities. In [Aïd et al., 2013] for example, hedging strategies have also been derived under a structural model. The authors have enlarged the model to include electricity forward contracts as hedging instruments. In our research, we follow a similar approach. We will see in our numerical evaluations that the hedging behavior completely changes as soon as electricity forwards are considered as hedging instruments. The main complexity arises from the fact that electricity cannot be stored efficiently so far. The fact leads electricity not to be applicable as a hedging instrument but only derivatives on electricity. As soon as a claim on electricity spot is to be hedged, a bridge from electricity spot to electricity forwards/futures has to be build.

The second step is to derive conditions under which structural models can be used to build replication portfolios. The basic result is given by Proposition 3.2 where we proof under certain conditions that delta hedging can be applied to replicate a claim. It shows that a replication portfolio can be derived as soon as (i) the expected electricity spot price as well as the claim is integrable, (ii) stochastic drivers are Markov chains and (iii) the Itô Lemma can be applied to the expected electricity spot price as well as to the claim. In order to hedge a virtual power plant, a strip of spread options has to be replicated. Therefore, Proposition 3.3 proves - under the restriction that all spread options are independent of each other - that the hedging strategy can be derived by (i) calculating hedging strategies for each spread option separately using hourly forward contracts and (ii) solving an optimization problem to come from hourly forward contracts to liquid futures contracts.

The third step is to estimate appropriate model parameters for the stochastic dynamics as well as for the bid stack parameters based on a historical data set. In order to be able to quantify parameter uncertainty, we derive asymptotically normally distributed estimators. Afterwards, [Bannör and Scherer, 2013] can be applied to quantify the embedded parameter uncertainty in the present value of a contingent claim. The uncertainty of the present value leads to uncertainty in the composition of our hedging portfolio (uncertainty of PV causes uncertainty of its derivatives). Based on our knowledge [Bannör and Scherer, 2013] has not been applied to structural electricity models so far. The main complexity arises from our hedging intention. It forces us to estimate a structural electricity spot model from historical electricity futures data (hedging instruments). Based on our knowledge this has not been done in research so far. In detail, we estimate the residual demand dynamic such that we match the historical dynamic of electricity futures prices. The translation between demand and electricity futures is implied by the struc-

tural model or the bid stack function respectively. The result how an asymptotically normally distributed estimator can be derived is given by Proposition 4.4.

Furthermore, we are obliged to estimate the bid stack function from a historical data set. A comprehensive contribution how to estimate a bid stack function from data of the German electricity market has been published in [Coulon et al., 2014]. The authors exploit bid and offer data of EPEX Spot to estimate the bid stack function. However, the paper does not give a transparent algorithm from raw data to the bid stack parameters. Therefore, we intend to build a transparent algorithm in this thesis. The result is given in Proposition 4.3 where we end up with an asymptotically normally distributed estimator for the bid stack function based on historical data.

In the fourth step, we analyze different approaches how to derive hedging strategies numerically. In detail, we give a numerical comparison of the difference quotient method, the likelihood ratio method and the pathwise derivative method. Furthermore, we analyze an appropriate estimator for the present value of a spread option in order to avoid a numerically expensive Monte Carlo pricing engine. We end up with an algorithm which generalizes the common known Kirk formula (cf. [Kirk, 1995]) to structural models (Chapter 5.2). This has based on our knowledge not been done in research so far. In order to implement the generalized Kirk formula we were forced to derive an analytic electricity option price formula first. For the structural model [Carmona et al., 2013] this has not been done before.

## 1.4 Structure of the Thesis

In Chapter 2, we introduce the structural model in scope of this thesis as well as the stochastic dynamics of the fuels and the electricity demand. Furthermore, we give a review of market data and describe the algorithm how the hourly price forward curve for the purpose of the thesis has been derived. Chapter 3 analyzes how replication strategies can be derived under structural models. In detail, we build the link between the spot model and the hedging instruments (forward contracts) and derive a forward model which is implied by the merit order of the structural spot model. We then give a Proposition on how to come from an hourly hedging strategy to a hedging strategy using exchange traded instruments, i.e. futures.

In Chapter 4 we estimate the model parameters (fuels, demand and bid stack parameters) based on a historical data set. Beyond that we show that the estimators are asymptotically normal enabling us to quantify parameter risk induced by the estimators. The quantification of parameter risk is done for a virtual power plant. In Chapter 5, we generalize the common known Kirk formula to structural models. For the application of the Kirk formula we were obliged to derive an option price formula for our model in scope. Due to its complexity, we included the

formula as well as the proof at the end of the according Chapter (cf. Chapter 5.4). In Chapter 6 we proceed to compare different numerical methods to calculate Greeks for a structural model. Again, some of the technical proofs are outsourced to the end of the Chapter (cf. Chapter 6.6 and 6.7). Finally, we perform a case study and calculate delta hedging strategies for a virtual power plant. Chapter 8 concludes.

## 1.5 Publications

Chapter 3 together with the case study in Chapter 7 is published in the Journal of Energy Markets [Harms and Kiesel, 2017]. Moreover, we are in the process of submitting Chapter 4 to the SIAM Journal of Financial Mathematics (SIFIN).

## 1.6 Implementation

The mathematical results of this thesis are validated against an according implementation in C++. We used the following routines of the QuantLib and boost library:

- QuantLib::BivariateCumulativeNormalDistributionWe04DP,
- QuantLib::CumulativeNormalDistribution,
- QuantLib::SimpsonIntegral,
- QuantLib::MersenneTwisterUniformRng,
- QuantLib::SVD
- QuantLib::SimulatedAnnealing,
- QuantLib::LevenbergMarquardt,
- QuantLib::BFGS.

All visualizations in this thesis have been created with gnuplot.

## Market Setting

### 2.1 A Structural Model for Electricity Markets

Structural electricity spot models enable to interconnect the influence of residual demand  $D_t$ , marginal fuel prices  $\mathbf{S}_t^F = (S_t^1, \dots, S_t^n)$  and other fundamental factors such as market capacity  $\bar{\xi}$ . The electricity price  $S_t^P$  is modeled by a function of the according fundamental factors. The market bid stack (cf. Figure 1.2) is used to combine all these input variables.

We assume the general representation of a market bid stack depending on a  $n \in \mathbb{N}$  dimensional vector of fuel prices  $\mathbf{S} = (s_1, \dots, s_n)$  (potential marginal fuels) and an arbitrary residual demand  $D$  by a function

$$f_{bs}(D, \mathbf{S}) : \mathbb{R} \times (\mathbb{R}^+)^n \rightarrow \mathbb{R}. \quad (2.1)$$

We define  $I := \{1, \dots, n\}$  to be the according index set. Let  $t_0 \geq 0$  be the valuation date. We assume  $t > t_0 \geq 0$  throughout the following Chapters.

In [Carmona et al., 2013], it is proposed to use single fuel bid stacks  $b_i$  for each fuel type  $i \in I$ . The single fuel bid stacks are aggregated appropriately to end up with the final market bid stack. Each single fuel bid stack is assumed to have the form

$$b_i(D, s_i) : [0, \bar{\xi}_i] \times \mathbb{R}^+ \rightarrow \mathbb{R}, \quad b_i(D, s_i) := s_i e^{k_i + m_i D}, \quad (2.2)$$

where  $\bar{\xi}_i \in \mathbb{R}^+$  represents the individual capacity of fuel type  $i$ ,  $k_i \in \mathbb{R}$  and  $m_i > 0$ . Parameter  $k_i$  is used to set the minimum power production price for fuel  $i$  ( $D = 0$ ). Parameter  $m_i$  determines the steepness of the stack as well as the maximum power production price for fuel  $i$  for  $D = \bar{\xi}_i$ . The total capacity is given by  $\bar{\xi} := \sum_{i \in I} \bar{\xi}_i$ .

The power price for the residual demand  $D_t \in [0, \bar{\xi}]$  is consequently determined by the price such that the aggregated volume of produced electricity per fuel type approaches the market residual demand<sup>1</sup>:

$$S_t^P = f_{bs}(D_t, \mathbf{S}_t^F) = \min_{i \in I} b_i(0, S_t^i) \vee \sup \left\{ p \in \mathbb{R} : \sum_{i \in I} b^{-1}(\cdot, S_t^i)(p) < D_t \right\}. \quad (2.3)$$

---

<sup>1</sup>For a proof we refer to [Carmona et al., 2013].



In [Carmona et al., 2013], closed form solutions for forwards and spread option prices have been derived for the case  $n = 2$ . Furthermore, the model has been extended to capture negative and high demand. We collect a selection of their results (which we use in the thesis) for the convenience of the reader in Appendix A. In the following, we work with  $n = 2$ .

**Remark 2.1 (Only two marginal Fuels?)** *We intent to calibrate our model against German electricity data. However, it is well known that two marginal fuels are not enough to explain the full complexity of electricity markets like in Western Europe. Table 2.2 gives an overview on average available capacities in 2015 of the German electricity market based on information of the EEX transparency website<sup>2</sup>. It can be extracted that the electricity price is driven by at least nuclear, lignite, coal, gas and oil. However, as it is already done in [Coulon et al., 2014], nuclear belongs to the so called must-run stack implying that nuclear power plants produce electricity independently of the power price. Therefore, the residual demand - which is the demand after production of renewables and nuclear - is what we use as input for the bid stack function.*

*Furthermore, we build a cluster of lignite and coal for hedging purposes. By neglecting the impact of oil (we include that part in the spike part of the bid stack), we end up with a simplified bid stack model using only two marginal fuels.*

In Chapter A.3, an extension to spot price thresholds can be found. We believe it to be the first time that a price threshold is considered for structural electricity models. For example, EPEX Spot restricts the electricity spot price of an auction to be between -500 and 3000 EUR/MWh. We find price thresholds to become material as soon as we price derivatives with maturities beyond six months (cf. Figure A.1); at least for hours with high demand.

In Chapter 4, the exponential bid stack is estimated based on historical market data. Before, we use the next Remark to outline that each parameter may also be derived in a simplified manner merely from fundamental observables in the market.

Parameters	Coal	Gas
$k$	$-\log(40) + \log(5)$	$-\log(14.9) + \log(35)$
$m$	0.0695	0.0694
$\bar{\xi}$	29.94	7.78
$m_N$	0.5	
$m_S$	0.5	

Table 2.1: Bid Stack Parameters

<sup>2</sup>Licensed data by University Duisburg-Essen.



**Remark 2.2 (Choice of Bid Stack Parameters)** *The choice of bid stack parameters in Table 2.1 is based on fundamentals of the German electricity market: Parameter  $k$  was chosen such that coal (including lignite) starts producing electricity at a price of 5 EUR/MWh and gas at 35 EUR/MWh. We choose capacity with the help of the EEX transparency website. The average (ex ante) capacity for 2015 is given in Table 2.2.*

Power Plant	Average Capacity in MW
biomass	0.04
coal	12.23
coal-derived-gas	0.40
garbage	0.18
gas	7.78
lignite	17.71
oil	1.60
other	0.25
pumped-storage	5.15
run-of-the-river	0.60
seasonal-store	0.47
uranium	10.20
wind-offshore	0.65

Table 2.2: Available Capacity (ex ante, day ahead) published by EEX Transparency website throughout the year 2015 (yearly average)

Parameters  $m_c, m_g$  were chosen such that - at  $t_0$  - the maximum power price with coal as the single marginal fuel is 40 and with gas as single marginal fuel is 60 EUR/MWh. By choosing  $m_N, m_S$  to be 0.5 we achieve a price interval from -142 to 115 EUR/MWh (for negative demand: -10 MW; for spikes: 10 MW above total capacity).

## 2.2 The Dynamics for Fuels and Demand and a Risk-Neutral Measure

As it was done in [Carmona et al., 2013], we assume independence between the demand and fuels dynamics. We therefore define one filtration  $\mathcal{F}^{\mathbf{W}}$  created by Brownian motions  $\mathbf{W} = (W^{(1)}, \dots, W^{(n)})$  of the fuels and another independent filtration  $\mathcal{F}^D$  created by the Brownian Motion  $W^D$  of the demand process. The final filtration is defined as  $\mathcal{F} := \mathcal{F}^{\mathbf{W}} \vee \mathcal{F}^D$  (augmented and completed to satisfy usual conditions). We work on the probability basis  $(\Omega, \mathcal{F}, (\mathcal{F}_t)_{t \geq t_0}, \mathbb{Q})$ .

We briefly summarize the dynamics of the fuels and the demand together with the calibration against observable market data.

Let  $\mathbf{W}_t = (W_t^{(1)}, \dots, W_t^{(n)}, W_t^D)$  be a vector of correlated Brownian motions and let  $\alpha_t^{(i)}, \mathbf{v}_t^{(i)} \in L^1[t_0, \infty) \forall i \in I$  and  $\alpha_t^D, \mathbf{v}_t^D \in \mathcal{L}^1[t_0, \infty)$  (integrability with respect to the Lebesgue measure).

Let  $s^{(i)}(t) : \mathbb{R}^+ \rightarrow \mathbb{R}$  ( $i \in I$ ) and  $s^D(t) : \mathbb{R}^+ \rightarrow \mathbb{R}$  be deterministic seasonality functions.

The dynamics of the correlated fuel process  $\mathbf{S}_t^F = (S_t^1, \dots, S_t^n)$  and demand process  $D_t$  are constructed using  $n+1$  time-dependent Ornstein-Uhlenbeck processes  $X_t^{(1)}, \dots, X_t^{(n)}, Y_t$  as follows:

$$\left\{ \begin{array}{ll} dX_t^{(i)} = -\alpha_t^{(i)} X_t^{(i)} dt + \mathbf{v}_t^{(i)} dW_t^{(i)} & \forall i \in I \\ dY_t = -\alpha_t^D Y_t dt + \mathbf{v}_t^D dW_t^D \\ S_t^{(i)} = \exp(s^{(i)}(t) + X_t^{(i)}) & \forall i \in I \\ D_t = s^D(t) + Y_t \\ dW_t^{(i)} dW_t^{(j)} = \rho_{ij} dt & \forall i, j \in I \\ dW_t^D dW_t^{(i)} = 0 & \forall i \in I. \end{array} \right. \quad (2.4)$$

Let  $\mathbf{S}_{t_0} = (s_{t_0}^1, \dots, s_{t_0}^n) \in (\mathbb{R}^+)^n$  and  $D_{t_0} = d_{t_0} \in \mathbb{R}$  be given. The solution of the above stochastic differential equations for  $X_t^{(1)}, \dots, X_t^{(n)}, Y_t$  and therefore the form of the corresponding fuel and demand processes  $\mathbf{S}_t^F, D_t$  is known to be ( $\forall i \in I$ )

$$S_t^{(i)} = \exp \left( s^{(i)}(t) + \exp \left( - \int_{t_0}^t \alpha_s^{(i)} ds \right) \ln(s_{t_0}^i) + \int_{t_0}^t \mathbf{v}_s^{(i)} \exp \left( - \int_s^t \alpha_u^{(i)} du \right) dW_s^{(i)} \right) \quad (2.5)$$

$$D_t = s^D(t) + \exp \left( - \int_{t_0}^t \alpha_s^D ds \right) d_{t_0} + \int_{t_0}^t \mathbf{v}_s^D \exp \left( - \int_s^t \alpha_u^D du \right) dW_s^D. \quad (2.6)$$

As  $\mathbf{S}_t$  is lognormally distributed (and  $D_t$  normally distributed respectively) the expected future spot price can be calculated by calculating mean and the variance of  $X_t^i$  for  $i = 1, \dots, n$ :

$$\begin{aligned} \mathbb{E}^{\mathbb{Q}} [S_t^{(i)} | \mathcal{F}_{t_0}] &= \exp \left( s^{(i)}(t) + \mathbb{E}^{\mathbb{Q}} [X_t^i | \mathcal{F}_{t_0}] + \frac{1}{2} \mathbb{V}^{\mathbb{Q}} [X_t^i | \mathcal{F}_{t_0}] \right) \\ &= \exp \left( s^{(i)}(t) + \exp \left( - \int_{t_0}^t \alpha_s^{(i)} ds \right) \ln(s_{t_0}^i) \right. \\ &\quad \left. + \frac{1}{2} \int_{t_0}^t \left( \mathbf{v}_s^{(i)} \right)^2 \exp \left( -2 \int_s^t \alpha_u^{(i)} du \right) ds \right) \end{aligned} \quad (2.7)$$

$$\mathbb{E}^{\mathbb{Q}} [D_t | \mathcal{F}_{t_0}] = s^D(t) + \mathbb{E}^{\mathbb{Q}} [Y_t | \mathcal{F}_{t_0}] = s^D(t) + \exp \left( - \int_{t_0}^t \alpha_s^D ds \right) d_{t_0} \quad (2.8)$$

As it is proposed in [Eydeland and Wolyniec, 2003] we use the freedom degree in seasonality to cope with the shape of the fuels' forward curves. Therefore, we get the no-arbitrage condition regarding forward contracts at the same time.

Let  $F_{t_0, t}^i$  denote the price of a forward with delivery in  $t$  as of  $t_0$  and underlying  $i \in I \cup \{P\}$  (we will use the index  $P$  for electricity as underlying). Using (2.7) it follows for the fuels with

forward price  $F_{t_0,t}^i \in \mathbb{R}^+$  for each  $i \in I$ :

$$s^{(i)}(t) = \ln(F_{t_0,t}^i) - \mathbb{E}^{\mathbb{Q}}[X_t^i | \mathcal{F}_{t_0}] - \frac{1}{2} \mathbb{V}^{\mathbb{Q}}[X_t^i | \mathcal{F}_{t_0}] \quad \forall i = 1, \dots, n. \quad (2.9)$$

The choice of demand seasonality could be measured using historical information. However, we decided to use the freedom degree in demand seasonality to price an hourly electricity forward curve free of arbitrage. Consequently, a risk-neutral measure for each fuel and power is derived. It leads to the principle which we will call *implied demand seasonality*.

**Definition 2.1 (Implied Demand Seasonality)** Let  $f_{bs}(\cdot, \cdot)$  be a market bid stack given by (2.1) and let the demand be of the form  $D_t = s^D(t) + Y_t$  where  $Y_t$  is given by (2.4). Given an electricity forward price  $F_{t_0,t}^P \in \mathbb{R}$  for a fix  $t > t_0$ , we assume  $s_t^{ID} \in \mathbb{R}$  to solve the equation

$$F_{t_0,t}^P = \mathbb{E}^{\mathbb{Q}}[f_{bs}(s_t^{ID} + Y_t, \mathbf{S}_t^F) | \mathcal{F}_{t_0}]. \quad (2.10)$$

We call  $s_t^{ID}$  to be the implied demand seasonality induced by the forward price  $F_{t_0,t}^P$ . For a set of different  $t$ ,  $s^D(t)$  is defined by  $s^D(t) := s_t^{ID}$ .

By performing the above calibration, we achieve to price the power forward curve without arbitrage. At the same time, the implied power forward dynamic becomes a martingale under  $\mathbb{Q}$  which is important for hedging purposes (cf. Chapter 3).

Time dependent volatility  $v_t^{(i)}, v_t^D \quad \forall i = 1, \dots, n$  and mean-reversion speed  $\alpha_t^{(i)}, \alpha_t^D$  are assumed to be left-continuous step functions being able to be expressed by

$$\begin{aligned} \forall T > 0 \exists t_0 < t_1 < \dots < t_{d(T)} = T \quad \forall i = (1), \dots, (n), D \quad \forall t \leq T : \\ \begin{cases} v_t^i = \sum_{j=1}^{d(T)} \mathbb{I}_{(t_{j-1}, t_j]}(t) v_{t_j}^i \\ \alpha_t^i = \sum_{j=1}^{d(T)} \mathbb{I}_{(t_{j-1}, t_j]}(t) \alpha_{t_j}^i \end{cases} \end{aligned} \quad (2.11)$$

with  $\mathbb{I}(\cdot)$  representing the indicator function. We define  $v^{i,j} := v_{t_j}^i$ ,  $\alpha^{i,j} := \alpha_{t_j}^i$  for  $i = (1), \dots, (n), D$ ,  $j = 1, \dots, d(T)$ . We will need (2.11) to calculate Vegas with the help of the likelihood ratio method in Chapter 6.

**Remark 2.3** In some parts of the thesis (i.e. Chapter 6) we will use indexes  $n+1$  and  $D$  synonymously (i.e.  $v^{(n+1)} = v^D$ ).

## 2.3 From Market Data to an Hourly Price Forward Curve

We use market data as of year-end 2015 and time series data of 2015 to built price forward curves for different commodities (including electricity). Furthermore, we need time series data

Product	As of Date	Purpose	Market Data Provider
Futures Prices (Coal, Gas, Power)	1/1/2015- 31/12/2015	Generation of hourly price forward curves, Estimation of mean-reversion parameters	Bloomberg Terminal <sup>3</sup>
Spot Prices (Coal, Gas, Power)	1/1/2013- 31/12/2015	Generation of monthly, weekly and hourly seasonalities for the hourly price forward curves	Bloomberg Terminal
Day ahead auction data (electricity)	16/11/2015- 15/12/2015	Estimation of bid stack parameters	EPEX Spot <sup>4</sup>
EEX Transparency Data	16/11/2015- 15/12/2015	Estimation of bid stack parameters (fundamental information, i.e. capacities, renewables)	EEX <sup>5</sup>

Table 2.3: Summary of market data used for the thesis.

to calculate historical estimators for the model parameters of (2.4) and of the structural model (2.2). We summarize this universe of market data including its source in Table 2.3.

Based on the market data in Table 2.3, we have derived daily price forward curves for gas as well as coal and an hourly price forward curve for electricity. We have implemented the algorithm proposed in [Burger et al., 2014]. The resulting daily curves are depicted in Figure 2.1. We used the following modification of the algorithm:

1. detect outlier in baseload time series: if the difference between the 180 days median and the baseload price is larger than 3 times the volatility in the time series, replace the baseload price by the median plus volatility (if baseload price higher than median) or median minus volatility (else). We denote the resulting time series by  $y_i$  for  $i = 1, \dots, L$  ( $L$ : amount of historical data; in our case: 01/01/2013-30/12/2015).
2. Normalize baseload data (without outliers) using the historical yearly average  $y_{AVR}^j$  (cal-

<sup>3</sup>Licensed data by University Duisburg-Essen, House of Energy Markets and Finance

<sup>4</sup>Licensed data by University Duisburg-Essen, House of Energy Markets and Finance; University vendor contract

<sup>5</sup>Licensed data by University Duisburg-Essen, House of Energy Markets and Finance; University vendor contract

endar year;  $j = 2013, 2014, 2015$ ). We denote the normalized data by

$$\bar{y}_i := \frac{y_i}{\frac{\kappa(i)}{y_{AVR}}} \text{ for } i = 1, \dots, L.$$

Here,  $\kappa : \{1, \dots, L\} \rightarrow \{2013, 2014, 2015\}$  is a mapping of each data point to its corresponding year in which the data point lies.

3. Allocate each day to a cluster. We defined 5 weekly clusters (Tuesday to Thursday modeled as one cluster), 6 monthly clusters (Jan-Feb, Mar-Apr, May-Jun, Jul-Aug, Sep-Oct, Nov-Dec) as well as summer and winter bridge days and holidays leading to 34 different clusters.
4. Let  $D_j$  denote all days within cluster  $j$ . We minimize

$$\sum_{i=1}^L \left( \bar{y}_i - \sum_{j=1}^{34} \beta_j \mathbb{I}_{D_j}(t_i) \right)^2.$$

We get weights  $\beta_j$  quoted as a multiplier of a yearly average price.

5. We calculate multipliative factors for hourly prices by taking the mean of normalized hourly prices (normalized by daily baseload price). The results are depicted in Figure 2.2.
6. Using a yearly futures price for 2016, we can calculate an hourly price forward curve for power being arbitrage free to a yearly quote.
7. Scaling was used to get an arbitrage-free pricing forward curve for monthly and quarterly futures contracts.

In order to calculate a daily gas forward curve, we have slightly adjusted the above algorithm. The reason is that prices for each month of 2016 were available as of year end 2015. Therefore, we used weekly running averages as a quotation basis of the weights instead of a yearly average. In order to calculate a daily coal forward curve, we assumed the monthly futures for 2016 to be constant for each day of the month (no weekly seasonality).

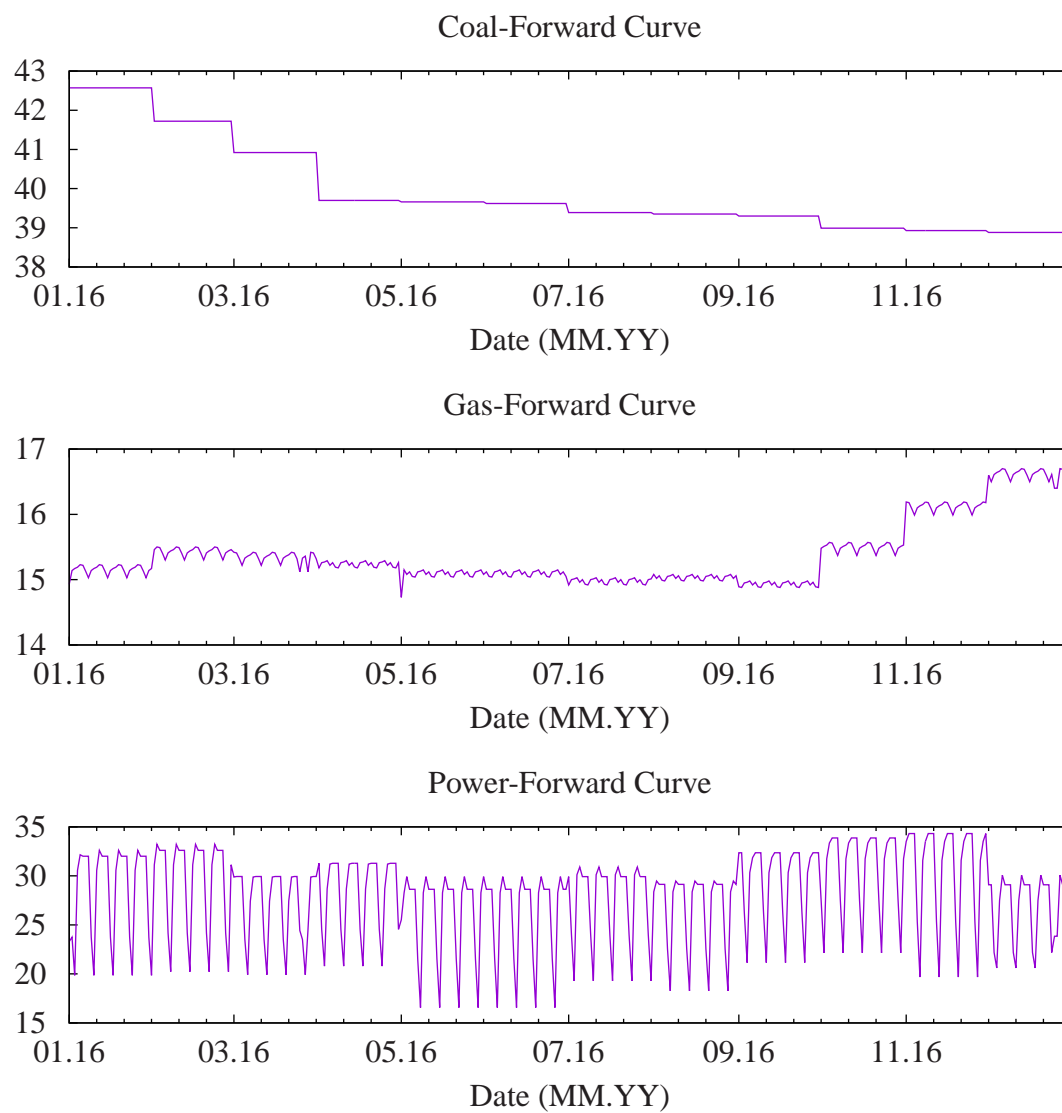


Figure 2.1: Daily price forward curves in EUR/MWh calculated as of year-end 2015.

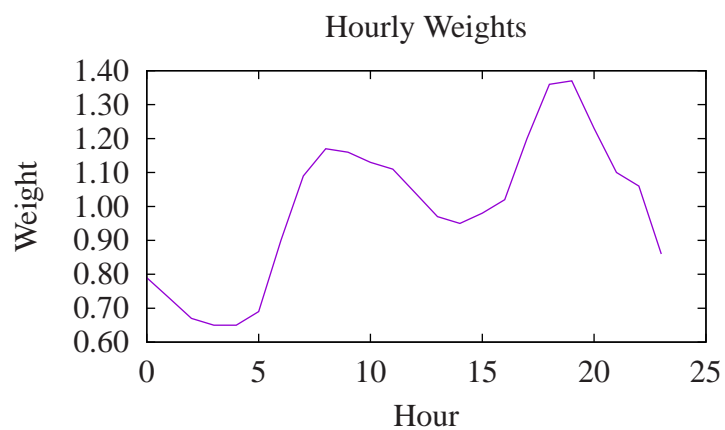


Figure 2.2: Hourly weights for electricity prices

## CHAPTER 3.

# The Idea - Hedging with Structural Models

Our aim is to derive a hedging strategy for a strip of arbitrary contingent claims (i.e. a virtual power plant) by using a structural electricity model as a reference model. In this Section we show how delta hedging can be applied.

## 3.1 Forward Dynamics

Hedging in commodity markets is - due to storage constraints - basically performed by trading in the futures/ forwards market. Thus, we deduce the forward dynamics from the spot dynamics as been defined in equation (2.4) in Chapter 2.2.

**Proposition 3.1 (Forward Dynamics)** *The forward dynamics for (2.4) with  $\mu_{t,T}^D := \mathbb{E}^{\mathbb{Q}}[D_T | \mathcal{F}_t]$  ( $T > t$ ) are*

$$dF_{t,T}^{(i)} = \exp\left(-\int_t^T \alpha_s^{(i)} ds\right) v_t^{(i)} F_{t,T}^{(i)} dW_t^{(i)} \quad d\mu_{t,T}^D = \exp\left(-\int_t^T \alpha_s^D ds\right) v_t^D dW_t^D. \quad (3.1)$$

**Proof.** We start with the fuels' forward dynamic. The conditioned forward price for  $t_0 < t < T$  using (2.8) is given by

$$\begin{aligned} F_{t,T}^{(i)} = \mathbb{E}^{\mathbb{Q}} \left[ S_T^{(i)} \middle| \mathcal{F}_t \right] &= \exp\left(s^{(i)}(T) + \exp\left(-\int_t^T \alpha_s^{(i)} ds\right) X_t^{(i)} \right. \\ &\quad \left. + \frac{1}{2} \int_t^T \left(v_s^{(i)}\right)^2 \exp\left(-2 \int_s^T \alpha_u^{(i)} du\right) ds \right). \end{aligned}$$

We define  $Z_t := \ln F_{t,T} := f(t, X_t^{(i)})$  and get by Itô's Lemma

$$\begin{aligned} d(\ln F_{t,T}) &= \frac{\partial f}{\partial t} dt + \frac{\partial f}{\partial X_t^{(i)}} dX_t^{(i)} + \frac{1}{2} \frac{\partial^2 f}{\partial (X_t^{(i)})^2} \left(v_t^{(i)}\right)^2 dt \\ &= \left[ \alpha_t^{(i)} \exp\left(-\int_t^T \alpha_s^{(i)} ds\right) X_t^{(i)} - \frac{1}{2} \left(v_t^{(i)}\right)^2 \exp\left(-2 \int_t^T \alpha_u^{(i)} du\right) \right] dt \\ &\quad + \exp\left(-\int_t^T \alpha_s^{(i)} ds\right) dX_t^{(i)} \end{aligned}$$

$$\stackrel{(2.4)}{=} -\frac{\left(v_t^{(i)}\right)^2}{2} \exp\left(-2 \int_t^T \alpha_u^{(i)} du\right) dt + v_t^{(i)} \exp\left(-\int_t^T \alpha_s^{(i)} ds\right) dW_t^{(i)}.$$

We apply Itô's Lemma again to  $\exp(Z_t) = F_{t,T}^{(i)}$  to obtain

$$\begin{aligned} dF_{t,T} &= \exp(Z_t) dZ_t + \frac{1}{2} \exp(Z_t) \left( v_t^{(i)} \exp\left(-\int_t^T \alpha_s^{(i)} ds\right) \right)^2 dt \\ &= F_{t,T}^{(i)} v_t^{(i)} \exp\left(-\int_t^T \alpha_s^{(i)} ds\right) dW_t^{(i)}. \end{aligned}$$

The conditioned expected demand in (2.8) is given by

$$\mu_{t,T}^D = \mathbb{E}^{\mathbb{Q}}[D_T | \mathcal{F}_t] = s^D(T) + \exp\left(-\int_t^T \alpha_s^D ds\right) Y_t.$$

Therefore, we get

$$\begin{aligned} d\mu_{t,T}^D &= \alpha_t^D \exp\left(-\int_t^T \alpha_s^D ds\right) Y_t dt + \exp\left(-\int_t^T \alpha_s^D ds\right) dY_t \\ &\stackrel{(2.4)}{=} \alpha_t^D \exp\left(-\int_t^T \alpha_s^D ds\right) Y_t dt + \exp\left(-\int_t^T \alpha_s^D ds\right) (-\alpha_t^D Y_t dt + v_t^D dW_t^D) \\ &= v_t^D \exp\left(-\int_t^T \alpha_s^D ds\right) dW_t^D. \end{aligned}$$

■

The dynamics in Proposition 3.1 can be generalized to

$$dF_{t,T}^{(i)} = a_i(F_{t,T}^{(i)}, t) dW_t^{(i)} \quad d\mu_{t,T}^D = a_D(t) dW_t^D \quad (3.2)$$

where  $a_i(F_{t,T}^{(i)}, t) : \mathbb{R}^+ \times \mathbb{R}^+ \rightarrow \mathbb{R}$ ,  $a_D(t) : \mathbb{R}^+ \rightarrow \mathbb{R}$  have to be integrable with respect to the Lebesgue measure (for  $t \geq t_0$  and  $i \in I$ ).

In order to derive a forward dynamic for electricity forwards, we use the bid stack function

$$S_t^P = f_{bs}(D_t, \mathbf{S}_t^F)$$

and assume

$$\text{A1 } \mathbb{E}^{\mathbb{Q}}[|f_{bs}(D_T, \mathbf{S}_T^F)|] < \infty \text{ (integrability),}$$

$$\text{A2 } \mathbb{E}^{\mathbb{Q}}[f_{bs}(D_T, \mathbf{S}_T^F) | \mathcal{F}_t] = \mathbb{E}^{\mathbb{Q}}[f_{bs}(D_T, \mathbf{S}_T^F) | (D_t, S_t^F)] \text{ (Markovian property).}$$

Consequently, the power forward price formula (which exist because of A1) can be expressed as a function  $F_{bs}$  depending on fuel forward prices and future expected demand:

$$F_{t,T}^P = F_{bs}(t, F_{t,T}^{(1)}, \dots, F_{t,T}^{(n)}, \mu_{t,T}^D),$$



A3  $F_{bs} \in C^{1,2}$  (in order to apply Itô's Lemma).

**Remark 3.1** *The structural electricity model defined in equation (2.3) fulfills conditions A1 to A3 for demand and fuels dynamics given by equation (2.4). The closed form formula for  $F_{bs}$  is given in Appendix A.2.*

We apply the Itô-Lemma to  $F_{bs}$  in order to derive the forward dynamics of a structural model (recall that  $F_{t,T}^{(i)}$  and  $\mu_{t,T}^D$  are uncorrelated):

$$\begin{aligned} dF_{t,T}^P &= \left[ \frac{\partial F_{bs}}{\partial t} + \frac{1}{2} \sum_{i,j \in I} \frac{\partial^2 F_{bs}}{\partial F_{t,T}^{(i)} \partial F_{t,T}^{(j)}} a_i(F_{t,T}^{(i)}, t) a_j(F_{t,T}^{(j)}, t) \rho_{ij} + \frac{1}{2} a_D^2(t) \frac{\partial^2 F_{bs}}{\partial (\mu_{t,T}^D)^2} \right] dt \\ &\quad + \sum_{i \in I} \frac{\partial F_{bs}}{\partial F_{t,T}^{(i)}} dF_{t,T}^{(i)} + \frac{\partial F_{bs}}{\partial \mu_{t,T}^D} d\mu_{t,T}^D \\ &=: \underbrace{a_P(F_{t,T}^{(1)}, \dots, F_{t,T}^{(n)}, t)}_{=0} dt + \sum_{i \in I} \frac{\partial F_{bs}}{\partial F_{t,T}^{(i)}} a_i(F_{t,T}^{(i)}, t) dW_t^{(i)} + \frac{\partial F_{bs}}{\partial \mu_{t,T}^D} a_D(t) dW_t^D. \end{aligned} \quad (3.3)$$

As  $F_{t,T}^P = \mathbb{E}^{\mathbb{Q}}[S_T^P | \mathcal{F}_t]$ , we have  $a_P(F_{t,T}^{(1)}, \dots, F_{t,T}^{(n)}, t) = 0$ , i.e. the electricity forward is a martingale under  $\mathbb{Q}$ .

## 3.2 Link to Cointegration

The dynamic in (3.3) is close to the principle of cointegration. In order to see that, we follow the idea of [de Jong and Schneider, 2009]. We start by giving the definition of cointegration (cf. [Hamilton, 1994]).

**Definition 3.1 (Integration of Order 0)** *A time series is integrated of order 0 if it admits a moving average representation with*

$$\sum_{k=0}^{\infty} |b_k|^2 < \infty,$$

where  $b = (b_1, b_2, \dots)$  is the possibly infinite vector of moving average weights (coefficients or parameters).

**Definition 3.2 (Covariance-Stationary)** *A time series  $X_t$  is covariance-stationary if and only if*

$$\begin{aligned} \mathbb{E}(X_t) &= \mu \quad \forall t > 0 \\ \mathbb{E}(X_t - \mu)(X_{t-j} - \mu) &= \gamma_j \quad \forall t > 0, j > 0. \end{aligned}$$

**Remark 3.2** *It can be shown that an integrable time series of order 0 is covariance-stationary (cf. [Hamilton, 1994], Chapter 3.3).*

**Definition 3.3 (Lag Operator)** *The lag operator is used to transfer a time series  $X_t$  for a fixed  $t \in \mathbb{N}$  to its prior value at  $X_{t-1}$ :  $LX_t \equiv X_{t-1}$ .*

**Definition 3.4 (Integration of order  $d$ )** *A time series  $X_t$  is called integrable of order  $d$  if and only if  $(1 - L)^d X_t$  is covariance-stationary.*

**Definition 3.5 (Cointegration)** *Let  $X_t^{(1)}, \dots, X_t^{(k)}$  be a series of time series variables, all of them being integrable of order 1. If a linear combination  $\sum_{i=1}^k \alpha_i X_t^{(i)}$  is integrated of order 0, then  $X_t^{(1)}, \dots, X_t^{(k)}$  are called cointegrated.*

In [de Jong and Schneider, 2009], cointegration between the difference of the front month futures price  $M_t^i$  and spot price  $S_t^i$  (both assumed to be integrable of order 1) of a set of commodities  $J := \{1, \dots, p\}$  is analyzed for each underlying  $i \in J$ . The set of commodities - where cointegration with commodity  $i$  is suspected - is denoted by  $J_i \subset J$ . They start with a mean-reversion model where the mean-reversion level is given by the front month futures price:

$$\begin{aligned} \ln(S_t^i) &= \ln(S_{t-1}^i) + \alpha_i(\ln(M_{t-1}^i) - \ln(S_{t-1}^i)) + u_{i,t} \\ \iff \ln(S_t^i) - \ln(M_{t-1}^i) &= (1 - \alpha_i)(\ln(S_{t-1}^i) - \ln(M_{t-1}^i)) + u_{i,t} \end{aligned}$$

where  $\alpha_i$  is the mean-reversion speed and  $u_{i,t}$  are normally distributed and correlated to other commodities. Using that idea they enlarge the model to include cointegration to other commodities. They end up with

$$\begin{aligned} \ln(S_t^i) - \ln(M_{t-1}^i) &= (1 - \alpha_i)(\ln(S_{t-1}^i) - \ln(M_{t-1}^i)) \\ &+ \sum_{j \in J_i} (1 - \alpha_{ij})(\ln(S_{t-1}^j) - \ln(M_{t-1}^j)) + u_{i,t}, \end{aligned}$$

where  $\alpha_{ij} \in \mathbb{R}$  are similarly interpreted as mean-reversion speeds. They used according time series data to derive the parameters  $\alpha_{ij}, \alpha_i$  and analyzed according statistical significance.

The interpretation of the above model is as follows: if the spot of underlying  $j$  largely deviates from its front month future, then this is likely to be transferred to underlying  $i$  as well (at least if  $1 - \alpha_{ij}$  is large). Within an empirical investigation they found that cointegration between power and gas is rather small. The authors argue that cointegration for both underlyings is more prominent in forward prices than in spot prices.

A structural electricity model naturally implies some kind of cointegration. For small  $\Delta t > 0$ , equation (3.3) yields:

$$F_{t+\Delta t, T}^P - F_{t, T}^P \approx \sum_{i \in I} \frac{\partial F_{bs}}{\partial F_{t, T}^{(i)}} (F_{t+\Delta t, T}^{(i)} - F_{t, T}^{(i)}) + \frac{\partial F_{bs}}{\partial \mu_{t, T}^D} (\mu_{t+\Delta t, T}^D - \mu_{t, T}^D).$$

For infinitesimal small time steps, we may interpret a structural electricity model to have cointegrated forwards<sup>1</sup> (changes in power forwards and fuels' forwards are approximately of linear dependence). The cointegration is directly implied by  $\frac{\partial F_{bs}}{\partial F_{t, T}^{(i)}}$  and therefore implicitly by the merit order of the energy market.

### 3.3 Replication Portfolio

We perform similar calculations for an arbitrary, discounted contingent claim  $\Psi : \mathbb{R} \times (\mathbb{R}^+)^2 \rightarrow \mathbb{R}$

$$e^{-r(T-t)} \Psi(S_T^P, S_T^F) = e^{-r(T-t)} \Psi(f_{bs}(D_T, S_T^F), S_T^F).$$

Again, we assume

B1  $\mathbb{E}^{\mathbb{Q}} [|\Psi(S_T^P, S_T^F)|] < \infty$  (*integrability*),

B2  $\mathbb{E}^{\mathbb{Q}} [\Psi(S_T^P, S_T^F) | \mathcal{F}_t] = \mathbb{E}^{\mathbb{Q}} [\Psi(S_T^P, S_T^F) | (D_t, S_t^F)]$  (*Markovian property*).

Consequently, the discounted risk-neutral expectation of  $\Psi$  (which exist because of B1) can be expressed as a function  $PV_{t, T}^{\Psi}$  depending on fuel forward prices and future expected demand:

$$PV_{t, T}^{\Psi} = F_{\Psi}(T-t, F_{t, T}^{(1)}, \dots, F_{t, T}^{(n)}, \mu_{t, T}^D)$$

B3  $F_{\Psi} \in C^{1,2}$  (in order to apply Itô's Lemma).

We apply the Itô-Lemma together with the product rule and equation (3.3) to yield for the discounted pricing formula

$$\begin{aligned} d(e^{-r(T-t)} PV_{t, T}^{\Psi}) = & e^{-r(T-t)} \left[ \frac{\partial F_{\Psi}}{\partial t} + \frac{1}{2} \sum_{i, j \in I} \frac{\partial^2 F_{\Psi}}{\partial F_{t, T}^{(i)} \partial F_{t, T}^{(j)}} a_i(F_{t, T}^{(i)}, t) a_j(F_{t, T}^{(j)}, t) \rho_{ij} \right. \\ & \left. + \frac{1}{2} a_D^2(t) \frac{\partial^2 F_{\Psi}}{\partial (\mu_{t, T}^D)^2} + r PV_{t, T}^{\Psi} \right] dt \\ & + e^{-r(T-t)} \sum_{i \in I} \frac{\partial F_{\Psi}}{\partial F_{t, T}^{(i)}} dF_{t, T}^{(i)} + e^{-r(T-t)} \frac{\partial F_{\Psi}}{\partial \mu_{t, T}^D} d\mu_{t, T}^D \end{aligned} \quad (3.4)$$

$$\stackrel{(3.3)}{=} e^{-r(T-t)} \sum_{i \in I} \left[ \frac{\partial F_{\Psi}}{\partial F_{t, T}^{(i)}} - \frac{\partial F_{\Psi}}{\partial \mu_{t, T}^D} \left( \frac{\partial F_{bs}}{\partial \mu_{t, T}^D} \right)^{-1} \frac{\partial F_{bs}}{\partial F_{t, T}^{(i)}} \right] dF_{t, T}^{(i)} \quad (3.5)$$

<sup>1</sup>We can only state *some kind* of cointegration as the relation ship between the forwards is obviously not linear.

$$+ e^{-r(T-t)} \frac{\partial F_{\Psi}}{\partial \mu_{t,T}^D} \left( \frac{\partial F_{bs}}{\partial \mu_{t,T}^D} \right)^{-1} dF_{t,T}^P.$$

Again, because  $PV_{t,T}^{\Psi} = \mathbb{E}^{\mathbb{Q}} \left[ e^{-r(T-t)} \Psi(S_T^P, \mathbf{S}_T^F) \middle| \mathcal{F}_t \right]$ , we know the discounted claim is a martingale under  $\mathbb{Q}$ .

In order to derive a replication strategy, we need to find a self-financing process

$$\phi := (\phi^{(0)}, \phi^{(1)}, \dots, \phi^{(n)}, \phi^P).$$

Let  $N_{t_0,t} := \exp(r(t-t_0))$  be a money market account. We define  $V_t := \sum_{i \in I} \phi_t^{(i)} F_{t,T}^i + \phi_t^{(0)} N_{t_0,t} + \phi_t^P F_{t,T}^P$ , ( $t \leq T$ ) with

$$dV_t = \sum_{i \in I} \phi_t^{(i)} dF_{t,T}^i + \phi_t^{(0)} dN_{t_0,t} + \phi_t^P dF_{t,T}^P.$$

Then, we get the following mapping for our hedging portfolio:

$$\left. \begin{aligned} \phi_t^{(i)} &= e^{-r(T-t)} \left[ \frac{\partial F_{\Psi}}{\partial F_{t,T}^{(i)}} - \frac{\partial F_{\Psi}}{\partial \mu_{t,T}^D} \left( \frac{\partial F_{bs}}{\partial \mu_{t,T}^D} \right)^{-1} \frac{\partial F_{bs}}{\partial F_{t,T}^{(i)}} \right], \text{ for } i \in I \\ \phi_t^P &= e^{-r(T-t)} \left[ \frac{\partial F_{\Psi}}{\partial \mu_{t,T}^D} \left( \frac{\partial F_{bs}}{\partial \mu_{t,T}^D} \right)^{-1} \right]. \end{aligned} \right\} \quad (3.6)$$

In order to ensure the self-financing character of the portfolio<sup>2</sup>, we choose  $\phi^{(0)}$  to be as described in [Fries, 2007] (Lemma 72):

$$\phi_t^{(0)} := \frac{V_{t_0}}{N_{t_0,t_0}} + \sum_{i \in I} \int_{t_0}^t \phi_s^{(i)} d \left( \frac{F_{s,T}^{(i)}}{N_{t_0,s}} \right) + \int_{t_0}^t \phi_s^P d \left( \frac{F_{s,T}^P}{N_{t_0,s}} \right) - \sum_{i \in I} \phi_t^{(i)} \frac{F_{t,T}^{(i)}}{N_{t_0,t}} - \phi_t^P \frac{F_{t,T}^P}{N_{t_0,t}}.$$

**Example 3.1 (Forwards)** For example, if the claim  $\Psi$  is simply an electricity forward, we would get from (3.6)

$$\phi_t^{(i)} \equiv 0, \text{ for } i \in I \quad \phi_t^P = e^{-r(T-t)}$$

resulting in a back-to-back hedge of the forward (due to  $F_{\Psi} \equiv F_{bs}$ ).

An interesting implication can be deduced when analyzing the replication strategy at  $t_0$ . Recall that the calibration of the demand process  $D_t$  is such that the power forward curve is priced free of arbitrage (according to Definition 2.1 of *implied demand seasonality*). Technically, we define an implicit function  $g(t_0, F_{t_0,T}^{(1)}, \dots, F_{t_0,T}^{(n)}, F_{t_0,T}^P)$  by

$$F_{bs}(t_0, F_{t_0,T}^{(1)}, \dots, F_{t_0,T}^{(n)}, g(t_0, F_{t_0,T}^{(1)}, \dots, F_{t_0,T}^{(n)}, F_{t_0,T}^P)) - F_{t_0,T}^P = 0 \quad (3.7)$$

<sup>2</sup>Because there is no restriction on  $\phi^{(0)}$  besides adapted to  $\mathcal{F}_t$ , we can always find a  $\phi^{(0)}$  such that our process  $\phi$  is self-financing. For further information we refer to [Fries, 2007].

and set  $\mu_{t_0}^D := g(t_0, F_{t_0,T}^{(1)}, \dots, F_{t_0,T}^{(n)}, F_{t_0,T}^P)$ .

We use the implicit form of  $\mu_{t_0,T}^D$  in (3.7), the inverse function theorem (for the derivative in direction  $F_{t_0,T}^P$ ) and the implicit function theorem (for the derivative in direction  $F_{t,T}^{(i)}$ ) to get

$$\frac{\partial}{\partial F_{t_0,T}^P} \left( F_{\Psi}(F_{t_0,T}^{(1)}, \dots, F_{t_0,T}^{(n)}, \mu_{t_0,T}^D) \right) = \frac{\partial F_{\Psi}}{\partial \mu_{t_0,T}^D} \frac{\partial \mu_{t_0,T}^D}{\partial F_{t_0,T}^P} = \frac{\partial F_{\Psi}}{\partial \mu_{t_0,T}^D} \left( \frac{\partial F_{bs}}{\partial \mu_{t_0,T}^D} \right)^{-1}$$

and

$$\begin{aligned} \frac{\partial}{\partial F_{t_0,T}^{(i)}} \left( F_{\Psi}(F_{t_0,T}^{(1)}, \dots, F_{t_0,T}^{(n)}, \mu_{t_0,T}^D) \right) &= \frac{\partial F_{\Psi}}{\partial F_{t_0,T}^{(i)}} + \frac{\partial F_{\Psi}}{\partial \mu_{t_0,T}^D} \frac{\partial \mu_{t_0,T}^D}{\partial F_{t_0,T}^{(i)}} \\ &= \frac{\partial F_{\Psi}}{\partial F_{t_0,T}^{(i)}} - \frac{\partial F_{\Psi}}{\partial \mu_{t_0,T}^D} \left( \frac{\partial F_{bs}}{\partial \mu_{t_0,T}^D} \right)^{-1} \frac{\partial F_{bs}}{\partial F_{t_0,T}^{(i)}}. \end{aligned}$$

Therefore, we altogether get

$$\left. \begin{aligned} \phi_{t_0}^{(i)} &= e^{-r(T-t_0)} \frac{\partial}{\partial F_{t_0,T}^{(i)}} \left( F_{\Psi}(F_{t_0,T}^{(1)}, \dots, F_{t_0,T}^{(n)}, \mu_{t_0,T}^D) \right), \text{ for } i \in I \\ \phi_{t_0}^P &= e^{-r(T-t_0)} \frac{\partial}{\partial F_{t_0,T}^P} \left( F_{\Psi}(F_{t_0,T}^{(1)}, \dots, F_{t_0,T}^{(n)}, \mu_{t_0,T}^D) \right) \end{aligned} \right\} \quad (3.8)$$

which is exactly delta hedging.

**Remark 3.3 (Assumptions on  $\mu_{t_0,T}^D$ )** In order to derive the delta hedging strategy, we need to verify that  $\frac{\partial \mu_{t_0,T}^D}{\partial F_{t_0,T}^P}$  exists. Due to the relationship

$$\left( \frac{\partial F_{bs}}{\partial \mu_{t_0,T}^D} \right)^{-1} = \frac{\partial \mu_{t_0,T}^D}{\partial F_{t_0,T}^P}$$

given by the inverse function theorem, we can employ Assumption A3 on  $F_{bs}$  and differentiate  $\mu_{t_0,T}^D$  in direction of  $F_{t,T}^P$  - at least for  $\frac{\partial F_{bs}}{\partial \mu_{t_0,T}^D} \neq 0$ . This is ensured by Lemma A.1 which proves strong monotony of  $F_{bs}$  in expected demand. Due to the implicit function theorem and the condition  $\frac{\partial F_{bs}}{\partial \mu_{t_0,T}^D} \neq 0$ , we can also build the derivative of  $\mu_{t_0,T}^D$  in direction of  $F_{t,T}^{(i)}$ .

We summarize the results of this Chapter in the next

**Proposition 3.2 (Delta Hedging for Structural Models)** Let  $T > t_0$  be fix. Let the fuels' processes  $S_t^{(1)}, \dots, S_t^{(n)}$  ( $n \in \mathbb{N}$ ) and electricity (residual) demand process  $D_t$  be such that the corresponding hourly forward prices  $F_{t,T}^{(1)}, \dots, F_{t,T}^{(n)}$  and the expected demand  $\mu_{t,T}$  follow the dynamics described in equation (3.2). Accordingly, we denote the power forward price by  $F_{t,T}^P$ .

We define the electricity spot price  $S_t^P$  by a bid stack function  $f_{bs} : \mathbb{R} \times (\mathbb{R}^+)^n \rightarrow \mathbb{R}$  satisfying assumptions A1 to A3 and set  $S_t^P := f_{bs}(D_t, \mathbf{S}_t^F)$ . Similarly, we assume a contingent claim  $\Psi(\mathbf{S}_t^F, S_t^P) : (\mathbb{R}^+)^n \times \mathbb{R} \rightarrow \mathbb{R}$  maturing in  $T$  to satisfy assumptions B1 to B3.

The delta hedging strategy given by (3.8) then delivers a replicating portfolio of the claim  $\Psi$  (completeness). Furthermore, the present value of the claim  $\Psi$  is a martingale under  $\mathbb{Q}$ .

**Proof.** The proposition follows from the calculations performed above in this Chapter. Completeness follows from (3.5): each risk factor can be expressed as a hedging instrument (fuel forwards and power forwards respectively). ■

**Remark 3.4 (Proposition 3.2)** *As it stands, Proposition 3.2 only seems to be of theoretical importance: we get a replication strategy under the unrealistic assumption that fuels and electricity forwards with a delivery period of one time point (day/hour) are traded in the market. However, the Proposition will be helpful in Chapter 3.5 where we propose how to come from deltas of hourly forward prices to traded futures prices.*

## 3.4 Practical Interpretations

### 3.4.1 Liquidity

Throughout the thesis, we assume a market participant assesses a market for a certain derivative to be either liquid or illiquid (nothing in between). We will assume that a market participant will only buy a derivative in a liquid market. Market volume (i.e. Figure 3.1) and bid-ask-spreads respectively might be used as an appropriate measure to assess liquidity.

Consequently, a market participant avoids to trade a certain derivative in the market in case he assesses the according market to be illiquid (i.e. too high bid-ask-spreads). Instead of trading in an illiquid market, he or she may prefer to hedge electricity by highly correlated assets in a liquid market - so called cross-commodity hedging. Cross-commodity hedging has found a lot of interest from practitioners and academics during the few decades. Popular approaches are minimum variance hedges or utility-based approaches (i.e. [Cotter and Hanly, 2015, Černý, 2009]). There is also a strand of research on how to isolate the non-hedgeable risk from the hedgeable one. The non-hedgeable risk in an incomplete market can be separated by orthogonalizing risk factors appropriately (cf. [Ankirchner et al., 2013]). Afterward, algorithms to quantify the non-hedgeable variance can be derived.

Translated to our model setup, a market participant may use the implied power forward dynamics in (3.5) only for replication purposes if the power futures market is liquid<sup>3</sup>. Otherwise, he or

<sup>3</sup>In this context, our definition of liquidity also allows to assess a futures market to be liquid up to a certain maturity (liquidity is defined for each contract separately).

she may start from (3.4) where the demand dynamic is not replaced by the power forward dynamic. Consequently, changes in power prices are now hedged by building up positions in fuel forward contracts: if it is likely for coal to be marginal in that hour, an outright of coal futures might be built up. Even several fuels might be marginal at the same time. [Aïd et al., 2013] investigates hedging with the marginal fuel for a different structural model. However, it has to be kept in mind that demand is a non-hedgeable risk factor so that the model is incomplete as a whole. Without incorporating additional instruments to hedge demand uncertainty (i.e. weather or wind derivatives), a lower threshold for the non-hedgeable variance is given by the variance of the demand (demand is already orthogonal to other risk factors in our model (2.4) due to zero correlation). The inclusion of weather or wind derivatives to reduce the non-hedgeable (demand) variance is beyond the scope of this thesis.

In order to distinguish the case of power forwards liquidity and illiquidity, we define the liquidity threshold date.

**Definition 3.6 (Power Liquidity Threshold Date (PLTD))** *Let futures data be given by Definition 1.1 and hourly forwards data be given by Definition 1.2 respectively. Then, we call*

$$t_{PLTD} := \max_{t \in \mathcal{T}} \left\{ \exists i \in \{1, \dots, n_P\} \text{ with } t \in [t_i^a, t_i^b) : F^P(t_i^a, t_i^b) \text{ is a liquid futures contract.} \right\}$$

*the power liquidity threshold date.*

**Example 3.2 (Power Liquidity Threshold Date for the German Market)** *The trading volume data at European Energy Exchange (EEX; cf. Figure 3.1) may be an appropriate measure to choose  $t_{PLTD}$ . Depending on risk aversion even futures with a relatively low trading volume (i.e. yearly futures with delivery in three years) are bought by market participants.*

In the following, we will refer to a high  $t_{PLTD}$  whenever we intend to analyze a liquid power futures market. We will refer to a low  $t_{PLTD}$  whenever we intend to analyze an illiquid power futures market.

A simple analysis of hedging a power forward contract using fuel forward contracts can be found in Section 7.2.

### 3.4.2 Volatility

In order that delta hedging with an electricity structural spot model earns the fair value during the life time of the contract, an appropriate volatility has to be used and hourly forward contracts need to be traded. However, the choice of volatility is complex in this context.

In this thesis, we propose to calibrate fuels and demand model volatility of Section 2.2 against historical spot data and mean-reversion speed against historical forwards data. By doing that,



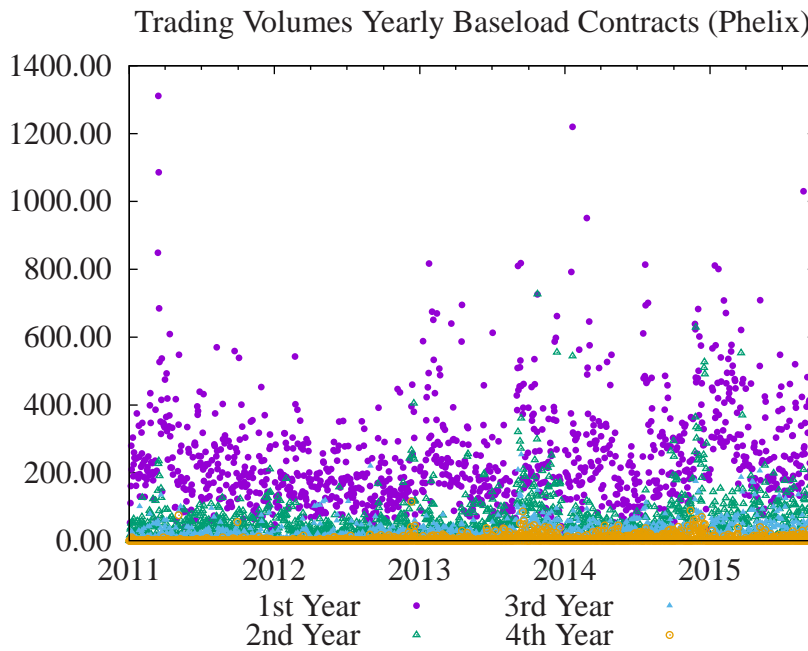


Figure 3.1: Trading Volumes of a 1Y Baseload contract Phelix at Bloomberg measured in total number of shares traded on a security on the current day.

fuels' and demand dynamics reflect both, the dynamics of the hedging instruments as well as the spot dynamics for the contingent claim.

The model volatility of the demand turns out to be crucial. Because we imply the expected demand from an hourly electricity price forward curve (Definition 2.1), the risk factor demand is directly linked to electricity instead of demand. Consequently, we calibrate the demand mean-reversion speed and volatility against electricity data. For details on the estimation procedure, we refer to Chapter 4.

**Remark 3.5 (Implied Volatilities)** *For practitioners it may be possible to imply volatilities from observable option prices. However, because options in Western European Markets are mainly traded OTC (cf. [Fiorenzani et al., 2012]), public option prices can rarely be observed. This is the reason why we prefer to work with historical estimators instead. Even though, practitioners might have enough information based on their OTC activity.*

### 3.5 From Forward Deltas to Futures Deltas

So far, hedging is performed by hypothetically trading hourly forward contracts. However, those contracts can typically not be traded in practice. Therefore, it has to be analyzed on how to come from hourly deltas to deltas of i.e. exchange traded instruments (futures).



Due to our choice of seasonality function  $s^{(i)}(t)$  ( $i = c, g, P$ ), a bump of a forward price at  $t > t_0$  will only affect the seasonality  $s^{(i)}(t)$  at  $t$  (we refer to (2.9) and Definition 2.1). Therefore - depending on the contingent claim -, we can intuitively calculate all hourly deltas (*delta curve*) regarding power, coal or gas with altogether two valuations: i. e. one valuation with a positive bump and one with a negative bump of the whole forward curve. Altogether this leads to six valuations.

In fact, path-independent spread options fulfill the necessary restriction: a bump in  $t$  will only affect an option maturing in  $t$ . Therefore, we can at first calculate the delta curve of each hourly forward curve (coal, gas, power). Afterward, we perform an optimization procedure on how to best cover the delta curve with futures contracts in the market.

We formulate this idea in a Proposition. In order to state it, we need the following Condition.

**Condition 3.1** *Let the notation of futures and forwards data be given by Definition 1.1 and 1.2. We assume the following equivalence between a futures contract  $F_{t_0}^i(t_l^a, t_l^b)$  ( $l = 1, \dots, n_i$ ) and forward prices  $F_{t_0, t}^i$  ( $i \in I \cup \{P\}$ ,  $t \in \mathcal{T}$ ):*

$$F_{t_0}^i(t_l^a, t_l^b) + \delta \Leftrightarrow F_{t_0, t_j}^i + \delta \quad \forall j = 1, \dots, m : t_l^a \leq t_j \leq t_l^b, \delta \in \mathbb{R}$$

Whereas " $\Leftarrow$ " is naturally given, " $\Rightarrow$ " has to be assumed. The reason is that i. e. a bump in a power forward contract can also be caused by new information about plant outages. However, we believe the vast majority of cases are caused by changes in the fuels or power.

**Proposition 3.3 (From Forward Deltas to Futures Deltas)** *We assume a structural electricity model fulfilling assumptions A1 to A3 (Section 3) together with fuels and demand processes from Section 2.2 to be given. A contingent claim is given by*

$$\Psi(S_t^P, S_t^F) : \mathbb{R} \times (\mathbb{R}^+)^n \rightarrow \mathbb{R}.$$

Furthermore, we assume futures data in Definition 1.1 and forwards data in Definition 1.2 to be given together with Condition 3.1.

We denote the maturity-dependent delta curves of  $\Psi$  for  $i \in I \cup \{P\}$  by  $\mathbf{D}^i \in \mathbb{R}^m$  and by  $\mathbf{h}^i \in \mathbb{R}^{n_i}$  a vector storing at  $h_j^i$  the total volume of  $F_{t_0}^i(t_j^a, t_j^b)$ .

The optimal futures portfolio  $(\bar{\mathbf{h}}^c, \bar{\mathbf{h}}^g, \bar{\mathbf{h}}^P)$  to hedge the claim

$$\sum_{t \in \mathcal{T}} \Psi(S_t^P, S_t^F)$$

as of  $t_0$  ( $r \in \mathbb{R}$ ) under a norm  $\|\cdot\| : \mathbb{R}^m \rightarrow \mathbb{R}$  is then given by solving the following set of linear optimization problems

$$\bar{\mathbf{h}}^i = \min_{\mathbf{h} \in \mathbb{R}^{n_i}} \|\mathbf{D}^i - \mathbf{V}^i \mathbf{h}\| \quad \text{for } i \in I \cup P.$$

Here,  $\mathbf{V}^i \in \mathbb{R}^{m \times n_i}$  and  $V_{kl}$  contains the volume of commodity  $i$  that is delivered in  $t_k$  by  $F_{t_0}^i(t_l^a, t_l^b)$   $k = 1, \dots, m$  and  $l = 1, \dots, n_i$ .

**Proof.** We define

$$PV_{\mathcal{T}}^{\Psi} := \sum_{t \in \mathcal{T}} e^{-r(t-t_0)} \mathbb{E}^{\mathbb{Q}} [\Psi(S_t^P, \mathbf{S}_t^F) | \mathcal{F}_{t_0}]$$

and have to show that

$$\frac{\partial}{\partial F_{t_0}^i(t_l^a, t_l^b)} PV_{\mathcal{T}}^{\Psi} = \sum_{t_k: t_l^a \leq t_k \leq t_l^b} \frac{\partial}{\partial F_{t_0, t_k}^i} PV_{\mathcal{T}}^{\Psi}, \quad \forall i \in I \cup \{P\} \quad l = 1, \dots, n_i.$$

If this condition holds we can reconstruct each  $\frac{\partial}{\partial F_{t_0}^i(t_l^a, t_l^b)} PV_{\mathcal{T}}^{\Psi}$  by using  $\frac{\partial}{\partial F_{t_0, t_k}^i} PV_{\mathcal{T}}^{\Psi}$  which is given by  $\mathbf{D}^c$ ,  $\mathbf{D}^g$ ,  $\mathbf{D}^P$  as a condition in the Proposition. This means that we can first calculate  $\frac{\partial}{\partial F_{t_0, t_k}^i} PV_{\mathcal{T}}^{\Psi}$  and afterwards decide on how to allocate our hedging products to capture the delta curve best. This is what the Proposition mainly states.

We denote  $\mathbf{F}_{t_0, t} := (F_{t_0, t}^1, \dots, F_{t_0, t}^n)$ . We have

$$\begin{aligned} & \frac{\partial}{\partial F_{t_0}^i(t_l^a, t_l^b)} PV_{\mathcal{T}}^{\Psi} \\ &= \sum_{t \in \mathcal{T}} e^{-r(t-t_0)} \frac{\partial}{\partial F_{t_0}^i(t_l^a, t_l^b)} \mathbb{E}^{\mathbb{Q}} [\Psi(S_t^P, \mathbf{S}_t^F) | \mathcal{F}_{t_0}] \\ &\stackrel{(*)}{=} \sum_{t \in \mathcal{T}} e^{-r(t-t_0)} \frac{\partial}{\partial F_{t_0}^i(t_l^a, t_l^b)} \mathbb{E}^{\mathbb{Q}} [\Psi(S_t^P(\mathbf{F}_{t_0, t}, F_{t_0, t}^P), \mathbf{S}_t^F(\mathbf{F}_{t_0, t})) | \mathcal{F}_{t_0}] \\ &= \sum_{t_k: t_l^a \leq t_k \leq t_l^b} e^{-r(t_k-t_0)} \frac{\partial}{\partial F_{t_0}^i(t_l^a, t_l^b)} \mathbb{E}^{\mathbb{Q}} [\Psi(S_{t_k}^P(\mathbf{F}_{t_0, t_k}, F_{t_0, t_k}^P), \mathbf{S}_{t_k}^F(\mathbf{F}_{t_0, t_k})) | \mathcal{F}_{t_0}] \\ &\stackrel{(**)}{=} \sum_{t_k: t_l^a \leq t_k \leq t_l^b} e^{-r(t_k-t_0)} \frac{\partial}{\partial F_{t_0, t_k}^i} \mathbb{E}^{\mathbb{Q}} [\Psi(S_{t_k}^P(\mathbf{F}_{t_0, t_k}, F_{t_0, t_k}^P), \mathbf{S}_{t_k}^F(\mathbf{F}_{t_0, t_k})) | \mathcal{F}_{t_0}] \\ &= \sum_{t_k: t_l^a \leq t_k \leq t_l^b} \frac{\partial}{\partial F_{t_0, t_k}^i} PV_{\mathcal{T}}^{\Psi}. \end{aligned}$$

Equality (\*) holds because of Condition 3.1 and the no-arbitrage conditions (Definition 2.1 and (2.9); underlyings' seasonality at time  $t_k$  merely depends on forwards maturing in  $t_k$ ).

(\*\*) holds because the derivative can be written as the limit of a difference quotient. Afterwards, Condition 3.1 can be applied:

$$\begin{aligned} & \frac{\partial}{\partial F_{t_0}^g(t_l^a, t_l^b)} \mathbb{E}^{\mathbb{Q}} [(S_{t_k}^P(F_{t_0, t_k}^c, F_{t_0, t_k}^g, F_{t_0, t_k}^P) - h_R S_{t_k}^g(F_{t_0, t_k}^g) - K)^+ | \mathcal{F}_{t_0}] \\ &= \lim_{\delta \rightarrow 0} \left( \mathbb{E}^{\mathbb{Q}} \left[ (S_{t_k}^P(F_{t_0, t_k}^c, F_{t_0, t_k}^g(F_{t_0}^g(t_l^a, t_l^b) + \delta), F_{t_0, t_k}^P) \right. \right. \\ &\quad \left. \left. - h_R S_{t_k}^g(F_{t_0, t_k}^g(F_{t_0}^g(t_l^a, t_l^b) + \delta)) - K)^+ | \mathcal{F}_{t_0} \right] \right. \\ &\quad \left. - \mathbb{E}^{\mathbb{Q}} \left[ (S_{t_k}^P(F_{t_0, t_k}^c, F_{t_0, t_k}^g(F_{t_0}^g(t_l^a, t_l^b) - \delta), F_{t_0, t_k}^P) \right. \right. \\ &\quad \left. \left. - h_R S_{t_k}^g(F_{t_0, t_k}^g(F_{t_0}^g(t_l^a, t_l^b) - \delta)) - K)^+ | \mathcal{F}_{t_0} \right] \right) / (2\delta) \end{aligned}$$

$$\begin{aligned}
&\stackrel{Cond.3.1}{=} \lim_{\delta \rightarrow 0} \left( \mathbb{E}^{\mathbb{Q}} \left[ (S_{t_k}^P(F_{t_0,t_k}^c, F_{t_0,t_k}^g + \delta, F_{t_0,t_k}^P) - h_R S_{t_k}^g(F_{t_0,t_k}^g + \delta) - K)^+ \mid \mathcal{F}_{t_0} \right] \right. \\
&\quad \left. - \mathbb{E}^{\mathbb{Q}} \left[ (S_{t_k}^P(F_{t_0,t_k}^c, F_{t_0,t_k}^g - \delta, F_{t_0,t_k}^P) - h_R S_{t_k}^g(F_{t_0,t_k}^g - \delta) - K)^+ \mid \mathcal{F}_{t_0} \right] \right) / (2\delta) \\
&= \frac{\partial}{\partial F_{t_0,t_k}^g} \mathbb{E}^{\mathbb{Q}} \left[ (S_{t_k}^P(F_{t_0,t_k}^c, F_{t_0,t_k}^g, F_{t_0,t_k}^P) - h_R S_{t_k}^g(F_{t_0,t_k}^g) - K)^+ \mid \mathcal{F}_{t_0} \right]
\end{aligned}$$

■

**Corollary 3.1** *We assume futures contracts to have non-overlapping deliveries ( $t_1^a \leq t_1^b < \dots < t_{n_i}^a \leq t_{n_i}^b$  for all  $i = c, g, P$ ) and to deliver equally distributed volumes. Then, Proposition 3.3 simplifies to*

$$\bar{\mathbf{h}}^i = \begin{pmatrix} \sum_{t \in \mathcal{T} \cap [t_1^a, t_1^b]} D_t^i \\ \vdots \\ \sum_{t \in \mathcal{T} \cap [t_{n_i}^a, t_{n_i}^b]} D_t^i \end{pmatrix} \quad \text{for } i = c, g, P.$$

In other words, we get the future deltas by summing up the hourly deltas in the according delivery period.

**Proof.** The optimal vector  $\mathbf{h}_i$  can be calculated by solving  $(\mathbf{V}^i)^T \mathbf{V}^i \mathbf{h} = (\mathbf{V}^i)^T \mathbf{D}^i$ . Because futures contracts are assumed to be non-overlapping and deliver equally distributed volumes,  $\mathbf{V}^i$  has a block matrix form (w.l.o.g we assume each hourly forward to belong to a futures contract)

$$(\mathbf{V}^i)^T = \begin{pmatrix} \delta_1 & \cdots & \delta_1 & 0 & \cdots & 0 & \cdots & 0 & \cdots & 0 \\ 0 & \cdots & 0 & \delta_2 & \cdots & \delta_2 & \cdots & 0 & \cdots & 0 \\ 0 & \cdots & 0 & 0 & \cdots & 0 & \ddots & 0 & \cdots & 0 \\ \vdots & \ddots & \vdots & \vdots & \ddots & \vdots & \ddots & \vdots & \ddots & \vdots \\ 0 & \cdots & 0 & 0 & \cdots & 0 & \cdots & \delta_{n_i} & \cdots & \delta_{n_i} \end{pmatrix} \in \mathbb{R}^{n_i \times m},$$

where  $\delta_j^{-1} := \left| \left\{ t \in \mathcal{T} : t_j^a < t < t_j^b \right\} \right|$ ,  $j = 1, \dots, n_i$ . ■



## CHAPTER 4.

# Historical Estimators and Parameter Risk

We believe that historical prices (observable auction data and forward price data respectively) as well as fundamental information<sup>1</sup> is required to calibrate a structural electricity spot model to a certain market. Some components of the structural electricity model in Chapter 2 are naturally given by fundamentals, i.e. the amount of renewables and nuclear production which is why we derive the residual demand of a certain day completely from fundamental data. However, we intend to build historical estimators for the remaining parameters like fuel capacities and the slope parameters of the bid stack. The reason is that i.e. the published fuel capacity of a market and the actual bidden volume of that fuel will not match in general. In detail, only part of the actual capacity is sold using the day ahead spot market causing the clearing volume of the day ahead market to be lower than the actual grid load (overall demand). The remaining part of capacity may have been sold OTC to its customers. For a detailed analysis of grid load and clearing volume of the day ahead auction data, we refer to [Coulon et al., 2014].

Based on the estimators, we decided to use asymptotic statistic for the estimators to quantify parameter risk. The approach is based on [Bannör and Scherer, 2013] and forces us to calculate a proxy of the asymptotic covariance matrix of the estimators. We proceed to explain the main idea of that approach before we start to build the actual estimators.

## 4.1 The Approach to Quantify Parameter Risk

The approach is based on [Bannör and Scherer, 2013]. It was applied for an electricity jump-diffusion spot model in [Bannör et al., 2013]. The authors follow Definition 1.11 on parameter risk to derive an algorithm for as follows.

Given a set of estimators  $\Theta$  (the historical estimator should be in  $\Theta$ ), we get a family of risk-neutral measures  $\{\mathbb{Q}_\theta\}_{\theta \in \Theta}$ , each leading in general to a different present value of the contingent claim  $X \in \mathcal{L}^1(\mathbb{P})$ . We denote the probability measure which allocates each present value (or equivalently probability measure  $\mathbb{Q}_\theta$ ) a probability given a set  $\vartheta \subset \Theta$  by  $R$  (cf. Definition 1.10). We seek to use a convex risk measure  $\rho$  which quantifies the risk in the

---

<sup>1</sup>i.e. <https://www.eex-transparency.com/>

uncertainty of choosing the best  $\theta \in \Theta$ . We calculate the *risk-captured price* of that contingent claim  $X$  by

$$\Gamma(X) := \rho \left( \theta \rightarrow \mathbb{E}^{\mathbb{Q}_\theta} [X | \mathcal{F}_{t_0}] \right).$$

**Definition 4.1 (Convex Risk Measure and Model Risk ([Bannör and Scherer, 2013]))** *A functional  $\Gamma$  incorporating model risk with respect to the model family  $\mathbb{Q}$  into contingent claims prices should fulfill the following properties:*

1. *Order preservation: if there exists a model-free order, it should be preserved when incorporating model uncertainty (cf. Definition 1.8), i.e. for contingent claims  $X, Y$ :*

$$X(\omega) \geq Y(\omega) \text{ for all } \omega \in \Omega \Rightarrow \Gamma(X) \geq \Gamma(Y).$$

2. *Diversification: Diversification of model uncertainty should not be penalized, i.e. a convex combination of two positions facing model uncertainty should not have a higher price than the convex combination of the individual prices, i.e.*

$$\Gamma(\lambda X + (1 - \lambda)Y) \leq \lambda \Gamma(X) + (1 - \lambda) \Gamma(Y)$$

*should hold for contingent claims  $X, Y$  and  $\lambda \in [0, 1]$ .*

3. *Model independence consistency: If a contingent claim  $X$  is consistently priced under all models (respective parameters), no model uncertainty is present and the model risk-captured price agrees with the risk-neutral price, i.e. no charge for model risk is added to the risk-neutral price:*

$$\mathbb{Q} \mapsto \mathbb{E}^{\mathbb{Q}}[X] \text{ is constant on } \mathcal{Q} \rightarrow \Gamma(X) = \mathbb{E}^{\mathbb{Q}}[X].$$

The authors have chosen to use the average value-at-risk (AVAR) with confidence level  $\alpha \in (0, 1)$  as convex risk measure:

$$AVAR(\alpha, \mathbb{P}, X) = \frac{1}{\alpha} \int_0^\alpha q_X^{\mathbb{P}}(1 - \beta) d\beta,$$

where  $q_X^{\mathbb{P}} : (0, 1) \rightarrow \mathbb{R}$  is the quantile function induced by the probability measure  $\mathbb{P}$ . The calculation of  $AVAR(\alpha, R, \mathbb{E}^{\mathbb{Q}}[X])$  is motivated by

$$\int_{\Theta} \mathbb{E}^{\mathbb{Q}}[X | \theta = \theta_0] R(d\theta_0) = \int_{\Theta} \mathbb{E}^{\mathbb{Q}_{\theta_0}}[X] R(d\theta_0) = \int_0^1 q_{\mathbb{E}^{\mathbb{Q}}[X]}^R(\beta) d\beta = AVAR(1, R, \mathbb{E}^{\mathbb{Q}}[X]).$$

The calculation leads to the quantification of parameter risk with respect to a certain quantile  $\alpha$ .

The idea in [Bannör and Scherer, 2013] is to approximate the probability measure  $R$  by the asymptotic distribution of the estimators for a sufficiently large historical data set of market data. Therefore the problem to calculate the AVAR is reduced to the calculation of an AVAR for a normally distributed random variable. The authors used [McNeal et al., 2005] to calculate the AVAR and arrived at the following algorithm to quantify parameter risk expressed as an add-on to the present value:

1. estimate model parameters  $\theta$  retrospectively using historical data and calculate their asymptotic covariance matrix  $\Sigma_\theta$ ,
2. calculate the gradient  $\nabla_\theta \mathbb{E}^{\mathbb{Q}_\theta} [X | \mathcal{F}_{t_0}]$  of the present value of the claim with respect to the model parameters,
3. for a given confidence level  $\alpha \in (0, 1)$  the risk adjustment is computed by calculating:

$$\frac{\phi(\Phi^{-1}(1 - \alpha))}{\alpha} \sqrt{\frac{(\nabla_\theta \mathbb{E}^{\mathbb{Q}_\theta} [X | \mathcal{F}_{t_0}])^T \Sigma_\theta \nabla_\theta \mathbb{E}^{\mathbb{Q}_\theta} [X | \mathcal{F}_{t_0}]}{N}}$$

where  $\phi$  denotes the standard normal density function and  $\Phi$  the standard normal distribution function.

## 4.2 Historical Estimators

For the purpose of analyzing time series data, we have to work with the real-world measure  $\mathbb{P}$  instead of a risk-neutral measure  $\mathbb{Q}$ . Consequently, our probability basis becomes  $(\Omega, \mathcal{F}, (\mathcal{F}_t)_{t \geq t_0}, \mathbb{P})$ .

We intend to find estimators of the model parameters of the structural model introduced in Chapter 2.

### 4.2.1 Fuels' Dynamics

We derive two different estimators (based on a one year data history): in the first approach, we estimate the model parameters based on historical spot data. In the second approach, we estimate the model parameters based on historical forwards/ futures data.

#### Spot Data

We use the deseasonalized logarithm of the gas and coal spot market  $X_t^c, X_t^g$  to calibrate (for simplicity: constant) mean-reversion speed, volatility parameters and correlation parameters  $\alpha_c, \alpha_g, \nu_c, \nu_g, \rho$  in (2.4).

**Remark 4.1 (Deseasonalization)** *In the Ornstein- Uhlenbeck model in Chapter 2 (cf. (2.4)), it holds under  $\mathbb{Q}$   $\forall i \in I$*

$$S_t^{(i)} = \exp \left( s^{(i)}(t) + X_t^{(i)} \right).$$

*Therefore, we have to derive a  $\tilde{s}^{(i)}(t)$  under the real world measure  $\mathbb{P}$  in order to get a time series for  $X_t^{(i)}$  under  $\mathbb{P}$  by*

$$X_t^{(i)} = \ln \left( \frac{S_t^{(i)}}{\exp(\tilde{s}^{(i)}(t))} \right).$$

*We derive  $\exp(\tilde{s}^{(i)}(t))$  by multiplying the seasonality weights ( $\beta_i$ ,  $i = 1, \dots, 34$ ) of the price forward curves in Chapter 1.2.1 to a running historical average of the electricity spot price. The result is an average seasonal spot price time series where  $X_t$  reflects the deviation factor of the spot price to its seasonal average. In terms of gas with weekly seasonality we applied a weekly average. In terms of coal with monthly seasonality, we applied a monthly average. The approach is consistent to the derivation of the weights (Chapter 2.3) where we also have derived weekly (monthly) running averages as a starting point.*

*From Girsanov's theorem we now the connection between Brownian motions under  $\mathbb{P}$  and  $\mathbb{Q}$  to be  $W_t = \tilde{W}_t - \int_{t_0}^t u_s^{(i)} ds$  (We denote a Brownian motion under  $\mathbb{P}$  instead of  $\mathbb{Q}$  by  $\tilde{W}_t$ ). Consequently, (2.4) can be used to yield*

$$\tilde{s}^{(i)}(t) = s^{(i)}(t) - \int_{t_0}^t u_s^{(i)} v_s^{(i)} \exp \left( - \int_s^t \alpha_u^{(i)} du \right) ds.$$

*A stepwise constant process  $u_t^{(i)}$  is uniquely defined by  $\tilde{s}^{(i)}(t)$  and  $s^{(i)}(t)$ .*

We will show that - by assuming the model parameters to be constant over time - the estimation of the joint fuels' dynamics reduces to the estimation of a VAR model. At first, we give the according Definition.

**Definition 4.2 (VAR( $p$ ) Process)** *As it is done in [Lütkepohl, 2007], we define a Gaussian stable  $K$ -dimensional VAR( $p$ ) process ( $p \in \mathbb{N}$ ) for a time series  $\mathbf{y}_t$  ( $t = 1, \dots, T$ ) by*

$$\mathbf{y}_t = \mathbf{v} + \mathbf{A}_1 \mathbf{y}_{t-1} + \dots + \mathbf{A}_p \mathbf{y}_{t-p} + \mathbf{u}_t.$$

*Here,  $\mathbf{y}_t = (y_{1t}, \dots, y_{Kt})^T \in \mathbb{R}^K$ ,  $\mathbf{v} = (v_1, \dots, v_K)^T \in \mathbb{R}^K$ ,  $\mathbf{A}_i \in \mathbb{R}^{K \times K}$  and  $\mathbf{u}_t$  is white noise with non-singular covariance matrix  $\Sigma_u$ .*

*By defining*

$$\mathbf{Z}_t := [1, \mathbf{y}_t, \dots, \mathbf{y}_{t-p+1}]^T,$$

*$\mathbf{Z} := [\mathbf{Z}_0, \dots, \mathbf{Z}_{T-1}]$ ,  $\mathbf{Y} := [\mathbf{y}_1, \dots, \mathbf{y}_T]$ ,  $\mathbf{B} := [\mathbf{v}, \mathbf{A}_1, \dots, \mathbf{A}_p]$  and  $\mathbf{U} := [\mathbf{u}_1, \dots, \mathbf{u}_T]$  this is equivalent to*

$$\mathbf{Y} = \mathbf{BZ} + \mathbf{U}.$$



In order to estimate the parameters, we use (2.5) (solution of the stochastic differential equations in (2.4)).

We get for  $\Delta t > 0$

$$\begin{aligned} \begin{pmatrix} X_{t+\Delta t}^c \\ X_{t+\Delta t}^g \end{pmatrix} &= \begin{pmatrix} e^{-\alpha_c \Delta t} & 0 \\ 0 & e^{-\alpha_g \Delta t} \end{pmatrix} \begin{pmatrix} X_t^c \\ X_t^g \end{pmatrix} + \begin{pmatrix} v_c \int_t^{t+\Delta t} e^{\alpha_c(s-t-\Delta t)} d\tilde{W}_s^{(c)} \\ v_g \int_t^{t+\Delta t} e^{\alpha_g(s-t-\Delta t)} d\tilde{W}_s^{(g)} \end{pmatrix} \\ &= \begin{pmatrix} e^{-\alpha_c \Delta t} & 0 \\ 0 & e^{-\alpha_g \Delta t} \end{pmatrix} \begin{pmatrix} X_t^c \\ X_t^g \end{pmatrix} \\ &\quad + \begin{pmatrix} v_c \int_t^{t+\Delta t} e^{\alpha_c(s-t-\Delta t)} d\tilde{B}_s^c \\ \rho v_g \int_t^{t+\Delta t} e^{\alpha_g(s-t-\Delta t)} d\tilde{B}_s^c + \sqrt{1-\rho^2} v_g \int_t^{t+\Delta t} e^{\alpha_g(s-t-\Delta t)} d\tilde{B}_s^g \end{pmatrix}. \end{aligned}$$

Using the Itô-Isometry and two standard normal distributions  $Z_1, Z_2 \stackrel{\mathcal{D}}{=} \mathcal{N}(0, 1)$ , this simplifies to

$$\begin{aligned} &\stackrel{\mathcal{D}}{=} \begin{pmatrix} e^{-\alpha_c \Delta t} & 0 \\ 0 & e^{-\alpha_g \Delta t} \end{pmatrix} \begin{pmatrix} X_t^c \\ X_t^g \end{pmatrix} \\ &\quad + \begin{pmatrix} \frac{v_c}{\sqrt{2\alpha_c}} \sqrt{1-e^{-2\alpha_c \Delta t}} & 0 \\ \frac{\rho v_g}{\sqrt{2\alpha_g}} \sqrt{1-e^{-2\alpha_g \Delta t}} & \frac{\sqrt{1-\rho^2} v_g}{\sqrt{2\alpha_g}} \sqrt{1-e^{-2\alpha_g \Delta t}} \end{pmatrix} \begin{pmatrix} Z_1 \\ Z_2 \end{pmatrix} \\ &=: \mathbf{A}_1 \begin{pmatrix} X_t^c \\ X_t^g \end{pmatrix} + u_t, \end{aligned}$$

being a VAR(1) model.  $u_t$  is normally distributed with mean zero and covariance matrix

$$\begin{aligned} \Sigma_u &= \begin{pmatrix} \frac{v_c^2}{2\alpha_c} (1-e^{-2\alpha_c \Delta t}) & \frac{\rho v_g v_c}{2\sqrt{\alpha_c \alpha_g}} \sqrt{1-e^{-2\alpha_c \Delta t}} \sqrt{1-e^{-2\alpha_g \Delta t}} \\ \frac{\rho v_g v_c}{2\sqrt{\alpha_c \alpha_g}} \sqrt{1-e^{-2\alpha_c \Delta t}} \sqrt{1-e^{-2\alpha_g \Delta t}} & \frac{v_g^2}{2\alpha_g} (1-e^{-2\alpha_g \Delta t}) \end{pmatrix} \\ &=: \begin{pmatrix} (\Sigma_u)_{11} & (\Sigma_u)_{12} \\ (\Sigma_u)_{21} & (\Sigma_u)_{22} \end{pmatrix}. \end{aligned}$$

We incorporate the diagonal character of  $\mathbf{A}_1 := \begin{pmatrix} a_{11} & a_{12} \\ a_{21} & a_{22} \end{pmatrix}$  into the model by defining the linear mapping

$$\begin{pmatrix} a_{11} \\ a_{21} \\ a_{12} \\ a_{22} \end{pmatrix} = \begin{pmatrix} a_{11} \\ 0 \\ 0 \\ a_{22} \end{pmatrix} = \underbrace{\begin{pmatrix} 1 & 0 \\ 0 & 0 \\ 0 & 0 \\ 0 & 1 \end{pmatrix}}_{=\mathbf{R}} \begin{pmatrix} a_{11} \\ a_{22} \end{pmatrix}.$$

We perform the estimation for  $\begin{pmatrix} a_{11} & a_{22} \end{pmatrix}^T$ . The maximum likelihood estimator as well as the asymptotic distribution of  $\mathbf{A}_1, \tilde{\Sigma}_u$  is analytically derived in [Lütkepohl, 2007] (cf. Proposition B.3). For the calibration of the coal and gas processes, we obtain

$$\begin{pmatrix} \tilde{\alpha}_c \\ \tilde{\alpha}_g \\ \tilde{v}_c \\ \tilde{v}_g \\ \tilde{\rho} \end{pmatrix} = \begin{pmatrix} -\ln(\tilde{a}_{11})/\Delta t \\ -\ln(\tilde{a}_{22})/\Delta t \\ \sqrt{2(\tilde{\Sigma}_u)_{11}\tilde{\alpha}_c/(1-e^{-2\tilde{\alpha}_c\Delta t})} \\ \sqrt{2(\tilde{\Sigma}_u)_{22}\tilde{\alpha}_g/(1-e^{-2\tilde{\alpha}_g\Delta t})} \\ 2(\tilde{\Sigma}_u)_{12}\sqrt{\tilde{\alpha}_g\tilde{\alpha}_c/\tilde{v}_c/\tilde{v}_g/\sqrt{1-e^{-2\tilde{\alpha}_c\Delta t}}/\sqrt{1-e^{-2\tilde{\alpha}_g\Delta t}}} \end{pmatrix} =: h\left(\tilde{a}_{11}, \tilde{a}_{22}, \begin{pmatrix} (\tilde{\Sigma}_u)_{11} \\ (\tilde{\Sigma}_u)_{21} \\ (\tilde{\Sigma}_u)_{22} \end{pmatrix}\right)$$

Here,  $\tilde{a}_{11}, \tilde{a}_{22}, \tilde{\Sigma}_u$  are the maximum likelihood estimators of the VAR(1) model. The estimation results are summarized in Table 4.1.

The asymptotic covariance matrix of the coal and gas stochastic process parameters can be calculated in two steps. At first, we calculate the asymptotic distribution of the VAR model parameters  $\mathbf{A}_1, \tilde{\Sigma}_u$  as been described in [Lütkepohl, 2007] (cf. Proposition B.3). Secondly, we use the delta method (cf. [van der Vaart, 2000] or B.1) for

$$h(\tilde{a}_{11}, \tilde{a}_{22}, ((\tilde{\Sigma}_u)_{11}, (\tilde{\Sigma}_u)_{21}, (\tilde{\Sigma}_u)_{22})^T)$$

to derive the asymptotic distribution of  $\alpha_c, \alpha_g, v_c, v_g$  and  $\rho$ .

We summarize the results in the next Proposition.

**Proposition 4.1 (Asymptotic Covariance Matrix: Fuels Spot Estimation)** Let  $\mathbf{y}_t := \begin{pmatrix} X_t^c \\ X_t^g \end{pmatrix}$ .

We define  $\mathbf{Z}_t := [1, \mathbf{y}_t]^T$ ,  $\mathbf{Z} := [Z_0, \dots, Z_{T-1}]$ ,  $\mathbf{Y} := [\mathbf{y}_1, \dots, \mathbf{y}_T]$ ,  $\mathbf{B} := [0, \mathbf{A}_1]$  and  $\mathbf{U} := [\mathbf{u}_1, \dots, \mathbf{u}_T]$ .

The maximum likelihood estimator of  $(\tilde{\alpha}_c, \tilde{\alpha}_g, \tilde{v}_c, \tilde{v}_g, \tilde{\rho})$  is then asymptotically normal with covariance matrix

$$(\nabla h(\mathbf{a}))^T \begin{bmatrix} [\mathbf{R}^T(\Gamma \otimes \Sigma_u^{-1})\mathbf{R}]^{-1} & 0 \\ 0 & 2\mathbf{D}_K^+(\Sigma_u \otimes \Sigma_u)(\mathbf{D}_K^+)^T \end{bmatrix} \nabla h(\mathbf{a}).$$

Here,  $\mathbf{a} := (\tilde{a}_{11}, \tilde{a}_{22}, ((\tilde{\Sigma}_u)_{11}, (\tilde{\Sigma}_u)_{21}, (\tilde{\Sigma}_u)_{22})^T)$  and  $\mathbf{D}_K^+$ ,  $\Gamma$  and  $\otimes$  are defined in Appendix B.2.

**Proof.** With the help of Proposition B.3, we know

$$(\tilde{a}_{11}, \tilde{a}_{21}, \tilde{a}_{12}, \tilde{a}_{22}, ((\tilde{\Sigma}_u)_{11}, (\tilde{\Sigma}_u)_{21}, (\tilde{\Sigma}_u)_{22})^T)$$

Model Parameter	Estimation Result
$\alpha_c$	15.16
$\alpha_g$	32.04
$v_c$	26.78%
$v_g$	38.89%
$\rho$	0.086

Table 4.1: Historical Estimation of a joint fuels' process (time series: 1 year)

to be asymptotically normal. We apply the delta method for

$$\begin{pmatrix} \tilde{a}_{11} \\ \tilde{a}_{21} \\ \tilde{a}_{12} \\ \tilde{a}_{22} \end{pmatrix} = \begin{pmatrix} 1 & 0 & 0 & 0 \\ 0 & 0 & 0 & 1 \end{pmatrix} \begin{pmatrix} \tilde{a}_{11} \\ \tilde{a}_{21} \\ \tilde{a}_{12} \\ \tilde{a}_{22} \end{pmatrix}$$

to get

$$\sqrt{T} \begin{bmatrix} \tilde{a}_{11} - a_{11} \\ \tilde{a}_{22} - a_{22} \\ (\tilde{\Sigma}_u)_{11} - (\Sigma_u)_{11} \\ (\tilde{\Sigma}_u)_{21} - (\Sigma_u)_{21} \\ (\tilde{\Sigma}_u)_{22} - (\Sigma_u)_{22} \end{bmatrix} \xrightarrow{\mathcal{D}} \mathcal{N} \left( 0, \begin{bmatrix} [\mathbf{R}^T (\Gamma \otimes \Sigma_u^{-1}) \mathbf{R}]^{-1} & 0 \\ 0 & 2\mathbf{D}_K^+ (\Sigma_u \otimes \Sigma_u) (\mathbf{D}_K^+)^T \end{bmatrix} \right).$$

The last step is to apply the delta method for  $h$  to get the final statement. ■

### Forward Data

The usage of fuel forward data for estimation enables to estimate a time-dependent mean-reversion speed parameter. Furthermore, we directly extract volatility from our hedging instruments instead from - in general - non-traded spot instruments. The estimation is straight forward: using the implied fuels' forward dynamics in Proposition 3.1, we apply the Itô-Lemma to get<sup>2</sup> ( $\tau > \Delta t > 0$  and  $i \in \{c, g\}$ ):

$$\begin{aligned} \ln F_{t+\Delta t, t+\tau}^{(i)} &= \ln F_{t, t+\tau}^{(i)} - \underbrace{\frac{1}{2} \int_t^{t+\Delta t} (v_s^{(i)})^2 \exp \left( -2 \int_s^{t+\tau} \alpha_u^{(i)} du \right) ds}_{=:(\sigma_\tau^{(i)})^2} \\ &\quad + \int_t^{t+\Delta t} v_s^{(i)} \exp \left( - \int_s^{t+\tau} \alpha_u^{(i)} du \right) dW_s^{(i)} \end{aligned}$$

<sup>2</sup>We integrate the stochastic differential equation  $d \ln F_{t+\Delta t, t+\Delta t+\tau}^{(i)}$  in the proof of Proposition 3.1 to get an equation instead of a discretization of a stochastic differential equation.

$$\begin{aligned}
\Longleftrightarrow: \Delta \ln F_{t+\Delta t, t+\tau}^{(i)} &= -\frac{1}{2}(\sigma_\tau^{(i)})^2 + \int_t^{t+\Delta t} v_s^{(i)} \exp\left(-\int_s^{t+\tau} \alpha_u^{(i)} du\right) dW_s^{(i)} \\
\Longleftrightarrow \Delta \ln F_{t+\Delta t, t+\tau}^{(i)} &= -\frac{1}{2}(\sigma_\tau^{(i)})^2 - \int_t^{t+\Delta t} u_s^{(i)} v_s^{(i)} \exp\left(-\int_s^{t+\tau} \alpha_u^{(i)} du\right) ds \\
&\quad + \int_t^{t+\Delta t} v_s^{(i)} \exp\left(-\int_s^{t+\tau} \alpha_u^{(i)} du\right) d\tilde{W}_s^{(i)}.
\end{aligned}$$

The last equivalence is necessary as merely  $\tilde{W}_t$  is a Brownian motion under  $\mathbb{P}$ .

**Remark 4.2 (Alternative Stochastic Differential Equation)** *There is at least a second approach to build a historical estimator: Whereas we derived  $dF_{t,T}^{(i)}$  in Proposition 3.1,  $dF_{t,t+\tau}^{(i)}$  can be analyzed instead. In the first approach (Proposition 3.1), forward prices are martingales due to a fix maturity  $T$ . In the second approach, we have to treat a running maturity  $t + \tau$  which leads the running forward price to face seasonality. In detail, we could instead analyze*

$$\begin{aligned}
\ln F_{t+\Delta t, t+\Delta t+\tau}^{(i)} &= \ln F_{t, t+\tau}^{(i)} + \int_t^{t+\Delta t} \left\{ \frac{\partial s^{(i)}(s+\tau)}{\partial t} - \alpha_{s+\tau}^{(i)} \exp\left(\int_s^{s+\tau} \alpha_u^{(i)} du\right) X_s^{(i)} \right. \\
&\quad \left. - \alpha_{s+\tau}^{(i)} \int_s^{s+\tau} \left(v_u^{(i)}\right)^2 \exp\left(\int_u^{s+\tau} \alpha_v^{(i)} dv\right) du \right. \\
&\quad \left. + \frac{1}{2} \left[ \left(v_{s+\tau}^{(i)}\right)^2 - \left(v_s^{(i)}\right)^2 \right] \exp\left(-2 \int_s^{s+\tau} \alpha_v^{(i)} dv\right) \right\} ds \\
&\quad + \int_t^{t+\Delta t} v_s^{(i)} \exp\left(-\int_s^{s+\tau} \alpha_u^{(i)} du\right) dW_s^{(i)}.
\end{aligned}$$

However, we believe it to be the more tractable method to fix the maturity of the forward and to automatically eliminate the seasonality by comparing  $\ln F_{t+\Delta t, t+\tau}^{(i)}$  to  $\ln F_{t, t+\tau}^{(i)}$ . An analysis of running forward prices was i.e. done in [Benth and Paraschiv, 2016].

Therefore,  $\Delta \ln F_{t+\Delta t, t+\tau}^{(i)}$  is normally distributed with variance  $(\sigma_\tau^{(i)})^2$  (Itô-Isometry). For a set of forward contracts with ascending deliveries  $\mathcal{M} = \{\tau_1^{(i)}, \dots, \tau_M^{(i)}\}$  ( $M \in \mathbb{N}$ ), we use an according set of historical forward prices  $F_{t_0, t_0+\tau}^{(i)}, \dots, F_{t_N, t_N+\tau}^{(i)}$  ( $i = c, g, \tau \in \mathcal{M}$ ). We estimate the fuels' dynamics by solving the following root-problem for each  $i = c, g$  (cf. [Clewlow and Strickland, 2000]; in order to avoid the inclusion of  $u_t^{(i)}$  into the estimation, we completely extract the information on  $\alpha_t^{(i)}$  from the variance  $\sigma_\tau^{(i)}$ . Otherwise,  $u_t^{(i)}$  would have to be recalculated during the estimation procedure leading to a mixture of measures  $\mathbb{P}$  and  $\mathbb{Q}$ ):

$$\left(\sigma_{\tau_k^{(i)}}\right)^2 - \frac{1}{N} \sum_{j=1}^N \left(\Delta \ln F_{t_j, t_j+\tau_k^{(i)}}^{(i)} - \overline{\Delta \ln F_{t, t+\tau_k^{(i)}}^{(i)}}\right)^2 = 0$$

which equals

$$\frac{1}{N} \sum_{j=1}^N \left\{ \underbrace{\left( \sigma_{\tau_k^{(i)}}^2 - \left( \Delta \ln F_{t_j, t_j + \tau_k^{(i)}}^{(i)} - \overline{\Delta \ln F_{t, t + \tau_k^{(i)}}^{(i)}} \right)^2 \right)}_{:= \Psi_F^{\alpha_t^{(i)}, v_t^{(i)}} \left( \Delta \ln F_{t_j, t_j + \tau_k^{(i)}}^{(i)}; \tau_k^{(i)} \right)} \right\} = 0, \quad \forall k = 1, \dots, M \quad (4.1)$$

where  $\overline{\Delta \ln F_{t, t + \tau_k^{(i)}}^{(i)}}$  denotes the sample mean over  $N$  different observations. Based on (4.1), we intend to estimate a vector of  $M$  mean-reversion speed parameters.

**Remark 4.3** Based on (4.1), we cannot estimate a time-dependent  $v_t^{(i)}$  ( $i \in \{c, g\}$ ). The reason is that we only observe  $v_t^{(i)}$  on  $[t, t + \Delta t]$  and  $\Delta t$  will be small. This is the reason why we assume  $v_t^{(i)} \equiv v^{(i)} > 0$ <sup>3</sup>. However, we can estimate  $\alpha_t^{(i)}$  on the whole interval  $[t, t + \tau_M^{(i)}]$ . We define it to be a piecewise constant function

$$\alpha_s^{(i)} := \sum_{j=1}^M \alpha_{t + \tau_j^{(i)}}^{(i)} \mathbb{I}_{s \in (t + \tau_{j-1}^{(i)}, t + \tau_j^{(i)}]}, \quad \tau_0^{(i)} := 0,$$

where  $s$  such that  $t + \tau_M^{(i)} > s > t > 0$ . We estimate  $\alpha_{t + \tau_j^{(i)}}^{(i)}$  as been defined in (2.11) stepwise based on historical data.

**Remark 4.4** The time series for an hourly or daily forward curve  $F_{t, t + \tau}^{(i)}$  is not observable in the market but merely futures contracts  $F^{(i)}(t_a, t_b)$ . Theoretically, the running stochastic differential equation in Remark 4.2 has to be used for futures contracts instead. However, practitioners merely have to store their forward curves on a daily basis to get the according time series which is why we believe our approach to have a broader relevance in practice.

The asymptotic distribution is given in the next Proposition.

**Definition 4.3 (Empirical Probability Measure)** We define the empirical probability measure  $\mathbb{P}_N$  on  $(\Omega, \mathcal{F})$  by

$$\mathbb{P}_N A := \frac{1}{N} \sum_{i=1}^N \mathbb{I}_A(x_i)$$

for observations  $x_i$  and  $A \in \mathcal{F}$ . For  $N \rightarrow \infty$  it converges against the real world measure  $\mathbb{P}$ .

**Notation 4.1** As it is common in statistics, we will use the notation  $\mathbb{P}X$  for a random variable  $X$  in order to express the expectation  $\mathbb{E}^{\mathbb{P}}X$  under  $\mathbb{P}$ .

<sup>3</sup>For more information on how to estimate model volatility, we refer to Chapter B.3

**Proposition 4.2 (Asymptotic Covariance Matrix: Fuel Forwards Estimation)** *Let  $M > 0$  be fix and the deterministic processes  $\alpha_t^{(i)}$  and  $v_t^{(i)}$  be given by Remark 4.3 for each  $i = c, g$ . We assume  $v_t^{(i)}$  to be known. The estimator  $\hat{\alpha}^{(i)} = (\hat{\alpha}_1^{(i)}, \dots, \hat{\alpha}_M^{(i)})$  solving (4.1) is then asymptotically normal for  $N \rightarrow \infty$  with covariance matrix*

$$(\mathbb{P}\dot{\Psi}_F)^{-1} \mathbb{P}(\Psi_F \Psi_F^T) (\mathbb{P}\dot{\Psi}_F)^{-T},$$

where we denote  $\mathbb{P}\Psi_F := \mathbb{P} \left[ \Psi_F^{\alpha_t^{(i)}, v_t^{(i)}} \left( \Delta \ln F_{t, t+\tau_k}^{(i)} \right) \right]$  and  $\Psi_F^{\alpha_t^{(i)}, v_t^{(i)}}$  as defined in (4.1).

**Proof.** (4.1) defines a Z-estimator which is why the Proposition follows from Theorem 5.21 in [van der Vaart, 2000] (cf. Proposition B.1). ■

In order to estimate correlation, we calculate the implied covariance matrix of  $\Delta \ln F_{t, t+\tau_k}^{(i)}$  ( $\tau \in T$ ):

$$\begin{aligned} & \begin{pmatrix} \int_t^{t+\Delta t} v_s^{(c)} \exp \left( - \int_s^{t+\tau} \alpha_u^{(c)} du \right) d\tilde{W}_s^{(c)} \\ \int_t^{t+\Delta t} v_s^{(g)} \exp \left( - \int_s^{t+\tau} \alpha_u^{(g)} du \right) d\tilde{W}_s^{(g)} \end{pmatrix} \\ &= \begin{pmatrix} \int_t^{t+\Delta t} v_s^{(c)} \exp \left( - \int_s^{t+\tau} \alpha_u^{(c)} du \right) d\tilde{B}_s^{(c)} \\ \int_t^{t+\Delta t} \rho_s v_s^{(g)} \exp \left( - \int_s^{t+\tau} \alpha_u^{(g)} du \right) d\tilde{B}_s^{(c)} + \int_t^{t+\Delta t} \sqrt{1 - \rho_s^2} v_s^{(g)} \exp \left( - \int_s^{t+\tau} \alpha_u^{(g)} du \right) d\tilde{B}_s^{(g)} \end{pmatrix} \\ &= \begin{pmatrix} \sqrt{\int_t^{t+\Delta t} (v_s^{(c)})^2 e^{-2 \int_s^{t+\tau} \alpha_u^{(c)} du} ds} & 0 \\ \sqrt{\int_t^{t+\Delta t} \rho_s^2 (v_s^{(g)})^2 e^{-2 \int_s^{t+\tau} \alpha_u^{(g)} du} ds} & \sqrt{\int_t^{t+\Delta t} (1 - \rho_s^2) (v_s^{(g)})^2 e^{-2 \int_s^{t+\tau} \alpha_u^{(g)} du} ds} \end{pmatrix} \begin{pmatrix} Z_1 \\ Z_2 \end{pmatrix}, \end{aligned}$$

where  $Z_1, Z_2 \stackrel{\mathcal{D}}{=} \mathcal{N}(0, 1)$ . The estimator for correlation can finally be computed by solving for each  $\tau = \tau_1^{(i)}, \dots, \tau_M^{(i)}$ :

$$\begin{aligned} & \sqrt{\int_t^{t+\Delta t} (v_s^{(c)})^2 \exp \left( -2 \int_s^{t+\tau} \alpha_u^{(c)} du \right) ds} \sqrt{\int_t^{t+\Delta t} \rho_s^2 (v_s^{(g)})^2 \exp \left( -2 \int_s^{t+\tau} \alpha_u^{(g)} du \right) ds} \\ &= \frac{1}{N} \sum_{j=1}^N \underbrace{\left( \Delta \ln F_{t_j, t_j+\tau}^{(c)} - \overline{\Delta \ln F_{t, t+\tau}^{(c)}} \right) \left( \Delta \ln F_{t_j, t_j+\tau}^{(g)} - \overline{\Delta \ln F_{t, t+\tau}^{(g)}} \right)}_{=:(\hat{\sigma}_{\tau, cg}^{(i)})^2} \end{aligned} \quad (4.2)$$

Equation (4.3) reveals that - similarly to  $v_t^{(i)}$  for  $i = c, g$  - we can only estimate  $\rho_t$  on  $[t, t + \Delta t]$ . This is the reason why we derive the solution under the assumption  $\rho_t \equiv \rho \in (-1, 1)$ . We get

$$\begin{aligned} & \rho \sqrt{\int_t^{t+\Delta t} (v_s^{(c)})^2 \exp \left( -2 \int_s^{t+\tau} \alpha_u^{(c)} du \right) ds} \sqrt{\int_t^{t+\Delta t} (v_s^{(g)})^2 \exp \left( -2 \int_s^{t+\tau} \alpha_u^{(g)} du \right) ds} = (\hat{\sigma}_{\tau, cg}^{(i)})^2 \\ & \iff: f_\rho^\tau(v_t^{(c)}, v_t^{(g)}, \alpha_t^{(c)}, \alpha_t^{(g)}; \hat{\sigma}_{\tau, cg}^{(i)}) \stackrel{!}{=} \rho. \end{aligned} \quad (4.3)$$

We have to solve (4.3) for  $M$  different  $\tau$  which is why we formulate a M estimator:

$$\min_{\rho \in (-1,1)} \left\{ \sum_{i=1}^M \left( \rho - f_{\rho}^{(i)}(v_t^{(c)}, v_t^{(g)}, \alpha_t^{(c)}, \alpha_t^{(g)}; \hat{\sigma}_{\tau, cg}^{(i)}) \right)^2 \right\} \quad (4.4)$$

In order to give the final result of the asymptotic distribution of  $v_t^{(c)}, v_t^{(g)}, \alpha_t^{(c)}, \alpha_t^{(g)}, \rho$ , we define:

$$F_{\rho}^{\tau} \begin{pmatrix} v_t^{(c)} \\ v_t^{(g)} \\ \alpha_t^{(c)} \\ \alpha_t^{(g)} \\ \sigma_{\tau, cg}^{(i)} \end{pmatrix} := \begin{pmatrix} v_t^{(c)} \\ v_t^{(g)} \\ \alpha_t^{(c)} \\ \alpha_t^{(g)} \\ f_{\rho}(v_t^{(c)}, v_t^{(g)}, \alpha_t^{(c)}, \alpha_t^{(g)}; \sigma_{\tau, cg}^{(i)}) \end{pmatrix}$$

**Corollary 4.1** ( $M = 1$ ) *Let the estimator of the model parameters  $\hat{\alpha}_t^{(c)}, \hat{\alpha}_t^{(g)}$  be given by Proposition 4.2 and for time-dependent correlation by (4.3). Let  $v_t^{(c)}, v_t^{(g)}$  be already known and  $M = 1$ . Then, the joint estimator  $\hat{\alpha}_t^{(c)}, \hat{\alpha}_t^{(g)}, \hat{\rho}_t$  is asymptotically normal with covariance matrix*

$$(\nabla F_{\rho}^{\tau})(\mathbb{P}\Psi_F)^{-1} \mathbb{P}(\Psi_F \Psi_F^T)(\mathbb{P}\Psi_F)^{-T} (\nabla F_{\rho}^{\tau})^T.$$

**Proof.** Application of the delta method (cf. Chapter B.1). ■

In order to compare the estimation against the spot data estimation, we assume the volatility  $v^{(i)}$  to be equal to the spot volatility given in Table 4.1<sup>4</sup>. Therefore, we end up to estimate a time dependent and stepwise constant mean-reversion function of dimension  $M$  for each fuel  $i = c, g$ .

The results of the estimation are depicted in Figure 4.1. We used the following generic futures prices from Bloomberg for estimation: 1st, 2nd, 3rd Month; 2nd, 3rd, 4th Quarter. We used historical daily data of 2015. Comparing the mean-reversion estimation based on forward data to the spot estimation (Table 4.1) it can be deduced the parameter to decrease by more than 50% even for the mean-reversion speed for short maturities (i.e. one month). By making this parameter time-dependent we can furthermore preserve a higher forward price volatility for longer maturities (mean-reversion speed close to zero for maturities longer than 6 months).

The estimation yields a forward volatility function being depicted in Figure 4.2. The decreasing volatility for increasing forward maturity is the common known Samuelson effect

[Samuelson, 1965, Eydeland and Wolyniec, 2003]. Whereas spot mean-reversion speed was estimated at 15 for coal and 32 for gas (Table 4.1), mean-reversion speed is decreasing to something close to zero for high forward maturities.

Based on the calibration above, we calculate parameter risk using [Bannör et al., 2013] in Chapter 4.1.

<sup>4</sup>In B.3 the approach is verified by taking a look at the limes.

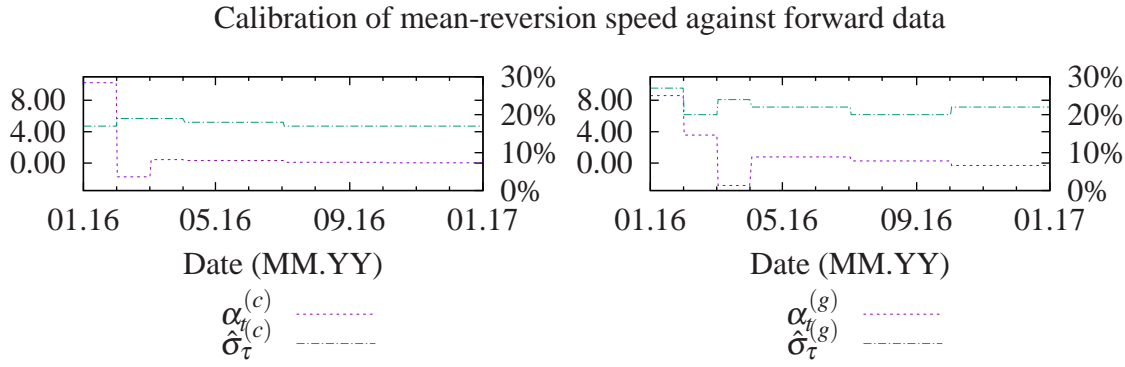


Figure 4.1: Left: Coal, right: Gas; Calibration of mean-reversion speed parameter  $\alpha_t^{(i)}$  for  $i = c, g$  using a stepwise function (Remark 4.3; left axis); Volatility was taken from Table 4.1; estimated future volatility on right axis.

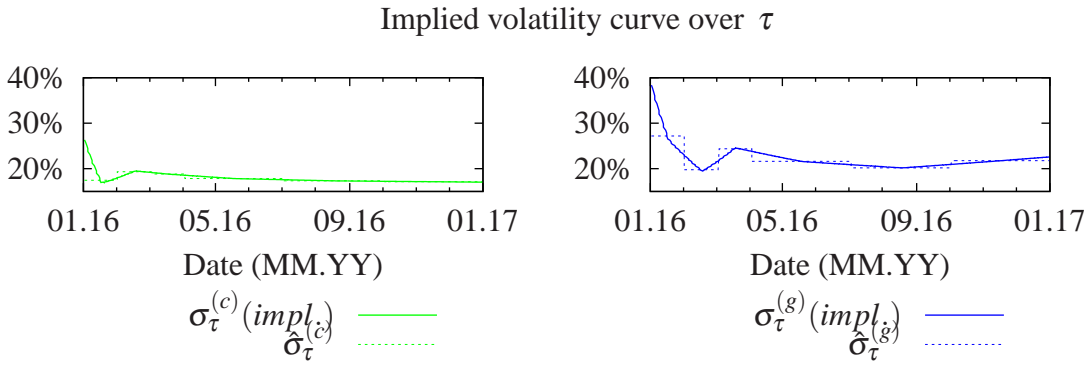


Figure 4.2: Left: Coal, right: Gas; Implied volatility function based on the estimation results in Figure 4.1

## 4.2.2 Bid Stack Parameters

In general, the estimation of the bid stack parameters is a trade off between information in bid and offer data and the usage of fundamental data respectively. In Remark 2.2, we have seen that the bid stack parameters can be completely derived based on fundamental data. However, beyond this transparency data, the observable bid and offer volumes carry a lot implied information about the bid stack as well. In this context it is important that only a subset of the total volume is traded within the day ahead market. Therefore, we believe the information in bid and offer data to be more relevant for our purposes.

Consequently, the aim is to estimate the bid stack parameters  $\{k_c, k_g, m_c, m_g, \bar{\xi}_c, \bar{\xi}_g, m_N, m_S\}$  based on historical bid and offer data of EPEX Spot. However, we assume historical renewables and nuclear production  $\hat{\xi}_R$  to be naturally given by fundamental data (EEX transparency website; cf. Chapter 2.3).



### The Idea

As proposed by [Coulon et al., 2014], several steps have to be performed in order to transfer the EPEX Spot data into a format which can be used to calibrate our structural model. We perform the following steps for a certain hour of a day:

1. Transform bid and offer curves  $(s, d)$  (i.e. from EPEX for German market; cf. Figure 4.3, left) into a price curve  $p$  with inelastic demand: It has to be calculated ( $\xi \hat{=}$  Demand,  $y \hat{=}$  Power Price,  $p_{min} \hat{=}$  Lowest bid/offer price,  $p_{max} \hat{=}$  Highest bid/offer price; cf. Figure 4.3, mid)

$$y = \hat{p}(\xi) \quad \xi = s^{-1}(y) + d^{-1}(p_{min}) - d^{-1}(y) - \hat{\xi}_R. \quad (4.5)$$

We slightly adjust the price curve by defining

$$p(\xi) := \hat{p}(\xi - \min\{\hat{p}^{-1}(0), 0\}).$$

Consequently, negative prices can only occur for negative residual demand.

2. Define  $[\underline{p}_{TS}, \bar{p}_{TS}]$  by  $\underline{p}_{TS} := p(0)$  and  $\bar{p}_{TS} := p(\bar{\xi})$ . Furthermore, we define

$$[d_{min}, d_{max}] := [p^{-1}(p_{min}), p^{-1}(p_{max})]$$

and  $\bar{d} := d_{max} - d_{min}$

3. We concentrate on in  $\hat{\xi} \in [0, \bar{\xi}]$  (thermal stack): scale the demand between 0 and 1 by

$$\xi = \omega(\hat{\xi}) := \frac{\hat{\xi}}{d_{max} - d_{min}} \in \left[0, \frac{\bar{\xi}}{d_{max} - d_{min}}\right],$$

we denote  $\bar{p}$  to be the price curve acting on  $[0, \frac{\bar{\xi}}{d_{max} - d_{min}}]$  with  $\bar{p} = p \circ \omega^{-1} : [0, \frac{\bar{\xi}}{d_{max} - d_{min}}] \rightarrow [\underline{p}_{TS}, \bar{p}_{TS}]$ .

4. Interpret the price curve as the inverse of a distribution function  $\Phi_{BS} : [\underline{p}_{TS}, \bar{p}_{TS}] \rightarrow [0, \frac{\bar{\xi}}{d_{max} - d_{min}}]$  conditioned on  $S_t^{(c)}, S_t^{(g)}, \xi_R$ .
5. Use the idea of a mixture density network (MDN; cf. [Bishop, 1994]) to estimate the conditional density function  $\phi_{BS}$  of  $\Phi_{BS}$  (cf. Figure 4.3, right) with a maximum likelihood estimator. By construction, we get

$$\int_{\underline{p}_{TS}}^{\bar{p}_{TS}} \phi_{BS}(y | S_t^{(c)}, S_t^{(g)}, \xi_R) dy = \frac{\bar{\xi}}{d_{max} - d_{min}}.$$

The remaining mass  $1 - \frac{\bar{\xi}}{d_{max} - d_{min}}$  is later used to approximate the spikes part and negative demand part.

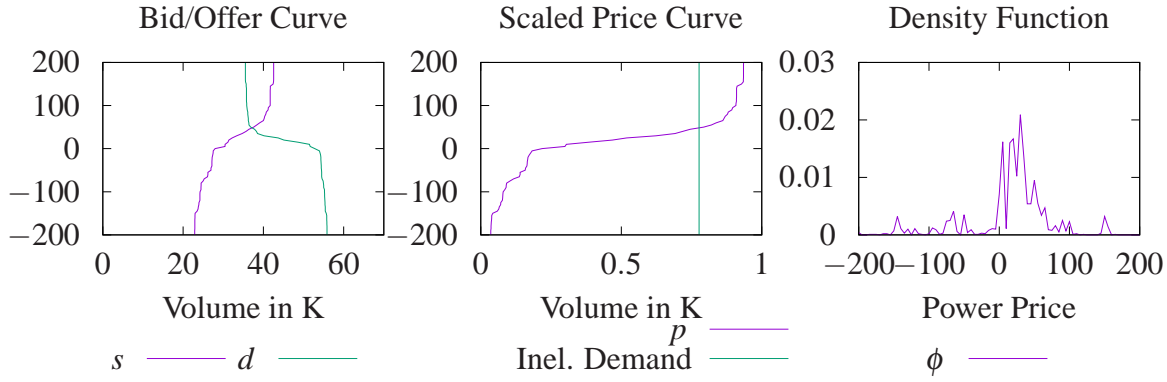


Figure 4.3: Example of a bid and offer curve at Epex Spot as of December, 8th 2015 (09:00h; German market) (left), its transformation into a price curve with inelastic demand (mid) and the implied density function

### Derivation of the Implied Bid Stack Density Function

The following calculations to derive an implied bid stack density function are not part of [Coulon et al., 2014]. We believe it to be the first time that the implied bid stack density function of the structural model in Chapter 2.1 is derived.

We intend to use a maximum likelihood estimator to estimate the MDN. In order to measure our model parameters as directly as possible, we derive a mixture density function which is implied from the our bid stack for function (Chapter 2.1):

We define  $\mathbf{z} := (S_t^{(c)}, S_t^{(g)}, \xi_R)$  and intent to estimate a density function  $\phi_{BS}(y|\mathbf{z})$  using a sum of density functions  $\phi_c, \phi_g, \phi_N, \phi_S$  such that

$$\phi_{BS}(y|\mathbf{z}) := \sum_{i \in I} \phi_i(y|\mathbf{z}) + \phi_N(y|\mathbf{z}) + \phi_S(y|\mathbf{z}), \quad (4.6)$$

where each density has to reflect the according part of the exponential bid stack. We start with the derivation of  $\phi_c, \phi_g$ :

Based on step four of the above stated transformation (cf. Figure 4.3, right), the inverse of the single exponential bid stack for the fuels  $b_i$  ( $i = c, g$ ; cf. Chapter 2.1) can be interpreted as a distribution function

$$\Phi_i(p|\mathbf{z}) := \int_a^p \phi_i(y|\mathbf{z}) dy, \quad a > 0.$$

For  $\xi \in [0, \bar{\xi}_i/\bar{d}]$  and  $p \in [p_{TS}, \bar{p}_{TS}]$ , we get the restriction

$$p = \Phi_i^{-1}(\xi|\mathbf{z}) \stackrel{!}{=} S_t^{(i)} \exp(k_i + m_i \bar{d} \xi).$$

This is equivalent to

$$\xi = \frac{\ln(p) - k_i - \ln(S_t^{(i)})}{m_i \bar{d}} = \int_{S_t^{(i)} \exp(k_i)}^p \frac{1}{m_i \cdot \bar{d} \cdot y} dy.$$

Therefore, we define

$$\phi_i(y|\mathbf{z}) := \begin{cases} 0 & , \text{ for } y < S_t^{(i)} \exp(k_i) = b_i(0, S_t^{(i)}) \\ \frac{1}{m_i \cdot \bar{d} \cdot y} & , \text{ for } y \in [b_i(0, S_t^{(i)}), b_i(\bar{\xi}_i, S_t^{(i)})] \\ 0 & , \text{ for } y > b_i(\bar{\xi}_i, S_t^{(i)}). \end{cases}$$

Due to  $\sum_{i \in I} \bar{\xi}_i = \bar{\xi}$  it follows

$$\int_{\underline{p}_{TS}}^{\bar{p}_{TS}} \phi_{BS}(y|\mathbf{z}) dy = \sum_{i \in I} \int_{\underline{p}_{TS}}^{\bar{p}_{TS}} \phi_i(y|\mathbf{z}) dy = \sum_{i \in I} \bar{\xi}_i / \bar{d} = \frac{\bar{\xi}}{\bar{d}}.$$

In order to end up with a distribution with probabilities from 0 to 1, the remaining mass  $1 - \bar{\xi}/\bar{d}$  is used to calibrate against negative prices  $b_N$  (mass:  $-d_{min}/\bar{d}$ ) and price spikes  $b_S$  (mass:  $(d_{max} - \bar{\xi})/\bar{d}$ ).

The derivation of the according density functions  $\phi_N, \phi_S$  is given at the end of this Chapter (cf. Chapter 4.5).

### Normal Density Function: An Intermediate Step

Because  $\phi_{BS}(y|\mathbf{z})$  is not differentiable with respect to

$$\theta := (k_c, k_g, m_c, m_g, \bar{\xi}_c, \bar{\xi}_g, m_N, m_S)$$

due to the non-differentiable indicator function, maximum likelihood methods are difficult to apply<sup>5</sup>. This is the reason why we perform an intermediate step and replace  $\phi_{BS}(y|\mathbf{z})$  by a sum of unconditioned, weighted normal densities  $\phi_{ND}(y)$ .

We use a sum of univariate and independent normal density functions  $\phi_{\mu_i, \sigma_i^2}, \dots, \phi_{\mu_S, \sigma_S^2}$  with  $S > 0$  to define a mixture density function

$$\phi_{ND}(y) := \sum_{i=1}^S \omega_i \cdot \phi_{\mu_i, \sigma_i^2}(y),$$

where  $\sum_{i=1}^S \omega_i = 1$  and  $\omega_i > 0 \ \forall i = 1, \dots, S$ .

Let  $(d_i, p_i)$  ( $i = 1, \dots, N$ ) denote all bid-price pairs leading - when stacked - to the price curve  $p$ <sup>6</sup>. The tuple is calculated from observable bid and offer data by the above transformation in (4.5).

We use a maximum likelihood estimator to estimate

$$\mathbf{w}^N := (\mu_1^N, \dots, \mu_S^N, \sigma_1^N, \dots, \sigma_S^N, \omega_1^N, \dots, \omega_S^N).$$

The likelihood function is

$$\mathcal{L}_{MDN}(\mathbf{w}) = \sum_{i=1}^N d_i \cdot \log \{ \phi_{ND}(p_i) \} \quad (4.7)$$

<sup>5</sup>For a maximum likelihood estimator directly applied to the defined density functions, we refer to the end of this Chapter (cf. Chapter 4.6).

<sup>6</sup>As done in [Coulon and Howison, 2009], we assume a bit of  $d_i$  MW to be  $d_i$  separate observations of 1 MW bids.

and was introduced in [Coulon and Howison, 2009]. A consistent estimator for the empirical Fisher information matrix  $(i, j = 1, \dots, 3S)$  is given by

$$I_{MDN}^{(i,j)} = \sum_{k=1}^N \left[ d_k \cdot \frac{\partial}{\partial(\mathbf{w})_i} \log\{\phi_{ND}(p_k)\} \frac{\partial}{\partial(\mathbf{w})_j} \log\{\phi_{ND}(p_k)\} \right] - \frac{1}{N} \sum_{k=1}^N \left[ d_k \cdot \frac{\partial}{\partial(\mathbf{w})_i} \log\{\phi_{ND}(p_k)\} \right] \cdot \sum_{k=1}^N \left[ d_k \cdot \frac{\partial}{\partial(\mathbf{w})_j} \log\{\phi_{ND}(p_k)\} \right].$$

For more information on maximum likelihood estimation and the calculation of the information matrix, we refer to [McLachlan and Krishnan, 2008] and [Scott, 2002] respectively.

**Remark 4.5** *The construction of the implied bid stack density restricts the total mass of all densities with negative mean to equal  $-\frac{d_{\min}}{d_{\max}-d_{\min}}$ . Therefore, weights of normal densities with negative mass have to sum up to that value. For simplicity, we impose the MDN problem to have one single density with negative mean and  $S-1$  densities with positive means.*

*Additionally, we want to avoid densities with positive mean to have too much mass for negative prices (only the first density should have negative mass). Therefore, we decided to restrict the mean to be at least twice of the volatility. This leads the distribution function to have a maximum of 4.55% mass for negative prices.*

In order to keep track of the restrictions on weights and volatilities, we use the following parametrization (for the weights, we adapted the approaches in [Alexandrovich, 2014] and [Bishop, 1994]):

$$\left\{ \begin{array}{ll} \mu_1 := -\exp(\alpha_1^\mu) & \\ \mu_i := 2\sigma_i + \exp(\alpha_i^\mu) & , i = 2, \dots, S \\ \sigma_i := \exp(\alpha_i^\sigma) & , i = 1, \dots, S \\ \omega_i := \frac{\exp(\alpha_i^\omega)}{\sum_{j=2}^{S-1} \exp(\alpha_j^\omega) + 1} \cdot (1 - \omega_1) & , i = 2, \dots, S-1 \\ \omega_S := 1 - \sum_{i=1}^{S-1} \omega_i & \end{array} \right\}. \quad (4.8)$$

Here,  $\alpha_i^\mu, \alpha_i^\sigma, \alpha_i^\omega \in \mathbb{R}$  for  $i = 1, \dots, S$ . Because  $\omega_1$  is known from the bid data (cf. Remark 4.5) and  $\omega_S$  is calculated using the other weights, both deliver no additional degree of freedom. This is why we assume  $\alpha^\omega \in \mathbb{R}^{S-2}$  in the following. It reveals to be much easier to calculate the Fisher Information matrix  $I_{MDN}$  in terms of this parametrization (i.e. no constraints on parameters):

$$I_{MDN, \alpha}^{(i,j)} = \sum_{k=1}^N \left[ d_k \cdot \frac{\partial}{\partial(\alpha)_i} \log\{\phi_{ND}(p_k)\} \frac{\partial}{\partial(\alpha)_j} \log\{\phi_{ND}(p_k)\} \right] - \frac{1}{N} \sum_{k=1}^N \left[ d_k \cdot \frac{\partial}{\partial(\alpha)_i} \log\{\phi_{ND}(p_k)\} \right] \cdot \sum_{k=1}^N \left[ d_k \cdot \frac{\partial}{\partial(\alpha)_j} \log\{\phi_{ND}(p_k)\} \right], \quad (4.9)$$

where  $\alpha := ((\alpha^\mu)^T, (\alpha^\sigma)^T, (\alpha^\omega)^T)$  and  $\mathbf{I}_{MDN, \alpha} \in \mathbb{R}^{(3S-2) \times (3S-2)}$ .

Maximizing (4.7) is time-consuming as it takes time to find appropriate start values for the optimization procedure (local vs. global maximum). In order to cope with that, we decided to optimize in two steps: (1) perform 10.000 paths of simulated annealing (we use the Mersenne Twister to include randomness) and (2) use the result to start a BFGS optimizer. Both algorithms were taken from the QuantLib library. Alternatively, we could have used i.e. a penalized Newton method or an EM algorithm as it was compared in [Alexandrovich, 2014].

We perform the estimation for each hour (overall  $T$  hours) in the data panel which yields for  $t = 1, \dots, T$  according vectors  $\alpha_t^N$  and  $\mathbf{z}_t$ .

### From Normal Densities to the Implied Bid Stack Density

In the next step, we estimate

$$\theta^{N,T} := (k_c^{N,T}, k_g^{N,T}, m_c^{N,T}, m_g^{N,T}, \bar{\xi}_c^{N,T}, \bar{\xi}_g^{N,T}, m_N^{N,T}, m_S^{N,T})$$

based on  $\alpha_t^N$  and  $\mathbf{z}_t$  (for  $t = 1, \dots, T$ ). In literature (i.e. [Wooldridge, 2010]), estimators like  $\theta^{N,T}$  are called *two-step-estimators*<sup>7</sup>. The estimator  $\theta^{N,T}$  in the second step is a M-estimator using the estimator  $\alpha_t^N$  with observables  $\mathbf{z}_t$  as input.

**Remark 4.6** As illustrated in [Coulon et al., 2014],  $S = 7$  delivers appropriate estimation results for the German power market. This large number is also supported by fundamentals: we know the power market to be at least driven by renewables, nuclear, lignite, hard coal, gas and oil. This is why the authors in [Coulon et al., 2014] generalize the exponential bid stack in Chapter 2.1 to more than two marginal fuels.

In order to test our algorithm, we indeed use  $S = 7$  to estimate the normal densities. However, we only work with four bid stack density functions:  $\phi_c, \phi_g, \phi_N, \phi_S$ .

As a result, we have to establish an algorithm on how to link a normal density to a bid stack density function. We decided to group several densities and either allocate a normal density to belong to gas or coal. There are several approaches to do that. We simply defined an interval for coal  $[2, 35]$  and for gas  $[35, 52]$ . Normal densities with mean in those intervals belong to the according fuel. Finally, we allocated all densities with mean higher than the gas interval to belong to the spike part.

We denote the resulting sets to store which normal density belongs to a which fuel by  $\Xi^i$  for  $i = c, g$ . For instance, it may hold  $\Xi_t^c = \{2, 3\}$  and  $\Xi_t^g = \{4, 5\}$ .

By doing that, capacities  $\xi_i$  ( $i \in I$ ) are directly implied by the weights:

$$\bar{\xi}_i = \frac{1}{T} \sum_{t=1}^T \sum_{j \in \Xi_i^t} \omega_t^j(\alpha_t^N) \cdot \bar{d}.$$

<sup>7</sup>We note that additional complexities arise because  $\alpha_t^N$  is based on a time series in  $N$  (cross section) and  $\theta^{N,T}$  on a time series in  $T$

In order to come from normal distributions to the implied bid stack distribution (cf. (4.6)), we use a modification of the Wasserstein distance applied to the cumulative distribution function:

$$\begin{aligned}\theta^{N,T} &= \arg \min_{\theta} \left\{ \sum_{t=1}^T \int_{p_{\min}}^{p_{\max}} \left| \Phi_{ND}^{(t)}(y) - \Phi_{BS}(y; \mathbf{z}_t) \right| dy \right\} \\ &=: \arg \min_{\theta} \{ \Psi_{BS,WD}(\theta, \mathbf{z}, \alpha_1^N, \dots, \alpha_T^N) \}.\end{aligned}\quad (4.10)$$

The following constraints on  $\theta$  have to hold:

$$\left\{ \begin{array}{l} k_c \in \mathbb{R} \\ k_g \in \mathbb{R} \\ m_c > 0 \\ m_g > 0 \\ m_N > 0 \\ m_S > 0 \\ \bar{\xi}_c > 0 \\ \bar{\xi}_g > 0 \end{array} \right\}$$

To solve the problem we use a BFGS optimizer in QuantLib. Additionally, we use Simulated Annealing to find an appropriate start value for the optimizer (QuantLib).

**Remark 4.7** *The estimation approach leads to the estimation of the thermal stack bid stack parameters from historical data. However, bid stack parameters have maximal freedom degree, i.e.  $k_i \in \mathbb{R}$  for  $i \in I$ . In order to transfer more information of the normal densities into the bid stack parameters, it may for instance be decided to include the term*

$$\sum_{i \in I} \sum_{t=1}^T \frac{\left[ k_i - \log \left( \frac{\sum_{j \in \Xi_i^t} \omega_j^i(\alpha_i^N) (\mu_j^i(\alpha_i^N) - \beta \sigma_j^i(\alpha_i^N))}{\sum_{j \in \Xi_i^t} \omega_j^i(\alpha_i^N)} \right) + \log(S_t^{(i)}) \right]^2}{k_i^2}$$

into (4.10). It would cause  $k_i$  to be closely connected to density functions which belong to fuel  $i$ . For instance, a choice of  $\beta = 2$  would cause  $k_i$  to be close to the left tail of the according densities and therefore close to a power price where fuel  $i$  might produce electricity. In other words, it restricts the minimal power price for an according fuel power plant to be close to the average left tail of the fuels' mixture densities.

We analyze the impact of this additional restriction on parameter risk in Chapter 4.4.

The result of the fit for a single hour is depicted in Figure 4.4 (based on the price curve in Figure 4.3). The blue line depicts the fit of the final calibration of bid stack parameters using the modified Wasserstein distance. It can be seen that the fit for positive residual demand is quite close, even for the spike part of the price curve. The reason for the higher differences in case of negative demand is the structure of the curve in that area: it seems to rather be a linear trend on that date and hour instead an exponential one.

The estimated parameters are summarized in Table 4.2. Unless the estimators for  $m_N$  and  $m_S$ , we found the values to be in the region of our qualitative estimation summarized in Table 2.1.

A calculation was also performed for a data set of several dates (each Tuesday between 17th November 2015 - 15th December 2015). The results of the fit are depicted in Chapter 4.4. For the purpose of this paper, the quantification of parameter risk will be based on a calibration of one day and the parameters in Table 4.2 respectively.

Table 4.2: Estimated Bid Stack Parameters based on an estimation on 08/12/2015, hour 9 using data from EPEX Spot.

Parameters	Coal	Gas
$k$	$-\log(40) + \log(8.99)$	$-\log(14.9) + \log(30.43)$
$m$	0.072	0.12
$\bar{\xi}$	22.42	4.84
$m_N$		1.10
$m_S$		0.90

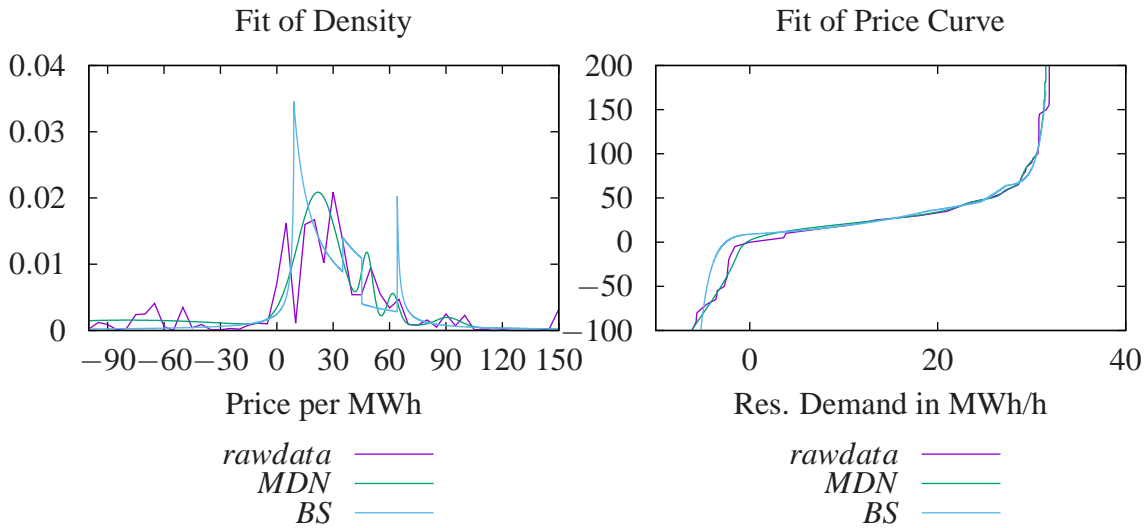


Figure 4.4: Normal MDN results together with the final calibrated exponential bid stack for the same day as being used in Figure 4.3 (left: fit of density; right: fit of price curve).

### Asymptotic Behavior of the Estimator and Parameter Risk

To calculate the asymptotic covariance matrix of  $\theta^{N,T}$ , we take  $T \ll N$  (as usual for panel data as proposed in [Wooldridge, 2010]). In that case, we interpret  $\theta^{N,T}$  in (4.10) (Wasserstein distance) as a function of  $\alpha_t^N$  and apply the delta method (cf. Appendix B.1). By doing that, we drop some of the complexity in the calculation of the asymptotic covariance. In detail, we neglect that we have used the

minimization of the adjusted Wasserstein-distance to come from  $\alpha_t^N$  to  $\theta^{N,T}$ . However, we believe the delta method to be an appropriate simplification for a first analysis.

To summarize, we have to calculate for each  $t = 1, \dots, T$  the inverse Fisher information matrix  $I_{MDN,\alpha}^{(t)} \in \mathbb{R}^{3S-2 \times 3S-2}$  in (4.9) of the normal MDN estimator in (4.7). We denote the gradient of  $\Psi_{BS,WD}(\theta, \mathbf{z})$  in (4.10) by

$$\nabla_{\alpha_1^N, \dots, \alpha_T^N} \Psi_{BS}(\theta, \mathbf{z}, \alpha_1^N, \dots, \alpha_T^N) \in \mathbb{R}^{(3S-2)T}.$$

Because different days (hours) are estimated independently from each other, the final Fisher- Information matrix  $I_{MDN,\alpha} \in \mathbb{R}^{(3S-2)T \times (3S-2)T}$  reveals - because of its score to be zero - to be a block matrix

$$I_{MDN,\alpha} = \text{diag}(I_{MDN,\alpha}^{(1)}, \dots, I_{MDN,\alpha}^{(T)}), \quad t = 1, \dots, T.$$

Consequently, the inverse is the inverse of the block matrices. Applying the delta method therefore leads to

$$\left( \nabla_{\alpha_1^N, \dots, \alpha_T^N} \Psi_{BS} \right)^T (I_{MDN,\alpha})^{-1} \nabla_{\alpha_1^N, \dots, \alpha_T^N} \Psi_{BS} = \sum_{t=1}^T \left( \nabla_{\alpha_t^N} \Psi_{BS} \right)^T \left( I_{MDN,\alpha}^{(t)} \right)^{-1} \nabla_{\alpha_t^N} \Psi_{BS}.$$

We summarize the results in the next Proposition.

**Proposition 4.3 (Asymptotic Covariance Matrix: Bid Stack Parameters)** *Let the two step estimator for the bid stack parameters in (4.10) be given. The asymptotic covariance matrix of  $\theta^{N,T}$  for fix  $T \in \mathbb{N}$  and  $N \rightarrow \infty$  is then given by*

$$\sum_{t=1}^T \left( \nabla_{\alpha_t^N} \Psi_{BS} \right)^T \left( I_{MDN,\alpha}^{(t)} \right)^{-1} \nabla_{\alpha_t^N} \Psi_{BS},$$

where  $I_{MDN,\alpha}^{(t)}$  is defined in (4.9).

**Proof.** The proposition is the result of prior calculations of Chapter 4.2.2. ■

In order to calculate parameter risk based on [Bannör et al., 2013], we have to calculate the first order derivatives of a contingent claim in direction of bid stack parameters. We give a short illustration in the next Section.

### Analysis of first order derivatives

For each bid stack parameter  $\vartheta \in \{k_c, k_g, m_c, m_g, \bar{\xi}_c, \bar{\xi}_g, m_N, m_S\}$ , we calculate

$$\frac{\partial PV_{\mathcal{T}}^{VPP}(h_R, K)}{\partial \vartheta} = \sum_{t \in \mathcal{T}} e^{-r(t-t_0)} \frac{\partial}{\partial \vartheta} \mathbb{E}^{\mathbb{Q}} \left[ (S_t^P - h_R \cdot S_t^F - K)^+ | \mathcal{F}_{t_0} \right].$$

In order to measure parameter risk appropriately, we believe to recalibrate our model against the power forward curve after a shift of a bid stack parameter. The reason is that even if we might have estimated the bid stack parameters inadequately, we are still calibrated against the power forward curve before starting our pricing. Only in case, we assume the power forwards not to be liquid, we would not recalibrate



our model after a shift. This approach is based on the same idea as being used later when we study the difference quotient method for calculating Greeks with a structural electricity model (cf. Chapter 6.2).

The results are depicted in Figure B.5 for a daily VPP for 2016. Compared to fuels' sensitivities in Figure B.4, the sensitivities are higher by a factor of more than 10. Compared to demand's sensitivities, the bid stack sensitivities are of similar dimension (cf. Figure B.6). However, in case of high expected demand, the derivative in direction of model parameters will be even higher; at least if (i) power forwards are illiquid and (ii) the model parameter belongs with high probability to the marginal fuel. Simplified, we would have to build the derivative of  $S_t^P = S_t^{(i)} \exp(k_i + m_i D_t)$  in direction of  $m_i$  leading to derivatives up to 500 and more (Figure B.5; i.e.  $D_t = 20MWh$  and  $S_t^P = 25$ ).

### 4.2.3 Demand Dynamic

Our aim is to estimate the demand dynamic based on a one year historical data set.

A first approach might be to directly estimate the dynamics of the expected demand  $\mu_{t,t+\tau}$  ( $\tau > 0$ ) by a maximum likelihood estimator from historical demand data. Using the expected demand dynamic in Proposition 3.1, we apply the Itô-Lemma to get ( $\tau > \Delta t > 0$ ;  $u_t^D$  similarly defined to Remark 4.1)):

$$\begin{aligned} \mu_{t+\Delta t,t+\tau} &= \mu_{t,t+\tau} + \int_t^{t+\Delta t} v_s^D \exp\left(-\int_s^{t+\tau} \alpha_u^D du\right) d\tilde{W}_s^D \\ \iff \Delta \mu_{t+\Delta t,t+\tau} &= \int_t^{t+\Delta t} v_s^D \exp\left(-\int_s^{t+\tau} \alpha_u^D du\right) dW_s^D. \\ \iff \Delta \mu_{t+\Delta t,t+\tau} &= -\int_t^{t+\Delta t} u_s^D v_s^D \exp\left(-\int_s^{t+\tau} \alpha_u^D du\right) ds + \int_t^{t+\Delta t} v_s^D \exp\left(-\int_s^{t+\tau} \alpha_u^D du\right) d\tilde{W}_s^D. \end{aligned}$$

The last equivalence again comes from switching from a Brownian motion under  $\mathbb{Q}$  to a Brownian motion under  $\mathbb{P}$  (Remark 4.1). Using the Itô-Isometry we conclude  $\Delta \mu_{t,t+\tau}$  to be normally distributed with variance

$$\begin{aligned} \sigma_\tau^2 &:= \int_t^{t+\Delta t} (v_s^D)^2 \exp\left(-2 \int_s^{t+\tau} \alpha_u^D du\right) ds \\ &=: f_\tau(v^D, \alpha^D) \end{aligned}$$

where  $v^D := (v_1^D, \dots, v_{d(\tau_M)}^D)$  and  $\alpha^D := (\alpha_1^D, \dots, \alpha_{d(\tau_M)}^D)$ . Again we estimate the model parameters completely from the variance  $f_\tau(v^D, \alpha^D)$  in order to avoid the incorporation of  $u_t^D$ .

For a given time series  $\mu_{t_0,t_0+\tau}, \dots, \mu_{t_N,t_N+\tau}$ , the maximum likelihood estimator is known to be

$$\hat{\sigma}_\tau^2 := \frac{1}{N} \sum_{i=1}^N (\Delta \mu_{t_i,t_i+\tau})^2 \quad (4.11)$$

and it holds

$$\sqrt{N}(\hat{\sigma}_\tau^2 - \sigma_\tau^2) \xrightarrow{\mathcal{D}} \mathcal{N}(0, 2\sigma_\tau^4).$$

**Remark 4.8 (Alternative Stochastic Differential Equation)** *As been explained in Remark 4.2, an alternative approach would be to derive  $d\mu_{t,t+\tau}$  instead of  $d\mu_{t,T}$  and to consider a running maturity of the forward price instead. It would lead to the following forward price dynamics:*

$$\begin{aligned} \mu_{t+\Delta t,t+\Delta t+\tau} = & \mu_{t,t+\tau} + \int_t^{t+\Delta t} \left[ \frac{\partial s^D(s+\tau)}{\partial t} - \alpha_{s+\tau}^D \exp\left(-\int_s^{s+\tau} \alpha_u^D du\right) Y_s \right] ds \\ & + \int_t^{t+\Delta t} v_s^D \exp\left(-\int_s^{s+\tau} \alpha_u^D du\right) d\tilde{W}_s^D \end{aligned}$$

Again, we believe it to be more tractable to automatically eliminate seasonality by comparing  $\mu_{t+\Delta t,t+\tau}$  to  $\mu_{t,t+\tau}$  in the data series.

As been stated in Chapter 3.4.2, we prefer to calibrate the demand process such that the induced power forward dynamic reflects historical power forward price volatility. Additionally, we intend to calibrate against forward prices with different maturities  $0 < \tau_1 < \dots < \tau_M$ . Therefore, we use the analytical power forward price formula in [Carmona et al., 2013] to manually derive an artificial time series of the implicit demand:

$$\mu_{t,t+\tau_j} := F_{BS}^{-1}(F_{t,t+\tau_j}^c, F_{t,t+\tau_j}^g; \cdot)(F_{t,t+\tau_j}^P)$$

Consequently, the demand time series  $\mu_{t_0,t_0+\tau_j}, \dots, \mu_{t_N,t_N+\tau_j}$  is implied by observable historical time series data of power forward and fuel forward prices  $F_{t_0,t_0+\tau_j}^i, \dots, F_{t_N,t_N+\tau_j}^i$  for  $i = c, g, P$  and  $j = 1, \dots, M$ . However,  $F_{BS}$  depends on demand volatility and therefore on the volatility process  $v^D$  and mean-reversion process  $\alpha^D$  respectively (cf. Chapter 2.2). Therefore, (4.11) becomes<sup>8</sup>

$$f_{\tau_j}(v^D, \alpha^D) = \frac{1}{N} \sum_{t=1}^N \left( \Delta F_{BS}^{-1}(F_{t,t+\tau_j}^c, F_{t,t+\tau_j}^g; \cdot)(F_{t,t+\tau_j}^P; v^D, \alpha^D) - \overline{\Delta F_{BS}^{-1}} \right)^2 \quad (4.12)$$

which we solve in direction  $\alpha^D$  ( $v^D$  assumed to be fix and known) by applying Newton's method. In order to calculate the asymptotical distribution, we rearrange (4.12) and define:

$$\begin{aligned} \frac{1}{N} \sum_{t=1}^N \left[ \underbrace{f_{\tau_j}(v^D, \alpha^D) - \left( \Delta F_{BS}^{-1}(F_{t,t+\tau_j}^c, F_{t,t+\tau_j}^g; \cdot)(F_{t,t+\tau_j}^P; v^D, \alpha^D) - \overline{\Delta F_{BS}^{-1}} \right)^2}_{=: \Psi(F_{t,t+\tau_j}^c, F_{t,t+\tau_j}^g, F_{t,t+\tau_j}^P, v^D, \alpha^D)} \right] &= 0 \quad (4.13) \\ \iff \mathbb{P}_N \left( \Psi(F_{t,t+\tau_j}^c, F_{t,t+\tau_j}^g, F_{t,t+\tau_j}^P, v^D, \alpha^D) \right) &= 0 \end{aligned}$$

In order to derive time-dependent variables  $\alpha_t^D$ , we model  $\alpha_t^D$  as a piecewise constant function (as been done for the fuels' dynamics in Remark 4.3). We assume  $v_t^D$  to be known.

**Proposition 4.4 (Asymptotic Covariance Matrix: Demand Forwards Estimation)** *We assume  $v^D \equiv v^D > 0$  to be known and solve (4.13) for  $j = 1, \dots, M$  iteratively to get a time dependent mean-reversion speed  $\alpha^D := (\alpha_1^D, \dots, \alpha_M^D)$  from of  $M$  different implied demand time series  $\mu_{t_0,t_0+\tau_j}, \dots, \mu_{t_N,t_N+\tau_j}$  ( $j = 1, \dots, M$ ).*

<sup>8</sup>We use the notation  $\overline{\Delta F_{BS}^{-1}}$  to denote the mean of the expected demand time series  $\mu_{t,T}^D$ .

Then, the estimator  $\hat{\alpha}^D$  is asymptotically normal for  $N \rightarrow \infty$  with covariance matrix

$$(\mathbb{P}\Psi)^{-1} \mathbb{P}(\Psi\Psi^T) (\mathbb{P}\Psi)^{-T},$$

where we denote  $\mathbb{P}\Psi := \mathbb{P} \left[ \Psi \left( F_{t,t+\tau_j}^c, F_{t,t+\tau_j}^g, F_{t,t+\tau_j}^P, v^D, \alpha^D \right) \right]$ .

**Proof.** (4.13) defines an Z-estimator which is why the Proposition follows from Theorem 5.21 in [van der Vaart, 2000] (and Appendix B.1 respectively). ■

**Remark 4.9 (Choice of  $v^D$ )** In Section B.3, we show that demand volatility  $v^D > 0$  has to be chosen such that the implied power spot volatility of the model equals historical power spot volatility. In order to build an according estimator based on historical data, we would be obliged to calculate an implied demand time series using the inverse of the bid stack function:

$$D_t := f_{bs}^{-1}(\cdot, \mathbf{S}_t^F)(S_t^P).$$

However, we cannot ensure  $f_{bs}^{-1}(\cdot, \mathbf{S}_t^F)$  to be well-defined in general (i.e. the bid stack function may contain jumps). This is the reason why we skip an according analysis in the following.

The calibration results are depicted in Figure 4.5. In Figure 4.6, we observe the common known Samuelson effect. However, we observe it for the implied demand dynamic. Therefore, the Samuelson effect in the power futures data translates into a Samuelson effect in the implied demand dynamic.

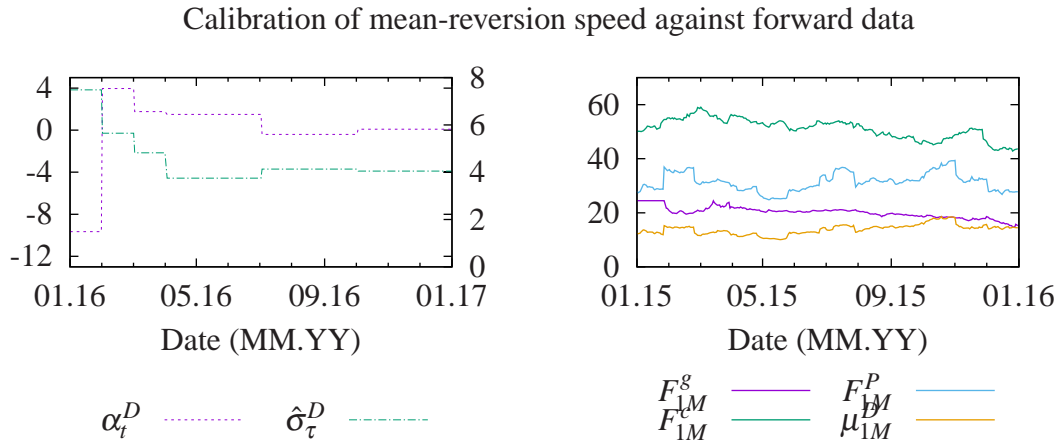


Figure 4.5: left: Calibration of mean-reversion speed parameter  $\alpha_t^D$  using a stepwise function (Remark 4.3) and the calibration results for the fuels in Figure 4.1(left axis); estimated future volatility on right axis. We used the following generic power futures prices from Bloomberg for estimation: 1st, 2nd, 3rd Month; 2nd, 3rd, 4th Quarter; historical daily data of 2015; Volatility was assumed to be 5 MWh. right: result for the corresponding demand time series for 2015 (orange: in MWh/h), we picked the front month futures as an example (in EUR/MWh).

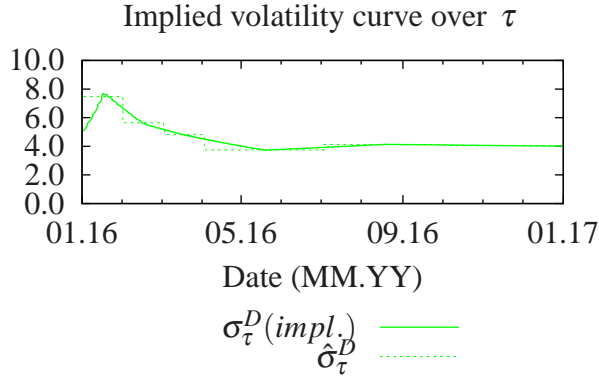


Figure 4.6: Implied volatility function of demand based on the estimation results in Figure 4.5

**Remark 4.10 (Quotation of volatility)** *We believe it important to note that the implied volatility is not quoted in percent as usual. The reason is that we do not model the demand returns (may be interpreted as percent) but instead the actual demand differences (raw Ornstein-Uhlenbeck-process). Consequently, our demand volatility naturally depends on the measurement of the demand. For the purpose of this paper we use MWh/h.*

### 4.3 Numerical Results for Parameter Risk

In this chapter we calculate parameter risk numerically based on the calibrations derived in the prior Chapters. Consequently, each parameter of the model (cf. Chapter 2) is either estimated from historical data or derived from a power forward curve (seasonality  $s^{(i)}(t), s^D(t)$ ,  $i \in I$ ). In detail, we used the historical forwards estimation in Chapter 4.2.1 and 4.2.3 to estimate fuels' and demand dynamics and Chapter 4.2.2 to estimate the exponential bid stack. The bid stack was estimated based on a one day history (for several days, we refer to Chapter 4.4).

In order to quantify parameter risk, we use the approach in Chapter 4.1. Therefore, the level of parameter risk will be based on the choice of a certain quantile  $\alpha \in (0, 1)$ . We will use 1% and 5% in the following. We start with some consistency checks to validate the implementation. For this purpose, we start analysing parameter risk when pricing power forward contracts (Chapter 4.3.1).

Afterwards, all quantifications in this Chapter are based on the pricing of a virtual coal power plant. For our analysis we assumed  $\mathcal{T}$  to contain a certain hour for the first half of the year 2016 (i.e. 08:00-09:00h) using  $t_0 = 31/12/2015$ ,  $h_R = 0.3 \left[ \frac{mt(\text{Coal})}{MWh(\text{Power})} \right]$ ,  $r = 0$  and  $K = 15$ . The valuation will be done with the help of a Monte Carlo method with 1.000.000 paths. In order to get used with the principle of implied demand, Figure 4.7 depicts the implied demand seasonality for hour 06:00-07:00 and 08:00-09:00 respectively of each Tuesday in 2016 based on the calibrated bid stack parametrization in Table 4.2.

The intrinsic value for hour 08:00-09:00 is 243.58 EUR/MWh and 23.14 EUR/MWh for hour 7.

**Remark 4.11** *It is well known that the bid stack for certain hours and weekdays is different from one*

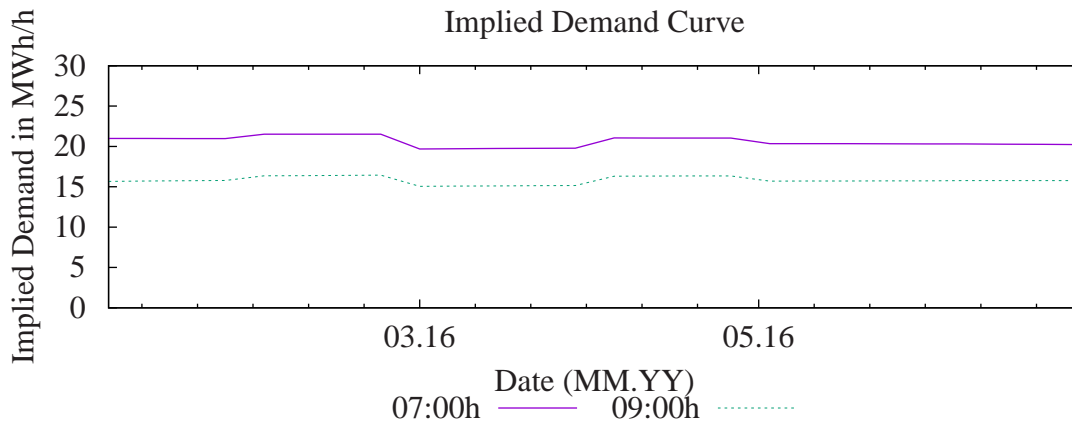


Figure 4.7: Implied demand by the price forward curves of Figure 2.1.

another (cf. [Coulon et al., 2014] for the German day ahead auction market). Consequently, a practitioner may build cluster of certain hours of a day and weekdays of a week. Afterwards, he or she may estimate different bid stack parameters for each cluster.

However, to illustrate the approach we believe it to be sufficient to concentrate on one of that clusters. We picked the morning hour from 08:00h to 9:00h on a typical Tuesday of the German day ahead auction market. In some cases we compare to hour 06:00 to 07:00.

### 4.3.1 Uncertainty in Price Forward Curves and Monte Carlo Risk

In order to validate the implementation -, we simply start to choose the payoff function to be an hourly power forward. We expect parameter risk for an hourly forward curve which belongs to liquid futures contracts to be zero<sup>9</sup> (high  $t_{PLTD}$ ). However, we will see that a Monte Carlo method leads to a non-zero risk due to convergence issues. We will call that risk *Monte Carlo risk*. For an hourly forward which to not belong to traded futures (low  $t_{PLTD}$ ), we expect to get a natural risk corridor surrounding the power forward curve.

We analyze both cases by calculating parameter risk in the bid stack parameters.

#### Monte Carlo Risk

Under the assumption of a high  $t_{PLTD}$ , we know electricity futures to be liquid. If we assume no uncertainty in the seasonality weights  $\beta_i$  ( $i = 1, \dots, 34$ ) of the hourly price forward curves, there is consequently no uncertainty about electricity forward prices. Our model should therefore calculate parameter risk of zero when pricing electricity forwards. In detail, the derivatives of the electricity forward prices in direction of model parameters should be zero. This should lead the algorithm in [Bannör et al., 2013]

<sup>9</sup>In practice, it might be equal to the assumption that a trader completely trusts the hourly pricing forward curve of the quant department, i.e. the hourly power forwards belong to liquid futures and daily/weekly/monthly seasonalities are known.

to deliver a zero.

However, because we use a Monte Carlo method, the derivatives are calculated by an upwards and downwards bump of the according model parameters followed by according revaluations. Due to the finite amount of paths within Monte Carlo, the difference does not have to be zero leading to a certain bias.

By calculating parameter risk for a strip of forward contracts we can therefore quantify Monte Carlo risk in our model. The results based on bid stack parameter risk quantifications (Chapter 4.2.2) are depicted in Table 4.3. For the purpose of this analysis, we just summed up all hourly forward prices for the first half of the year 2016. The PV of the whole strip was used as a basis to calculate parameter risk. The results show that we can trust our pricing engine up to one basis point of the present value of the VPP.

High $t_{PLTD}$ , hour 7			
Conf. Int.	PV in EUR/MWh	Parameter Risk in EUR/MWh	Risk in Bps.
0.01	730.5	0.01	0.10
0.5	730.5	0.00	0.03
High $t_{PLTD}$ , hour 9			
Conf. Int.	PV in EUR/MWh	Parameter Risk in EUR/MWh	Risk in Bps.
0.01	951.0	0.08	0.81
0.5	951.0	0.02	0.24

Table 4.3: Quantification of Monte Carlo pricing risk (risk in bid stack parameters) for hour 7 and hour 9 of a Tuesday in 2016.

### Parameter Risk in Power Forward Curves

Under the assumption of a low  $t_{PLTD}$ , we assume electricity forwards to be illiquid. Technically speaking this leads the derivatives of the electricity forward prices in direction of model parameters to be unequal to zero. Consequently, this will cause parameter risk to be unequal to zero. By calculating parameter risk for the whole forward curve, we get a corridor of parameter risk surrounding the forward curve implied by uncertainty in the bid stack (Chapter 4.2.2).

As an example, we performed the calculation for hour 06:00-07:00 and hour 08:00-09:00 of all Tuesdays in 2016 in Figure 4.8. It can be seen that parameter risk is highest for hours with high expected demand (hour 08:00-09:00). However, even for hour 06:00-07:00, we get a high risk in forward prices of up to 20% of the forward price. We believe the high uncertainty to be mainly caused by high derivatives of the VPP in direction of bid stack parameters. The issue was already discussed at the end of Chapter 4.2.2. Economically, we might deduce that even a small uncertainty in bid stack parameters can lead to high uncertainty in forward prices due to the high slope of the bid stack for high demand.

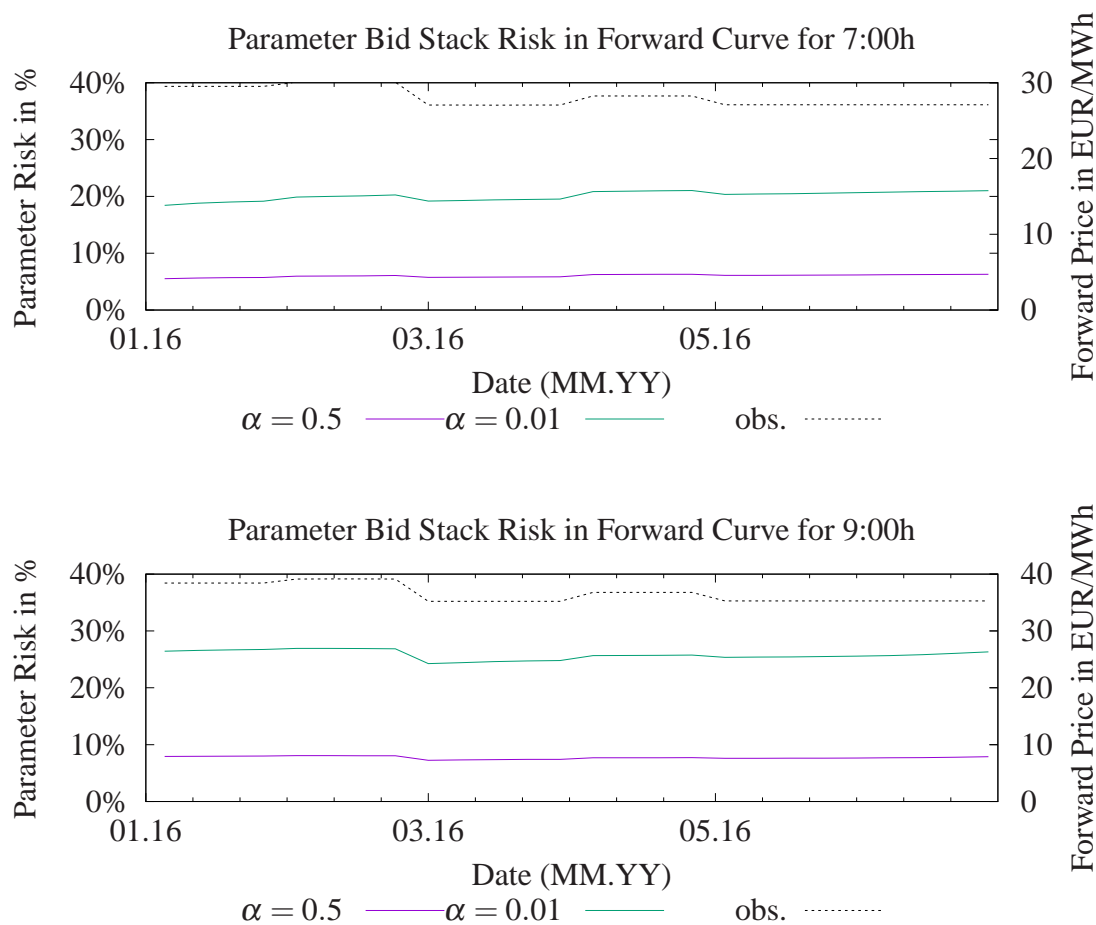


Figure 4.8: Bid Stack Parameter Risk of the power forward curve in Figure 2.1 for hour 7 and 9; green and purple lines are measured on left axis; black dashed line is measured on right axis.

### 4.3.2 Fuels Dynamics

We proceed to quantify parameter risk for the given virtual power plant with heat rate and strike given at the beginning of this Chapter.

#### Spot Calibration

Parameter risk applied to the VPP is calculated in Table 4.4 for two different choices of quantiles  $\alpha$ . Additionally, we quantified parameter risk for each payoff of the VPP separately (cf. Figure B.7). The according model parameter sensitivities are depicted in Figure B.3. It can be seen that the sensitivities are highest for coal volatility followed by gas volatility and fuel correlation.

High $t_{PLTD}$			
Conf. Int.	PV in EUR/MWh	Parameter Risk in EUR/MWh	Risk in Bps.
0.01	243.6	0.01	0.35
0.5	243.6	0.00	0.10
Low $t_{PLTD}$			
Conf. Int.	PV in EUR/MWh	Parameter Risk in EUR/MWh	Risk in Bps.
0.01	243.6	0.69	28.43
0.5	243.6	0.21	8.52

Table 4.4: Summary of the quantification of parameter risk in fuel dynamics for a coal VPP using the approach in [Bannör et al., 2013] (cf. Chapter 4.1) and historical spot estimation.

### Forward Calibration

The resulting parameter risk of the VPP can be found in Table 4.5 for different confidence levels  $\alpha > 0$ . By taking a separate view to each of the payoff functions of the VPP, parameter risk can be analyzed distributed over the lifetime of the contract. Results are depicted in Figure B.8, model sensitivities are depicted in Figure B.4.

Comparing the results in Table 4.5 to the spot estimation in Table 4.4, we at first see that the fair value of the VPP is roughly the same. The main reason is that the VPP is far in the money for hour 08:00-09:00. For a high  $t_{PLTD}$ , parameter risk is increasing by a factor of 10 whereas parameter risk for a low  $t_{PLTD}$  remains the same.

High $t_{PLTD}$			
Conf. Int.	PV in EUR/MWh	Parameter Risk in EUR/MWh	Risk in Bps.
0.01	245.1	0.20	8.24
0.5	245.1	0.06	2.47
Low $t_{PLTD}$			
Conf. Int.	PV in EUR/MWh	Parameter Risk in EUR/MWh	Risk in Bps.
0.01	245.1	0.69	27.97
0.5	245.1	0.21	8.36

Table 4.5: Summary of the quantification of parameter risk in fuel dynamics for a coal VPP using the approach in [Bannör et al., 2013] (cf. Chapter 4.1) and historical forwards estimation.



### 4.3.3 Bid Stack Parameters

The results for a daily VPP (one hour for each day: 8:00h-9:00h) is depicted in Figure B.9. Aggregating all the payoff functions again to one final VPP, we get a quantification of parameter risk depicted in Table 4.6.

It can be deduced from Table 4.6 that risk in the bid stack is one of the leading risk factors in our model. Risk for low liquidity in power forwards is higher by a factor of at least 100 compared to risk in the fuels dynamics. The result is as expected. By assuming power forwards not to be liquidly traded, the bid stack parameters immediately have an exponentially impact on the payoff function. This especially holds for the modeling of spikes  $m_S$ . The curve is quite steep in the spike area leading small changes to have a significant effect on the payoff.

We have also performed an according calculation where the bid stack is not estimated against one bid stack but instead the bid stacks of five different days (Chapter 4.4). We calculated the parameter risk in bid stack parameters for power forwards of hour 06:00-07:00 and 08:00-09:00. It turns out that risk remains in a similar corridor.

High $t_{PLTD}$			
Conf. Int.	PV in EUR/MWh	Parameter Risk in EUR/MWh	Risk in Bps.
0.01	245.1	0.77	31.43
0.5	245.1	0.23	9.42
Low $t_{PLTD}$			
Conf. Int.	PV in EUR/MWh	Parameter Risk in EUR/MWh	Risk in Bps.
0.01	245.1	239.3	9763
0.5	245.1	71.64	2923

Table 4.6: Summary of the quantification of parameter risk in bid stack parameters for a coal VPP using the approach in [Bannör et al., 2013] (cf. Chapter 4.1; hour 08:00-09:00).

**Remark 4.12 (Different Parameter Risk for different hours a day)** *From a qualitative perspective, ones might argue that parameter risk in the bid stack might depend on how steep the bid stack is in the area of the expected electricity price. Whereas hour 08:00-09:00 of a day has quite a high weight compared to other hours of a day, the weight of hour 06:00-07:00 is lower leading our VPP to be roughly at the money for the year 2016. From Table 4.7 it can be seen that parameter risk in bid stack parameters is - at least for low power forwards liquidity - indeed lower than for hour 08:00-09:00.*

High $t_{PLTD}$			
Conf. Int.	PV in EUR/MWh	Parameter Risk in EUR/MWh	Risk in Bps.
0.01	54.38	8.19	1506
0.5	54.38	2.45	450.8
Low $t_{PLTD}$			
Conf. Int.	PV in EUR/MWh	Parameter Risk in EUR/MWh	Risk in Bps.
0.01	54.38	94.25	17330
0.5	54.38	28.22	5188

Table 4.7: Summary of the quantification of parameter risk in bid stack parameters for a coal VPP using the approach in [Bannör et al., 2013] (cf. Chapter 4.1) and historical forwards estimation in Chapter 4.2.1 and 4.2.3. However, we price a VPP for Tuesday, hour 06:00-07:00 (instead of hour 08:00-09:00).

#### 4.3.4 Demand Dynamic

Aggregated parameter risk in the demand dynamic for the whole VPP is summarized in Table 4.8 for hour 08:00-09:00 and in Table 4.9 for hour 06:00-07:00 respectively. It can be seen that parameter risk is slightly higher than risk in fuels and in the same dimension as the bid stack. Furthermore, hour 06:00-07:00 has higher parameter risk than hour 08:00-09:00 at least for power forwards assumed to belong to tradeable futures. One reason for that can be that hour 08:00-09:00 is far more in the money than hour 06:00-07:00. Consequently, hour 06:00-07:00 should naturally have a higher sensitivity regarding changes in volatility than hour 08:00-09:00. In detail, a spread option far in the money will have a positive payoff for most  $\omega \in \Omega$ , therefore the insurance against negative payoffs does not deliver any more value. However, we cannot conclude the same for a low  $t_{PLTD}$ . In this case, changes in volatility also result in changes in the payoff function (bid stack) making an analysis more complicated.

High $t_{PLTD}$			
Conf. Int.	PV in EUR/MWh	Parameter Risk in EUR/MWh	Risk in Bps.
0.01	245.1	3.47	141.4
0.5	245.1	1.04	42.35
Low $t_{PLTD}$			
Conf. Int.	PV in EUR/MWh	Parameter Risk in EUR/MWh	Risk in Bps.
0.01	245.1	25.51	1040
0.5	245.1	7.64	311.6

Table 4.8: Summary of the quantification of parameter risk in demand for a coal VPP using the approach in [Bannör et al., 2013] (cf. Chapter 4.1) and historical forwards estimation (hour 08:00-09:00).

High $t_{PLTD}$			
Conf. Int.	PV in EUR/MWh	Parameter Risk in EUR/MWh	Risk in Bps.
0.01	54.38	7.08	1301
0.5	54.38	2.12	389.5
Low $t_{PLTD}$			
Conf. Int.	PV in EUR/MWh	Parameter Risk in EUR/MWh	Risk in Bps.
0.01	54.38	10.63	1955
0.5	54.38	3.18	585.3

Table 4.9: Summary of the quantification of parameter risk in demand and historical forwards estimation (hour 06:00-07:00 instead of hour 08:00-09:00).

## 4.4 An Extension - Bid Stack Estimation and Parameter Risk for Several Days

The prior evaluations have been performed based on a one-day bid stack estimator. In this Chapter, we show practically that it is indeed possible to calibrate against several dates and to quantify parameter risk afterwards.

As an example we took the time frame from 17th November 2015 from 15th December 2015 leading to altogether five Tuesdays. We intend to estimate a bid stack for hour 06:00-07:00h and 08:00-09:00h. The results are depicted in Figure 4.9. It can clearly be seen that the calibrated bid stack is in the middle of all bid stacks in scope of the estimation. The parameters are depicted in Table 4.10.

As a next step we calculate parameter risk in the bid stack parameters of the hourly power forward curve. For the optimization procedure in (4.10) we include the additional restriction of Remark 4.7 using  $\beta = 2$ . The results are depicted in Figure 4.10. Because the bid stack becomes slightly steeper for power prices at roughly 30 to 35 EUR/MWh (cf. Figure 4.9; right), it is reasonable that parameter risk increases slightly for long term deliveries (compared to Figure 4.8). However, for short term deliveries parameter risk reduces strongly. The reason is that we included the additional restriction for  $k_i$  for  $i \in I$  (Remark 4.7). The restriction reduces uncertainty about the bid stack factors and therefore parameter risk.

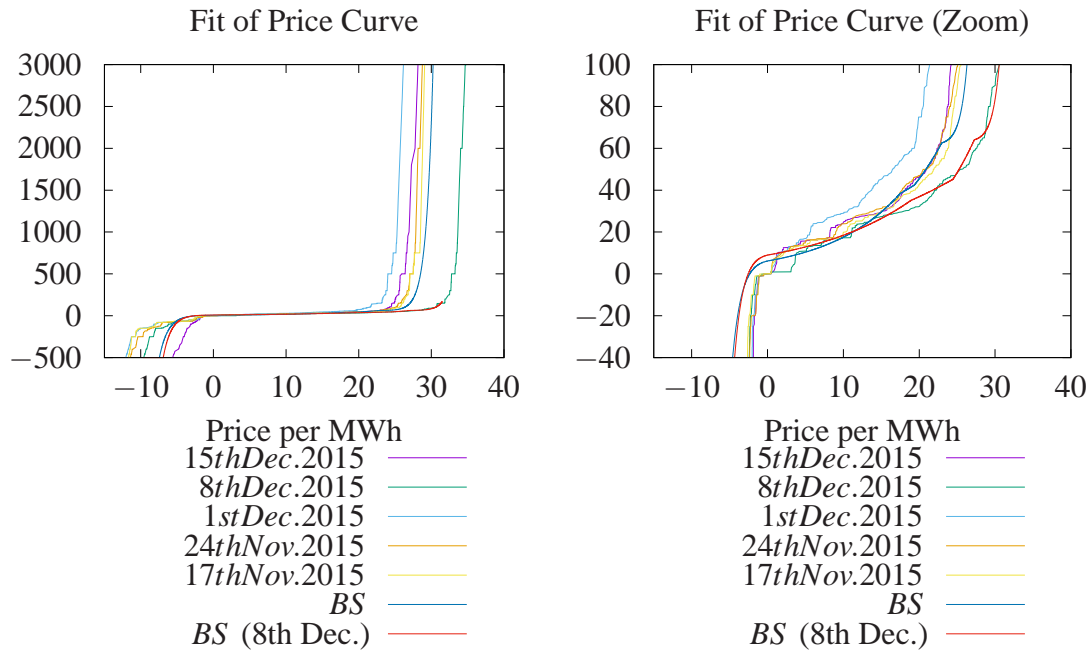


Figure 4.9: Estimation of a bid stack based on 5 different Tuesdays in November and December 2015.

Table 4.10: Estimated Bid Stack Parameters based on an estimation from 17th November until 15th December 2015, hour 9 using data from EPEX Spot.

Parameters	Coal	Gas
$k$	$-\log(40) + \log(6.16)$	$-\log(14.9) + \log(34.08)$
$m$	0.10	0.11
$\bar{\xi}$	18.45	4.53
$m_N$		1.10
$m_S$		0.84

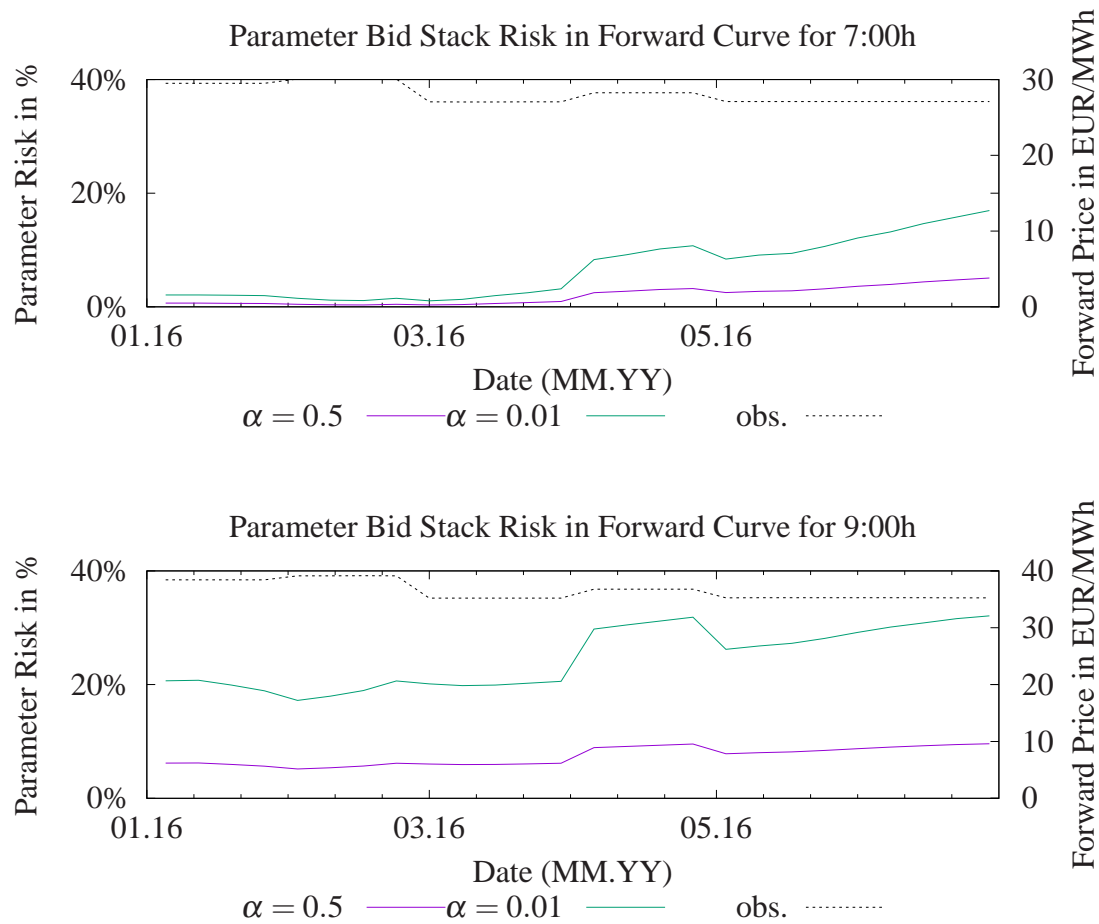


Figure 4.10: Parameter Risk in Bid Stack to measure risk in power forward curve. Estimation of bid stack was done using several bid and offer curves of different Tuesdays in winter 2015 (cf. Figure 4.9).

## 4.5 Derivation of the Density Function implied by an Exponential Bid Stack

### 4.5.1 Bid Stack Parameters for Negative Demand

After the calculation of the price curve in (4.5), we have to estimate  $b_N$  on  $\xi \in [d_{min}, 0]$ . In order to be able to interpret  $b_N$  as the inverse of a distribution function, we have to transform the demand to  $[0, \frac{-d_{min}}{d_{max}-d_{min}}]$  by

$$\hat{\xi} = \frac{\xi - d_{min}}{d_{max} - d_{min}}.$$

$b_N$  therefore changes for  $i_- = \operatorname{argmin}_{i \in I} \{S_t^{(i)} \exp(k_i)\}$  to

$$b_N(\hat{\xi}) = S_t^{(i_-)} \exp(k_{i_-}) - \exp(-m_N(d_{max} - d_{min})\hat{\xi} - d_{min}m_N) + 1.$$

This is for  $b_N(\hat{\xi}) \stackrel{!}{=} p \in [p_{min}, p(0)]$  and  $\bar{d} := d_{max} - d_{min}$  equivalent to

$$\hat{\xi} = -\frac{\ln \{S_t^{(i_-)} \exp(k_{i_-}) + 1 - p\}}{m_N \bar{d}} - d_{min} / \bar{d}$$

which leads to

$$\hat{\xi} = \int_{S_t^{(i_-)} \exp(k_{i_-}) + 1 - \exp(-d_{min}m_N)}^p \frac{1}{m_N \bar{d}(-y + S_t^{(i_-)} \exp(k_{i_-}) + 1)} dy.$$

Consequently, we define the density function  $\phi_N$  to be

$$\phi_N(p|\mathbf{z}) = \begin{cases} 0 & p > S_t^{(i_-)} \exp(k_{i_-}), \\ 0 & p < S_t^{(i_-)} \exp(k_{i_-}) + 1 - \exp(-d_{min}m_N), \\ \frac{1}{m_N \bar{d}(-p + S_t^{(i_-)} \exp(k_{i_-}) + 1)} & \text{else} \end{cases}$$

and we get

$$\int_{p_{min}}^{p_{max}} \phi_N(y|\mathbf{z}) dy = -d_{min} / \bar{d},$$

at least for  $p_{min} < S_t^{(i_-)} \exp(k_{i_-}) + 1 - \exp(-d_{min}m_N)$ .

### 4.5.2 Bid Stack Parameters for Price Spikes

The derivation is similar to the derivation of  $\phi_N$ . After the calculation of the price curve in (4.5), we have to estimate  $b_S$  on  $\xi \in [\bar{\xi}, d_{max}]$ . In order to be able to interpret  $b_S$  as the inverse of a distribution function, we transform the demand to  $[0, \frac{d_{max}-\bar{\xi}}{d_{max}-d_{min}}]$  by

$$\hat{\xi} = \frac{\xi - \bar{\xi}}{d_{max} - d_{min}}.$$

$b_S$  therefore changes for  $i_+ = \operatorname{argmax}_{i \in I} \{S_t^{(i)} \exp(k_i + m_i \bar{\xi}_i)\}$  to

$$b_S(\hat{\xi}) = b_{i_+}(\bar{\xi}_{i_+}, S_t^{(i_+)}) + \exp(m_S(d_{\max} - d_{\min})\hat{\xi}) - 1.$$

This is for  $b_S(\hat{\xi}) \stackrel{!}{=} p \in [p(\bar{\xi}), p_{\max}]$  and  $\bar{d} := d_{\max} - d_{\min}$  equivalent to

$$\hat{\xi} = \frac{\ln \left\{ 1 - b_{i_+}(\bar{\xi}_{i_+}, S_t^{(i_+)}) + p \right\}}{m_S \bar{d}}$$

which leads to

$$\hat{\xi} = \int_{b_{i_+}(\bar{\xi}_{i_+}, S_t^{(i_+)})}^p \frac{1}{m_S \bar{d} (y - b_{i_+}(\bar{\xi}_{i_+}, S_t^{(i_+)}) + 1)} dy.$$

Consequently, we define the density function  $\phi_S$  to be

$$\phi_S(p|\mathbf{z}) = \begin{cases} 0 & p > b_{i_+}(\bar{\xi}_{i_+}, S_t^{(i_+)}) - 1 + \exp((d_{\max} - \bar{\xi})m_S), \\ 0 & p < b_{i_+}(\bar{\xi}_{i_+}, S_t^{(i_+)}) - 1 + \exp((d_{\max} - \bar{\xi})m_S), \\ \frac{1}{m_S \bar{d} (p - b_{i_+}(\bar{\xi}_{i_+}, S_t^{(i_+)}) + 1)} & \text{else} \end{cases}$$

and we get

$$\int_{p_{\min}}^{p_{\max}} \phi_S(y|\mathbf{z}) dy = (d_{\max} - \bar{\xi})/\bar{d},$$

at least for  $p_{\max} > b_{i_+}(\bar{\xi}_{i_+}, S_t^{(i_+)}) - 1 + \exp((d_{\max} - \bar{\xi})m_S)$ .

## 4.6 Additional Analysis: Maximum Likelihood to Estimate the Bid Stack

The maximum likelihood function to be maximized for  $\phi(y|\mathbf{z})$  is given by

$$\begin{aligned} \mathcal{L}(\theta) &= \log \left\{ \prod_{i=1}^N \left[ \sum_{j \in I} \phi_j(p_i|\mathbf{z}) + \phi_N(p_i|\mathbf{z}) + \phi_S(p_i|\mathbf{z}) \right]^{d_i + \xi_R} \right\} \\ &= \sum_{i=1}^N (d_i + \xi_R) \log \left\{ \phi_c(p_i|\mathbf{z}; k_c, m_c, \bar{\xi}_c) + \phi_g(p_i|\mathbf{z}; k_g, m_g, \bar{\xi}_g) \right. \\ &\quad \left. + \phi_N(p_i|\mathbf{z}; k_c, k_g, m_N) + \phi_S(p_i|\mathbf{z}; k_c, k_g, m_c, m_g, \bar{\xi}_c, \bar{\xi}_g, m_S) \right\}. \end{aligned}$$

So far, we assume the estimation of the bid stack parameters to be based on one single price curve as of a certain hour of a certain day. By treating bid and offer curves  $s, d$  to be time-dependent variables  $s_t, d_t$ , we get a time-dependent price curve  $(d_{it}, p_t(d_{it}) =: p_{it})$ . We interpret the data for a fixed  $t$  to be the cross section and for  $i = 1, \dots, N$  and  $t = 1, \dots, T$  to be a panel with  $N \gg T$  (cf. [Wooldridge, 2010]). The result maximum likelihood estimator is called a partial (pooled) maximum likelihood estimator maximizing

$$\begin{aligned}
\mathcal{L}_T(\theta) &= \sum_{i=1}^N \sum_{t=1}^T (d_{it} + \xi_{R,t}) \log \{ \phi_c(p_{it} | \mathbf{z}_t; k_c, m_c, \bar{\xi}_c) + \phi_g(p_{it} | \mathbf{z}_t; k_g, m_g, \bar{\xi}_g) \\
&\quad + \phi_N(p_{it} | \mathbf{z}_t; k_c, k_g, m_N, m_S) + \phi_S(p_{it} | \mathbf{z}_t; k_c, k_g, m_c, m_g, \bar{\xi}_c, \bar{\xi}_g, m_N, m_S) \} \\
&=: \sum_{i=1}^N l_{BS}(\mathbf{d}_i, \mathbf{p}_i | \mathbf{z}; k_c, k_g, m_c, m_g, \bar{\xi}_c, \bar{\xi}_g, m_N, m_S),
\end{aligned} \tag{4.14}$$

where  $\mathbf{d}_i := (d_{i1}, \dots, d_{iT})$ ,  $\mathbf{p}_i := (p_{i1}, \dots, p_{iT})$  and  $\mathbf{z} := (\mathbf{z}_1, \dots, \mathbf{z}_T)$ .

For a fix  $T$  and  $N \rightarrow \infty$   $\mathcal{L}_T$  is a M-estimator. However, the support of each of the densities is (a) finite and (b) has to be optimized when maximizing the likelihood function. We therefore preferred to apply an intermediate step using normal densities in this thesis instead (cf. Chapter 4.2.2).



## CHAPTER 5.

# A Generalization of the Kirk Formula for Structural Electricity Models

In the prior Chapter, we have analyzed parameter uncertainty for a structural electricity model and quantified parameter risk for a virtual power plant of a time horizon of half a year. The reason for that time horizon is that the power price volatility becomes high when analyzing hours with high demand in the future. In Figure 5.1, we see that pricing uncertainty of a Monte Carlo method with 1 million paths is increasing tremendously between a delivery of 6 and 12 months. Furthermore, Figure A.1 reveals that even the present value of options to buy electricity at the regulatory price threshold (Western European markets: 3.000 EUR/MWh) increase significantly for hours with high demand. It turns out that we have to consider the regulatory price threshold whenever we intent to calculate present values with maturities beyond six months. For more information we refer to Chapter A.3.

It is therefore worth to analyze whether Monte Carlo method may be replaced by some (semi-) analytic pricing formula like the common known Kirk formula for spread options with non-zero strikes (cf. [Kirk, 1995]). This is what we are going to investigate in the following.

In order to validate our algorithm we intend to work with some less complex structural models as well. We give an introduction in the next Chapter.

## 5.1 Additional Models

### 5.1.1 A simple Bid Stack

We analyze the exponential bid stack in Chapter 2.1 for  $n = 1$  and  $n = 0$  respectively. For the bid stack function we get

$$f_{bs}(d, s) : \mathbb{R}^+ \times [0, \bar{\xi}] \rightarrow \mathbb{R}, \quad f_{bs}(d, s) := se^{k+md}, \quad (5.1)$$

where  $\bar{\xi}$  still represents the capacity of the marginal fuel. We set  $S_t^P := f_{bs}(D_t, S_t^F)$ .

**Proposition 5.1 (Close Form Formulas for Bid Stack with one Fuel)** *By assuming*

1.  $\log(S_t^F) \stackrel{\mathcal{D}}{=} N(\mu_t^F, (\sigma_t^F)^2),$
2.  $X_t \stackrel{\mathcal{D}}{=} N(\mu_t^D, (\sigma_t^D)^2),$

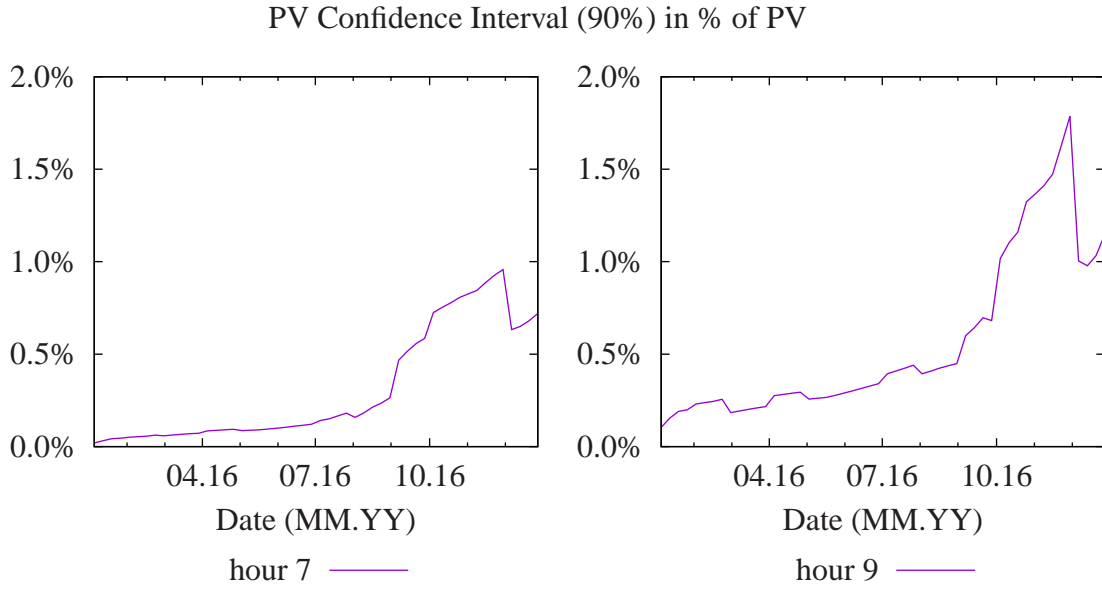


Figure 5.1: Monte Carlo pricing uncertainty (90% confidence interval as percentage of PV; 1 million paths) over maturity for a VPP delivering electricity in hour 06:00-07:00 and 08:00-09:00 respectively on each Tuesday of 2016.

3. independence between  $\log(S_t^F)$  and  $X_t$ ,

4.  $D_t = \min(\bar{\xi}, \max(0, X_t))$ ,

the expected electricity forward price  $F_t^P$  is given by:

$$F_t^P = F_t^F \exp\left(k + m\mu_t^D + \frac{1}{2}m^2(\sigma_t^D)^2\right) \left[ \Phi_1\left(\frac{\bar{\xi} - \mu_t^D}{\sigma_t^D} - \sigma_t^D m\right) - \Phi_1\left(\frac{-\mu_t^D}{\sigma_t^D} - \sigma_t^D m\right) \right] \quad (5.2)$$

$$+ F_t^F \exp(k) \Phi_1\left(-\frac{\mu_t^D}{\sigma_t^D}\right) + F_t^F \exp(k + m\bar{\xi}) \Phi_1\left(\frac{\mu_t^D - \bar{\xi}}{\sigma_t^D}\right), \quad (5.3)$$

where  $F_t^F$  denotes the fuel's forward price maturing in  $t$ . By setting  $\mu_t^F \equiv 0, \sigma_t^F \equiv 0$  we get a bid stack without any marginal fuel.

An analytical formula for European Call options with strike  $K > 0$  is available:

$$\begin{aligned} C_t^P(K) = & e^{-r(t-t_0) + \frac{m^2(\sigma_t^D)^2}{2}} f_{bs}(\mu_t^D, F_t^F) \Phi_2\left(\left(\frac{\bar{\xi} - \mu_t^D}{\sigma_t^D} - m\sigma_t^D\right), \frac{d_2(\mu_t^D) + m^2(\sigma_t^D)^2}{\sigma_{F,D}}, \frac{-m\sigma_t^D}{\sigma_{F,D}}\right) \\ & - e^{-r(t-t_0)} K \Phi_2\left(\left(\frac{\bar{\xi} - \mu_t^D}{\sigma_t^D}\right), \frac{d_1(\mu_t^D)}{\sigma_{F,D}}, \frac{-m\sigma_t^D}{\sigma_{F,D}}\right) \\ & + e^{-r(t-t_0)} (f_{bs}(0, F_t^F) \Phi_1(d_2(0)/\sigma_t^F) - K \Phi_1(d_1(0)/\sigma_t^F)) \Phi_1\left(\frac{-\mu_t^D}{\sigma_t^D}\right) \\ & + e^{-r(t-t_0)} (f_{bs}(\bar{\xi}, F_t^F) \Phi_1(d_2(\bar{\xi})/\sigma_t^F) - K \Phi_1(d_1(\bar{\xi})/\sigma_t^F)) \Phi_1\left(\frac{\mu_t^D - \bar{\xi}}{\sigma_t^D}\right) \end{aligned}$$

where

$$d_1(x) = \ln(F_t^F/K) - \frac{1}{2}\sigma_F^2 + k + mx, \quad d_2(x) = d_1(x) + \sigma_F^2, \quad \sigma_{F,D} = \sqrt{\sigma_F^2 + m^2(\sigma_t^D)^2}.$$

Similarly, for the bid stack without any fuel we get

$$\begin{aligned} C_t^P(K) = & e^{-r(t-t_0)} \left\{ f_{bs}(\mu_t^D, 1) \exp\left(\frac{1}{2}m^2(\sigma_t^D)^2\right) \right. \\ & \left[ \Phi_1\left(\frac{\bar{\xi} - \mu_t^D}{\sigma_t^D} - m\sigma_t^D\right) - \Phi_1\left(\frac{a - \mu_t^D}{\sigma_t^D} - m\sigma_t^D\right) \right] \\ & - K \left[ \Phi_1\left(\frac{\bar{\xi} - \mu_t^D}{\sigma_t^D}\right) - \Phi_1\left(\frac{a - \mu_t^D}{\sigma_t^D}\right) \right] \\ & \left. + (\exp(k) - K)^+ \Phi_1\left(\frac{-\mu_t^D}{\sigma_t^D}\right) + (\exp(k + m\bar{\xi}) - K)^+ \Phi_1\left(\frac{\mu_t^D - \bar{\xi}}{\sigma_t^D}\right) \right\}. \end{aligned}$$

where  $a$  is defined in (5.4).

**Proof.** The following proof is not part of [Carmona et al., 2013] but was derived during our investigations. Based on our knowledge, option and forward price formula have not been published yet for the structural electricity model with exponential bid stack and up to one marginal fuel.

Derivation of the Forward Price Formula:

Following the principle of risk-neutral valuation it holds for  $t \geq t_0$  (in order to shorten notation, we leave out the time index in mean and variance)

$$\begin{aligned} F_{t_0,t}^P &= \mathbb{E}^{\mathbb{Q}}[S_t^P | \mathcal{F}_t] = \int_{\mathbb{R}} \int_0^{\bar{\xi}} \exp(\mu_F + \sigma^F z + k + mD) \phi_1(z) dz \frac{1}{\sigma_D} \phi_1\left(\frac{D - \mu_D}{\sigma^D}\right) dD \\ &\quad + \int_{\mathbb{R}} \int_{-\infty}^0 \exp(\mu_F + \sigma^F z + k) \phi_1(z) dz \frac{1}{\sigma_D} \phi_1\left(\frac{D - \mu_D}{\sigma^D}\right) dD \\ &\quad + \int_{\mathbb{R}} \int_{\bar{\xi}}^{\infty} \exp(\mu_F + \sigma^F z + k + m\bar{\xi}) \phi_1(z) dz \frac{1}{\sigma_D} \phi_1\left(\frac{D - \mu_D}{\sigma^D}\right) dD \\ &= F_t^F \int_{\mathbb{R}} \int_0^{\bar{\xi}} \exp(k + mD) \phi_1(z - \sigma_F) dz \frac{1}{\sigma_D} \phi_1\left(\frac{D - \mu_D}{\sigma^D}\right) dD \\ &\quad + f_{bs}(0, F_t^F) \int_{\mathbb{R}} \int_{-\infty}^0 \phi_1(z - \sigma_F) dz \frac{1}{\sigma_D} \phi_1\left(\frac{D - \mu_D}{\sigma^D}\right) dD \\ &\quad + f_{bs}(\bar{\xi}, F_t^F) \int_{\mathbb{R}} \int_{\bar{\xi}}^{\infty} \phi_1(z - \sigma_F) dz \frac{1}{\sigma_D} \phi_1\left(\frac{D - \mu_D}{\sigma^D}\right) dD \\ &= f_{bs}(\mu_D, F_t^F) \int_{\frac{-\mu_F}{\sigma_F}}^{\frac{\bar{\xi} - \mu_F}{\sigma_D}} \exp(m\sigma_D D) \phi_1(D) dD \\ &\quad + f_{bs}(0, F_t^F) \int_{-\infty}^{\frac{-\mu_F}{\sigma_F}} \phi_1(D) dD + f_{bs}(\bar{\xi}, F_t^F) \int_{\frac{\bar{\xi} - \mu_F}{\sigma_D}}^{\infty} \phi_1(D) dD \end{aligned}$$

leading to what is stated in Proposition 5.1.

### Derivation of the European Call Option Formula for $n = 0$

Following the principle of risk-neutral valuation it holds for  $t \geq t_0$  (in order to shorten notation, we leave out the time index in mean and variance; W.l.o.g we assume  $r = 0$ )

$$\begin{aligned}
 C_t^P &= \mathbb{E}^{\mathbb{Q}}[(S_t^P - K)^+ | \mathcal{F}_t] = \int_0^{\bar{\xi}} (\exp(k + mD) - K)^+ \frac{1}{\sigma_D} \phi_1\left(\frac{D - \mu_D}{\sigma_D}\right) dD \\
 &\quad + (\exp(k) - K)^+ \int_{-\infty}^0 \frac{1}{\sigma_D} \phi_1\left(\frac{D - \mu_D}{\sigma_D}\right) dD \\
 &\quad + (\exp(k + m\bar{\xi}) - K)^+ \int_{\bar{\xi}}^{\infty} \frac{1}{\sigma_D} \phi_1\left(\frac{D - \mu_D}{\sigma_D}\right) dD \\
 &= \int_0^{\bar{\xi}} (\exp(k + mD) - K)^+ \frac{1}{\sigma_D} \phi_1\left(\frac{D - \mu_D}{\sigma_D}\right) dD \\
 &\quad + (\exp(k) - K)^+ \Phi_1\left(\frac{-\mu_D}{\sigma_D}\right) + (\exp(k + m\bar{\xi}) - K)^+ \Phi_1\left(\frac{\mu_D - \bar{\xi}}{\sigma_D}\right).
 \end{aligned}$$

The integrand of the first term is non-negative for  $D \geq \frac{\ln(K) - k}{m}$  leading to

$$\int_0^{\bar{\xi}} (\exp(k + mD) - K)^+ \frac{1}{\sigma_D} \phi_1\left(\frac{D - \mu_D}{\sigma_D}\right) dD = \int_a^{\bar{\xi}} (\exp(k + mD) - K) \frac{1}{\sigma_D} \phi_1\left(\frac{D - \mu_D}{\sigma_D}\right) dD$$

where

$$a := \begin{cases} \frac{\ln(K) - k}{m} & 0 < \frac{\ln(K) - k}{m} < \bar{\xi} \\ 0 & 0 \geq \frac{\ln(K) - k}{m} \\ \bar{\xi} & \frac{\ln(K) - k}{m} \geq \bar{\xi} \end{cases}. \quad (5.4)$$

Finally, we get

$$\begin{aligned}
 &\int_a^{\bar{\xi}} (\exp(k + mD) - K) \frac{1}{\sigma_D} \phi_1\left(\frac{D - \mu_D}{\sigma_D}\right) dD \\
 &= \int_{\frac{a - \mu_D}{\sigma_D}}^{\frac{\bar{\xi} - \mu_D}{\sigma_D}} (\exp(k + m\mu_D + m\sigma_D D) - K) \phi_1(D) dD \\
 &= f_{bs}(\mu_D, 1) \exp\left(\frac{1}{2} m^2 \sigma_D^2\right) \left[ \Phi_1\left(\frac{\bar{\xi} - \mu_D}{\sigma_D} - m\sigma_D\right) - \Phi_1\left(\frac{a - \mu_D}{\sigma_D} - m\sigma_D\right) \right] \\
 &\quad - K \left[ \Phi_1\left(\frac{\bar{\xi} - \mu_D}{\sigma_D}\right) - \Phi_1\left(\frac{a - \mu_D}{\sigma_D}\right) \right]
 \end{aligned}$$

being what is stated in Proposition 5.1.

### Derivation of the European Call Option Formula for $n = 1$

Following the principle of risk-neutral valuation it holds for  $t \geq t_0$  (in order to shorten notation, we leave out the time index in mean and variance; W.l.o.g we assume  $r = 0$ )

$$C_t^P = \mathbb{E}^{\mathbb{Q}}[(S_t^P - K)^+ | \mathcal{F}_t]$$

$$\begin{aligned}
&= \int_{\mathbb{R}} \int_0^{\bar{\xi}} (\exp(\mu_F + \sigma^F z + k + mD) - K)^+ \phi_1(z) dz \frac{1}{\sigma_D} \phi_1\left(\frac{D - \mu_D}{\sigma^D}\right) dD \\
&\quad + \int_{\mathbb{R}} \int_{-\infty}^0 (\exp(\mu_F + \sigma^F z + k) - K)^+ \phi_1(z) dz \frac{1}{\sigma_D} \phi_1\left(\frac{D - \mu_D}{\sigma^D}\right) dD \\
&\quad + \int_{\mathbb{R}} \int_{\bar{\xi}}^{\infty} (\exp(\mu_F + \sigma^F z + k + m\bar{\xi}) - K)^+ \phi_1(z) dz \frac{1}{\sigma_D} \phi_1\left(\frac{D - \mu_D}{\sigma^D}\right) dD \\
&= \int_{-d_1(D)/\sigma_F}^{\infty} \int_0^{\bar{\xi}} (\exp(\mu_F + \sigma^F z + k + mD) - K) \phi_1(z) dz \frac{1}{\sigma_D} \phi_1\left(\frac{D - \mu_D}{\sigma^D}\right) dD \\
&\quad + \int_{-d_1(0)/\sigma_F}^{\infty} \int_{-\infty}^0 (\exp(\mu_F + \sigma^F z + k) - K) \phi_1(z) dz \frac{1}{\sigma_D} \phi_1\left(\frac{D - \mu_D}{\sigma^D}\right) dD \\
&\quad + \int_{-d_1(\bar{\xi})/\sigma_F}^{\infty} \int_{\bar{\xi}}^{\infty} (\exp(\mu_F + \sigma^F z + k + m\bar{\xi}) - K) \phi_1(z) dz \frac{1}{\sigma_D} \phi_1\left(\frac{D - \mu_D}{\sigma^D}\right) dD \\
&= F_t^F \int_0^{\bar{\xi}} (\exp(k + mD) \Phi_1(d_1(D)/\sigma_F + \sigma_F) - K \Phi_1(d_1(D)/\sigma_F)) \frac{1}{\sigma_D} \phi_1\left(\frac{D - \mu_D}{\sigma^D}\right) dD \\
&\quad + F_t^F (\exp(k) \Phi_1(d_1(0)/\sigma_F + \sigma_F) - K \Phi_1(d_1(0)/\sigma_F)) \int_{-\infty}^0 \frac{1}{\sigma_D} \phi_1\left(\frac{D - \mu_D}{\sigma^D}\right) dD \\
&\quad + F_t^F (\exp(k + m\bar{\xi}) \Phi_1(d_1(\bar{\xi})/\sigma_F + \sigma_F) - K \Phi_1(d_1(\bar{\xi})/\sigma_F)) \int_{\bar{\xi}}^{\infty} \frac{1}{\sigma_D} \phi_1\left(\frac{D - \mu_D}{\sigma^D}\right) dD \\
&= F_t^F \int_0^{\bar{\xi}} (\exp(k + mD) \Phi_1(d_1(D)/\sigma_F + \sigma_F) - K \Phi_1(d_1(D)/\sigma_F)) \frac{1}{\sigma_D} \phi_1\left(\frac{D - \mu_D}{\sigma^D}\right) dD \\
&\quad + F_t^F (\exp(k) \Phi_1(d_1(0)/\sigma_F + \sigma_F) - K \Phi_1(d_1(0)/\sigma_F)) \Phi_1\left(\frac{-\mu_D}{\sigma^D}\right) \\
&\quad + F_t^F (\exp(k + m\bar{\xi}) \Phi_1(d_1(\bar{\xi})/\sigma_F + \sigma_F) - K \Phi_1(d_1(\bar{\xi})/\sigma_F)) \Phi_1\left(\frac{\mu_D - \bar{\xi}}{\sigma^D}\right).
\end{aligned}$$

The last terms are already what is stated in Proposition 5.1. For the first term, we apply Lemma 5.6 with

$$q_1 = m\sigma_D \quad l_1 = k + m\mu_D \quad q_2 = \frac{m\sigma_D}{\sigma_F} \quad l_2 = d_1(\mu_D)/\sigma_F + \sigma_F \quad a_1 = \frac{\bar{\xi} - \mu_D}{\sigma_D} \quad a_2 = \frac{-\mu_D}{\sigma_D}$$

for the bid stack term and

$$q_1 = 0 \quad l_1 = 0 \quad q_2 = \frac{m\sigma_D}{\sigma_F} \quad l_2 = d_1(\mu_D)/\sigma_F \quad a_1 = \frac{\bar{\xi} - \mu_D}{\sigma_D} \quad a_2 = \frac{-\mu_D}{\sigma_D}$$

for the strike term leading to the assertion in Proposition 5.1. ■

### 5.1.2 Geometric Brownian Motions for Fuels and Demand

Let  $\mathbf{X}_t = (X_t^1, \dots, X_t^n)$  be a vector of correlated Brownian Motions and let  $q_t^{(i)}, v_t^{(i)}, r_t, q_t^D, v^D \in \mathcal{L}^1[t_0, \infty)$  (integrability with respect to the Lebesgue measure,  $i \in I$ ) and  $t \geq t_0$ . The dynamics of the correlated fuel process  $\mathbf{S}_t^F = (S_t^1, \dots, S_t^n)$  and demand process  $D_t$  are given by

$$\begin{aligned}
dS_t^{(i)} &= (r_t - q_t^{(i)}) S_t^{(i)} dt + v^{(i)} S_t^{(i)} dW_t^{(i)} & \forall i \in I \\
dD_t &= q_t^D dt + v^D dW_t^D \\
dW_t^{(i)} dW_t^{(j)} &= \rho_{ij} dt & \forall i, j \in I
\end{aligned}$$

$$dW_t^D dW_t^{(i)} = 0 \quad \forall i \in I.$$

Let  $\mathbf{S}_{t_0} = (s_1, \dots, s_n) \in (\mathbb{R}^+)^n$  and  $D_{t_0} = d \in \mathbb{R}$  be given. The solution of the above stochastic differential equations is known to be given by ( $\forall i \in I$ )

$$S_t^{(i)} = S_{t_0}^{(i)} \exp \left( \int_{t_0}^t (r_s - q_s - \frac{1}{2} (v^{(i)})^2) ds + v^{(i)} dW_s^{(i)} \right)$$

$$D_t = \int_{t_0}^t q_s^D ds + v^D W_t^D.$$

Forward prices for  $i = 1, \dots, n$  are given by:

$$\mathbb{E}^{\mathbb{Q}} [S_t^{(i)} | \mathcal{F}_{t_0}] = S_{t_0}^{(i)} \exp \left( \int_{t_0}^t (r_s - q_s) ds \right) \quad (5.5)$$

$$\mathbb{E}^{\mathbb{Q}} [D_t | \mathcal{F}_{t_0}] = \int_{t_0}^t q_s^D ds. \quad (5.6)$$

We switch the drift of our framework to the risk neutral world setup by choosing  $q_t^{(i)}$  such that we price forwards free of arbitrage. For the demand, we again use Definition 2.1 of implied demand.

## 5.2 From the Idea to the Algorithm

As a starting point we use [Alos et al., 2011] where the authors derive a generalization of the Kirk's formula to include stochastic emission costs in addition to stochastic fuel costs. In the following we adapt this idea to the pricing in structural electricity models. As an example, we test our formula against exponential bid stacks with different amount of marginal fuels in Chapter 5.3.

For simplicity, we choose the fuels to follow a geometric Brownian motion and the demand to follow a Bachelier dynamic (cf. Chapter 5.1.1). For  $\Psi(S_T^P) := (S_T^P - K)^+$ ,  $K \in \mathbb{R}$ , the following conditions are fulfilled for the exponential structural model in Chapter 2.1 for  $n = 0, 1, 2$ :

$$\text{K1 } \mathbb{E}^{\mathbb{Q}} [|\Psi(S_T^P)|] < \infty \text{ (integrability),}$$

$$\text{K2 } \mathbb{E}^{\mathbb{Q}} [\Psi(S_T^P) | \mathcal{F}_t] = \mathbb{E}^{\mathbb{Q}} [\Psi(S_T^P) | (D_t, S_t^F)] \text{ (Markovian property).}$$

Consequently, the discounted risk-neutral expectation of  $\Psi$  (which exist because of B1) can be expressed as a function  $PV_{t,T}^{EC}$  depending on fuel forward prices and future expected demand:

$$PV_{t,T}^{EC} = V_{EC}(F_{t,T}^{(c)}, F_{t,T}^{(g)}, \mu_{t,T}^D, T - t)$$

$$\text{K3 } V_{EC} \in C^{1,2} \text{ (in order to apply Itô's Lemma).}$$

In order to underline the dependency to model parameters we write

$$V_{EC}(F_{t,T}^{(c)}, F_{t,T}^{(g)}, \mu_{t,T}^D; v^C, v^G, v^D, \rho_{cg}, T - t).$$

Under the risk neutral measure, it holds for the present value of a dark spark spread option with strike  $K$  and heat rate  $h_R \in \mathbb{R}$

$$PV = e^{-r(T-t)} \mathbb{E}^{\mathbb{Q}} [(S_T^P - h_R S_T^G - K)^+ | \mathcal{F}_t]$$

$$= e^{-r(T-t)} \mathbb{E}^{\mathbb{Q}} \left[ V_{EC}(F_{t,T}^c, F_{t,T}^g, \mu_{t,T}^D, h_R F_{t,T}^G + K; v^C, v^G, v^D, \rho_{cg}, T-t) \middle| \mathcal{F}_t \right].$$

By defining

$$G(t) := e^{r(T-t)} V_{EC}(F_{t,T}^c, F_{t,T}^g, \mu_{t,T}^D, h_R F_{t,T}^G + K; v^C, v^G, v^D, \rho_{cg}, T-t)$$

and applying the Itô-Lemma, we get

$$\begin{aligned} &= V_{EC}(F_{t,T}^c, F_{t,T}^g, \mu_{t,T}^D, h_R F_{t,T}^G + K; v^c, v^g, v^D, \rho_{cg}, T-t) \\ &+ \mathbb{E}^{\mathbb{Q}} \left[ \int_t^T e^{-r(s-t)} \left( \frac{\partial V_{EC}}{\partial t} - r V_{EC} \right) ds \right. \\ &+ \frac{1}{2} \int_t^T e^{-r(s-t)} \left( \frac{\partial^2 V_{EC}}{\partial (F_{t,T}^g)^2} (v^g)^2 (F_{s,T}^G)^2 + \frac{\partial^2 V_{EC}}{\partial (F_{t,T}^c)^2} (v^c)^2 (F_{s,T}^c)^2 \right. \\ &\left. \left. + \frac{\partial^2 V_{EC}}{\partial (\mu_{t,T}^D)^2} (v^D)^2 + 2 \frac{\partial^2 V_{EC}}{\partial F_{t,T}^g \partial F_{t,T}^c} \rho_{cg} v^g v^c F_{s,T}^c F_{s,T}^g \right) ds \middle| \mathcal{F}_t \right]. \end{aligned}$$

As conducted in [Alos et al., 2011] we intend to choose the demand volatility  $v^D$  such that the conditional expectation term vanishes for  $s = t$ . This lead to a price formula only being accurate for small  $T - t$ . Therefore, we have to solve the root problem

$$\begin{aligned} 0 &\stackrel{!}{=} \frac{\partial V_{EC}}{\partial t} - r V_{EC} + \frac{1}{2} \left( \frac{\partial^2 V_{EC}}{\partial (F_{t,T}^g)^2} (v^g)^2 (F_{t,T}^G)^2 + \frac{\partial^2 V_{EC}}{\partial (F_{t,T}^c)^2} (v^c)^2 (F_{t,T}^c)^2 \right. \\ &\left. + \frac{\partial^2 V_{EC}}{\partial (\mu_{t,T}^D)^2} (v^D)^2 + 2 \frac{\partial^2 V_{EC}}{\partial F_{t,T}^g \partial F_{t,T}^c} \rho_{cg} v^g v^c F_{t,T}^c F_{t,T}^g \right). \end{aligned} \quad (5.7)$$

We solve (5.7) with the help of the Newton method. Due to that method, derivatives of order three have to be calculated using i.e. the difference quotient method. Therefore, small bumps and numerical methods with high accuracy have to be used to solve the equation.

## 5.3 Numerical Results

We will test the accuracy of the formula for the three following bid stack approaches:

1. exponential bid stack without a fuel,
2. exponential bid stack with single fuel (coal),
3. exponential bid stack with two marginal fuels (gas and coal).

The calculations for the exponential bid stack with two marginal fuels are based on the estimation of Chapter 4 (using the spot estimation for the fuels and  $v^D \equiv 5$ ). For the exponential bid stack without a fuel we used  $k = 0$  and  $m = 0.17$ . For the exponential bid stack with coal as a single fuel we used the estimation in Chapter 4 but added the gas capacity to coal. As input for the model in Chapter 5.1.1, we simply used the volatility estimators in Chapter 4.2.1 although they are derived under an Ornstein-Uhlenbeck model (cf. Chapter 2.2). Because the option price formula does not have a close form solution

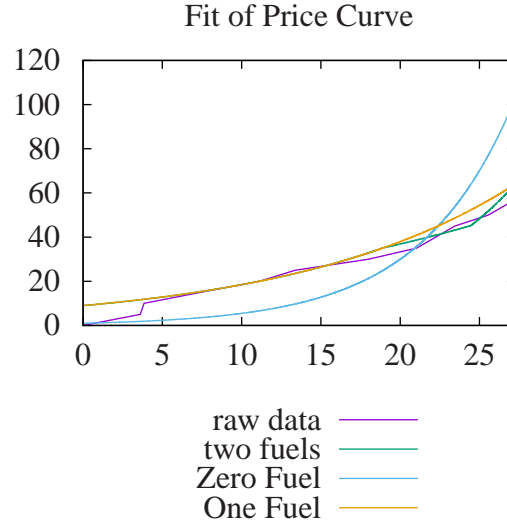


Figure 5.2: Three different bid stacks to be compared when applying the Kirk formula for structural electricity models as of  $t_0 = 31/12/2016$ ; 'raw data' depicts the bid stack of 08/12/2016 as it has been observed for hour 08:00-09:00 at EPEX Spot.

for  $m_S, m_N > 0$ , we have chosen them to be zero. The different bid stacks are depicted in Figure 5.2. Beyond the x-axis the bid stacks was extended by constant extrapolation ( $m_N = m_S = 0$ ).

In order to stress the merit order, we use three different scenarios for correlation:  $\rho = -0.8, 0, 0.8$ . Under  $\rho = 0.8$  there is a high probability for the merit order to remain as it is induced by forward prices whereas  $\rho = -0.8$  has a higher probability to create paths where the merit order changes.

We analyze the VPP given in Chapter 1.2.4 for hour 06:00-07:00h and 08:00-09:00h for maturities from 0 to 2 years as of year-end 2015. The results are depicted in Figure 5.3 to 5.5. In order to compare our results we choose a Monte Carlo method with an amount of paths such that the runtime of the Monte Carlo method is similar to the runtime of the Kirk formula (cf. Table 5.1). Afterwards, we compare the price of our Kirk formula against the confidence interval (90%) of the Monte Carlo method. In order to measure an error, we used a Monte Carlo method with 1 million paths as reference value.

It can be seen that for all choices of bid stack ( $n = 0, 1, 2$ ) and different hours the generalized Kirk formula is numerically quite competitive. For a time horizon up to 2 years, the VPP can be priced with an error of roughly 1%, whereas the confidence interval of the Monte Carlo method is in most cases above 2%. The best results are obtained for small correlation. In fact, the historical correlation was estimated below 0.1 (Table 4.2) being a good basis in general to use the Kirk formula for the structural models above.

The limitation of the Kirk formula is of course given by the fact that the results cannot be improved any further whereas a Monte Carlo method increases its accuracy by increasing its overall paths. On the other hand, the Kirk formula accuracy does not depend on volatility whereas higher volatility will lead a Monte Carlo method to loose accuracy.

In case of an exponential bid stack with two marginal fuels (Figure 5.4), the runtime is significantly increasing. This is due to the complex formula for European call options (cf. Chapter 5.4). The Newton



algorithm to find the root needs up to 3 iterations for a accuracy below 0.01.

Altogether, the main reason why we will proceed using a Monte Carlo method for the remaining part of the thesis is the model limitation to a geometric Brownian motion. In case of an Ornstein-Uhlenbeck process, the power forward dynamics will additionally depend on  $\int_{t_0}^t \alpha_u du$  (cf. Proposition 3.1). Therefore, the assumption of  $|t - t_0|$  to be small, will lead to an additional error. Additionally, we cannot introduce time dependent parameters which is why we cannot use a model being calibrated against historical fuel and power forwards data.

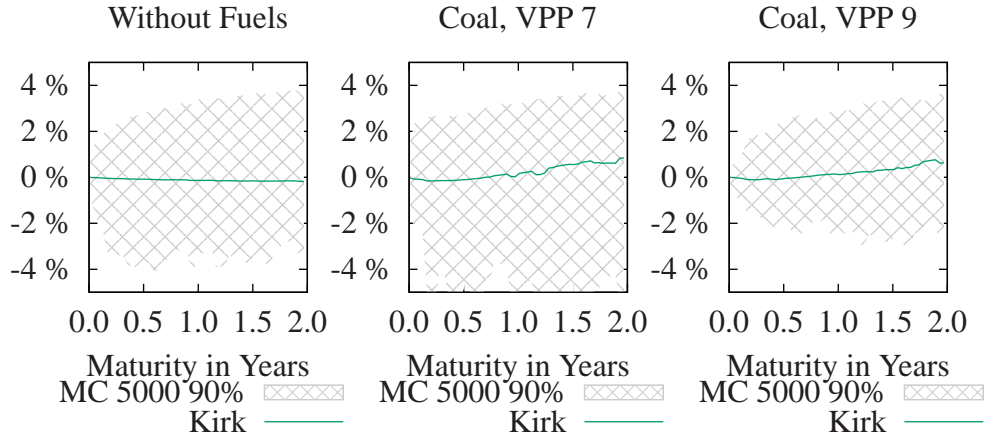


Figure 5.3: Relative error of General Kirk formula over delivery applied to an exponential bid stack with and without using a fuel in the bid stack model; left: hour 08:00-09:00 , middle: hour 06:00-07:00 , right: hour 08:00-09:00.

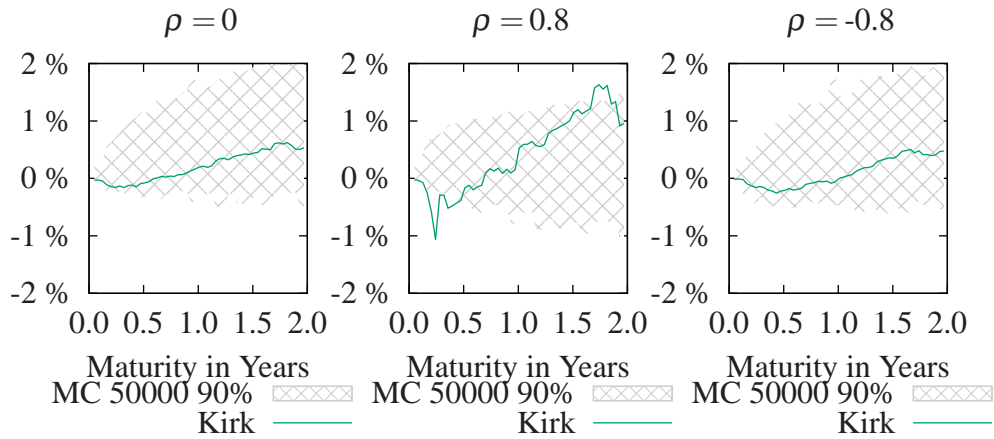


Figure 5.4: Relative error of General Kirk formula over delivery applied to an exponential bid stack with two marginal fuels and three different fuel correlations for hour 08:00-09:00

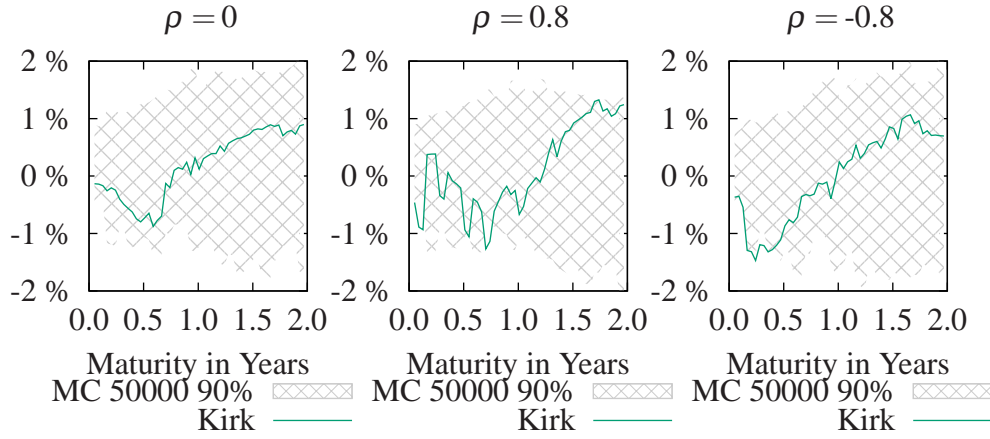


Figure 5.5: Relative error of General Kirk formula over delivery applied to an exponential bid stack with two marginal fuels and three different fuel correlations for hour 06:00-07:00

Table 5.1: Average numerical Effort in ms to perform one valuation for Figure 5.3 to 5.5

Bid Stack Approach	Kirk Formula	Monte Carlo
No Fuels	7	9.7
1 Fuel	10.9	11.4
2 Fuels	86	111

## 5.4 Derivation of the European Call Option Formula

Based on our knowledge, this is the first time where the European Call Option Formula for the exponential bid stack with two marginal fuels (cf. [Carmona et al., 2013]; Chapter 2.1) is derived.

We derive a close form formula to price European call options on the electricity spot price. We assume lognormally distributed fuels  $\mathbf{S}_t^F$  and (truncated-) normally distributed demand  $D_t$  fulfilling the condition<sup>1</sup>

$$\begin{pmatrix} \ln(\mathbf{S}_t^F) \\ D_t \end{pmatrix} := \begin{pmatrix} \ln(S_t^1) \\ \vdots \\ \ln(S_t^n) \\ D_t \end{pmatrix} \stackrel{\mathcal{D}}{=} \mathcal{N} \left( \begin{pmatrix} \mu_t^1 \\ \vdots \\ \mu_t^n \\ \mu_t^D \end{pmatrix}, \Sigma_t \right) =: \mathcal{N} \left( \begin{pmatrix} \mu_t^F \\ \mu_t^D \end{pmatrix}, \Sigma_t \right) \quad (5.8)$$

with  $|\Sigma_t| > 0 \forall t > t_0$ .

The derivation is similar to the derivations in [Carmona et al., 2013] where close form formulas for forwards and spread options have been derived. However, more complex terms will appear due to the constant strike  $K > 0$ . For the derivation we start to integrate over the fuels and keep the demand fix.

Due to the complexity of formulas, we decided to concentrate on presenting the results in this Chapter. The main proofs are presented afterward in Chapter 5.4.1 to Chapter 5.4.4. The main outcome of the

<sup>1</sup>I.e. the Ornstein-Uhlenbeck model in Chapter 2.2 fulfills the condition.

Chapter - being the European call option formula - is given in Corollary 5.1 (p. 89).

**Proposition 5.2 (Power Call Option Formula for an Arbitrary Demand Density)** *Let the exponential bid stack in Chapter 2.1 together with according notations in Appendix A be given. Additionally, let the fuels be lognormally distributed as given in (5.8) and let the demand  $D_t$  be independent of  $\mathcal{F}_t^W$  with density function  $\phi_d : [0, \bar{\xi}] \rightarrow \mathbb{R}_+$ . Then, for a given strike  $K > 0$  and maturity  $t \geq t_0$ , it holds for the according European call price  $C_t^P$  at  $t_0$*

$$C_t^P(K) = \int_0^{\bar{\xi}_{i-}} f_{low}(D, \mathbf{F}_t) \phi_d(D) dD + \int_{\bar{\xi}_{i-}}^{\bar{\xi}_{i+}} f_{mid}(D, \mathbf{F}_t) \phi_d(D) dD + \int_{\bar{\xi}_{i+}}^{\bar{\xi}} f_{high}(D, \mathbf{F}_t) \phi_d(D) dD \\ - K \left( \int_0^{\bar{\xi}_{i-}} k_{low}(D, \mathbf{F}_t) \phi_d(D) dD + \int_{\bar{\xi}_{i-}}^{\bar{\xi}_{i+}} k_{mid}(D, \mathbf{F}_t) \phi_d(D) dD + \int_{\bar{\xi}_{i+}}^{\bar{\xi}} k_{high}(D, \mathbf{F}_t) \phi_d(D) dD \right)$$

where for  $(\xi, \mathbf{x}) \in [0, \bar{\xi}] \cup \mathbb{R}_+^2$   $f_{low}, f_{mid}, f_{high}$  and  $k_{low}, k_{mid}, k_{high}$  are derived in Lemma 5.1 to 5.3.

**Proof.** By applying the tower property of sub-algebras and using  $\mathcal{F} = \mathcal{F}^W \vee \mathcal{F}^D$  (cf. Chapter 2.2), we get

$$C_t^P(K) = e^{-r(t-t_0)} \mathbb{E}^Q \left[ (S_t^P - K)^+ \mid \mathcal{F}_{t_0}^W \vee \mathcal{F}_{t_0}^D \right] = e^{-r(t-t_0)} \mathbb{E}^Q \left[ \mathbb{E}^Q \left[ (S_t^P - K)^+ \mid \mathcal{F}_{t_0}^W \vee \mathcal{F}_t^D \right] \mid \mathcal{F}_{t_0}^W \vee \mathcal{F}_{t_0}^D \right] \\ \stackrel{App.A.1}{=} e^{-r(t-t_0)} \mathbb{E}^Q \left[ \mathbb{E}^Q \left[ \left( b_{low}(D_t, S_t) \mathbb{I}_{[0, \bar{\xi}_{i-}]}(D_t) + b_{mid}(D_t, S_t) \mathbb{I}_{(\bar{\xi}_{i-}, \bar{\xi}_{i+}]}(D_t) \right. \right. \right. \\ \left. \left. \left. + b_{high}(D_t, S_t) \mathbb{I}_{(\bar{\xi}_{i+}, \bar{\xi}]}(D_t) - K \right)^+ \mid \mathcal{F}_{t_0}^W \vee \mathcal{F}_t^D \right] \mid \mathcal{F}_{t_0}^W \vee \mathcal{F}_{t_0}^D \right] \\ = e^{-r(t-t_0)} \int_0^{\bar{\xi}} \mathbb{E}^Q \left[ \left( b_{low}(D, S_t) \mathbb{I}_{[0, \bar{\xi}_{i-}]}(D) + b_{mid}(D, S_t) \mathbb{I}_{(\bar{\xi}_{i-}, \bar{\xi}_{i+}]}(D) \right. \right. \\ \left. \left. + b_{high}(D, S_t) \mathbb{I}_{(\bar{\xi}_{i+}, \bar{\xi}]}(D) - K \right)^+ \mid \mathcal{F}_{t_0}^W \vee \mathcal{F}_t^D \right] \phi_d(D) dD \\ = e^{-r(t-t_0)} \int_0^{\bar{\xi}_{i-}} \mathbb{E}^Q \left[ (b_{low}(D, S_t) - K) \mathbb{I}_{b_{low}(D, S_t) > K}(D) \mid \mathcal{F}_{t_0}^W \vee \mathcal{F}_t^D \right] \phi_d(D) dD \\ + e^{-r(t-t_0)} \int_{\bar{\xi}_{i-}}^{\bar{\xi}_{i+}} \mathbb{E}^Q \left[ (b_{mid}(D, S_t) - K) \mathbb{I}_{b_{mid}(D, S_t) > K}(D) \mid \mathcal{F}_{t_0}^W \vee \mathcal{F}_t^D \right] \phi_d(D) dD \\ + e^{-r(t-t_0)} \int_{\bar{\xi}_{i+}}^{\bar{\xi}} \mathbb{E}^Q \left[ (b_{high}(D, S_t) - K) \mathbb{I}_{b_{high}(D, S_t) > K}(D) \mid \mathcal{F}_{t_0}^W \vee \mathcal{F}_t^D \right] \phi_d(D) dD$$

which is why the Proposition is defined by summands of *low*, *mid* and *high*. The calculation of the expectations over fuel dynamics is performed in Lemma 5.1 to 5.3. It leads to the definitions of  $f_{low}, f_{mid}, f_{high}$  and  $k_{low}, k_{mid}, k_{high}$ . ■

**Definition 5.1 (Expressions for the Option Price Formula)** *Additionally to the definitions in Appendix A.2 of  $R_i(\xi_1, \xi_2), b_i, b_{cg}, \alpha_i, \beta, \gamma, \sigma$  with  $i = c, g$  we define*

$$R_i^K(\xi) := \ln(K) - \ln(F_t^i) - k_i - m_i \xi \\ R_\alpha^K(\xi) := \ln(K) - \alpha_c \ln(F_t^c) - \alpha_g \ln(F_t^g) + \alpha_c \sigma_c^2 / 2 + \alpha_g \sigma_g^2 / 2 - \gamma \xi - \beta - \sigma(\alpha)^2, \\ \sigma^2(\alpha) := \sigma_c^2 \alpha_c^2 + 2\rho \alpha_c \sigma_c \sigma_g \alpha_g + \sigma_g^2 \alpha_g^2,$$

$$\begin{aligned}
v^2(\kappa, v) &:= \kappa^2 \sigma_D^2 + v^2 \quad (\kappa, v > 0), \\
R_{\Delta}^{c,low}(\xi) &:= R_{\alpha}^K(\xi) + \sigma^2(\alpha) + \alpha_g \cdot [R_c(\xi, 0) + 0.5(\sigma^2 + \sigma_c^2 - \sigma_g^2)], \\
R_{\Delta}^{g,low}(\xi) &:= R_{\alpha}^K(\xi) + \sigma^2(\alpha) - \alpha_g \cdot [R_g(\xi, 0) + 0.5(\sigma^2 - \sigma_c^2 + \sigma_g^2)], \\
R_{\Delta}^{K,high}(\xi^i, \xi^j; x) &:= (\sigma_c(R_g^K(\xi^j) + \sigma_g^2/2) - \sigma_g \rho(R_c^K(\xi^i) + \sigma_c^2/2)) / (\sigma_c - \sigma_g \rho) / x, \\
R_{\Delta}^{g,high}(\xi) &:= (R_{\alpha}^K(\xi) + \sigma^2(\alpha) - (R_g(\xi - \bar{\xi}^c, \bar{\xi}^c) + 0.5(\sigma^2 - \sigma_c^2 + \sigma_g^2))\alpha_g) / \sigma_c \\
R_{\Delta}^{c,high}(\xi) &:= (R_{\alpha}^K(\xi) + \sigma^2(\alpha) + (R_c(\xi - \bar{\xi}^g, \bar{\xi}^g) + 0.5(\sigma^2 + \sigma_c^2 - \sigma_g^2))\alpha_g) / \sigma_c \\
R_i^{K,s}(\xi) &:= \ln(K + 1 - \exp(m_s(\xi - \bar{\xi}^i))) - \ln(F_t^i) - k_i - m_i \bar{\xi}^i \\
R_i^{K,n}(\xi) &:= \ln(K - 1 + \exp(-m_n \xi)) - \ln(F_t^i) - k_i
\end{aligned}$$

Let  $\Phi_2(\cdot, \cdot; \rho)$  be the notation for the bivariate cumulative standard normal distribution with correlation  $\rho \in (-1; 1)$ .

**Lemma 5.1 (Low-Cases)** *Given the assumptions in Proposition 5.2 and Definition 5.1,  $f_{low}$  and  $k_{low}$  are given by*

$$f_{low}(\xi, \mathbf{x}) = f_{low}^c(\xi, \mathbf{x}) + f_{low}^g(\xi, \mathbf{x}) + f_{low}^{cg}(\xi, \mathbf{x}),$$

where

$$\begin{aligned}
f_{low}^c(\xi, \mathbf{x}) &= b_c(\xi, \mathbf{x}) [\Phi_1(R_c(\xi, 0)/\sigma) - \Phi_2(R_c^K(\xi)/\sigma_c - \sigma_c/2, R_c(\xi, 0)/\sigma; (\sigma_c - \sigma_g \rho)/\sigma)] \\
f_{low}^g(\xi, \mathbf{x}) &= b_g(\xi, \mathbf{x}) [\Phi_1(R_g(\xi, 0)/\sigma) - \Phi_2((R_c^K(0) + 0.5\sigma_c^2)/\sigma_c - \sigma_g \rho, R_g(\xi, 0)/\sigma; -(\sigma_c - \sigma_g \rho)/\sigma) \\
&\quad - \Phi_1(R_g^K(\xi)/\sigma_g - \sigma_g/2) + \Phi_2((R_c^K(0) + 0.5\sigma_c^2)/\sigma_c - \sigma_g \rho, R_g^K(\xi)/\sigma_g - \sigma_g/2; \rho)] \\
f_{low}^{cg}(\xi, \mathbf{x}) &= b_{cg}(\xi, \mathbf{x}) e^{\frac{-\alpha_c \alpha_g \sigma^2}{2}} [1 + f_{low}^{cg,c}(\xi, \mathbf{x}) + f_{low}^{cg,g}(\xi, \mathbf{x})] \\
f_{low}^{cg,c}(\xi, \mathbf{x}) &= -\Phi_1(R_c(\xi, 0)/\sigma + \alpha_g \sigma) \\
&\quad + \Phi_2(R_{\Delta}^{c,low}(\xi)/\sigma_c - \sigma_c \alpha_c - \sigma_g \alpha_g \rho, R_c(\xi, 0)/\sigma + \alpha_g \sigma, (\sigma_c - \sigma_g \rho)/\sigma) \\
&\quad - \Phi_2(R_{\Delta}^{c,low}(\xi)/\sigma_c - \sigma_c \alpha_c - \sigma_g \alpha_g \rho, -R_{\alpha}^K(\xi)/\sigma(\alpha), -(\sigma_c \alpha_c + \sigma_g \alpha_g \rho)/\sigma(\alpha)) \\
f_{low}^{cg,g}(\xi, \mathbf{x}) &= -\Phi_1(R_g(\xi, 0)/\sigma + \alpha_c \sigma) \\
&\quad + \Phi_2(R_{\Delta}^{g,low}(\xi)/\sigma_c - \sigma_c \alpha_c - \sigma_g \alpha_g \rho, R_g(\xi, 0)/\sigma + \alpha_c \sigma, -(\sigma_c - \sigma_g \rho)/\sigma) \\
&\quad - \Phi_2(R_{\Delta}^{g,low}(\xi)/\sigma_c - \sigma_c \alpha_c - \sigma_g \alpha_g \rho, R_{\alpha}^K(\xi)/\sigma(\alpha), (\sigma_c \alpha_c + \sigma_g \alpha_g \rho)/\sigma(\alpha))]
\end{aligned}$$

and

$$k_{low}(\xi, \mathbf{x}) = k_{low}^c(\xi, \mathbf{x}) + k_{low}^g(\xi, \mathbf{x}) + k_{low}^{cg}(\xi, \mathbf{x}),$$

where

$$\begin{aligned}
k_{low}^c(\xi, \mathbf{x}) &= -\Phi_2(R_c^K(\xi)/\sigma_c + \sigma_c/2, (R_c(\xi, 0) + 0.5 \cdot (\sigma^2 + \sigma_c^2 - \sigma_g^2))/\sigma; (\sigma_c - \sigma_g \rho)/\sigma) \\
k_{low}^g(\xi, \mathbf{x}) &= -\Phi_2((R_c^K(0) + 0.5\sigma_c^2)/\sigma_c, (R_g(\xi, 0) + 0.5 \cdot (\sigma^2 + \sigma_g^2 - \sigma_c^2))/\sigma; -(\sigma_c - \sigma_g \rho)/\sigma)
\end{aligned}$$

$$\begin{aligned}
& -\Phi_1(R_g^K(\xi)/\sigma_g + \sigma_g/2) + \Phi_2((R_c^K(0) + 0.5\sigma_c^2)/\sigma_c, R_g^K(\xi)/\sigma_g + \sigma_g/2; \rho) \\
k_{low}^{cg}(\xi, \mathbf{x}) &= 1 + k_{low}^{cg,c}(\xi, \mathbf{x}) + k_{low}^{cg,g}(\xi, \mathbf{x}) \\
k_{low}^{cg,c}(\xi, \mathbf{x}) &= \Phi_2(R_{\Delta}^{c,low}(\xi)/\sigma_c, (R_c(\xi, 0) + 0.5 \cdot (\sigma^2 + \sigma_c^2 - \sigma_g^2))/\sigma, (\sigma_c - \sigma_g)/\sigma) \\
& - \Phi_2(R_{\Delta}^{c,low}(\xi)/\sigma_c, (-R_{\alpha}^K(\xi) - \sigma^2(\alpha))/\sigma(\alpha), -(\sigma_c\alpha_c + \sigma_g\alpha_g\rho)/\sigma(\alpha)) \\
k_{low}^{cg,g}(\xi, \mathbf{x}) &= \Phi_2(R_{\Delta}^{g,low}(\xi)/\sigma_c, (R_g(\xi, 0) + 0.5 \cdot (\sigma^2 + \sigma_g^2 - \sigma_c^2))/\sigma, -(\sigma_c - \sigma_g)/\sigma) \\
& - \Phi_2(R_{\Delta}^{g,low}(\xi)/\sigma_c, (R_{\alpha}^K(\xi) + \sigma^2(\alpha))/\sigma(\alpha), (\sigma_c\alpha_c + \sigma_g\alpha_g\rho)/\sigma(\alpha)).
\end{aligned}$$

**Proof.** We refer to Chapter 5.4.1. ■

**Lemma 5.2 (High-Cases)** *Given the assumptions in Proposition 5.2 and Definition 5.1,  $f_{high}$  and  $k_{high}$  are given by*

$$\begin{aligned}
f_{high}(\xi, \mathbf{x}) &= f_{high}^c(\xi, \mathbf{x}) + f_{high}^g(\xi, \mathbf{x}) + f_{high}^{cg}(\xi, \mathbf{x}) \\
f_{high}^c(\xi, \mathbf{x}) &= b_c(\xi - \bar{\xi}^g, \mathbf{x}) [\Phi_1(-R_c(\xi - \bar{\xi}^g, \bar{\xi}^g)/\sigma) \\
& - \Phi_2(R_c^K(\xi - \bar{\xi}^g)/\sigma_c - \sigma_c/2, -R_c(\xi - \bar{\xi}^g, \bar{\xi}^g)/\sigma; -(\sigma_c - \sigma_g\rho)/\sigma)] \\
f_{high}^g(\xi, \mathbf{x}) &= b_g(\xi - \bar{\xi}^c, \mathbf{x}) [\Phi_1(-R_g(\xi - \bar{\xi}^c, \bar{\xi}^c)/\sigma) \\
& - \Phi_2(R_c^K(\bar{\xi}^c)/\sigma_c + \sigma_c/2 - \sigma_g\rho, -R_g(\xi - \bar{\xi}^c, \bar{\xi}^c)/\sigma; (\sigma_c - \sigma_g\rho)/\sigma) \\
& + \Phi_2(R_c^K(\bar{\xi}^c)/\sigma_c + \sigma_c/2 - \sigma_g\rho, -R_g^K(\xi - \bar{\xi}^c)/\sigma_g + \sigma_g/2; -\rho)] \\
f_{high}^{cg}(\xi, \mathbf{x}) &= b_{cg}(d, \mathbf{x}) e^{-\alpha_c\alpha_g\sigma^2/2} [-1 + f_{high}^{cg,c}(\xi, \mathbf{x}) + f_{high}^{cg,g}(\xi, \mathbf{x})] \\
f_{high}^{cg,c}(\xi, \mathbf{x}) &= \Phi_1(R_c(\xi - \bar{\xi}^g, \bar{\xi}^g)/\sigma + \alpha_c\sigma) \\
& + \Phi_2(R_{\Delta}^{c,High}(\xi) - (\alpha_c\sigma_c + \alpha_g\sigma_g\rho), -R_c(\xi - \bar{\xi}^g, \bar{\xi}^g)/\sigma - \alpha_g\sigma; -(\sigma_c - \sigma_g\rho)/\sigma) \\
& - \Phi_2(R_{\Delta}^{c,High}(\xi) - (\alpha_c\sigma_c + \alpha_g\sigma_g\rho), R_{\alpha}^K(\xi)/\sigma(\alpha); (\alpha_c\sigma_c + \alpha_g\sigma_g\rho)/\sigma(\alpha)) \\
f_{high}^{cg,g}(\xi, \mathbf{x}) &= \Phi_1(R_g(\xi - \bar{\xi}^c, \bar{\xi}^c)/\sigma + \alpha_c\sigma) \\
& - \Phi_2(R_{\Delta}^{g,High}(\xi) - (\alpha_c\sigma_c + \alpha_g\sigma_g\rho), -R_{\alpha}^K(\xi)/\sigma(\alpha); -(\alpha_c\sigma_c + \alpha_g\sigma_g\rho)/\sigma(\alpha)) \\
& + \Phi_2(R_{\Delta}^{g,High}(\xi) - (\alpha_c\sigma_c + \alpha_g\sigma_g\rho), -R_g(\xi - \bar{\xi}^c, \bar{\xi}^c)/\sigma - \alpha_c\sigma; (\sigma_c - \sigma_g\rho)/\sigma)] \\
k_{high}(\xi, \mathbf{x}) &= k_{high}^c(\xi, \mathbf{x}) + k_{high}^g(\xi, \mathbf{x}) + k_{high}^{cg}(\xi, \mathbf{x}) \\
k_{high}^c(\xi, \mathbf{x}) &= -\Phi_2(R_c^K(\xi - \bar{\xi}^g)/\sigma_c + 0.5\sigma_c, (-R_c(\xi - \bar{\xi}^g, \bar{\xi}^g) + 0.5(\sigma_g^2 - \sigma_c^2 - \sigma^2))/\sigma; \frac{-\sigma_c - \sigma_g\rho}{\sigma}) \\
k_{high}^g(\xi, \mathbf{x}) &= -\Phi_2(R_c^K(\bar{\xi}^c)/\sigma_c + \sigma_c/2, (-R_g(\xi - \bar{\xi}^c, \bar{\xi}^c) - 0.5(\sigma^2 - \sigma_c^2 + \sigma_g^2))/\sigma; (\sigma_c - \sigma_g\rho)/\sigma) \\
& + \Phi_2(R_c^K(\bar{\xi}^c)/\sigma_c + \sigma_c/2, -R_g^K(\xi - \bar{\xi}^c)/\sigma_g - \sigma_g/2; -\rho) \\
k_{high}^{cg}(\xi, \mathbf{x}) &= 1 + k_{high}^{cg,c}(\xi, \mathbf{x}) + k_{high}^{cg,g}(\xi, \mathbf{x}) \\
k_{high}^{cg,c}(\xi, \mathbf{x}) &= \Phi_2(R_{\Delta}^{c,High}(\xi), (-R_c(\xi - \bar{\xi}^g, \bar{\xi}^g) - 0.5(\sigma^2 + \sigma_c^2 - \sigma_g^2))/\sigma; -(\sigma_c - \sigma_g\rho)/\sigma) \\
& - \Phi_2(R_{\Delta}^{c,High}(\xi), R_{\alpha}^K(\xi)/\sigma(\alpha) + \sigma(\alpha); (\alpha_c\sigma_c + \alpha_g\sigma_g\rho)/\sigma(\alpha)) \\
k_{high}^{cg,g}(\xi, \mathbf{x}) &= -\Phi_2(R_{\Delta}^{g,High}(\xi), -R_{\alpha}^K(\xi)/\sigma(\alpha) - \sigma(\alpha); -(\alpha_c\sigma_c + \alpha_g\sigma_g\rho)/\sigma(\alpha)) \\
& + \Phi_2(R_{\Delta}^{g,High}(\xi), (-R_g(\xi - \bar{\xi}^c, \bar{\xi}^c) - 0.5(\sigma^2 + \sigma_g^2 - \sigma_c^2))/\sigma; (\sigma_c - \sigma_g\rho)/\sigma)
\end{aligned}$$

**Proof.** We refer to Chapter 5.4.2. ■

**Lemma 5.3 (Mid-Cases)** *Given the assumptions in Proposition 5.2 and Definition 5.1,  $f_{mid}$  and  $k_{mid}$  are given by*

$$f_{mid}(\xi, \mathbf{x}) = f_{high}^{i^+}(\xi, \mathbf{x}) + f_{low}^{i^+}(\xi, \mathbf{x}) + b_{cg}(d, \mathbf{x})e^{-\alpha_c \alpha_g \sigma^2 / 2} \left[ f_{high}^{cg, i^+}(\xi, \mathbf{x}) + f_{low}^{cg, i^+}(\xi, \mathbf{x}) \right]$$

$$k_{mid}(\xi, \mathbf{x}) = k_{high}^{i^+}(\xi, \mathbf{x}) + k_{low}^{i^+}(\xi, \mathbf{x}) + 2 + k_{high}^{cg, i^+}(\xi, \mathbf{x}) + k_{low}^{cg, i^+}(\xi, \mathbf{x}),$$

where  $i^+, i^-$  are defined in Appendix A.1.

**Proof.** Just the same calculations as performed in low/high but keeping in mind that only the fuel with higher capacity has to be considered. ■

**Proposition 5.3 (Extension of Proposition 5.2 to Negative Prices and Price Spikes)** *We allow the demand density function  $\phi_d$  in Proposition 5.2 to be defined on  $\mathbb{R}$ . In order to involve negative power prices and price spikes, the following terms have to be added to those in Proposition 5.2 to calculate the present value of a European call option with strike  $K$  maturing in  $t$ :*

$$\int_{-\infty}^0 f_n(D, \mathbf{F}_t) \phi_d(D) dD + \int_{\bar{\xi}}^{\infty} f_s(D, \mathbf{F}_t) \phi_d(D) dD,$$

where

$$f_n(d, \mathbf{x}) = \sum_{i \in I} b_i(0, x_i) \Phi(R_i(0, 0)/\sigma) + 1 - \exp(-m_n d) - K$$

$$+ \delta_N(d) \cdot \{$$

$$- b_c(0, x_c) \Phi_2((R_c^{K,n}(d) - \sigma_c^2/2)/\sigma_c, R_c(0, 0)/\sigma; (\sigma_c - \sigma_g \rho)/\sigma)$$

$$- b_g(0, x_g) [\Phi_1((R_g^{K,n}(d) - \sigma_g^2/2)/\sigma_g)$$

$$+ \Phi_2((R_c^{K,n}(d) + \sigma_c^2/2)/\sigma_c - \sigma_g \rho, R_g(0, 0)/\sigma; -(\sigma_c - \sigma_g \rho)/\sigma)$$

$$- \Phi_2((R_c^{K,n}(d) + \sigma_c^2/2)/\sigma_c - \sigma_g \rho, (R_g^{K,n}(d) - \sigma_g^2/2)/\sigma_g; \rho)]$$

$$+ (1 - \exp(-m_n d) - K) [$$

$$- \Phi_2((R_c^{K,n}(d) + \sigma_c^2/2)/\sigma_c, (R_c(0, 0) + 0.5(\sigma^2 - \sigma_g^2 + \sigma_c^2))/\sigma; (\sigma_c - \sigma_g \rho)/\rho)$$

$$- \Phi((R_g^{K,n}(d) + \sigma_g^2/2)/\sigma_g)$$

$$- \Phi_2((R_c^{K,n}(d) + \sigma_c^2/2)/\sigma_c, (R_g(0, 0) + 0.5(\sigma^2 - \sigma_c^2 + \sigma_g^2))/\sigma; -(\sigma_c - \sigma_g \rho)/\rho)$$

$$+ \Phi_2(R_c^{K,n}(d) + \sigma_c^2/2)/\sigma_c, (R_g^{K,n}(d) + \sigma_g^2/2)/\sigma_g; \rho)] \}$$

$$f_s(d, \mathbf{x}) = \sum_{i \in I} b_i(\bar{\xi}^i, x_i) \Phi(-R_i(\bar{\xi}^i, \bar{\xi}^j)/\sigma) + \exp(m_s(d - \bar{\xi})) - 1 - K$$

$$+ \delta_S(d) \cdot \{$$

$$- b_c(\bar{\xi}^c, x_c) \Phi_2((R_c^{K,s}(d) - \sigma_c^2/2)/\sigma_c, -R_c(\bar{\xi}^c, \bar{\xi}^g)/\sigma; -(\sigma_c - \sigma_g \rho)/\sigma)$$

$$+ b_g(\bar{\xi}^g, x_g) [\Phi_2((R_c^{K,s}(d) + \sigma_c^2/2)/\sigma_c - \sigma_g \rho, (-R_g^{K,s}(d) + \sigma_g^2/2)/\sigma_g; -\rho)$$

$$- \Phi_2((R_c^{K,s}(d) + \sigma_c^2/2)/\sigma_c - \sigma_g \rho, -R_g(\bar{\xi}^g, \bar{\xi}^c)/\sigma; (\sigma_c - \sigma_g \rho)/\sigma)]$$

$$+ (\exp(m_s(d - \bar{\xi})) - 1 - K) [$$

$$- \Phi_2((R_c^{K,s}(d) + \sigma_c^2/2)/\sigma_c, (-R_c(\bar{\xi}^c, \bar{\xi}^g) + 0.5(-\sigma^2 + \sigma_g^2 - \sigma_c^2))/\sigma; -(\sigma_c - \sigma_g \rho)/\sigma)$$

$$\begin{aligned}
& + \Phi_2 \left( (R_c^{K,s}(d) + \sigma_c^2/2)/\sigma_c, (-R_g^{K,s}(d) - \sigma_g^2/2)/\sigma_g; -\rho \right) \\
& - \Phi_2 \left( (R_c^{K,s}(d) + \sigma_c^2/2)/\sigma_c, (-R_g(\bar{\xi}^g, \bar{\xi}^c) - 0.5(\sigma^2 - \sigma_c^2 + \sigma_g^2))/\sigma; (\sigma_c - \sigma_g\rho)/\sigma \right) \}
\end{aligned}$$

and

$$\begin{aligned}
\delta_N(d) &= \begin{cases} 1 & , \text{ if } K + \exp(-m_n d) - 1 > 0 \\ 0 & , \text{ else} \end{cases} \\
\delta_S(d) &= \begin{cases} 1 & , \text{ if } K - \exp(m_s(d - \bar{\xi})) + 1 > 0 \\ 0 & , \text{ else} \end{cases}.
\end{aligned}$$

**Proof.** We refer to Chapter 5.4.3. ■

As a next step we generalize Proposition 5.2 by assuming a more general demand density function having non-zero values not only on  $[0, \bar{\xi}]$  but on  $\mathbb{R}$  instead.

**Corollary 5.1** *Let  $D_t := \min \{ \bar{\xi}, \max \{ 0, X_t \} \}$  be a truncated demand process with  $X_t$  being normal distributed with mean  $\mu_D$  and variance  $\sigma_D^2$ . Furthermore, let the assumptions of Proposition 5.2 hold. We assume the power price to have the form given in Chapter A.1 but with  $m_n = 0$ ,  $m_s = 0$  (cf. Remark 5.1). Then, the price of a European call option with strike  $K > 0$  and maturity  $t \in [t_0, T]$  is given by*

$$C_t^P(K) = F_t^P + F_{low}(K) + F_{high}(K) - K \cdot (K_{low}(K) + K_{high}(K)) + N(K) + S(K),$$

where  $F_t^P$  is the power forward price and  $F_{low}(K)$  and  $F_{high}(K)$  are derived in Lemma 5.4 to 5.5.

**Proof.** Whereas  $F_{low}(K)$  and  $F_{high}(K)$  are derived in Lemma 5.4 to 5.5, we can straight give the form of  $N(K)$  and  $S(K)$ .

Because we haven chosen  $m_n = 0$  and  $m_s = 0$ ,  $f_n(d, \mathbf{x})$  and  $f_s(d, \mathbf{x})$  do not depend on the demand anymore. Furthermore,  $R_i^{K,s}(D) = R_i^K(D - \bar{\xi})$  and  $R_i^{K,n}(D) = R_i^K(0)$ . We get

$$\begin{aligned}
N(K) &= f_n(0, \mathbf{F}_t) \cdot \Phi_1 \left( \frac{-\mu_D}{\sigma_D} \right) & S(K) &= f_s(0, \mathbf{F}_t) \cdot \Phi_1 \left( \frac{\mu_D - \bar{\xi}}{\sigma_D} \right).
\end{aligned}$$

■

**Remark 5.1 (Negative Prices and Spikes)** *Due to the non-linearity of the demand in the definition of  $R_i^{K,s}$  and  $R_i^{K,n}$  ( $i = c, g$ ), we cannot apply Lemma 5.7 to derive a more general analytical solution of Corollary 5.1 being able to incorporate spikes and negative prices.*

*If necessary the integration over demand in Proposition 5.3 would have to be performed using i.e. numerical integration techniques. However, this is not performed in this thesis.*

Before we give the constituents to the formula in detail we define - for an arbitrary  $y \in \mathbb{R}$  -

$$\mathbf{x}^{i,L}(y) := \begin{pmatrix} \frac{\bar{\xi}^i - \mu_D}{\sigma_D} - y\sigma_D \\ \frac{-\mu_D}{\sigma_D} - y\sigma_D \end{pmatrix}, \quad \mathbf{x}^{i,H}(y) := \begin{pmatrix} \frac{\bar{\xi}^i - \mu_D}{\sigma_D} - y\sigma_D \\ \frac{\bar{\xi}^i - \mu_D}{\sigma_D} - y\sigma_D \end{pmatrix}, \quad \mu_D(y) := \mu_D + y\sigma_D^2.$$

Furthermore, we denote the trivariate standard normal cumulative density function by  $\Phi_3(x_1, x_2, x_3; (\rho_{21}, \rho_{31}, \rho_{32})^T)$ . We define for  $x_1, x_2, y, z \in \mathbb{R}$ ,  $\rho_{21}, \rho_{31}, \rho_{32} \in (-1, 1)$

$$\Phi_3 \left( \begin{pmatrix} x_1 \\ x_2 \end{pmatrix}, y, z; (\rho_{21}, \rho_{31}, \rho_{32})^T \right) := \Phi_3(x_1, y, z; (\rho_{21}, \rho_{31}, \rho_{32})^T) - \Phi_3(x_2, y, z; (\rho_{21}, \rho_{31}, \rho_{32})^T).$$



**Lemma 5.4 (Low)** *Given the assumptions in Proposition 5.2, Corollary 5.1 and Definition 5.1,  $F_{low}(K)$  is given by*

$$\begin{aligned}
F_{low}(K) = & \exp\left(\frac{m_c^2 \sigma_d^2}{2}\right) b_c(\mu_d, F_t^c) \left[ -\Phi_3 \left( \mathbf{x}^{c,L}(m_c), \frac{R_c^K(\mu_D(m_c)) - \sigma_c^2/2}{v(m_c, \sigma_c)}, \frac{R_c(\mu_D(m_c), 0)}{v(m_c, \sigma)}; \begin{pmatrix} \frac{m_c \sigma_D}{v(m_c, \sigma_c)} \\ \frac{m_c \sigma_D}{v(m_c, \sigma)} \\ \frac{\sigma_c^2 - \sigma_g \sigma_c \rho + m_c^2 \sigma_D^2}{v(m_c, \sigma_c) v(m_c, \sigma)} \end{pmatrix} \right) \right] \\
& + \exp\left(\frac{m_g^2 \sigma_d^2}{2}\right) b_g(\mu_d, F_t^g) \left[ -\Phi_3 \left( \mathbf{x}^{g,L}(m_g), (R_c^K(0) + 0.5 \sigma_c^2)/\sigma_c - \sigma_g \rho, \frac{R_g(\mu_D(m_g), 0)}{v(m_g, \sigma)}; \begin{pmatrix} 0 \\ \frac{m_g \sigma_D}{v(m_g, \sigma)} \\ \frac{-(\sigma_c - \sigma_g \rho)}{v(m_g, \sigma)} \end{pmatrix} \right) \right. \\
& + \Phi_3 \left( \mathbf{x}^{g,L}(m_g), (R_c^K(0) + 0.5 \sigma_c^2)/\sigma_c - \sigma_g \rho, \frac{R_g^K(\mu_D(m_g)) - \sigma_g^2/2}{v(m_g, \sigma_g)}; \begin{pmatrix} 0 \\ \frac{m_g \sigma_D}{v(m_g, \sigma_g)} \\ \frac{\rho \sigma_g}{v(m_g, \sigma_g)} \end{pmatrix} \right) \\
& \left. - \Phi_2 \left( \mathbf{x}^{g,L}(m_g), \frac{R_g^K(\mu_D(m_g)) - \sigma_g^2/2}{v(m_g, \sigma_g)}; \frac{m_g \sigma_D}{v(m_g, \sigma_g)} \right) \right] \\
& + \exp(\eta) b_{cg}(\mu_d, \mathbf{F}_t) \left[ \Phi_3 \left( \mathbf{x}^{c,L}(\gamma), \frac{R_{\Delta}^{c,low}(\mu_D(\gamma)) - (\alpha_c \sigma_c + \sigma_g \alpha_g \rho) \sigma_c}{v(\gamma + \alpha_g m_c, \sigma_c)}, \frac{R_c(\mu_D(\gamma), 0) + \sigma^2 \alpha_g}{v(m_c, \sigma)}; \begin{pmatrix} \frac{(\gamma + \alpha_g m_c) \sigma_D}{v(\gamma + \alpha_g m_c, \sigma_c)} \\ \frac{m_c \sigma_D}{v(m_c, \sigma)} \\ \frac{(\sigma_c - \sigma_g \rho) \sigma_c + (\gamma + \alpha_g m_c) m_c \sigma_D^2}{v(\gamma + \alpha_g m_c, \sigma_c) v(m_c, \sigma)} \end{pmatrix} \right) \right. \\
& - \Phi_3 \left( \mathbf{x}^{c,L}(\gamma), \frac{R_{\Delta}^{c,low}(\mu_D(\gamma)) - (\alpha_c \sigma_c + \sigma_g \alpha_g \rho) \sigma_c}{v(\gamma + \alpha_g m_c, \sigma_c)}, \frac{-R_{\alpha}^K(\mu_D(\gamma))}{v(\gamma, \sigma(\alpha))}; \begin{pmatrix} \frac{(\gamma + \alpha_g m_c) \sigma_D}{v(\gamma + \alpha_g m_c, \sigma_c)} \\ \frac{-\gamma \sigma_D}{v(\gamma, \sigma(\alpha))} \\ \frac{(-\sigma_c \alpha_c - \sigma_g \alpha_g \rho) \sigma_c - (\gamma + \alpha_g m_c) \gamma \sigma_D^2}{v(\gamma + \alpha_g m_c, \sigma_c) v(\gamma, \sigma(\alpha))} \end{pmatrix} \right) \\
& \left. + \Phi_3 \left( \mathbf{x}^{g,L}(\gamma), \frac{R_{\Delta}^{g,low}(\mu_D(\gamma)) - (\alpha_c \sigma_c + \sigma_g \alpha_g \rho) \sigma_c}{v(\gamma - \alpha_g m_g, \sigma_c)}, \frac{R_g(\mu_D(\gamma), 0) + \sigma^2 \alpha_c}{v(m_g, \sigma)}; \begin{pmatrix} \frac{(\gamma - \alpha_g m_g) \sigma_D}{v(\gamma - \alpha_g m_g, \sigma_c)} \\ \frac{m_g \sigma_D}{v(m_g, \sigma)} \\ \frac{-(\sigma_c - \sigma_g \rho) \sigma_c - (\gamma - \alpha_g m_g) \sigma_D^2 m_g}{v(m_g, \sigma) v(\gamma - \alpha_g m_g, \sigma_c)} \end{pmatrix} \right) \right]
\end{aligned}$$

$$-\Phi_3 \left( \mathbf{x}^{g,L}(\gamma), \frac{R_{\Delta}^{g,low}(\mu_D(\gamma)) - (\alpha_c \sigma_c + \sigma_g \alpha_g \rho) \sigma_c}{v(\gamma - \alpha_g m_g, \sigma_c)}, \frac{R_{\alpha}^K(\mu_D(\gamma))}{v(\gamma, \sigma(\alpha))}; \begin{pmatrix} \frac{(\gamma - m_g \alpha_g) \sigma_D}{v(\gamma - \alpha_g m_g, \sigma_c)} \\ \frac{\gamma \sigma_D}{v(\gamma, \sigma(\alpha))} \\ \frac{(\sigma_c \alpha_c + \alpha_g \sigma_g \rho) \sigma_c - (\gamma - m_g \alpha_g) \sigma_D^2 \gamma}{v(\gamma, \sigma(\alpha)) v(\gamma - \alpha_g m_g, \sigma_c)} \end{pmatrix} \right) \Bigg]$$

Respectively,  $K_{low}$  is given by

$$\begin{aligned} K_{low}(K) = & -\Phi_3 \left( \mathbf{x}^{c,L}(0), \frac{R_c^K(\mu_D(0)) + \sigma_c^2/2}{v(m_c, \sigma_c)}, \frac{R_c(\mu_D(0), 0) + \frac{1}{2}(\sigma^2 + \sigma_c^2 - \sigma_g^2)}{v(m_c, \sigma)}; \begin{pmatrix} \frac{m_c \sigma_D}{v(m_c, \sigma_c)} \\ \frac{m_c \sigma_D}{v(m_c, \sigma)} \\ \frac{\sigma_c^2 - \sigma_g \sigma_c \rho + m_c^2 \sigma_D^2}{v(m_c, \sigma_c) v(m_c, \sigma)} \end{pmatrix} \right) \\ & -\Phi_3 \left( \mathbf{x}^{g,L}(0), (R_c^K(0) + 0.5 \sigma_c^2)/\sigma_c, \frac{R_g(\mu_D(0), 0) + \frac{1}{2}(\sigma^2 - \sigma_c^2 + \sigma_g^2)}{v(m_g, \sigma)}; \begin{pmatrix} 0 \\ \frac{m_g \sigma_D}{v(m_g, \sigma)} \\ \frac{-(\sigma_c - \sigma_g \rho)}{v(m_g, \sigma)} \end{pmatrix} \right) \\ & +\Phi_3 \left( \mathbf{x}^{g,L}(0), (R_c^K(0) + 0.5 \sigma_c^2)/\sigma_c, \frac{R_g^K(\mu_D(m_g)) + \sigma_g^2/2}{v(m_g, \sigma_g)}; \begin{pmatrix} 0 \\ \frac{m_g \sigma_D}{v(m_g, \sigma_g)} \\ \frac{\rho \sigma_g}{v(m_g, \sigma_g)} \end{pmatrix} \right) \\ & -\Phi_2 \left( \mathbf{x}^{g,L}(0), \frac{R_g^K(\mu_D(m_g)) + \sigma_g^2/2}{v(m_g, \sigma_g)}; \frac{m_g \sigma_D}{v(m_g, \sigma_g)} \right) \\ & +\Phi_3 \left( \mathbf{x}^{c,L}(0), \frac{R_{\Delta}^{c,low}(\mu_D(0))}{v(\gamma + \alpha_g m_c, \sigma_c)}, \frac{R_c(\mu_D(0), 0) + \frac{1}{2}(\sigma^2 + \sigma_c^2 - \sigma_g^2)}{v(m_c, \sigma)}; \begin{pmatrix} \frac{(\gamma + \alpha_g m_c) \sigma_D}{v(\gamma + \alpha_g m_c, \sigma_c)} \\ \frac{m_c \sigma_D}{v(m_c, \sigma)} \\ \frac{(\sigma_c - \sigma_g \rho) \sigma_c + (\gamma + \alpha_g m_c) m_c \sigma_D^2}{v(\gamma + \alpha_g m_c, \sigma_c) v(m_c, \sigma)} \end{pmatrix} \right) \\ & -\Phi_3 \left( \mathbf{x}^{c,L}(0), \frac{R_{\Delta}^{c,low}(\mu_D(0))}{v(\gamma + \alpha_g m_c, \sigma_c)}, \frac{-R_{\alpha}^K(\mu_D(0)) - \sigma^2(\alpha)}{v(\gamma, \sigma(\alpha))}; \begin{pmatrix} \frac{(\gamma + \alpha_g m_c) \sigma_D}{v(\gamma + \alpha_g m_c, \sigma_c)} \\ \frac{-\gamma \sigma_D}{v(\gamma, \sigma(\alpha))} \\ \frac{-(\sigma_c \alpha_c - \sigma_g \alpha_g \rho) \sigma_c - (\gamma + \alpha_g m_c) \gamma \sigma_D^2}{v(\gamma + \alpha_g m_c, \sigma_c) v(\gamma, \sigma(\alpha))} \end{pmatrix} \right) \end{aligned}$$

$$\begin{aligned}
& + \Phi_3 \left( \mathbf{x}^{g,L}(0), \frac{R_{\Delta}^{g,low}(\mu_D(0))}{v(\gamma - \alpha_g m_g, \sigma_c)}, \frac{R_g(\mu_D(0), 0) + \frac{1}{2}(\sigma^2 - \sigma_c^2 + \sigma_g^2)}{v(m_g, \sigma)}, \left( \begin{array}{c} \frac{(\gamma - m_g \alpha_g) \sigma_D}{v(\gamma - \alpha_g m_g, \sigma_c)} \\ \frac{m_g \sigma_D}{v(m_g, \sigma)} \\ \frac{-(\sigma_c - \sigma_g \rho) \sigma_c - (\gamma - m_g \alpha_g) \sigma_D^2 m_g}{v(m_g, \sigma) v(\gamma - \alpha_g m_g, \sigma_c)} \end{array} \right) \right) \\
& - \Phi_3 \left( \mathbf{x}^{g,L}(0), \frac{R_{\Delta}^{g,low}(\mu_D(0))}{v(\gamma - \alpha_g m_g, \sigma_c)}, \frac{R_{\alpha}^K(\mu_D(0)) + \sigma^2(\alpha)}{v(\gamma, \sigma(\alpha))}, \left( \begin{array}{c} \frac{(\gamma - m_g \alpha_g) \sigma_D}{v(\gamma - \alpha_g m_g, \sigma_c)} \\ \frac{\gamma \sigma_D}{v(\gamma, \sigma(\alpha))} \\ \frac{(\sigma_c \alpha_c + \alpha_g \sigma_g \rho) \sigma_c - (\gamma - m_g \alpha_g) \sigma_D^2 \gamma}{v(\gamma, \sigma(\alpha)) v(\gamma - \alpha_g m_g, \sigma_c)} \end{array} \right) \right)
\end{aligned}$$

**Proof.** We refer to Chapter 5.4.4. ■

**Lemma 5.5 (High)** *Given the assumptions in Proposition 5.2, Corollary 5.1 and Definition 5.1,  $F_{high}(K)$  is given by*

$$\begin{aligned}
F_{high}(K) = & \exp \left( \frac{m_c^2 \sigma_d^2}{2} \right) b_c(\mu_d - \bar{\xi}^g, F_t^c) \left[ -\Phi_3 \left( \mathbf{x}^{g,H}(m_c), \frac{R_c^K(\mu_D(m_c) - \bar{\xi}^g) - \sigma_c^2/2}{v(m_c, \sigma_c)}, \frac{-R_c(\mu_D(m_c) - \bar{\xi}^g, \bar{\xi}^g)}{v(m_c, \sigma)}, \left( \begin{array}{c} \frac{m_c \sigma_D}{v(m_c, \sigma_c)} \\ \frac{-m_c \sigma_D}{v(m_c, \sigma)} \\ \frac{-\sigma_c^2 + \sigma_g \sigma_c \rho - m_c^2 \sigma_D^2}{v(m_c, \sigma_c) v(m_c, \sigma)} \end{array} \right) \right) \right] \\
& + \exp \left( \frac{m_g^2 \sigma_d^2}{2} \right) b_g(\mu_d - \bar{\xi}^c, F_t^g) \left[ -\Phi_3 \left( \mathbf{x}^{c,H}(m_g), (R_c^K(\bar{\xi}^c) + 0.5 \sigma_c^2) / \sigma_c - \sigma_g \rho, \frac{-R_g(\mu_D(m_g) - \bar{\xi}^c, \bar{\xi}^c)}{v(m_g, \sigma)}, \left( \begin{array}{c} 0 \\ \frac{-m_g \sigma_D}{v(m_g, \sigma)} \\ \frac{(\sigma_c - \sigma_g \rho)}{v(m_g, \sigma)} \end{array} \right) \right) \right] \\
& + \Phi_3 \left( \mathbf{x}^{c,H}(m_g), (R_c^K(\bar{\xi}^c) + 0.5 \sigma_c^2) / \sigma_c - \sigma_g \rho, \frac{-R_g^K(\mu_D(m_g) - \bar{\xi}^c) + \sigma_g^2/2}{v(m_g, \sigma_g)}, \left( \begin{array}{c} 0 \\ \frac{-m_g \sigma_D}{v(m_g, \sigma_g)} \\ \frac{-\rho \sigma_g}{v(m_g, \sigma_g)} \end{array} \right) \right) \right] \\
& + \exp(\eta) b_{cg}(\mu_d, \mathbf{F}_t) \left[ \Phi_3 \left( \mathbf{x}^{g,H}(\gamma), \frac{R_{\Delta}^{c,high}(\mu_D(\gamma)) - (\alpha_c \sigma_c + \sigma_g \alpha_g \rho) \sigma_c}{v(\gamma + \alpha_g m_c, \sigma_c)}, \frac{-R_c(\mu_D(\gamma) - \bar{\xi}^g, \bar{\xi}^g) - \sigma^2 \alpha_g}{v(m_c, \sigma)}, \left( \begin{array}{c} \frac{(\gamma + \alpha_g m_c) \sigma_D}{v(\gamma + \alpha_g m_c, \sigma_c)} \\ \frac{-m_c \sigma_D}{v(m_c, \sigma)} \\ \frac{-(\sigma_c - \sigma_g \rho) \sigma_c - (\gamma + \alpha_g m_c) m_c \sigma_D^2}{v(\gamma + \alpha_g m_c, \sigma_c) v(m_c, \sigma)} \end{array} \right) \right) \right]
\end{aligned}$$

$$\begin{aligned}
& -\Phi_3 \left( \mathbf{x}^{g,H}(\gamma), \frac{R_{\Delta}^{c,high}(\mu_D(\gamma)) - (\alpha_c \sigma_c + \sigma_g \alpha_g \rho) \sigma_c}{v(\gamma + \alpha_g m_c, \sigma_c)}, \frac{R_{\alpha}^K(\mu_D(\gamma))}{v(\gamma, \sigma(\alpha))}; \left( \begin{array}{c} \frac{(\gamma + \alpha_g m_c) \sigma_D}{v(\gamma + \alpha_g m_c, \sigma_c)} \\ \frac{\gamma \sigma_D}{v(\gamma, \sigma(\alpha))} \\ \frac{(\sigma_c \alpha_c + \sigma_g \alpha_g \rho) \sigma_c + (\gamma + \alpha_g m_c) \gamma \sigma_D^2}{v(\gamma + \alpha_g m_c, \sigma_c) v(\gamma, \sigma(\alpha))} \end{array} \right) \right) \\
& -\Phi_3 \left( \mathbf{x}^{c,H}(\gamma), \frac{R_{\Delta}^{g,high}(\mu_D(\gamma)) - (\alpha_c \sigma_c + \sigma_g \alpha_g \rho) \sigma_c}{v(\gamma - \alpha_g m_g, \sigma_c)}, \frac{-R_{\alpha}^K(\mu_D(\gamma))}{v(\gamma, \sigma(\alpha))}; \left( \begin{array}{c} \frac{(\gamma - m_g \alpha_g) \sigma_D}{v(\gamma - \alpha_g m_g, \sigma_c)} \\ \frac{-\gamma \sigma_D}{v(\gamma, \sigma(\alpha))} \\ \frac{-(\sigma_c \alpha_c + \sigma_g \alpha_g \rho) \sigma_c + (-\gamma + m_g \alpha_g) \sigma_D^2 \gamma}{v(\gamma - \alpha_g m_g, \sigma_c) v(\gamma, \sigma(\alpha))} \end{array} \right) \right) \\
& +\Phi_3 \left( \mathbf{x}^{c,H}(\gamma), \frac{R_{\Delta}^{g,high}(\mu_D(\gamma)) - (\alpha_c \sigma_c + \sigma_g \alpha_g \rho) \sigma_c}{v(\gamma - \alpha_g m_g, \sigma_c)}, \frac{-R_g(\mu_D(\gamma) - \bar{\xi}^g, \bar{\xi}^c) - \sigma^2 \alpha_c}{v(m_g, \sigma)}; \left( \begin{array}{c} \frac{(\gamma - m_g \alpha_g) \sigma_D}{v(\gamma - \alpha_g m_g, \sigma_c)} \\ \frac{-m_g \sigma_D}{v(m_g, \sigma)} \\ \frac{\sigma_c (\sigma_c - \sigma_g \rho) + m_g \sigma_D^2 (-\gamma + m_g \alpha_g)}{v(\gamma - \alpha_g m_g, \sigma_c) v(m_g, \sigma)} \end{array} \right) \right) \Bigg]
\end{aligned}$$

Respectively,  $K_{high}$  is given by

$$\begin{aligned}
K_{high}(K) = & -\Phi_3 \left( \mathbf{x}^{g,H}(0), \frac{R_c^K(\mu_D(0) - \bar{\xi}^g) + \sigma_c^2/2}{v(m_c, \sigma_c)}, \frac{-R_c(\mu_D(0) - \bar{\xi}^g, \bar{\xi}^g) + 0.5(\sigma_g^2 - \sigma_c^2 - \sigma^2)}{v(m_c, \sigma)}; \left( \begin{array}{c} \frac{m_c \sigma_D}{v(m_c, \sigma_c)} \\ \frac{-m_c \sigma_D}{v(m_c, \sigma)} \\ \frac{-\sigma_c^2 + \sigma_g \sigma_c \rho - m_c^2 \sigma_D^2}{v(m_c, \sigma_c) v(m_c, \sigma)} \end{array} \right) \right) \\
& -\Phi_3 \left( \mathbf{x}^{c,H}(0), (R_c^K(\bar{\xi}^c) + 0.5\sigma_c^2)/\sigma_c, \frac{-R_g(\mu_D(0) - \bar{\xi}^g, \bar{\xi}^c) - 0.5(\sigma^2 - \sigma_c^2 + \sigma_g^2)}{v(m_g, \sigma)}; \left( \begin{array}{c} 0 \\ \frac{-m_g \sigma_D}{v(m_g, \sigma)} \\ \frac{(\sigma_c - \sigma_g \rho)}{v(m_g, \sigma)} \end{array} \right) \right) \\
& +\Phi_3 \left( \mathbf{x}^{c,H}(0), (R_c^K(\bar{\xi}^c) + 0.5\sigma_c^2)/\sigma_c, \frac{-R_g^K(\mu_D(0) - \bar{\xi}^c) - \sigma_g^2/2}{v(m_g, \sigma_g)}; \left( \begin{array}{c} 0 \\ \frac{-m_g \sigma_D}{v(m_g, \sigma_g)} \\ \frac{-\rho \sigma_g}{v(m_g, \sigma_g)} \end{array} \right) \right) \\
& +\Phi_3 \left( \mathbf{x}^{g,H}(0), \frac{R_{\Delta}^{c,high}(\mu_D(0))}{v(\gamma + \alpha_g m_c, \sigma_c)}, \frac{-R_c(\mu_D(0) - \bar{\xi}^g, \bar{\xi}^g) - 0.5(\sigma^2 + \sigma_c^2 - \sigma_g^2)}{v(m_c, \sigma)}; \left( \begin{array}{c} \frac{(\gamma + \alpha_g m_c) \sigma_D}{v(\gamma + \alpha_g m_c, \sigma_c)} \\ \frac{-m_c \sigma_D}{v(m_c, \sigma)} \\ \frac{-(\sigma_c - \sigma_g \rho) \sigma_c - (\gamma + \alpha_g m_c) m_c \sigma_D^2}{v(\gamma + \alpha_g m_c, \sigma_c) v(m_c, \sigma)} \end{array} \right) \right)
\end{aligned}$$

$$\begin{aligned}
& -\Phi_3 \left( \mathbf{x}^{g,H}(0), \frac{R_{\Delta}^{c,high}(\mu_D(0))}{v(\gamma + \alpha_g m_c, \sigma_c)}, \frac{R_{\alpha}^K(\mu_D(0)) + \sigma^2(\alpha)}{v(\gamma, \sigma(\alpha))}; \left( \begin{array}{c} \frac{(\gamma + \alpha_g m_c) \sigma_D}{v(\gamma + \alpha_g m_c, \sigma_c)} \\ \frac{\gamma \sigma_D}{v(\gamma, \sigma(\alpha))} \\ \frac{(\sigma_c \alpha_c + \sigma_g \alpha_g \rho) \sigma_c + (\gamma + \alpha_g m_c) \gamma \sigma_D^2}{v(\gamma + \alpha_g m_c, \sigma_c) v(\gamma, \sigma(\alpha))} \end{array} \right) \right) \\
& -\Phi_3 \left( \mathbf{x}^{c,H}(0), \frac{R_{\Delta}^{g,high}(\mu_D(0))}{v(\gamma - \alpha_g m_g, \sigma_c)}, \frac{-R_{\alpha}^K(\mu_D(0)) - \sigma^2(\alpha)}{v(\gamma, \sigma(\alpha))}; \left( \begin{array}{c} \frac{(\gamma - m_g \alpha_g) \sigma_D}{v(\gamma - \alpha_g m_g, \sigma_c)} \\ \frac{-\gamma \sigma_D}{v(\gamma, \sigma(\alpha))} \\ \frac{-(\sigma_c \alpha_c + \sigma_g \alpha_g \rho) \sigma_c + (-\gamma + m_g \alpha_g) \sigma_D^2 \gamma}{v(\gamma - \alpha_g m_g, \sigma_c) v(\gamma, \sigma(\alpha))} \end{array} \right) \right) \\
& +\Phi_3 \left( \mathbf{x}^{c,H}(0), \frac{R_{\Delta}^{g,high}(\mu_D(0))}{v(\gamma - \alpha_g m_g, \sigma_c)}, \frac{-R_g(\mu_D(0)) - \bar{\xi}^c, \bar{\xi}^c - 0.5(\sigma^2 + \sigma_g^2 - \sigma_c^2)}{v(m_g, \sigma)}; \left( \begin{array}{c} \frac{(\gamma - m_g \alpha_g) \sigma_D}{v(\gamma - \alpha_g m_g, \sigma_c)} \\ \frac{-m_g \sigma_D}{v(m_g, \sigma)} \\ \frac{\sigma_c (\sigma_c - \sigma_g \rho) + m_g \sigma_D^2 (-\gamma + m_g \alpha_g)}{v(\gamma - \alpha_g m_g, \sigma_c) v(m_g, \sigma)} \end{array} \right) \right)
\end{aligned}$$

**Proof.** The proof is - similar to the proof of Lemma 5.4 - a straight application of Lemma 5.7. ■

### 5.4.1 Proof: Derivation for a fix Demand; Low Demand

For the next proofs we need the following Lemma from [Carmona et al., 2013].

**Lemma 5.6** *The following relationship holds between  $\phi_1$ ,  $\Phi_1$  and  $\Phi_2$ :*

$$\int_{-\infty}^a \exp(l_1 + q_1 x) \phi_1(x) \Phi_1(l_2 + q_2 x) dx = \exp\left(l_1 + \frac{q_1^2}{2}\right) \Phi_2\left(a - q_1, \frac{l_2 + q_1 q_2}{\sqrt{1 + q_2^2}}; \frac{-q_2}{\sqrt{1 + q_2^2}}\right),$$

for all  $l_1, l_2, q_1, q_2 \in \mathbb{R}$  and  $a \in \mathbb{R} \cup \{\infty\}$ .

**Proof.** Cf. [Carmona et al., 2013]. ■

In the following, we proof Lemma 5.1 (p. 86).

**Proof.** Referring to (5.8), it holds for a given  $\rho \in (-1; 1)$

$$\begin{pmatrix} \ln(S_t^c) \\ \ln(S_t^g) \end{pmatrix} \stackrel{\mathcal{D}}{\sim} \mathcal{N}\left(\begin{pmatrix} \mu_t^c \\ \mu_t^g \end{pmatrix}, \begin{pmatrix} (\sigma_t^c)^2 & \rho \sigma_t^c \sigma_t^g \\ \rho \sigma_t^c \sigma_t^g & (\sigma_t^g)^2 \end{pmatrix}\right) \quad (5.9)$$

which is - due to an application of the Cholesky decomposition - equivalent to

$$\begin{pmatrix} \ln(S_t^c) \\ \ln(S_t^g) \end{pmatrix} = \begin{pmatrix} \mu_t^c + \sigma_t^c Z_1 \\ \mu_t^g + \rho \sigma_t^g Z_1 + \sqrt{1 - \rho^2} \sigma_t^g Z_2 \end{pmatrix} \quad (5.10)$$

for two random variables  $Z_1, Z_2 \stackrel{\mathcal{D}}{\sim} \mathcal{N}(0, 1)$ . We short the notation by writing

$$\begin{pmatrix} S_t^c(Z_1) \\ S_t^g(Z_1, Z_2) \end{pmatrix} := \begin{pmatrix} \exp(\mu_t^c + \sigma_t^c Z_1) \\ \exp(\mu_t^g + \rho \sigma_t^g Z_1 + \sqrt{1 - \rho^2} \sigma_t^g Z_2) \end{pmatrix}$$

Let  $\phi^{\mu, \Sigma}(\ln(s^c), \ln(s^g))$  denote the bivariate normal density function of the lognormally distributed state variables  $S_t^c$  and  $S_t^g$  with covariance matrix  $\Sigma$  as given in (5.9).

Following the proof of Proposition 5.2 we have to calculate for  $D \in [0, \bar{\xi}^-]$

$$\begin{aligned} \mathbb{E}^{\mathbb{Q}} \left[ (b_{\text{low}}(D, S_t)(D) - K)^+ \mid \mathcal{F}_{t_0}^{\mathbf{W}} \vee \mathcal{F}_t^D \right] &\stackrel{\text{App.A.1}}{=} \int_{(\mathbb{R}^+)^2} \left( b_c(D, s^c) \mathbb{I}_{\{b_c(D, s^c) < b_g(0, s^g)\}} \right. \\ &\quad \left. + b_g(D, s^g) \mathbb{I}_{\{b_g(D, s^g) < b_c(0, s^c)\}} + b_{cg}(D, \mathbf{s}) \mathbb{I}_{\{b_c(D, s^c) \geq b_g(0, s^g), b_g(D, s^g) \geq b_c(0, s^c)\}} - K \right)^+ \\ &\quad \cdot \phi^{\mu, \Sigma}(\ln(s^c), \ln(s^g)) d(\ln(s^c), \ln(s^g)) \end{aligned}$$

where we can split the integrals using the (disjoint) indicator terms which yields

$$\begin{aligned} &= \int_{\mathbb{I}_{\{b_c(D, s^c) < b_g(0, s^g)\}}} \left( b_c(D, s^c) \mathbb{I}_{\{b_c(D, s^c) < b_g(0, s^g)\}} - K \right)^+ \phi^{\mu, \Sigma}(\ln(s^c), \ln(s^g)) d(\ln(s^c), \ln(s^g)) \\ &+ \int_{\mathbb{I}_{\{b_g(D, s^g) < b_c(0, s^c)\}}} \left( b_g(D, s^g) \mathbb{I}_{\{b_g(D, s^g) < b_c(0, s^c)\}} - K \right)^+ \phi^{\mu, \Sigma}(\ln(s^c), \ln(s^g)) d(\ln(s^c), \ln(s^g)) \\ &\quad + \int_{\mathbb{I}_{\{b_c(D, s^c) \geq b_g(0, s^g), b_g(D, s^g) \geq b_c(0, s^c)\}}} \left( b_{cg}(D, \mathbf{s}) \mathbb{I}_{\{b_c(D, s^c) \geq b_g(0, s^g), b_g(D, s^g) \geq b_c(0, s^c)\}} - K \right)^+ \\ &\quad \cdot \phi^{\mu, \Sigma}(\ln(s^c), \ln(s^g)) d(\ln(s^c), \ln(s^g)). \end{aligned}$$

By condition we have  $K > 0$  which gives us the relation

$$(b_i(D, \mathbf{s}) \mathbb{I}_{\{A\}}(D) - K)^+ > 0 \Leftrightarrow \mathbb{I}_{\{A\}}(D) (b_i(D, \mathbf{s}) - K)^+ > 0$$

for arbitrary  $A \subset (\mathbb{R}^+)^2$ ,  $\mathbf{s} \in (\mathbb{R}^+)^2$ ,  $D \in \mathbb{R}$ ,  $i \in \{c, g, cg\}$ .

Considering this condition and performing a transformation to integrate over  $Z_1, Z_2$  leads us to

$$\mathbb{E}^{\mathbb{Q}} [ (b_{\text{low}}(D, S_t)(D) - K)^+ \mid \mathcal{F}_{t_0}^{\mathbf{W}} \vee \mathcal{F}_t^D ] \quad (5.11)$$

$$\begin{aligned} &= \int_{\mathbb{I}_{\{b_c(D, s^c(z_1)) < b_g(0, s^g(z_1, z_2))\}}} (b_c(D, s^c(z_1)) - K)^+ \phi_1(z_1) \phi_1(z_2) dz_1 dz_2 \\ &+ \int_{\mathbb{I}_{\{b_g(D, s^g(z_1, z_2)) < b_c(0, s^c(z_1))\}}} (b_g(D, s^g(z_1, z_2)) - K)^+ \phi_1(z_1) \phi_1(z_2) dz_1 dz_2 \\ &+ \int_{\mathbb{I}_{\{b_c(D, s^c(z_1)) \geq b_g(0, s^g(z_1, z_2)), b_g(D, s^g(z_1, z_2)) \geq b_c(0, s^c(z_1))\}}} (b_{cg}(D, \mathbf{s}(z_1, z_2)) - K)^+ \phi_1(z_1) \phi_1(z_2) dz_1 dz_2 \quad (5.12) \\ &=: I_1 + I_2 + I_3. \end{aligned}$$

In order to simplify the notation, we will - in the following - leave out the character indicating the time dependence in the variables (i.e  $\mu_c := \mu_t^c$ ; additionally commodity specification moves to bottom).

Calculation of  $I_1$  :

The condition for a non-zero payoff is (using the definition of  $b_c(\cdot)$  in (2.2) and (5.10)):

$$z_1 > \frac{\ln(K) - \mu_c - k_c - m_c D}{\sigma_c} = \frac{R_c^K(D) + 0.5\sigma_c^2}{\sigma_c} \quad (5.13)$$

The integration limit can be expressed as

$$\begin{aligned} z_2 &> \frac{\mu_c - \mu_g + k_c - k_g + m_c D + (\sigma_c - \sigma_g \rho) z_1}{\sigma_g \sqrt{1 - \rho^2}} \\ &= \frac{-R_c(D, 0) - 0.5(\sigma^2 + \sigma_c^2 - \sigma_g^2) + (\sigma_c - \sigma_g \rho) z_1}{\sigma_g \sqrt{1 - \rho^2}} =: l^a + q^a z_1 \quad (5.14) \end{aligned}$$

where we used the Definitions in Definition 5.1 and Appendix A.2. Therefore, it holds

$$\begin{aligned} I_1 &= \int_{\frac{R_c^K(D) + 0.5\sigma_c^2}{\sigma_c}}^{\infty} \int_{l^a + q^a z_1}^{\infty} b_c(D, s^c(z_1)) \phi_1(z_1) \phi_1(z_2) dz_1 dz_2 - K \int_{\frac{R_c^K(D) + 0.5\sigma_c^2}{\sigma_c}}^{\infty} \int_{l^a + q^a z_1}^{\infty} \phi_1(z_1) \phi_1(z_2) dz_1 dz_2 \\ &=: I_1^P + I_1^K. \end{aligned}$$

We use the definition of  $b_c(\cdot)$  in (2.2), perform the transformation  $\bar{z}_1 = z_1 - \sigma_c$  and apply the risk-neutral relation  $F_c = \exp(\mu_c + 0.5\sigma_c^2)$  to yield

$$\begin{aligned} I_1^P &= b_c(D, F_c) \int_{\frac{R_c^K(D) - 0.5\sigma_c^2}{\sigma_c}}^{\infty} \Phi_1(-l^a - q^a(z_1 + \sigma_c)) \phi_1(z_1) dz_1 \\ &= b_c(D, F_c) \left[ \int_{-\infty}^{\infty} \Phi_1(-l^a - q^a(z_1 + \sigma_c)) \phi_1(z_1) dz_1 - \int_{-\infty}^{\frac{R_c^K(D) - 0.5\sigma_c^2}{\sigma_c}} \Phi_1(-l^a - q^a(z_1 + \sigma_c)) \phi_1(z_1) dz_1 \right] \end{aligned}$$

We now apply Lemma 5.6 with  $q_1 = l_1 = 0$ ,  $l_2 = -l^a - q^a \sigma_c$ ,  $q_2 = -q^a$  and  $a = \frac{R_c^K(D) - 0.5\sigma_c^2}{\sigma_c}, \infty$  yielding

$$\frac{-q_2}{\sqrt{1+q_2^2}} = \frac{\sigma_c - \rho\sigma_g}{\sigma_g\sqrt{1-\rho^2}} \frac{\sigma_g\sqrt{1-\rho^2}}{\sigma} \quad \frac{l_2 + q_1q_2}{\sqrt{1+q_2^2}} = \frac{R_c(D,0) + 0.5(\sigma^2 + \sigma_c^2 - \sigma_g^2) - \sigma_c(\sigma_c - \sigma_g\rho)}{\sigma}$$

and therefore  $f_{low}^c(D, \mathbf{F})$  in Proposition 5.3. Similar calculations but without the transformation  $\bar{z}_1 = z_1 - \sigma_c$  yield  $k_{low}^c(D, \mathbf{F})$  for  $I_1^K$ .

Calculation of  $I_2$  :

The condition for a non-zero payoff is (using the definition of  $b_g(\cdot)$  in (2.2) and (5.10)):

$$z_2 > \frac{\ln(K) - \mu_g - k_g - m_g D - \sigma_g \rho z_1}{\sigma_g \sqrt{1-\rho^2}} = \frac{R_g^K(D) + 0.5\sigma_g^2 - \sigma_g \rho z_1}{\sigma_g \sqrt{1-\rho^2}} \quad (5.15)$$

The integration limit can be expressed as

$$\begin{aligned} z_2 &< \frac{\mu_c - \mu_g + k_c - k_g - m_g D + (\sigma_c - \sigma_g \rho) z_1}{\sigma_g \sqrt{1-\rho^2}} \\ &= \frac{R_g(D,0) + 0.5(\sigma^2 - \sigma_c^2 + \sigma_g^2) + (\sigma_c - \sigma_g \rho) z_1}{\sigma_g \sqrt{1-\rho^2}} =: l^b + q^b z_1 \end{aligned} \quad (5.16)$$

In order to assure (5.15) and (5.16) to be fulfilled for the same  $z_2$ , we need the additional restriction

$$\begin{aligned} \frac{R_g^K(D) + 0.5\sigma_g^2 - \sigma_g \rho z_1}{\sigma_g \sqrt{1-\rho^2}} &< \frac{R_g(D,0) + 0.5(\sigma^2 - \sigma_c^2 + \sigma_g^2) + (\sigma_c - \sigma_g \rho) z_1}{\sigma_g \sqrt{1-\rho^2}} \\ \Leftrightarrow \quad z_1 &> \frac{R_c^K(0) + 0.5\sigma_c^2}{\sigma_c} \end{aligned} \quad (5.17)$$

Therefore, it holds

$$\begin{aligned} I_2 &= \int_{\frac{R_c^K(0) + 0.5\sigma_c^2}{\sigma_c}}^{\infty} \int_{\frac{R_g^K(D) + 0.5\sigma_g^2 - \sigma_g \rho z_1}{\sigma_g \sqrt{1-\rho^2}}}^{l^b + q^b z_1} b_g(D, s^g(z_1, z_2)) \phi_1(z_1) \phi_1(z_2) dz_1 dz_2 \\ &\quad - K \int_{\frac{R_c^K(0) + 0.5\sigma_c^2}{\sigma_c}}^{\infty} \int_{\frac{R_g^K(D) + 0.5\sigma_g^2 - \sigma_g \rho z_1}{\sigma_g \sqrt{1-\rho^2}}}^{l^b + q^b z_1} \phi_1(z_1) \phi_1(z_2) dz_1 dz_2 =: I_2^P + I_2^K. \end{aligned}$$

We use the definition of  $b_g(\cdot)$  in (2.2), perform the transformation  $\bar{z}_1 = z_1 - \sigma_g \sqrt{1-\rho^2}$  and use  $F_g = \exp(\mu_g + 0.5\sigma_g^2)$  to yield

$$\begin{aligned} I_2^P &= b_g(D, F_g) \exp(-\sigma_g^2 \rho^2 / 2) \int_{\frac{R_c^K(0) + 0.5\sigma_c^2}{\sigma_c}}^{\infty} \exp(\sigma_g \rho z_1) \\ &\quad \cdot \left[ \Phi_1 \left( l^b + q^b z_1 - \sigma_g \sqrt{1-\rho^2} \right) - \Phi_1 \left( \frac{R_g^K(D) + 0.5\sigma_g^2 - \sigma_g \rho z_1}{\sigma_g \sqrt{1-\rho^2}} - \sigma_g \sqrt{1-\rho^2} \right) \right] \phi_1(z_1) dz_1. \end{aligned}$$

Now we apply Lemma 5.6 on both terms resulting in four terms. For the first we set

$$q_1 = \sigma_g \rho \quad l_1 = 0 \quad q_2 = q^b \quad l_2 = l^b - \sigma_g \sqrt{1-\rho^2} \quad a = \frac{R_c^K(0) + 0.5\sigma_c^2}{\sigma_c}$$

<sup>2</sup>The term  $-K\Phi_1((R_c(D,0) + 0.5(\sigma^2 + \sigma_c^2 - \sigma_g^2))/\sigma)$  will appear with opposite sign in  $I_3$  and is therefore not depicted in Proposition 5.3.



and for the second term

$$q_1 = \sigma_g \rho \quad l_1 = 0 \quad q_2 = \frac{-\sigma_g \rho}{\sigma_g \sqrt{1-\rho^2}} \quad l_2 = \frac{R_g^K(D) + 0.5\sigma_g^2}{\sigma_g \sqrt{1-\rho^2}} - \sigma_g \sqrt{1-\rho^2} \quad a = \frac{R_c^K(0) + 0.5\sigma_c^2}{\sigma_c}.$$

Calculating the right side of Lemma 5.6 directly leads to the four terms of  $f_{low}^g(D, \mathbf{F})$ . The calculation of  $I_2^K$  is similar leading to  $k_{low}^g(D, \mathbf{F})$ <sup>3</sup> but without applying the transformation  $\bar{z}_1 = z_1 - \sigma_g \sqrt{1-\rho^2}$  and setting  $q_1 = 0$  when applying Lemma 5.6.

Calculation of  $I_3$  :

The condition for a non-zero payoff is (using the definition of  $b_{cg}(\cdot)$  in Appendix A.1 and (5.10)):

$$z_2 > \frac{\ln(K) - \mu_g \alpha_g - \mu_c \alpha_c - \beta - \gamma D - (\sigma_g \rho \alpha_g + \sigma_c \alpha_c) z_1}{\sigma_g \alpha_g \sqrt{1-\rho^2}} = \frac{R_\alpha^K(D) + \sigma(\alpha)^2 - (\sigma_g \rho \alpha_g + \sigma_c \alpha_c) z_1}{\sigma_g \alpha_g \sqrt{1-\rho^2}} \quad (5.18)$$

$$=: \tilde{l}(K, z_1)$$

where we used the Definitions in Definition 5.1. The integration limit can be expressed as

$$\begin{aligned} \mathbb{I}_{\{b_c(D, s^c(z_1)) \geq b_g(0, s^g(z_1, z_2)), b_g(D, s^g(z_1, z_2)) \geq b_c(0, s^c(z_1))\}} &= 1 - \mathbb{I}_{\{b_c(D, s^c(z_1)) < b_g(0, s^g(z_1, z_2))\}} \\ &\quad - \mathbb{I}_{\{b_g(D, s^g(z_1, z_2)) < b_c(0, s^c(z_1))\}} \end{aligned}$$

and therefore we use conditions (5.14) and (5.16) to yield

$$\begin{aligned} I_3 &= \left[ \int_{\mathbb{R}} \int_{\mathbb{R}} \tilde{l}(K, z_1) - \int_{\mathbb{R}} \int_{\max(\tilde{l}(K, z_1), l^a + q^a z_1)}^{\infty} - \int_{\mathbb{R}} \int_{\tilde{l}(K, z_1)}^{l^b + q^b z_1} \right] \\ &\quad \left( \exp(\mu_c \alpha_c + \mu_g \alpha_g + (\sigma_c \alpha_c + \sigma_g \alpha_g \rho) z_1 + \sigma_g \alpha_g \sqrt{1-\rho^2} z_2 + \beta + \gamma D) - K \right) \phi(z_1) \phi(z_2) dz_1 dz_2 \\ &= \left[ \int_{\mathbb{R}} \int_{\mathbb{R}} \tilde{l}(K, z_1) - \int_{\mathbb{R}} \int_{\max(\tilde{l}(K, z_1), l^a + q^a z_1)}^{\infty} - \int_{\mathbb{R}} \int_{\tilde{l}(K, z_1)}^{l^b + q^b z_1} \right] \\ &\quad \left( b_{cg}(D, \mathbf{F}) \exp \left( -\frac{\alpha_c \sigma_c^2}{2} - \frac{\alpha_g \sigma_g^2}{2} + (\sigma_c \alpha_c + \sigma_g \alpha_g \rho) z_1 + \sigma_g \alpha_g \sqrt{1-\rho^2} z_2 \right) - K \right) \phi(z_1) \phi(z_2) dz_1 dz_2 \\ &=: I_3^1 - I_3^2 - I_3^3 - K^1 + K^2 + K^3, \end{aligned}$$

where  $I$ -terms refer to the exponential terms and  $K$ -terms refer to the strike terms.

In order to calculate  $I_3^1$ , we perform the transformation  $\bar{z}_2 = z_2 - \sigma_g \alpha_g \sqrt{1-\rho^2}$ , use  $F_i = \exp(\mu_i + 0.5\sigma_i^2)$  and apply Lemma 5.6 with

$$q_1 = \sigma_c \alpha_c + \sigma_g \alpha_g \rho \quad l_1 = 0 \quad q_2 = \frac{\sigma_c \alpha_c + \sigma_g \alpha_g \rho}{\sigma_g \alpha_g \sqrt{1-\rho^2}} \quad l_2 = \frac{-R_\alpha^K(D) - \sigma^2(\alpha) + \sigma_g^2 \alpha_g^2 (1-\rho^2)}{\sigma_g \alpha_g \sqrt{1-\rho^2}}$$

<sup>3</sup>The term  $-K\Phi_1((R_g(D, 0) + 0.5(\sigma^2 + \sigma_g^2 - \sigma_c^2))/\sigma)$  will appear with opposite sign in  $I_3$  and is therefore not depicted in Proposition 5.3.

and  $a = \infty$  to get<sup>4</sup>

$$I_3^1 = b_{cg}(D, \mathbf{F}) \exp\left(\frac{-\alpha_g \alpha_c \sigma^2}{2}\right) \underbrace{\Phi_1\left(\frac{-R_\alpha^K(D)}{\sigma(\alpha)}\right)}_{=1-\Phi_1\left(\frac{R_\alpha^K(D)}{\sigma(\alpha)}\right)}.$$

Similarly, but without the transformation and  $q_1 = 0$  when applying Lemma 5.6, we get

$$K^1 = K \left(1 - \Phi_1\left(\frac{R_\alpha^K(D) + \sigma^2(\alpha)}{\sigma(\alpha)}\right)\right).$$

The second term of  $K^1$  will together with the second term of  $K^3$  sum up to zero.

In order to calculate  $I_3^2$ , we have to consider the additional condition

$$\max(\tilde{l}(K, z_1), l^a + q^a z_1) = \begin{cases} l^a + q^a z_1, & z_1 > R_\Delta^{c,low}(D)/\sigma_c \\ \tilde{l}(K, z_1), & \text{else} \end{cases}$$

yielding

$$\begin{aligned} I_3^2 &= \left[ \int_{R_\Delta^{c,low}(D)}^\infty \int_{l^a + q^a z_1}^\infty + \int_{-\infty}^{R_\Delta^{c,low}(D)} \int_{\tilde{l}(K, z_1)}^\infty \right] \\ &\quad \exp(\mu_c \alpha_c + \mu_g \alpha_g + (\sigma_c \alpha_c + \sigma_g \alpha_g \rho) z_1 + \sigma_g \alpha_g \sqrt{1 - \rho^2} z_2 + \beta + \gamma D) \phi(z_1) \phi(z_2) dz_1 dz_2 \\ &=: I_3^{2,a} + I_3^{2,b}. \end{aligned}$$

In order to calculate  $I_3^{2,a}$ , we perform the transformation  $\bar{z}_2 = z_2 - \sigma_g \alpha_g \sqrt{1 - \rho^2}$ , use  $F_i = \exp(\mu_i + 0.5\sigma_i^2)$  and apply Lemma 5.6 with

$$q_1 = \sigma_c \alpha_c + \sigma_g \alpha_g \rho \quad l_1 = 0 \quad q_2 = -q^a \quad l_2 = -l^a + \alpha_g \sigma_g \sqrt{1 - \rho^2}$$

and  $a = R_\Delta^{c,low}(D)$  to get

$$\begin{aligned} I_3^{2,a} &= b_{cg}(D, \mathbf{F}) \exp\left(\frac{-\alpha_g \alpha_c \sigma^2}{2}\right) \left( \Phi_1\left(\frac{R_c(D, 0)}{\sigma} + \alpha_g \sigma\right) \right. \\ &\quad \left. - \Phi_2\left(\frac{R_\Delta^{c,low}(D)}{\sigma_c} - (\sigma_c \alpha_c + \sigma_g \alpha_g \rho), \frac{R_c(D, 0)}{\sigma} + \alpha_g \sigma; \frac{\sigma_c - \sigma_g \rho}{\sigma}\right) \right). \end{aligned}$$

---

<sup>4</sup>The term  $b_{cg}(D, \mathbf{F}) \exp\left(\frac{-\alpha_g \alpha_c \sigma^2}{2}\right)$  comes from  $(\alpha_c + \alpha_g = 1)$ :

$$\begin{aligned} &b_{cg}(D, \mathbf{F}) \exp\left(-\frac{\alpha_c \sigma_c^2}{2} - \frac{\alpha_g \sigma_g^2}{2} + \frac{\sigma_g^2 \alpha_g^2 (1 - \rho^2)}{2} + \frac{(\sigma_c \alpha_c + \sigma_g \alpha_g \rho)^2}{2}\right) \\ &= b_{cg}(D, \mathbf{F}) \exp\left(-\frac{\alpha_c \sigma_c^2}{2} - \frac{\alpha_g \sigma_g^2}{2} + \frac{\sigma_g^2 \alpha_g (1 - \alpha_c)(1 - \rho^2)}{2} + \frac{(\sigma_c \alpha_c + \sigma_g \alpha_g \rho)^2}{2}\right) \\ &= b_{cg}(D, \mathbf{F}) \exp\left(\frac{-\alpha_c \sigma_c^2 - \alpha_g \sigma_g^2 + \sigma_g^2 \alpha_g (1 - \rho^2) - \sigma_g^2 \alpha_g \alpha_c (1 - \rho^2) + \sigma_c^2 \alpha_c (1 - \alpha_g) + 2\sigma_c \sigma_g \alpha_c \alpha_g + \sigma_g^2 \alpha_g (1 - \alpha_c) \rho^2}{2}\right) \\ &= b_{cg}(D, \mathbf{F}) \exp\left(\frac{-\alpha_g \alpha_c (\sigma_g^2 - 2\sigma_c \sigma_g + \sigma_c^2)}{2}\right) = \exp\left(\frac{-\alpha_g \alpha_c \sigma}{2}\right). \end{aligned}$$

In order to calculate  $I_3^{2,b}$ , we perform the transformation  $\bar{z}_2 = z_2 - \sigma_g \alpha_g \sqrt{1 - \rho^2}$ , use  $F_i = \exp(\mu_i + 0.5\sigma_i^2)$  and apply Lemma 5.6 with

$$q_1 = \sigma_c \alpha_c + \sigma_g \alpha_g \rho \quad l_1 = 0 \quad q_2 = \frac{\sigma_c \alpha_c + \sigma_g \alpha_g \rho}{\alpha_g \sigma_g \sqrt{1 - \rho^2}} \quad l_2 = \frac{-R_\alpha^K(D) - \sigma(\alpha)^2 + \sigma_g^2 \alpha_g^2 (1 - \rho^2)}{\alpha_g \sigma_g \sqrt{1 - \rho^2}}$$

and  $a = R_\Delta^{c,low}(D)$  to get

$$I_3^{2,b} = b_{cg}(D, \mathbf{F}) \exp\left(\frac{-\alpha_g \alpha_c \sigma^2}{2}\right) \Phi_2\left(\frac{R_\Delta^{c,low}(D)}{\sigma_c} - (\sigma_c \alpha_c + \sigma_g \alpha_g \rho), \frac{-R_\alpha^K(D)}{\sigma(\alpha)}; \frac{-\sigma_c \alpha_c - \sigma_g \alpha_g \rho}{\sigma(\alpha)}\right).$$

Similary, we define  $K^2 := K^{2,a} + K^{2,b}$  and perform the above calculations without the transformation and using  $q_1 = 0$  to get

$$\begin{aligned} K^{2,a} &= K \left( \Phi_1 \left( \frac{-R_c(D, 0) - \frac{1}{2}(\sigma^2 + \sigma_c^2 - \sigma_g^2)}{\sigma} \right) \right. \\ &\quad \left. - \Phi_2 \left( \frac{R_\Delta^{c,low}(D)}{\sigma_c}, \frac{R_c(D, 0) + \frac{1}{2}(\sigma^2 + \sigma_c^2 - \sigma_g^2)}{\sigma}; \frac{\sigma_c - \sigma_g \rho}{\sigma} \right) \right), \\ K^{2,b} &= K \Phi_2 \left( \frac{R_\Delta^{c,low}(D)}{\sigma_c}, \frac{-R_\alpha^K(D) - \sigma^2(\alpha)}{\sigma(\alpha)}; \frac{-\sigma_c \alpha_c - \sigma_g \alpha_g \rho}{\sigma(\alpha)} \right). \end{aligned}$$

In order to calculate  $I_3^3$ , we have to consider the additional condition

$$\tilde{l}(K, z_1) < l^b + q^b z_1 \Leftrightarrow z_1 > R_\Delta^{g,low}(D)/\sigma_c$$

which yields (by applying the transformation  $\bar{z}_2 := z_2 - \sigma_g \alpha_g \sqrt{1 - \rho^2}$ )

$$\begin{aligned} I_3^3 &= \exp(\mu_c \alpha_c + \mu_g \alpha_g + \beta + \gamma D + \sigma_g^2 \alpha_g^2 (1 - \rho^2)/2) \cdot \\ &\quad \int_{R_\Delta^{g,low}(D)/\sigma_c}^{\infty} \exp((\sigma_c \alpha_c + \sigma_g \alpha_g \rho) z_1) \cdot \\ &\quad \left[ \Phi \left( l^b + q^b z_1 - \sigma_g \alpha_g \sqrt{1 - \rho^2} \right) - \Phi \left( \tilde{l}(K, z_1) - \sigma_g \alpha_g \sqrt{1 - \rho^2} \right) \right] \phi(z_1) dz_1. \end{aligned}$$

For the first summand we apply Lemma 5.6 with

$$q_1 = \sigma_c \alpha_c + \sigma_g \alpha_g \rho \quad l_1 = 0 \quad q_2 = q^b \quad l_2 = l^b - \alpha_g \sigma_g \sqrt{1 - \rho^2} \quad a = R_\Delta^{g,low}(D)/\sigma_c$$

and for the second summand with

$$q_1 = \sigma_c \alpha_c + \sigma_g \alpha_g \rho \quad l_1 = 0 \quad q_2 = -\frac{\sigma_c \alpha_c + \sigma_g \alpha_g \rho}{\alpha_g \sigma_g \sqrt{1 - \rho^2}} \quad l_2 = \frac{R_\alpha^K(D) + \sigma(\alpha)^2 - \sigma_g^2 \alpha_g^2 (1 - \rho^2)}{\alpha_g \sigma_g \sqrt{1 - \rho^2}}$$

and  $a = R_\Delta^{g,low}(D)/\sigma_c$ . Further simplifications lead to

$$\begin{aligned} I_3^3 &= b_{cg}(D, \mathbf{F}) \exp\left(\frac{-\alpha_g \alpha_c \sigma^2}{2}\right) \left( \Phi_1 \left( \frac{R_g(D, 0) + \alpha_c \sigma^2}{\sigma} \right) - \Phi_1 \left( \frac{R_\alpha^K(D)}{\sigma(\alpha)} \right) \right. \\ &\quad \left. - \Phi_2 \left( R_\Delta^{g,low}(D)/\sigma_c - \sigma_c \alpha_c - \sigma_g \alpha_g \rho, \frac{R_g(D, 0) + \alpha_c \sigma^2}{\sigma}, \frac{-(\sigma_c - \sigma_g \rho)}{\sigma} \right) \right) \end{aligned}$$

$$+\Phi_2\left(R_{\Delta}^{g,low}(D)/\sigma_c - \sigma_c\alpha_c - \sigma_g\alpha_g\rho, \frac{R_{\alpha}^K(D)}{\sigma(\alpha)}, \frac{\sigma_c\alpha_c + \sigma_g\alpha_g\rho}{\sigma(\alpha)}\right).$$

We perform similar calculations for  $K^3$  without transformation ( $\bar{z}_2 = z_2 - \sigma_g\alpha_g\sqrt{1-\rho^2}$ ) and using  $q_1 = 0$  to derive

$$\begin{aligned} K^3 = & K \left( \Phi_1\left(\frac{R_g(D,0) + \frac{1}{2}(\sigma^2 + \sigma_g^2 - \sigma_c^2)}{\sigma}\right) - \Phi_1\left(\frac{R_{\alpha}^K(D) + \sigma^2(\alpha)}{\sigma(\alpha)}\right) \right. \\ & - \Phi_2\left(R_{\Delta}^{g,low}(D)/\sigma_c, \frac{R_g(D,0) + \frac{1}{2}(\sigma^2 + \sigma_g^2 - \sigma_c^2)}{\sigma}, \frac{-(\sigma_c - \sigma_g\rho)}{\sigma}\right) \\ & \left. + \Phi_2\left(R_{\Delta}^{g,low}(D)/\sigma_c, \frac{R_{\alpha}^K(D) + \sigma^2(\alpha)}{\sigma(\alpha)}, \frac{\sigma_c\alpha_c + \sigma_g\alpha_g\rho}{\sigma(\alpha)}\right) \right) .. \end{aligned}$$

Taking the difference  $I_3^1 - I_3^2 - I_3^3$  and  $K^1 - K^2 - K^3$  leads to  $f_{low}^{cg}(\cdot, \cdot)$  and  $k_{low}^{cg}(\cdot, \cdot)$ . ■

### 5.4.2 Proof: Derivation for a fix Demand; High Demand

In this Chapter, we proof Lemma 5.2 (p. 87).

**Proof.** Similar to the proof of the low-case in Chapter 5.4.1, we define  $I_1, I_2, I_3$  by

$$\begin{aligned} & \mathbb{E}^{\mathbb{Q}} \left[ (b_{\text{high}}(D, S_t)(D) - K)^+ \mid \mathcal{F}_{t_0}^{\mathbf{W}} \vee \mathcal{F}_t^D \right] = \\ & \int_{\mathbb{I}_{\{b_c(D - \bar{\xi}^g, s^c(z_1)) > b_g(\bar{\xi}^g, s^g(z_1, z_2))\}}} (b_c(D - \bar{\xi}^g, s^c(z_1)) - K)^+ \phi_1(z_1) \phi_1(z_2) dz_1 dz_2 \\ & + \int_{\mathbb{I}_{\{b_g(D - \bar{\xi}^c, s^g(z_1, z_2)) > b_c(\bar{\xi}^c, s^c(z_1))\}}} (b_g(D - \bar{\xi}^c, s^g(z_1, z_2)) - K)^+ \phi_1(z_1) \phi_1(z_2) dz_1 dz_2 \\ & + \int_{\mathbb{I}_{\{b_c(D - \bar{\xi}^g, s^c(z_1)) \leq b_g(\bar{\xi}^g, s^g(z_1, z_2)), b_g(D - \bar{\xi}^c, s^g(z_1, z_2)) \leq b_c(\bar{\xi}^c, s^c(z_1))\}}} (b_{cg}(D, s(z_1, z_2)) - K)^+ \phi_1(z_1) \phi_1(z_2) dz_1 dz_2 \quad (5.19) \\ & =: I_1 + I_2 + I_3 \end{aligned}$$

In order to simplify notation, we will again leave out the character indicating the time dependence in the variables (i.e  $\mu_c := \mu_t^c$ ; additionally commodity specification moves to bottom).

Calculation of  $I_1$  :

The condition for a non-zero payoff is (using the definition of  $b_c(\cdot)$  (2.2) and (5.10)):

$$z_1 > \frac{\ln(K) - \mu_c - k_c - m_c(D - \bar{\xi}^g)}{\sigma_c} = \frac{R_c^K(D - \bar{\xi}^g) + 0.5\sigma_c^2}{\sigma_c} \quad (5.20)$$

The integration limit can be expressed as

$$\begin{aligned} z_2 & < \frac{\mu_c - \mu_g + k_c - k_g + m_c(D - \bar{\xi}^g) - m_g\bar{\xi}^g + (\sigma_c - \sigma_g\rho)z_1}{\sigma_g\sqrt{1-\rho^2}} \\ & = \frac{-R_c(D - \bar{\xi}^g, \bar{\xi}^g) - 0.5(\sigma^2 + \sigma_c^2 - \sigma_g^2) + (\sigma_c - \sigma_g\rho)z_1}{\sigma_g\sqrt{1-\rho^2}} =: l^a + q^a z_1 \quad (5.21) \end{aligned}$$

Therefore, it holds

$$\begin{aligned} I_1 &= \int_{\frac{R_c^K(D-\bar{\xi}^g)+0.5\sigma_c^2}{\sigma_c}}^{\infty} \int_{-\infty}^{l^a+q^a z_1} b_c(D-\bar{\xi}^g, s^c(z_1)) \phi_1(z_1) \phi_1(z_2) dz_1 dz_2 \\ &\quad - K \int_{\frac{R_c^K(D-\bar{\xi}^g)+0.5\sigma_c^2}{\sigma_c}}^{\infty} \int_{-\infty}^{l^a+q^a z_1} \phi_1(z_1) \phi_1(z_2) dz_1 dz_2 \\ &=: I_1^P + I_1^K \end{aligned}$$

The next steps are similar to those in Chapter 5.4.1: Lemma 5.6 can be applied with  $q_1 = l_1 = 0$ ,  $l_2 = l_2^a + q_2^a \sigma_c$ ,  $q_2 = q_2^a$  and  $a = \frac{R_c^K(D-\bar{\xi}^g)-0.5\sigma_c^2}{\sigma_c}$  yielding  $f_{high}^c(D, \mathbf{F})$  in Proposition 5.3.

Similar calculations but without the transformation  $\bar{z}_1 = z_1 - \sigma_c$  yield  $k_{high}^c(D, \mathbf{F})$  for  $I_1^K$ <sup>5</sup>.

Calculation of  $I_2$ :

The condition for a non-zero payoff is (using the definition of  $b_g(\cdot)$  in (2.2) and (5.10)):

$$\begin{aligned} z_2 &> \frac{\ln(K) - \mu_g - k_g - m_g(D - \bar{\xi}^c) - \sigma_g \rho z_1}{\sigma_g \sqrt{1 - \rho^2}} = \frac{R_g^K(D - \bar{\xi}^c) + 0.5\sigma_g^2 - \sigma_g \rho z_1}{\sigma_g \sqrt{1 - \rho^2}} \\ &=: l_g(K, D) + q_g z_1 \end{aligned} \quad (5.22)$$

The integration limit can be expressed as

$$\begin{aligned} z_2 &> \frac{\mu_c - \mu_g + k_c - k_g - m_g(D - \bar{\xi}^c) + m_c \bar{\xi}^c + (\sigma_c - \sigma_g \rho) z_1}{\sigma_g \sqrt{1 - \rho^2}} \\ &= \frac{R_g(D - \bar{\xi}^c, \bar{\xi}^c) + 0.5(\sigma^2 - \sigma_c^2 + \sigma_g^2) + (\sigma_c - \sigma_g \rho) z_1}{\sigma_g \sqrt{1 - \rho^2}} =: l^b + q^b z_1 \end{aligned} \quad (5.23)$$

In order to assure (5.10) and (5.15) to be fulfilled for the same  $z_2$ , we need the additional restriction

$$\max \left( l_g(K, D) + q_g z_1, l^b + q^b z_1 \right) = \begin{cases} l^b + q^b z_1, & z_1 > (R_c^K(\bar{\xi}^c) + 0.5\sigma_c^2)/\sigma_c \\ l_g(K, D) + q_g z_1, & \text{else} \end{cases}.$$

Therefore, it holds

$$\begin{aligned} I_2 &= \int_{-\infty}^{\frac{R_c^K(\bar{\xi}^c)+0.5\sigma_c^2}{\sigma_c}} \int_{l_g(K, D) + q_g z_1}^{\infty} b_g(D - \bar{\xi}^c, s^g(z_1, z_2)) \phi_1(z_1) \phi_1(z_2) dz_1 dz_2 \\ &\quad + \int_{\frac{R_c^K(\bar{\xi}^c)+0.5\sigma_c^2}{\sigma_c}}^{\infty} \int_{l^b + q^b z_1}^{\infty} b_g(D - \bar{\xi}^c, s^g(z_1, z_2)) \phi_1(z_1) \phi_1(z_2) dz_1 dz_2 \\ &\quad - K \int_{-\infty}^{\frac{R_c^K(\bar{\xi}^c)+0.5\sigma_c^2}{\sigma_c}} \int_{l_g(K, D) + q_g z_1}^{\infty} \phi_1(z_1) \phi_1(z_2) dz_1 dz_2 \\ &\quad - K \int_{\frac{R_c^K(\bar{\xi}^c)+0.5\sigma_c^2}{\sigma_c}}^{\infty} \int_{l^b + q^b z_1}^{\infty} \phi_1(z_1) \phi_1(z_2) dz_1 dz_2 =: I_2^{P,1} + I_2^{P,2} + I_2^{K,1} + I_2^{K,2} \end{aligned}$$

<sup>5</sup>The term  $-K\Phi_1((-R_c(D - \bar{\xi}^g, \bar{\xi}^g) - 0.5(\sigma^2 + \sigma_c^2 - \sigma_g^2))/\sigma)$  will appear with opposite sign in  $I_3$  and is therefore not depicted in Proposition 5.3.

and now using the definition of  $b_g(\cdot)$  in (2.2), performing the transformation  $\bar{z}_1 = z_1 - \sigma_g \sqrt{1 - \rho^2}$ , using  $F_g = \exp(\mu_g + 0.5\sigma_g^2)$  and applying Lemma 5.6 with

$$q_1 = \sigma_g \rho \quad l_1 = 0 \quad q_2 = -q^b \quad l_2 = -l^b + \sigma_g \sqrt{1 - \rho^2} \quad a = \frac{R_c^K(\bar{\xi}^c) + 0.5\sigma_c^2}{\sigma_c}$$

for  $I_2^{P,1}$  and for  $I_2^{P,2}$  with

$$q_1 = \sigma_g \rho \quad l_1 = 0 \quad q_2 = -q_g \quad l_2 = -l_g(K, D) + \sigma_g \sqrt{1 - \rho^2}$$

and  $a = \frac{R_c^K(\bar{\xi}^c) + 0.5\sigma_c^2}{\sigma_c}$  leads to the three terms of  $f_{high}^g(D, \mathbf{F})$  in Lemma 5.2. The calculation of  $I_2^K$  is similar leading to  $k_{low}^g(D, \mathbf{F})$ <sup>6</sup> but without applying the transformation  $\bar{z}_1 = z_1 - \sigma_g \sqrt{1 - \rho^2}$  and setting  $q_1 = 0$  when applying Lemma 5.6.

#### Calculation of $I_3$ :

The condition for a non-zero payoff is (using the definition of  $b_{cg}(\cdot)$  in Appendix A.1 and (5.10)):

$$\begin{aligned} z_2 &> \frac{\ln(K) - \mu_g \alpha_g - \mu_c \alpha_c - \beta - \gamma D - (\sigma_g \rho \alpha_g + \sigma_c \alpha_c) z_1}{\sigma_g \alpha_g \sqrt{1 - \rho^2}} = \frac{R_c^K(D) + \sigma(\alpha)^2 - (\sigma_g \rho \alpha_g + \sigma_c \alpha_c) z_1}{\sigma_g \alpha_g \sqrt{1 - \rho^2}} \\ &=: \tilde{l}(K) + \tilde{q}(K) z_1 \end{aligned} \quad (5.24)$$

The integration limit can be expressed as

$$\begin{aligned} &\mathbb{I}\{b_c(D - \bar{\xi}^g, s^c(z_1)) \leq b_g(\bar{\xi}^g, s^g(z_1, z_2)), b_g(D - \bar{\xi}^c, s^g(z_1, z_2)) \leq b_c(\bar{\xi}^c, s^c(z_1))\} \\ &= 1 - \mathbb{I}\{b_c(D - \bar{\xi}^g, s^c(z_1)) > b_g(\bar{\xi}^g, s^g(z_1, z_2))\} - \mathbb{I}\{b_g(D - \bar{\xi}^c, s^g(z_1, z_2)) > b_c(\bar{\xi}^c, s^c(z_1))\} \end{aligned}$$

and therefore we use conditions (5.21) and (5.23) to yield

$$\begin{aligned} I_3 &= \left[ \int_{\mathbb{R}} \int_{\mathbb{R}} \tilde{l}(K) + \tilde{q}(K) z_1 - \int_{\mathbb{R}} \int_{\tilde{l}(K) + \tilde{q}(K) z_1}^{l^a + q^a z_1} - \int_{\mathbb{R}} \int_{\max(\tilde{l}(K) + \tilde{q}(K) z_1, l^b + q^b z_1)}^{\infty} \right. \\ &\quad \left. \left( \exp(\mu_c \alpha_c + \mu_g \alpha_g + (\sigma_c \alpha_c + \sigma_g \alpha_g \rho) z_1 + \sigma_g \alpha_g \sqrt{1 - \rho^2} z_2 + \beta + \gamma D) - K \right) \phi(z_1) \phi(z_2) dz_1 dz_2 \right. \\ &= : I_3^1 - I_3^2 - I_3^3 - K^1 + K^2 + K^3, \end{aligned}$$

where  $I$ -terms refer to the exponential terms and  $K$ -terms refer to the strike terms.

In order to calculate  $I_3^1$ , we perform the transformation  $\bar{z}_2 = z_2 - \sigma_g \alpha_g \sqrt{1 - \rho^2}$ , use  $F_i = \exp(\mu_i + 0.5\sigma_i^2)$  and apply Lemma 5.6 with

$$q_1 = \sigma_c \alpha_c + \sigma_g \alpha_g \rho \quad l_1 = 0 \quad q_2 = -\tilde{q}(K) \quad l_2 = -\tilde{l}(K) + \sigma_g \alpha_g \sqrt{1 - \rho^2} \quad a = \infty$$

<sup>6</sup>The term  $-K\Phi_1((-R_g(D - \bar{\xi}^c, \bar{\xi}^c) - 0.5(\sigma^2 + \sigma_g^2 - \sigma_c^2))/\sigma)$  will appear with opposite sign in  $I_3$  and is therefore not depicted in Proposition 5.3.

to get

$$I_3^1 = b_{cg}(D, \mathbf{F}) \exp\left(\frac{-\alpha_g \alpha_c \sigma^2}{2}\right) \underbrace{\Phi_1\left(\frac{-R_\alpha^K(D)}{\sigma(\alpha)}\right)}_{=1-\Phi_1\left(\frac{R_\alpha^K(D)}{\sigma(\alpha)}\right)}.$$

Similarly, but without the transformation and  $q_1 = 0$  when applying Lemma 5.6 yields

$$K^1 = K \left( 1 - \Phi_1\left(\frac{R_\alpha^K(D) + \sigma^2(\alpha)}{\sigma(\alpha)}\right) \right).$$

The second term of  $K^1$  will together with the second term of  $K^3$  sum up to zero.

In order to calculate  $I_3^2$ , we have to consider the additional condition

$$\tilde{l}(K) + \tilde{q}(K)z_1 < l^a + q^a z_1 \Leftrightarrow z_1 > R_\Delta^{c,high}(D)/\sigma_c$$

which yields

$$\begin{aligned} I_3^2 = & \exp(\mu_c \alpha_c + \mu_g \alpha_g + \beta + \gamma D + \sigma_g^2 \alpha_g^2 (1 - \rho^2)/2) \cdot \\ & \int_{R_\Delta^{c,high}(D)/\sigma_c}^{\infty} \exp((\sigma_c \alpha_c + \sigma_g \alpha_g \rho)z_1) \cdot \\ & \left[ \Phi\left(l^a + q^a z_1 - \sigma_g \alpha_g \sqrt{1 - \rho^2}\right) - \Phi\left(\tilde{l}(K) + \tilde{q}(K)z_1 - \sigma_g \alpha_g \sqrt{1 - \rho^2}\right) \right] \phi(z_1) dz_1. \end{aligned}$$

For the first summand we apply Lemma 5.6 with

$$q_1 = \sigma_c \alpha_c + \sigma_g \alpha_g \rho \quad l_1 = 0 \quad q_2 = q^a \quad l_2 = l^a - \alpha_g \sigma_g \sqrt{1 - \rho^2} \quad a = R_\Delta^{c,high}(D)$$

and for the second summand with

$$q_1 = \sigma_c \alpha_c + \sigma_g \alpha_g \rho \quad l_1 = 0 \quad q_2 = \tilde{q}(K) \quad l_2 = \tilde{l}(K) - \sigma_g \alpha_g \sqrt{1 - \rho^2} \quad a = R_\Delta^{c,high}(D).$$

Further simplifications lead to

$$\begin{aligned} I_3^2 = & b_{cg}(D, \mathbf{F}) \exp\left(\frac{-\alpha_g \alpha_c \sigma^2}{2}\right) \left( \Phi_1\left(\frac{-R_c(D - \bar{\xi}^g, \bar{\xi}^g) - \alpha_g \sigma^2}{\sigma}\right) - \Phi_1\left(\frac{R_\alpha^K(D)}{\sigma(\alpha)}\right) \right. \\ & - \Phi_2\left(R_\Delta^{c,high}(D)/\sigma_c - \sigma_c \alpha_c - \sigma_g \alpha_g \rho, \frac{-R_c(D - \bar{\xi}^g, \bar{\xi}^g) - \alpha_g \sigma^2}{\sigma}, \frac{-(\sigma_c - \sigma_g \rho)}{\sigma}\right) \\ & \left. + \Phi_2\left(R_\Delta^{c,high}(D)/\sigma_c - \sigma_c \alpha_c - \sigma_g \alpha_g \rho, \frac{R_\alpha^K(D)}{\sigma(\alpha)}, \frac{\sigma_c \alpha_c + \sigma_g \alpha_g \rho}{\sigma(\alpha)}\right) \right). \end{aligned}$$

We perform similar calculations for  $K^2$  without transformation and using  $q_1 = 0$  to derive

$$\begin{aligned} K^2 = & K \left( \Phi_1\left(\frac{-R_c(D - \bar{\xi}^g, \bar{\xi}^g) - \frac{1}{2}(\sigma^2 - \sigma_g^2 + \sigma_c^2)}{\sigma}\right) - \Phi_1\left(\frac{R_\alpha^K(D) + \sigma^2(\alpha)}{\sigma(\alpha)}\right) \right. \\ & - \Phi_2\left(R_\Delta^{c,high}(D)/\sigma_c, \frac{-R_c(D - \bar{\xi}^g, \bar{\xi}^g) - \frac{1}{2}(\sigma^2 - \sigma_g^2 + \sigma_c^2)}{\sigma}, \frac{-(\sigma_c - \sigma_g \rho)}{\sigma}\right) \\ & \left. + \Phi_2\left(R_\Delta^{c,high}(D)/\sigma_c, \frac{R_\alpha^K(D) + \sigma^2(\alpha)}{\sigma(\alpha)}, \frac{\sigma_c \alpha_c + \sigma_g \alpha_g \rho}{\sigma(\alpha)}\right) \right). \end{aligned}$$

In order to calculate  $I_3^3$ , we have to consider the additional condition

$$\max\left(\tilde{l}(K) + \tilde{q}(K)z_1, l^b + q^b z_1\right) = \begin{cases} l^b + q^b z_1, & z_1 > R_{\Delta}^{g,high}(D)/\sigma_c \\ \tilde{l}(K) + \tilde{q}(K)z_1, & \text{else} \end{cases}$$

yielding

$$\begin{aligned} I_3^3 &= \left[ \int_{R_{\Delta}^{g,high}(D)}^{\infty} \int_{l^b + q^b z_1}^{\infty} + \int_{-\infty}^{R_{\Delta}^{g,high}(D)} \int_{\tilde{l}(K) + \tilde{q}(K)z_1}^{\infty} \right] \\ &\quad \exp(\mu_c \alpha_c + \mu_g \alpha_g + (\sigma_c \alpha_c + \sigma_g \alpha_g \rho) z_1 + \sigma_g \alpha_g \sqrt{1 - \rho^2} z_2 + \beta + \gamma D) \phi(z_1) \phi(z_2) dz_1 dz_2 \\ &=: I_3^{3,a} + I_3^{3,b}. \end{aligned}$$

In order to calculate  $I_3^{3,a}$ , we perform the transformation  $\bar{z}_2 = z_2 - \sigma_g \alpha_g \sqrt{1 - \rho^2}$ , use  $F_i = \exp(\mu_i + 0.5\sigma_i^2)$  and apply Lemma 5.6 with

$$q_1 = \sigma_c \alpha_c + \sigma_g \alpha_g \rho \quad l_1 = 0 \quad q_2 = -q^b \quad l_2 = -l^b + \alpha_g \sigma_g \sqrt{1 - \rho^2} \quad a = R_{\Delta}^{g,high}(D)$$

to get

$$\begin{aligned} I_3^{3,a} &= b_{cg}(D, \mathbf{F}) \exp\left(\frac{-\alpha_g \alpha_c \sigma^2}{2}\right) \left( \Phi_1\left(\frac{-R_g(D - \bar{\xi}^c, \bar{\xi}^c)}{\sigma} - \alpha_c \sigma\right) \right. \\ &\quad \left. - \Phi_2\left(\frac{R_{\Delta}^{g,high}(D)}{\sigma_c} - (\sigma_c \alpha_c + \sigma_g \alpha_g \rho), \frac{-R_g(D - \bar{\xi}^c, \bar{\xi}^c)}{\sigma} - \alpha_c \sigma; \frac{\sigma_c - \sigma_g \rho}{\sigma}\right) \right). \end{aligned}$$

In order to calculate  $I_3^{3,b}$ , we perform the transformation  $\bar{z}_2 = z_2 - \sigma_g \alpha_g \sqrt{1 - \rho^2}$ , use  $F_i = \exp(\mu_i + 0.5\sigma_i^2)$  and apply Lemma 5.6 with

$$q_1 = \sigma_c \alpha_c + \sigma_g \alpha_g \rho \quad l_1 = 0 \quad q_2 = -\tilde{q}(K) \quad l_2 = -\tilde{l}(K) + \sigma_g \alpha_g \sqrt{1 - \rho^2} \quad a = R_{\Delta}^{g,high}(D).$$

to get

$$I_3^{3,b} = b_{cg}(D, \mathbf{F}) \exp\left(\frac{-\alpha_g \alpha_c \sigma^2}{2}\right) \Phi_2\left(\frac{R_{\Delta}^{g,high}(D)}{\sigma_c} - (\sigma_c \alpha_c + \sigma_g \alpha_g \rho), \frac{-R_{\alpha}^K(D)}{\sigma(\alpha)}; \frac{-\sigma_c \alpha_c - \sigma_g \alpha_g \rho}{\sigma(\alpha)}\right).$$

Similary, we define  $K^3 := K^{3,a} + K^{3,b}$  and perform the above calculations without the transformation and using  $q_1 = 0$  to get

$$\begin{aligned} K^{3,a} &= K \left( \Phi_1\left(\frac{-R_g(D - \bar{\xi}^c, \bar{\xi}^c) - \frac{1}{2}(\sigma^2 - \sigma_c^2 + \sigma_g^2)}{\sigma}\right) \right. \\ &\quad \left. - \Phi_2\left(\frac{R_{\Delta}^{g,high}(D)}{\sigma_c}, \frac{-R_g(D - \bar{\xi}^c, \bar{\xi}^c) - \frac{1}{2}(\sigma^2 - \sigma_c^2 + \sigma_g^2)}{\sigma}; \frac{\sigma_c - \sigma_g \rho}{\sigma}\right) \right), \\ K^{3,b} &= K \Phi_2\left(\frac{R_{\Delta}^{g,high}(D)}{\sigma_c}, \frac{-R_{\alpha}^K(D) - \sigma^2(\alpha)}{\sigma(\alpha)}; \frac{-\sigma_c \alpha_c - \sigma_g \alpha_g \rho}{\sigma(\alpha)}\right). \end{aligned}$$

Taking the difference  $I_3^1 - I_3^2 - I_3^3$  and  $K^1 - K^2 - K^3$  leads to  $f_{high}^{cg}(\cdot, \cdot)$  and  $k_{high}^{cg}(\cdot, \cdot)$ . ■



### 5.4.3 Proof: Derivation for a fix Demand; Spikes and Negative Prices

In this Chapter, we proof Proposition 5.3 (p. 88).

#### Negative Prices

##### Proof.

We perform a similar proof as performed in Lemma 5.1 and 5.2 and use the tower property to calculate the fair value for a fixed  $D \in (-\infty, 0)$  at a first step. Furthermore, we use the Cholesky decomposition in (5.10) to calculate the integral over the fuels. Given the form of the power spot price in Chapter A.1 including negative prices and price spikes, we have to calculate

$$f_n(D, \mathbf{F}_t) = \int_{\mathbb{R}} \int_{\mathbb{R}} (\min\{s_c(z_1) \exp(k_c), s_g(z_1, z_2) \exp(k_g)\} - \exp(-m_n D) + 1 - K)^+ \phi_1(z_1) \phi_1(z_2) dz_1 dz_2.$$

It holds

$$\begin{aligned} s_c(z_1) \exp(k_c) < s_g(z_1, z_2) \exp(k_g) &\Leftrightarrow z_2 > \frac{R_g(0, 0) + (\sigma_c - \sigma_g \rho) z_1 + \frac{1}{2}(\sigma^2 + \sigma_g^2 - \sigma_c^2)}{\sigma_g \sqrt{1 - \rho^2}} \\ &= \frac{-R_c(0, 0) + (\sigma_c - \sigma_g \rho) z_1 + \frac{1}{2}(-\sigma^2 + \sigma_g^2 - \sigma_c^2)}{\sigma_g \sqrt{1 - \rho^2}} \\ &=: l_2^n + q_2^n z_1. \end{aligned} \quad (5.25)$$

For the case  $-\exp(-m_n D) + 1 - K > 0$  ( $\delta_N(D) = 0$ ), the payoff is non-zero for all choices of  $z_1$  and  $z_2$  and  $f_n(D, \mathbf{F}_t)$  becomes

$$\begin{aligned} f_n(D, \mathbf{F}_t) &= b_c(0, F_t^c) \int_{\mathbb{R}} \int_{l_2^n + q_2^n(z_1 + \sigma_c)}^{\infty} \phi_1(z_1) \phi_1(z_2) dz_1 dz_2 \\ &\quad + b_g(0, F_t^g) \int_{\mathbb{R}^+} \int_{-\infty}^{l_2^n + q_2^n(z_1 + \sigma_g \rho) - \sigma_g \sqrt{1 - \rho^2}} \phi_1(z_1) \phi_1(z_2) dz_1 dz_2 \\ &\quad - \exp(-m_n D) + 1 - K. \end{aligned}$$

Applying Lemma 5.6 with

$$q_1 = 0 \quad l_1 = 0 \quad q_2 = -q_2^n \quad l_2 = -l_2^n - q_2^n \sigma_c \quad a = \infty$$

for the first term and

$$q_1 = 0 \quad l_1 = 0 \quad q_2 = q_2^n \quad l_2 = l_2^n + q_2^n \sigma_g \rho - \sigma_g \sqrt{1 - \rho^2} \quad a = \infty$$

for the second term yields

$$f_n(D, \mathbf{F}_t) = \sum_{i \in I} b_i(0, F_t^i) \Phi(R_i(0, 0)/\sigma) + 1 - \exp(-m_n D) - K$$

being what is stated in Proposition 5.3 for  $\delta_N(D) = 0$ .

For the case  $\delta_N(D) = 1$  ( $-\exp(-m_n D) + 1 - K < 0$ ), we get the following restriction for a non-zero payoff

$$\begin{aligned} & \begin{cases} z_1 > \frac{\ln(K + \exp(-m_n D) - 1) - \mu_c - k_c}{\sigma_c} & \text{if } z_2 > l_2^n + q_2^n z_1 \\ z_2 > \frac{\ln(K + \exp(-m_n D) - 1) - \mu_g - k_g - \sigma_g \rho z_1}{\sigma_g \sqrt{1 - \rho^2}}, & \text{else} \end{cases} \\ & = \begin{cases} z_1 > \frac{R_c^{K,n}(D) + \sigma_c^2/2}{\sigma_c} & \text{if } z_2 > l_2^n + q_2^n z_1 \\ z_2 > \frac{R_g^{K,n}(D) + \sigma_g^2/2 - \sigma_g \rho z_1}{\sigma_g \sqrt{1 - \rho^2}}, & \text{else} \end{cases}. \end{aligned}$$

For the case  $z_2 \leq l_2^n + q_2^n z_1$ , we get the additional restriction

$$z_1 > \frac{R_c^{K,n}(K) + \sigma_c^2/2}{\sigma_c}$$

which is altogether leading to

$$\begin{aligned} f_n(D, \mathbf{F}_t) &= \int_{\frac{R_c^{K,n}(K) + \sigma_c^2/2}{\sigma_c}}^{\infty} \int_{l_2^n + q_2^n z_1}^{\infty} (s_c(z_1) \exp(k_c) - \exp(-m_n D) + 1 - K) \phi_1(z_1) \phi_1(z_2) dz_1 dz_2 \\ &+ \int_{\frac{R_c^{K,n}(K) + \sigma_c^2/2}{\sigma_c}}^{\infty} \int_{\frac{R_g^{K,n}(K) + \sigma_g^2/2 - \sigma_g \rho z_1}{\sigma_g \sqrt{1 - \rho^2}}}^{l_2^n + q_2^n z_1} (s_g(z_1, z_2) \exp(k_g) - \exp(-m_n D) + 1 - K) \phi_1(z_1) \phi_1(z_2) dz_1 dz_2. \end{aligned}$$

Similar to the prior proofs in Chapter 5.4, we at first split the sum into a strike-term ( $-\exp(-m_n D) + 1 - K$ ) and a bid-stack-term. Then, we use Lemma 5.6 to calculate the above integrals. This procedure leads to three bivariate terms for the bid-stack-term and other three bivariate terms for the ( $-\exp(-m_n D) + 1 - K$ )-term as it is summarized in Proposition 5.3. ■

## Spikes

### Proof.

We perform a similar proof as performed in Lemma 5.1 and 5.2 and use the tower property to calculate the fair value for a fixed  $D \in (\bar{\xi}, \infty)$  at a first step. Furthermore, we use the Cholesky decomposition in (5.10) to calculate the integral over the fuels. Given the form of the power spot price in Chapter A.1, we have to calculate

$$\begin{aligned} f_s(D, \mathbf{F}_t) &= \int_{\mathbb{R}} \int_{\mathbb{R}} (\max\{b_c(\bar{\xi}^c, s_c(z_1)), b_g(\bar{\xi}^g, s_g(z_1, z_2))\} + \exp(m_s(D - \bar{\xi})) - 1 - K)^+ \\ &\quad \cdot \phi_1(z_1) \phi_1(z_2) dz_1 dz_2. \end{aligned}$$

It holds

$$\begin{aligned} s_c(z_1) \exp(k_c + \bar{\xi}^c) < s_g(z_1, z_2) \exp(k_g + \bar{\xi}^g) &\Leftrightarrow z_2 > \frac{R_g(\bar{\xi}^g, \bar{\xi}^c) + (\sigma_c - \sigma_g \rho) z_1 + \frac{1}{2}(\sigma^2 + \sigma_g^2 - \sigma_c^2)}{\sigma_g \sqrt{1 - \rho^2}} \\ &= \frac{-R_c(\bar{\xi}^c, \bar{\xi}^g) + (\sigma_c - \sigma_g \rho) z_1 + \frac{1}{2}(-\sigma^2 + \sigma_g^2 - \sigma_c^2)}{\sigma_g \sqrt{1 - \rho^2}} \\ &=: l_2^s + q_2^s z_1. \end{aligned}$$

For the case  $+\exp(m_s(D - \bar{\xi})) - 1 - K > 0$  ( $\delta_S(D) = 0$ ), the payoff is non-zero for all choices of  $z_1$  and  $z_2$  and  $f_s(D, \mathbf{F}_t)$  becomes

$$\begin{aligned} f_s(D, \mathbf{F}_t) = & b_c(\bar{\xi}^c, F_t^c) \int_{\mathbb{R}^+} \int_{-\infty}^{l_2^s + q_2^s(z_1 + \sigma_c)} \phi_1(z_1) \phi_1(z_2) dz_1 dz_2 \\ & + b_g(\bar{\xi}^g, F_t^g) \int_{\mathbb{R}^+} \int_{l_2^s + q_2^s(z_1 + \sigma_g \rho) - \sigma_g \sqrt{1 - \rho^2}}^{\infty} \phi_1(z_1) \phi_1(z_2) dz_1 dz_2 \\ & + \exp(m_s(D - \bar{\xi})) - 1 - K. \end{aligned}$$

Applying Lemma 5.6 with

$$q_1 = 0 \quad l_1 = 0 \quad q_2 = q_2^s \quad l_2 = l_2^s + q_2^s \sigma_c \quad a = \infty$$

for the first term and

$$q_1 = 0 \quad l_1 = 0 \quad q_2 = -q_2^s \quad l_2 = -l_2^s - q_2^s \sigma_g \rho + \sigma_g \sqrt{1 - \rho^2} \quad a = \infty$$

for the second term yields

$$f_s(D, \mathbf{F}_t) = \sum_{i \in I} b_i(\bar{\xi}^i, F_t^i) \Phi(R_i(\bar{\xi}^i, \bar{\xi}^j)/\sigma) + \exp(m_s(D - \bar{\xi})) - 1 - K$$

being what is stated in Proposition 5.3 for  $\delta_S(D) = 0$ .

For the case  $\delta_S(D) = 1$  ( $\exp(m_s(D - \bar{\xi})) - 1 - K < 0$ ), we get the following restriction for a non-zero payoff

$$\begin{aligned} & \begin{cases} z_1 > \frac{\ln(K - \exp(m_s(D - \bar{\xi}))) + 1 - \mu_c - k_c - m_c \bar{\xi}^c}{\sigma_c} & \text{if } z_2 < l_2^s + q_2^s z_1 \\ z_2 > \frac{\ln(K - \exp(m_s(D - \bar{\xi}))) + 1 - \mu_g - k_g - m_g \bar{\xi}^g - \sigma_g \rho z_1}{\sigma_g \sqrt{1 - \rho^2}}, & \text{else} \end{cases} \\ & = \begin{cases} z_1 > \frac{R_c^{K,s}(D) + \sigma_c^2/2}{\sigma_c} & \text{if } z_2 < l_2^s + q_2^s z_1 \\ z_2 > \frac{R_g^{K,s}(D) + \sigma_g^2/2 - \sigma_g \rho z_1}{\sigma_g \sqrt{1 - \rho^2}}, & \text{else} \end{cases}. \end{aligned}$$

For the case  $z_2 \geq l_2^s + q_2^s z_1$ , we get the additional restriction

$$\max \left\{ l_2^s + q_2^s z_1, \frac{R_g^{K,s}(D) + \sigma_g^2/2 - \sigma_g \rho z_1}{\sigma_g \sqrt{1 - \rho^2}} \right\} = \begin{cases} l_2^s + q_2^s z_1 & , \text{if } z_1 > \frac{R_c^{K,s}(K) + \sigma_c^2/2}{\sigma_c} \\ \frac{R_g^{K,s}(D) + \sigma_g^2/2 - \sigma_g \rho z_1}{\sigma_g \sqrt{1 - \rho^2}} & \text{else} \end{cases}$$

which is altogether leading to

$$\begin{aligned} f_s(D, \mathbf{F}_t) = & \int_{\frac{R_c^{K,s}(K) + \sigma_c^2/2}{\sigma_c}}^{\infty} \int_{-\infty}^{l_2^s + q_2^s z_1} (b_c(\bar{\xi}^c, s_c(z_1)) + \exp(m_s(D - \bar{\xi})) - 1 - K) \phi_1(z_1) \phi_1(z_2) dz_1 dz_2 \\ & + \int_{\frac{R_c^{K,s}(K) + \sigma_c^2/2}{\sigma_c}}^{\infty} \int_{l_2^s + q_2^s z_1}^{\infty} (b_g(\bar{\xi}^g, s_g(z_1, z_2)) + \exp(m_s(D - \bar{\xi})) - 1 - K) \phi_1(z_1) \phi_1(z_2) dz_1 dz_2 \\ & + \int_{-\infty}^{\frac{R_c^{K,s}(K) + \sigma_c^2/2}{\sigma_c}} \int_{\frac{R_g^{K,s}(D) + \sigma_g^2/2 - \sigma_g \rho z_1}{\sigma_g \sqrt{1 - \rho^2}}}^{\infty} (b_g(\bar{\xi}^g, s_g(z_1, z_2)) + \exp(m_s(D - \bar{\xi})) - 1 - K) \end{aligned}$$

$$\cdot \phi_1(z_1)\phi_1(z_2)dz_1dz_2.$$

Similar to the prior proofs in Chapter 5.4, we first separate the integrand in a strike-term and a bid-stack-term and use Lemma 5.6 to calculate the above integrals. This procedure leads to three bivariate terms for the bid-stack-term and other three bivariate terms for the  $(\exp(m_s D) - 1 - K)$ -term as it is summarized in Proposition 5.3. ■

#### 5.4.4 Proof: Exemplary Derivation for truncated normal distributed Demand; Low Case

In this Chapter, we illustrate the approach how to proof Lemma 5.4 (p. 91) and Lemma 5.5 (p. 93).

In order to enable integration over demand, we need the following Lemma by [Gupta, 1963] in [Genz and Bretz, 2009].

**Lemma 5.7** *It holds the following relationship between  $\Phi_3, \Phi_2$  and  $\phi_1$ :*

$$\Phi_3(x_1, x_2, x_3; (\rho_{21}, \rho_{31}, \rho_{32})^T) = \int_{-\infty}^{x_1} \Phi_2 \left( \frac{x_2 - \rho_{21}y}{\sqrt{1 - \rho_{21}^2}}, \frac{x_3 - \rho_{31}y}{\sqrt{1 - \rho_{31}^2}}, \frac{\rho_{32} - \rho_{21}\rho_{31}}{\sqrt{(1 - \rho_{21}^2)(1 - \rho_{31}^2)}} \right) \phi_1(y) dy.$$

**Proof.** We refer to [Gupta, 1963]. ■

**Proof.** We show the proof exemplary for  $f_{low}^c$  as the proof is in all cases - where bivariate cumulative distribution functions have to be integrated - a straight application of Lemma 5.7. The first term of  $f_{low}^c$  belongs to the forward price formula (which is a separate part of the option price formula in Corollary 5.1). We get (to shortage notation we leave out the time index in mean and variance variables):

$$\begin{aligned} & \int_0^{\xi^c} f_{low}^c(D, \mathbf{F}_t) \phi_D(D) dD = \int_0^{\xi^c} b_c(D, \mathbf{x}) \Phi_1(R_c(D, 0)/\sigma) \phi_D(D) dD \\ & - F_t^c \exp(k_c) \int_0^{\xi^c} \exp(m_c D) \Phi_2 \left( \frac{R_c^K(D)}{\sigma_c} - \sigma_c/2, \frac{R_c(D, 0)}{\sigma}, \frac{\sigma_c - \sigma_g \rho}{\sigma} \right) \frac{\phi_1 \left( \frac{D - \mu_D}{\sigma_D} \right)}{\sigma_D} dD \\ & = \int_0^{\xi^c} b_c(D, \mathbf{x}) \Phi_1(R_c(D, 0)/\sigma) \phi_D(D) dD \\ & - F_t^c \exp(k_c) \int_{\frac{-\mu_D}{\sigma_D}}^{\frac{\xi^c - \mu_D}{\sigma_D}} \exp(m_c(\sigma_D D + \mu_D)) \\ & \cdot \Phi_2 \left( \frac{R_c^K(\sigma_D D + \mu_D)}{\sigma_c} - \sigma_c/2, \frac{R_c(\sigma_D D + \mu_D, 0)}{\sigma}, \frac{\sigma_c - \sigma_g \rho}{\sigma} \right) \phi_1(D) dD \\ & = \int_0^{\xi^c} b_c(D, \mathbf{x}) \Phi_1(R_c(D, 0)/\sigma) \phi_D(D) dD \\ & - b_c(\mu_D, F_t^c) \exp \left( \frac{m_c^2 \sigma_D^2}{2} \right) \int_{\frac{-\mu_D}{\sigma_D} - m_c \sigma_D}^{\frac{\xi^c - \mu_D}{\sigma_D} - m_c \sigma_D} \\ & \cdot \Phi_2 \left( \frac{R_c^K(\mu_D + m_c \sigma_D^2) - m_c \sigma_D D}{\sigma_c} - \frac{\sigma_c}{2}, \frac{R_c(\mu_D + m_c \sigma_D^2, 0) - \sigma_D m_c D}{\sigma}, \frac{\sigma_c - \sigma_g \rho}{\sigma} \right) \phi_1(D) dD. \end{aligned}$$

With the help of Lemma 5.7 we have to solve for the second term

$$\frac{m_c \sigma_D}{\sigma_c} \stackrel{!}{=} \frac{\rho_{21}}{\sqrt{1 - \rho_{21}^2}} \quad \frac{\sigma_D m_c}{\sigma} \stackrel{!}{=} \frac{\rho_{31}}{\sqrt{1 - \rho_{31}^2}} \quad \frac{\sigma_c - \sigma_g \rho}{\sigma} \stackrel{!}{=} \frac{\rho_{32} - \rho_{21} \rho_{31}}{\sqrt{1 - \rho_{21}^2} \sqrt{1 - \rho_{31}^2}}$$

being equivalent to

$$\begin{aligned} \rho_{21} &= \frac{m_c \sigma_D}{\sqrt{\sigma_c^2 + m_c^2 \sigma_D^2}} \stackrel{Def. 5.1}{=} \frac{m_c \sigma_D}{v(m_c, \sigma_c)} \\ \rho_{31} &= \frac{m_c \sigma_D}{\sqrt{\sigma^2 + m_c^2 \sigma_D^2}} \stackrel{Def. 5.1}{=} \frac{m_c \sigma_D}{v(m_c, \sigma)} \\ \rho_{32} &= \frac{\sigma_c^2 - \sigma_c \sigma_g \rho + m_c^2 \sigma_D^2}{v(m_c, \sigma) v(m_c, \sigma_c)}. \end{aligned}$$

It remains to calculate

$$x_2 = \left( \frac{R_c^K(\mu_D + m_c \sigma_D^2)}{\sigma_c} - \frac{\sigma_c}{2} \right) \sqrt{1 - \rho_{21}^2} \quad x_3 = \frac{R_c(\mu_D + m_c \sigma_D^2, 0)}{\sigma} \sqrt{1 - \rho_{31}^2}$$

leading to the first trivariate integral in Lemma 5.4. ■



## CHAPTER 6.

# Numerical Greek Calculation

There are various approaches to derive Greeks of an arbitrary contingent claim  $\Psi(S_t^F, S_t^P)$ . The starting point in quantitative finance is often to express the present value of the claim as a function of potential hedging instruments, i.e. futures (cf. Definition 1.1). Afterwards, according derivatives can directly be calculated to end up with the most common Greeks: delta, gamma and vega respectively (cf. Chapter 1.2.3).

In order to be able to identify open exposures on certain trading days/hours instead of trading time frames  $[t^a, t^b]$ , we prefer to work with an hourly forward curve (cf. Definition 1.2), though hourly forwards can typically not be traded in the market. In Chapter 3.5, we derive Proposition 3.3 which provides - under certain conditions - an algorithm to get from a daily/hourly hedging strategy to a hedging strategy of actively traded forwards/ futures contracts.

In Proposition 3.2, we have shown that replication strategies for contingent claims using structural models can - under certain conditions - be derived by calculating the partial derivatives (sensitivities) of the present value ( $PV_t$ ) at time  $t \geq t_0$  in direction of the hedging instruments (delta hedging). In this context, we want to distinguish between sensitivities regarding *model parameters*  $\vartheta \in \mathbb{R}^k$  (the Greeks) and *hedging instruments*  $f$ , i.e. an hourly forward (cf. Definition 1.2).

The connection between both is for an arbitrary forward  $f$  of Definition 1.2 given by the chain rule as follows:

$$\frac{\partial}{\partial f} PV_t = \sum_{j=1}^k \frac{\partial PV_t}{\partial \vartheta_j} \frac{\partial \vartheta_j}{\partial f}. \quad (6.1)$$

Further information on this distinction can be found in [Li, 1999].

**Example 6.1 (Application to the Ornstein- Uhlenbeck Model)** *The model parameters of the Ornstein-Uhlenbeck model in Chapter 2.2 are given by*

1.  $\alpha_t^{(1)}, \dots, \alpha_t^{(n)}$  and  $\alpha_t^D$ ,
2.  $v_t^{(1)}, \dots, v_t^{(n)}$  and  $v_t^D$ ,
3.  $s^{(1)}(t), \dots, s^{(n)}(t)$  and  $s^D(t)$ ,
4.  $p_{ij}$  for  $i, j \in I$ ,
5.  $S_{t_0}^{(1)}, \dots, S_{t_0}^{(n)}$  and  $D_{t_0}$ .

Forward prices are not part of the set of model parameters which is why they are instead included manually into our model by calibration.

Mean-reversion speeds, volatilities and correlations are estimated from historical data which is why they do not depend on forward prices. The same holds for spot fuel prices and spot demand. The derivatives of those model parameters in direction of forward prices are consequently zero.

However, seasonalities are used for calibration against forward prices which leads to

$$\begin{aligned}\frac{\partial s^{(i)}(t)}{\partial f} &\neq 0, \text{ for } f = F_{t_0,t}^{(i)} \text{ and } i \in I \\ \frac{\partial s^D(t)}{\partial f} &\neq 0, \text{ for } f = F_{t_0,t}^{(i)} \text{ and } i \in (I \cup \{D\}).\end{aligned}$$

It follows

$$\frac{\partial}{\partial F_{t_0,t}^{(i)}} PV_t = \frac{\partial PV_t}{\partial s^{(i)}(t)} \frac{\partial s^{(i)}(t)}{\partial F_{t_0,t}^{(i)}} + \frac{\partial PV_t}{\partial s^D(t)} \frac{\partial s^D(t)}{\partial F_{t_0,t}^{(i)}}, \quad (6.2)$$

$$\frac{\partial}{\partial F_{t_0,t}^P} PV_t = \frac{\partial PV_t}{\partial s^D(t)} \frac{\partial s^D(t)}{\partial F_{t_0,t}^P}. \quad (6.3)$$

We conclude:

1. Fuel seasonalities  $s^{(i)}$  for  $i \in I$  change after changing a fuel forward price,
2. Demand seasonality  $s^D(t)$  changes after either changing the fuel forward prices or electricity forward prices.

## 6.1 Numerical Techniques - An Overview

By using the notation in Definition 1.2, the present value  $PV_{t_0}$  of a claim  $\Psi(\mathbf{S}_t^F, \mathbf{S}_t^P)$  can be expressed as

$$PV_{t_0}(\mathbf{F}) = \mathbb{E}^{\mathbb{Q}} [\Psi(\mathbf{S}_t^F(\mathbf{F}), \mathbf{S}_t^P(\mathbf{F})) | \mathcal{F}_{t_0}]. \quad (6.4)$$

Let  $f := F_{t_0,t_l}^k$  with  $k \in \{1, \dots, n, P\}$  and  $l \in \{1, \dots, m\}$  be an hourly forward based on Definition 1.2. The aim is to calculate  $\frac{\partial}{\partial f} PV_t(\mathbf{S}_t^F(\mathbf{F}), \mathbf{S}_t^P(\mathbf{F}))$ .

**Notation 6.1** The notation  $\frac{\partial}{\partial f} PV_t(\mathbf{S}_t^F(\mathbf{F}), \mathbf{S}_t^P(\mathbf{F}))$  is motivated from (2.5) which is

$$\begin{aligned}S_t^{(i)} &= \exp \left( s^{(i)}(t) + \exp \left( - \int_{t_0}^t \alpha_s^{(i)} ds \right) \ln(s_i) + \int_{t_0}^t v_s^{(i)} \exp \left( - \int_s^t \alpha_u^{(i)} du \right) dW_s^{(i)} \right) \\ D_t &= s^D(t) + \exp \left( - \int_{t_0}^t \alpha_s^D ds \right) d + \int_{t_0}^t v_s^D \exp \left( - \int_s^t \alpha_u^D du \right) dW_s^D.\end{aligned}$$

The dependency  $S_t^{(i)}(\mathbf{F})$  and  $D_t(\mathbf{F})$  comes from choosing the seasonality function such that forward prices are priced arbitrage free (equation (2.9) and Definition 2.1).



The notation above indicates that we intent to use the spot dynamics in order to calculate Greeks in direction of forward prices. In general, forward dynamics might be the more intuitive way to compute forward Greeks. It would lead the notation rather to be  $\frac{\partial}{\partial f}PV_t(F_{t_0,t}^1, \dots, F_{t_0,t}^n, F_{t_0,t}^P)$ . However, we have seen in Chapter 3 that power forward dynamics may not be tractable for structural electricity models (cf. equation (3.3)). This is why we intent to use the spot dynamics to calculate forward Greeks instead.

Of course, if a close formula for the present value of the contingent claim exists, we would analytically calculate the derivative of the present value in direction a hedging instrument. However, in our case pricing formulas are either not available or quite complex (see [Carmona et al., 2013] for forwards and spread options; Chapter 5.4 for call options) which is why we prefer to use Monte Carlo techniques. We start with a short summary of numerical methods being common for Greek calculation (cf. [Glassermann, 2003]).

1. Difference quotient method: uses the differential quotient to approximate the derivative in direction of the hedging instrument:

$$\frac{\partial}{\partial f}PV_t(S_t^F(\mathbf{F}), S_t^P(\mathbf{F})) \approx \frac{PV_t(\mathbf{F} + \mathbf{h}) - PV_t(\mathbf{F} - \mathbf{h})}{2h}, \quad (6.5)$$

where  $\mathbf{h} = (h_1^1, \dots, h_m^1, \dots, h_1^n, \dots, h_m^n, h_1^P, \dots, h_m^P) \in \mathbb{R}^{m(n+1)}$  with  $h_j^i = h > 0$  for exactly one component and  $h_j^i = 0$  for the others.

2. likelihood ratio method: Assuming an existing close form density function  $f_{\mathbf{F}}(\cdot)$ , the hedging instruments are transformed from the claim into the density function (and additionally assuming integration and differentiation can be interchanged<sup>1</sup>)

$$\frac{\partial}{\partial f}PV_t(S_t^F(\mathbf{F}), S_t^P(\mathbf{F})) = \int_{\Omega} \Psi(\mathbf{x}) \frac{\partial}{\partial f}f_{\mathbf{F}}(\mathbf{x})d\mathbf{x}$$

3. pathwise derivative method: Assuming the claim is differentiable, the problem may be transformed (assuming integration and differentiation can be interchanged):

$$\frac{\partial}{\partial f}PV_t(S_t^F(\mathbf{F}), S_t^P(\mathbf{F})) = \mathbb{E}^{\mathbb{Q}} \left[ \frac{\partial}{\partial f}\Psi(S_t^F(\mathbf{F}), S_t^P(\mathbf{F})) \middle| \mathcal{F}_{t_0} \right]$$

4. adjoint algorithmic differentiation: Exploits the numerical implementation of the present value function into each sub-function and uses the chain rule to aggregate each derivative of each function to the derivative of the present value function. It is a method for an efficient implementation of the pathwise derivative method. Further information can be found in [Giles and Glassermann, 2006].

We will not investigate adjoint algorithmic differentiation in this thesis. However, current progress in the research of calculating Greeks for multi-asset options was achieved in [Bianchetti et al., 2016]: they show that the difference quotient method is able to compete with adjoint algorithmic differentiation by using a high dimensional Quasi Monte Carlo method.

In order to find appropriate methods for a structured model, it has to be considered that (a) close form formulas may not be derivable for all claims and (b) the bid stack might contain jumps and may therefore not be continuous.

<sup>1</sup>In [Glassermann, 2003] weak conditions for this interchange are derived

## 6.2 Difference Quotient Method

The difference quotient method can be implemented straight forward but leads to higher computation times in general. The reason is that at least two valuations of the contingent claim have to be performed. In case of multi asset options however, [Bianchetti et al., 2016] has shown that the difference quotient can even compete with the fast adjoint algorithmic differentiation - at least if quasi Monte Carlo methods are applied. Fuel sensitivities of an arbitrary contingent claim

$$\frac{\partial}{\partial F_{t_0,t}^k} PV_t(\mathbf{F}) = \frac{\partial}{\partial F_{t_0,t}^k} \mathbb{E}^{\mathbb{Q}} [\Psi(\mathbf{S}_t^F(\mathbf{F}), \mathbf{S}_t^P(\mathbf{F})) | \mathcal{F}_{t_0}],$$

with  $k \in \{1, \dots, n\}$  are calculated by shifting  $F_{t_0,t}^k$  upwards and downwards as described in (6.5). Let us assume a structural electricity model where the power spot price depends on the fuels  $1, \dots, n$  and demand (i.e. the exponential bid stack with two marginal fuels). If we would not recalibrate the implied demand seasonality after performing a shift of the fuels, we would violate the chain rule (6.1) as illustrated in Example 6.1. The reason is that  $\frac{\partial s^D(t)}{\partial F_{t_0,t}^k}$  is part of (6.2) being not zero in general (cf. Appendix A.2 for an example of the forward price formula for the exponential bid stack with two marginal fuels as been described in Chapter 2.1).

**Remark 6.1 (Link to Hedging in Practice)** In [Morini, 2011], the above complexity of recalibration after shifts in market data was discussed in the context of the SABR model. Starting point is that a trader expects implied volatilities to move to the right after an upwards shift of the underlying. Thus, the right shift has to be captured by the SABR model as well. However, the typical negative correlation between prices and volatility leads the implied volatilities erroneously to shift to the left. Practitioners avoid that behavior by forcing the volatility of volatility to remain unchanged after a shift. At first, this might be a contradiction of model implications. However, it seems to be a common model adjustment in practice in order to get market movements right.

Translated to our case, it may at first sound natural for a structural electricity model that a shift in fuel forward prices leads to a shift in power forwards. However, we assume this only to hold for a non-liquid power forwards market. Otherwise, we perform step (3) and therefore include power forwards as hedging instruments. This is why we end up with two different hedging strategies depending on power forwards liquidity.

**Remark 6.2** There is another technical argument why the implied demand has to be recalculated after a fuel shift. As given by (6.5), the difference quotient method forces us to use a vector  $\mathbf{h}$  being zero for all components except one. However, if we did not recalibrate the implied demand after a fuel shift, the power forward price in our model would consequently change as well. The outcome would be a shift of the fuels forward as well as the power forward which would not be in line with the principal of the difference quotient method.

Consequently, the following steps are necessary to implement the difference quotient:

1. Upwards shift of the according fuel forward price,
2. recalibrate the fuel's drift,
3. recalibrate the implied demand seasonality,
4. calculate  $PV_t$ ,
5. perform the same for a downwards shift of the according fuel forward price,
6. calculate quotient (6.5).

In case step 3 is skipped, we would assume power forwards to be illiquid (cf. Remark 6.1). In Chapter 3.4, we have defined the power liquidity threshold date (Definition 3.6). In case of a high  $t_{PLTD}$  we perform a recalibration after a shift. In case of a low  $t_{PLTD}$ , we do not perform a recalibration.

## 6.3 Likelihood Ratio Method

In this Chapter we analyze the likelihood ratio method (cf. [Glassermann, 2003]) to calculate Greeks in a structural electricity model.

We assume a fuel process  $\mathbf{S}_t^F$  and a demand process  $D_t$  to fulfill the condition

$$\begin{pmatrix} \ln(\mathbf{S}_t^F) \\ D_t \end{pmatrix} := \begin{pmatrix} \ln(S_t^1) \\ \vdots \\ \ln(S_t^n) \\ D_t \end{pmatrix} \stackrel{\mathcal{D}}{=} \mathcal{N} \left( \begin{pmatrix} \mu_t^1 \\ \vdots \\ \mu_t^n \\ \mu_t^D \end{pmatrix}, \Sigma_t \right) =: \mathcal{N} \left( \begin{pmatrix} \mu_t^F \\ \mu_t^D \end{pmatrix}, \Sigma_t \right) \quad (6.6)$$

with  $|\Sigma_t| > 0 \forall t > t_0$ .

**Lemma 6.1** *For the Ornstein-Uhlenbeck model in Chapter 2.2 it holds*

$$\begin{aligned} \mu_t^i &= \ln(F_{t_0,t}^i) - \frac{1}{2} \int_{t_0}^t \left( v_s^{(i)} \right)^2 \exp \left( -2 \int_s^t \alpha_u^{(i)} du \right) ds \quad \forall i = 1, \dots, n, \\ \mu_t^D &= s^D(t) + \exp \left( - \int_{t_0}^t \alpha_s^D ds \right) d_{t_0}, \\ (\Sigma_t)_{i,j} &= \begin{cases} \rho_{ij} \int_{t_0}^t v_s^{(i)} v_s^{(j)} \exp \left( - \int_s^t \left( \alpha_u^{(i)} + \alpha_u^{(j)} \right) du \right) ds & \forall i, j = \{1, \dots, n\} \\ 0 & i = n+1 \text{ or } j = n+1. \end{cases} \end{aligned}$$

**Proof.** We know for the Ornstein-Uhlenbeck model in Chapter 2.2 (for arbitrary  $i = 1, \dots, n$ )

$$\begin{aligned} \mu_t^i &\stackrel{(2.4)}{=} s^{(i)}(t) + \mathbb{E}^{\mathbb{Q}} [X_t^i | \mathcal{F}_{t_0}] \stackrel{(2.9)}{=} \ln(F_{t_0,t}^i) - \frac{1}{2} \int_{t_0}^t \left( v_s^{(i)} \right)^2 \exp \left( -2 \int_s^t \alpha_u^{(i)} du \right) ds, \\ \mu_t^D &= s^D(t) + \mathbb{E}^{\mathbb{Q}} [X_t^i | \mathcal{F}_{t_0}] \stackrel{(2.8)}{=} s^D(t) + \exp \left( - \int_{t_0}^t \alpha_s^D ds \right) d \end{aligned}$$

being the first statement of the Lemma. The form of  $\Sigma$  is implied by the Itô-Isometry. ■

Let  $\phi_{n+1}^{f, \Sigma_t, \mu_t} : \mathbb{R}^{n+1} \rightarrow \mathbb{R}^+$  be the according normal density function for (6.6) with  $f$  being a parameter the density is depending on (i.e. a forward price). Let  $\Psi(\mathbf{S}_t^F, S_t^P) \in \mathcal{L}^1(\mathbb{Q})$  be a contingent claim. The following calculations are a special case of the calculations in [Glassermann, 2003]:

$$\begin{aligned}
\frac{\partial}{\partial f} \mathbb{E}_f^{\mathbb{Q}} [\Psi(\mathbf{S}_t^F, S_t^P) | \mathcal{F}_{t_0}] &= \frac{\partial}{\partial f} \mathbb{E}_f^{\mathbb{Q}} [\Psi(\mathbf{S}_t^F, f_{bs}(D_t, \mathbf{S}_t^F)) | \mathcal{F}_{t_0}] \\
&= \int_{-\infty}^{\infty} \cdots \int_{-\infty}^{\infty} \Psi(\exp(\mathbf{x}^F), f_{bs}(x^D, \exp(\mathbf{x}^F))) \frac{\partial}{\partial f} \phi^{f, \Sigma_t, \mu_t}(\mathbf{x}^F, x^D) d\mathbf{x}^F dx^D \\
&= \mathbb{E}_f^{\mathbb{Q}} \left[ \Psi(\mathbf{S}_t^F, S_t^P) \frac{\frac{\partial}{\partial f} \phi^{f, \Sigma_t, \mu_t}(\ln(\mathbf{S}_t^F), D_t)}{\phi^{f, \Sigma_t, \mu_t}(\ln(\mathbf{S}_t^F), D_t)} \middle| \mathcal{F}_{t_0} \right] \\
&= \mathbb{E}_f^{\mathbb{Q}} \left[ \Psi(\mathbf{S}_t^F, S_t^P) \underbrace{\frac{d}{df} \ln(\phi^{f, \Sigma_t, \mu_t}(\ln(\mathbf{S}_t^F), D_t))}_{\text{defined as the score in [Glassermann, 2003]}} \middle| \mathcal{F}_{t_0} \right]
\end{aligned}$$

So far we have assumed that

A1 integration and differentiation can be interchanged (Lemma 6.1) and

A2 the bid stack  $f_{bs}$  itself does not depend on the parameter  $f$ .<sup>2</sup>

In order to calculate the score we use condition (6.6). The density function is given by

$$\begin{aligned}
\phi^{\Sigma_t, \mu_t}(\ln(\mathbf{S}_t^F), D_t) &= \frac{1}{\sqrt{(2\pi)^{n+1} |\Sigma_t|}} \exp \left( -\frac{1}{2} \cdot \right. \\
&\quad \left. ((\ln(\mathbf{S}_t^F) - \mu_t^F)^T, D_t - \mu_t^D) \Sigma_t^{-1} (\ln(\mathbf{S}_t^F) - \mu_t^F, D_t - \mu_t^D)^T \right).
\end{aligned} \tag{6.7}$$

Therefore, in case the parameter  $f$  is only located in the drift, the score can be calculated by (cf. [Glassermann, 2003])

$$\begin{aligned}
\frac{d}{df} \ln(\phi^{f, \Sigma_t, \mu_t}(\ln(\mathbf{S}_t^F), D_t)) &= ((\ln(\mathbf{S}_t^F) - \mu_t^F)^T, D_t - \mu_t^D) \Sigma_t^{-1} \begin{pmatrix} \dot{\mu}_t^F(f) \\ \dot{\mu}_t^D(f) \end{pmatrix} \\
&\stackrel{\mathcal{Q}}{=} \mathbf{Z}^T \mathbf{G}_t^{-1} \begin{pmatrix} \dot{\mu}_t^F(f) \\ \dot{\mu}_t^D(f) \end{pmatrix},
\end{aligned} \tag{6.8}$$

where  $\mathbf{Z}^T \stackrel{\mathcal{Q}}{=} (N(0, 1))^{n+1}$ ,  $\Sigma_t = \mathbf{G}_t \mathbf{G}_t^T$  being a Cholesky decomposition and  $\dot{\mu} := \frac{\partial \mu}{\partial f}$ . The last transformation holds in distribution by applying the relation

$$\begin{pmatrix} \ln(\mathbf{S}_t^F) \\ D_t \end{pmatrix} \stackrel{\mathcal{Q}}{=} \begin{pmatrix} \mu^F(f) \\ \mu^D(f) \end{pmatrix} + \mathbf{G}_t \mathbf{Z}. \tag{6.9}$$

So far, the result are still a special case of the calculations in [Glassermann, 2003].

<sup>2</sup>As long as we estimate the Bid Stack parameters  $k_i, m_i$  in (2.2) from a historical data set, the restriction will always be fulfilled.

### 6.3.1 Forward Deltas in a Framework with Historical Volatilities

The results above are used to calculate forward deltas in a framework with historical volatilities. In this case equation (6.1) becomes for  $f = F_{t_j}^i$

$$\frac{\partial}{\partial F_{t_j}^i} PV_t = \sum_{k=1}^n \frac{\partial PV_t}{\partial \mu_t^k} \frac{\partial \mu_t^k}{\partial F_{t_j}^i} + \frac{\partial PV_t}{\partial \mu_t^D} \frac{\partial \mu_t^D}{\partial F_{t_j}^i} + \sum_{k=1}^n \underbrace{\frac{\partial PV_t}{\partial \sigma_t^k} \frac{\partial \sigma_t^k}{\partial F_{t_j}^i}}_{=0, hist.} + \underbrace{\frac{\partial PV_t}{\partial \sigma_t^D} \frac{\partial \sigma_t^D}{\partial F_{t_j}^i}}_{=0, hist.}.$$

From our prior calculations we can allocate the terms as follows:

$$\begin{aligned} \frac{\partial PV_t}{\partial \mu_t^k} \frac{\partial \mu_t^k}{\partial F_{t_j}^i} &= \mathbb{E}_f^{\mathbb{Q}} [\Psi(\mathbf{S}_t^F, \mathbf{S}_t^P) (\mathbf{Z}^T \mathbf{G}_t^{-1})_k (\dot{\mu}_t^F(f))_k \mid \mathcal{F}_{t_0}] & k = 1, \dots, n \\ \frac{\partial PV_t}{\partial \mu_t^D} \frac{\partial \mu_t^D}{\partial F_{t_j}^i} &= \mathbb{E}_f^{\mathbb{Q}} [\Psi(\mathbf{S}_t^F, \mathbf{S}_t^P) (\mathbf{Z}^T \mathbf{G}_t^{-1})_D \dot{\mu}_t^D(f) \mid \mathcal{F}_{t_0}]. \end{aligned}$$

Before we proceed to derive the score for our Ornstein-Uhlenbeck model in Chapter 2.2 (Proposition 6.2), we proof that the model allows to apply the likelihood ratio method for lipschitz-continuous contingent claims (Interchange of Differentiation and Integration). For the proof we need the next Lemma which shows that for the model in Chapter 2.2  $\frac{\partial}{\partial F_{t_0,t}^P} \mu_t^D$  and  $\frac{\partial}{\partial F_{t_0,t}^i} \mu_t^D$  can be calculated by building the according derivative of the implied demand seasonality (Definition 2.1).

**Lemma 6.2 (Derivatives of the Implied Demand Seasonality)** *Under the model in Chapter 2, the derivatives of the implied demand seasonality  $s^D(t)$  in direction of the hedging instruments (Definition 1.2) are given by*

$$\begin{aligned} \frac{\partial}{\partial F_{t_0,t}^P} s^D(t) &= \frac{\partial}{\partial F_{t_0,t}^P} \mu_t^D = \begin{cases} \left[ \frac{\partial}{\partial \mu_t^D} F_{bs} \right]^{-1} & \text{if } t < t_{PLDT} \\ 0 & \text{else} \end{cases} \\ \frac{\partial}{\partial F_{t_0,t}^i} s^D(t) &= \frac{\partial}{\partial F_{t_0,t}^i} \mu_t^D = \begin{cases} - \left[ \frac{\partial}{\partial \mu_t^D} F_{bs} \right]^{-1} \frac{\partial}{\partial F_{t_0,t}^i} F_{bs} & \text{if } t < t_{FLTD}(i), i \in I \\ 0 & \text{else,} \end{cases} \end{aligned}$$

where  $F_{bs} := F_{bs}(t, F_{t,T}^{(1)}, \dots, F_{t,T}^{(n)}, \mu_t^D)$  represents the close form formula for the power forward price given in Appendix A.3. The derivatives are well defined, i.e.  $\frac{\partial}{\partial \mu_t^D} F_{bs} \neq 0$ .

**Proof.** The derivatives are well-defined due to Lemma A.1 which proves strong monotony of the electricity forward price formula  $F_{bs}$  in direction of  $\mu_t^D$ .

We use Lemma 6.1

$$\mu_t^D = s^D(t) + \exp \left( - \int_{t_0}^t \alpha_s^D ds \right) d_{t_0}$$

to calculate  $\frac{\partial}{\partial F_{t_0,t}^P} \mu_t^D(t)$  and  $\frac{\partial}{\partial F_{t_0,t}^i} \mu_t^D(t)$ . It turns out that the equivalent problem is to calculate the derivative of the implied demand seasonality in direction of a hedging instrument. The implied demand

seasonality for a certain  $t \geq t_0$  is implicitly given by the inverse of the electricity forward price  $F_{bs}^{-1}$  (Definition 2.1). However, the inverse of  $F_{bs}$  cannot be derived explicitly.

Instead, the derivative in direction of the power forward contract is for  $t < t_{PLTD}$  directly given by the inverse function theorem and zero otherwise (no dependence on any forward price). In terms of fuel forward contracts the derivative is given by the implicit function theorem (cf. [Forster, 2011]) if  $t < t_{FLTD}$  and zero otherwise. In order to apply the implicit function theorem, we use

$$F_{t_0,t}^P - F_{bs}(t, F_{t_0,t}^{(1)}, \dots, F_{t_0,t}^{(n)}, \mu_t^D) = 0.$$

We interpret  $\mu_t^D$  as a function of the fuel forwards, electricity forward and time  $t$ , yielding the implicit function to become  $\mu_t^D = g(t, F_{t,T}^{(1)}, \dots, F_{t,T}^{(n)}, F_{t,T}^P)$  (cf. Chapter 3). We build the derivative to get the assertion. ■

**Proposition 6.1 (Interchange of Differentiation and Integration)** *Let the exponential bid stack with two marginal fuels in Chapter 2.1 and stochastic processes for the fuels and demand in Chapter 2.2 together with forwards data in Definition 1.2 be given ( $\mathbf{F}$  denotes a vector containing all forward prices for power, gas and coal). We assume the model parameters except seasonality to be derived retrospectively using historical data (Chapter 4).*

*Then, it holds for an arbitrary hourly forward  $f$  of Definition 1.2*

$$\frac{\partial}{\partial f} \mathbb{E}^{\mathbb{Q}} [\Psi(\mathbf{S}_t^F(\mathbf{F}), S_t^P(\mathbf{F})) | \mathcal{F}_{t_0}] = \mathbb{E}^{\mathbb{Q}} \left[ \frac{\partial}{\partial f} \Psi(\mathbf{S}_t^F(\mathbf{F}), S_t^P(\mathbf{F})) \middle| \mathcal{F}_{t_0} \right]$$

*for a contingent claim  $\Psi$  being lipschitz continuous on  $(\mathbb{R}^+)^2 \times \mathbb{R}$  and  $t \in \mathcal{T}$ .*

**Proof.** We proof the interchange by verifying the requirements in [Glassermann, 2003] (see Appendix C.1). Let  $f$  be an arbitrary hourly forward of Definition 1.2.

Requirement A1(differentiable of spot prices with probability 1):  $S_t^{(i)}$  is given by (2.5). Thus,  $\frac{\partial}{\partial F_{t_0,T}^P} S_t^{(i)} = 0$  for  $i = 1, \dots, n$  as fuels' drift does not depend on power forward prices and model parameters are derived retrospectively using historical data. Furthermore,

$$\frac{\partial}{\partial F_{t_0,T}^{(i)}} S_t^{(i)} \stackrel{(2.5)}{=} S_t^{(i)} \frac{\partial s^{(i)}(t)}{\partial F_{t_0,T}^{(i)}} \stackrel{(2.9)}{=} \begin{cases} \frac{S_t^{(i)}}{F_{t_0,T}^{(i)}}, & \text{for } t = T \\ 0, & \text{else} \end{cases}$$

for  $i = 1, \dots, n$  which exists for positive  $F_{t_0,T}^{(i)}$ . Therefore, the fuels are differentiable in  $f$  with probability 1. Additionally, we have to proof

$$\frac{\partial}{\partial f} S_t^P = \begin{cases} \frac{\partial f_{bs}}{\partial D_t} \frac{\partial D_t}{\partial F_{t_0,T}^P} & , \text{ if } f = F_{t_0,t_1}^P, \dots, F_{t_0,t_m}^P \text{ and } t = T \\ \frac{\partial f_{bs}}{\partial S_t^{(i)}} \frac{\partial S_t^{(i)}}{\partial F_{t_0,T}^{(i)}} + \frac{\partial f_{bs}}{\partial D_t} \frac{\partial D_t}{\partial F_{t_0,T}^{(i)}} & , \text{ if } f = F_{t_0,t_1}^i, \dots, F_{t_0,t_m}^i \text{ (} i \in I \text{) and } t = T \\ 0 & \text{else} \end{cases}$$

to exist with probability 1. We start to show the bid stack function to be differentiable almost everywhere.

Due to Proposition A.2,  $b_{low}, b_{mid}, b_{high}$  of  $f_{bs}$  (cf. Appendix A.1) are lipschitz continuous on compact sets  $[0, \bar{\xi}^{i-}] \times [a, b]^2$ ,  $[\bar{\xi}^{i-}, \bar{\xi}^{i+}] \times [a, b]^2$  and  $[\bar{\xi}^{i+}, \bar{\xi}] \times [a, b]^2$  respectively for  $[a, b] \subset \mathbb{R}^+$  arbitrary but fix. Using the Rademacher's Theorem  $b_{low}, b_{mid}, b_{high}$  are differentiable almost everywhere on those sets. Because the transitions between  $b_{low}, b_{mid}, b_{high}, b_N, b_S$  are a zero set in  $\mathbb{R}^3$ , we get  $\bar{\Psi}$  to be differentiable almost everywhere on  $[0, \bar{\xi}] \times [a, b]^2$ . Because  $b_{low}, b_{mid}, b_{high}$  consist of exponential functions  $b_c, b_g, b_{cg}$  being differentiable almost everywhere, we can expand  $[a, b]$  to  $\mathbb{R}^+$  (transitions between  $b_{low}, b_{mid}, b_{high}, b_N, b_S$  remain to be a zero set in  $\mathbb{R}^3$ ).

Furthermore,  $b_N, b_S$  are differentiable on their definition intervals  $(-\infty, 0]$  and  $[\bar{\xi}, \infty)$  which is why  $f_{bs}$  is differentiable with probability 1 on  $(\mathbb{R}^+)^2 \times \mathbb{R}$ .

For the demand it holds  $\frac{\partial}{\partial f} D_t \stackrel{(2.6)}{=} \frac{\partial s^D(t)}{\partial f}$ . Lemma 6.2 ensures the derivative to be well-defined (existence).

Bringing all insights together, the power spot price is differentiable in  $f$  with probability 1. We denote the null set (where the power spot price is not differentiable) by  $N_{BS}$ .

Requirement A2 (spot prices act where  $\Psi$  is defined):  $\Psi$  is differentiable almost everywhere by condition (Rademacher's Theorem) leading to  $\mathbb{P}((S_t^F, S_t^P) \in D_\Psi) = \mathbb{P}((S_t^F, S_t^P) \in (\mathbb{R}^+)^2 \times \mathbb{R}) = 1$ .

Requirement A3 ( $\Psi$  lipschitz-continuous): Given by condition of the Lemma.

Requirement A4 (local lipschitz condition for spot prices): We have to show the lipschitz condition for the fuels and demand for arbitrary  $\omega \in \Omega$ . We get a random variable  $\kappa_\omega$  which has to fulfill  $\mathbb{E}[\kappa_\omega] < \infty$ . We define  $\Theta \subset (\mathbb{R}^+)^{2m} \times \mathbb{R}^m$  to be a compact set with  $\mathbf{F} \in \Theta$ . Let  $\mathbf{f}_1, \mathbf{f}_2 \in \Theta$  arbitrary but fix. We define

$$\mathbf{f}_1 := (f_1^1, \dots, f_1^{3m})^T, \mathbf{f}_2 := (f_2^1, \dots, f_2^{3m})^T$$

and get for  $t \in \mathcal{T}$  ( $t = t_j, j = 1, \dots, m$ ),  $i \in \{1, 2\}$  and  $\omega \in \Omega$

$$\begin{aligned} & \left| f_2^{(i-1)m+j} - f_1^{(i-1)m+j} \right| \underbrace{\exp \left( -\frac{1}{2} \mathbb{V}^Q [X_t^i | \mathcal{F}_{t_0}] + \int_{t_0}^t v_s^{(i)} \exp \left( -\int_s^t \alpha_u^{(i)} du \right) dW_s^{(i)} \right)}_{=: \kappa_{i,\omega}} \stackrel{(2.5) \& (2.9)}{=} \left| S_t^{(i)}(\mathbf{f}_2) - S_t^{(i)}(\mathbf{f}_1) \right| \\ & = \kappa_{i,\omega} \left| f_2^{(i-1)m+j} - f_1^{(i-1)m+j} \right| \leq \kappa_{i,\omega} \|\mathbf{f}_2 - \mathbf{f}_1\|_1 \end{aligned}$$

and  $\mathbb{E}[\kappa_{i,\omega}] = 1 < \infty$ .

Accordingly, we get for power (using the non-differentiability of  $f_{bs}$  on  $N_{BS}$  derived in Requirement A2)

$$\begin{aligned} & \left| S_t^P(\mathbf{f}_2) - S_t^P(\mathbf{f}_1) \right|^2 = \left| f_{bs}(D_t(\mathbf{f}_2), \mathbf{S}_t^F(\mathbf{f}_2)) - f_{bs}(D_t(\mathbf{f}_1), \mathbf{S}_t^F(\mathbf{f}_1)) \right|^2 \\ & \leq \underbrace{\sup_{d, \mathbf{s} \in \{d, \mathbf{s}: d := D_t(\mathbf{f}), \mathbf{s} := \mathbf{S}_t^F(\mathbf{f}), \mathbf{f} \in \Theta \setminus \{f_{bs}(D_t(\mathbf{f}), \mathbf{S}_t^F(\mathbf{f})) \in N_{BS}\}} \left\{ \|Df_{bs}(d, \mathbf{s})\|_\infty^2 \right\}}_{=: \kappa_{BS,\omega}^2} \left\| \begin{pmatrix} D_t(\mathbf{f}_2) - D_t(\mathbf{f}_1) \\ \mathbf{S}_t^F(\mathbf{f}_2) - \mathbf{S}_t^F(\mathbf{f}_1) \end{pmatrix} \right\|^2 \\ & \leq \kappa_{BS,\omega}^2 (\kappa_{1,\omega}^2 + \kappa_{2,\omega}^2 + \kappa_D^2) \|\mathbf{f}_2 - \mathbf{f}_1\|_1^2 \end{aligned}$$



where  $Df_{bs}(d, \mathbf{s})$  denotes the Jacobi matrix. Furthermore, we get

$$\begin{aligned} |D_t(\mathbf{f}_2) - D_t(\mathbf{f}_1)| &\stackrel{(2.6)}{=} \left| s_I^D(t_j; f_2^j, f_2^{m+j}, f_2^{2m+j}) - s_I^D(t_j; f_1^j, f_1^{m+j}, f_1^{2m+j}) \right| \\ &\leq \underbrace{\sup_{\mathbf{f} \in \Theta, t \in \mathcal{T}, k=1, \dots, 3m} \left\{ \left| \frac{\partial s_I^D(t; f^j, f^{m+j}, f^{2m+j})}{\partial f_k} \right| \right\}}_{=: \kappa_D} \|\mathbf{f}_2 - \mathbf{f}_1\|_1. \end{aligned}$$

We remind  $\kappa_D$  to be independent of  $\omega$  and smaller than infinity on a compact set due to Lemma 6.2. It remains to proof

$$\mathbb{E} \left[ \kappa_{BS, \omega} \sqrt{\kappa_{1, \omega}^2 + \kappa_{2, \omega}^2 + \kappa_D^2} \right] < \infty.$$

Following the notation of the spot formula in Appendix A.1,  $b_{low}$ ,  $b_{mid}$ ,  $b_{high}$ ,  $b_N$ ,  $b_S$  are a sum of exponential functions of order

$$\mathcal{O} \left( (S_t^{(c)})^{\alpha_c} (S_t^{(g)})^{\alpha_g} \exp(\gamma D_t), S_t^{(c)} \exp(m_c D_t), S_t^{(g)} \exp(m_g D_t), \exp(-m_N D_t), \exp(m_S D_t) \right)$$

being integrable for lognormally distributed fuels and normally distributed demand. Therefore,  $\kappa_{BS, \omega} = \sup\{\|Df_{bs}\|\}$  is integrable over  $\omega$ . Consequently,  $\kappa_{BS, \omega}^2 \kappa_{i, \omega}^2$  ( $i \in I$ ) is of order

$$\begin{aligned} \mathcal{O} \left( (S_t^{(c)})^{\alpha_c} (S_t^{(g)})^{\alpha_g} \exp(\gamma D_t), S_t^{(c)} \exp(m_c D_t), S_t^{(g)} \exp(m_g D_t), \exp(-m_N D_t), \exp(m_S D_t) \right) \\ \cdot \exp \left( \int_{t_0}^t \mathbf{v}_s^{(i)} \exp \left( - \int_s^t \alpha_u^{(i)} du \right) dW_s^{(i)} \right) \end{aligned}$$

which is altogether merely increasing the fuel's moment by one. Therefore, we end up with

$$\mathbb{E} \left[ \kappa_{BS, \omega} \sqrt{\kappa_{1, \omega}^2 + \kappa_{2, \omega}^2 + \kappa_D^2} \right] < \infty.$$

■

**Proposition 6.2 (Forward Delta Calculation)** *Let the Ornstein-Uhlenbeck model in Chapter 2.2 be given together with an arbitrary market bid stack  $f_{bs}(D_t, \mathbf{S}_t^F)$  defined by (2.1) and a set of calibration instruments given by Definition 1.2. We assume the bid stack parameters of  $f_{bs}$  not to be dependent on the calibration instruments.*

*Then, for a given contingent claim  $\Psi(\mathbf{S}_t^F, S_t^P)$  ( $t \in \mathcal{T}$ ) the score of a certain fuel forward  $F_{t_0, T}^i$  ( $i \in I$  and  $T \in \mathcal{T}$  arbitrary but fix) is given by*

$$\text{Score} \left( \frac{\partial}{\partial F_{t_0, T}^i} \right) = \begin{cases} \frac{1}{F_{t_0, T}^i} (\mathbf{Z}^T \mathbf{G}_t^{-1})_i + (\mathbf{Z}^T \mathbf{G}_t^{-1})_{n+1} \frac{\partial}{\partial F_{t_0, T}^i} s^D(T) & \text{if } T = t \\ 0 & \text{if } t \in \mathcal{T} \setminus \{T\}. \end{cases} \quad (6.10)$$

*In terms of the power forward Delta it holds*

$$\text{Score} \left( \frac{\partial}{\partial F_{t_0, T}^P} \right) = \begin{cases} (\mathbf{Z}^T \mathbf{G}_t^{-1})_{n+1} \frac{\partial}{\partial F_{t_0, T}^P} s^D(T) & \text{if } T = t \\ 0 & \text{if } t \in \mathcal{T} \setminus \{T\}. \end{cases} \quad (6.11)$$



**Proof.** We have to calculate (6.8) under the Ornstein- Uhlenbeck model in Chapter 2.2. Assumption A1 is fulfilled due to Proposition 6.1 and Assumption A2 is fulfilled by condition.

In terms of the fuels it holds due to Lemma 6.1 for  $i, j \in I$  :

$$\begin{aligned} \frac{\partial}{\partial F_{t_0, T}^i} \mu_t^j &= \frac{\partial}{\partial F_{t_0, T}^i} \left( \ln(F_t^j) - \frac{1}{2} \int_{t_0}^t (v_s^{(j)})^2 \exp \left( -2 \int_s^t \alpha_u^{(j)} du \right) ds \right) \\ &= \begin{cases} \frac{1}{F_{t_0, T}^i} & \text{if } i = j \text{ and } T = t \\ 0 & \text{else.} \end{cases} \end{aligned}$$

In terms of power it holds (because no power data is used to calibrate the mean of the log fuel prices; Lemma 6.1)

$$\frac{\partial}{\partial F_{t_0, T}^P} \mu_t^j = 0.$$

In order to calculate the derivative of  $\mu_D$  we have to calculate the derivative of the implied demand. For  $i \in I \cup \{P\}$ , it holds due to Lemma 6.1

$$\frac{\partial}{\partial F_{t_0, T}^i} \mu_D = \begin{cases} \frac{\partial}{\partial F_{t_0, T}^i} s^D(t) & \text{if } T = t \\ 0 & \text{else} \end{cases}$$

Inserting both derivatives into (6.8) yields the result. ■

**Remark 6.3 (Interpolation)** *The above proposition only holds for claims  $\Psi(\mathbf{S}_t^F, S_t^P)$  with  $t \in \mathcal{T}$ . Theoretically, if  $t \notin \mathcal{T}$  interpolation will have to be considered as well. However, when working with daily or hourly forward curves the effect tends to be small.*

### 6.3.2 Forward Gamma in a Framework with Historical Volatilities

Similar steps have been performed in order to calculate the second derivative (gamma) in direction of the fuel forward and power forward prices.

We start with the derivation of the likelihood ratio score. We still assume that merely the mean depends on  $f$ . It leads to

$$\frac{\partial^2}{\partial f^2} \mathbb{E}_f^{\mathbb{Q}} [\Psi(\mathbf{S}_t^F, S_t^P) | \mathcal{F}_{t_0}] = \mathbb{E}_f^{\mathbb{Q}} \left[ \Psi(\mathbf{S}_t^F, S_t^P) \frac{\frac{\partial^2}{\partial f^2} \phi^{f, \Sigma_t, \mu_t}(\ln(\mathbf{S}_t^F), D_t)}{\phi^{f, \Sigma_t, \mu_t}(\ln(\mathbf{S}_t^F), D_t)} \middle| \mathcal{F}_{t_0} \right].$$

Therefore, by taking the derivative, the scope has the form (cf. [Glassermann, 2003])

$$\begin{aligned} \frac{\frac{\partial^2}{\partial f^2} \phi^{f, \Sigma_t, \mu_t}(\ln(\mathbf{S}_t^F), D_t)}{\phi^{f, \Sigma_t, \mu_t}(\ln(\mathbf{S}_t^F), D_t)} &= \left( (\ln(\mathbf{S}_t^F) - \mu_t^F, D_t - \mu_t^D) \Sigma_t^{-1} \begin{pmatrix} \dot{\mu}_t^F(f) \\ \dot{\mu}_t^D(f) \end{pmatrix} \right)^2 \\ &\quad - (\dot{\mu}_t^F(f), \dot{\mu}_t^D(f)) \Sigma_t^{-1} \begin{pmatrix} \dot{\mu}_t^F(f) \\ \dot{\mu}_t^D(f) \end{pmatrix} \end{aligned}$$

$$\begin{aligned}
& + (\ln(\mathbf{S}_t^F) - \mu_t^F, D_t - \mu_t^D) \Sigma_t^{-1} \begin{pmatrix} \ddot{\mu}_t^F(f) \\ \ddot{\mu}_t^D(f) \end{pmatrix} \\
& \stackrel{\mathcal{Q}}{=} \left( \mathbf{Z}^T \mathbf{G}_t^{-1} \begin{pmatrix} \dot{\mu}_t^F(f) \\ \dot{\mu}_t^D(f) \end{pmatrix} \right)^2 - (\dot{\mu}_t^F(f), \dot{\mu}_t^D(f)) \Sigma_t^{-1} \begin{pmatrix} \dot{\mu}_t^F(f) \\ \dot{\mu}_t^D(f) \end{pmatrix} + \mathbf{Z}^T \mathbf{G}_t^{-1} \begin{pmatrix} \dot{\mu}_t^F(f) \\ \dot{\mu}_t^D(f) \end{pmatrix}
\end{aligned} \quad (6.12)$$

As it was done in the Chapter about the delta, the results above can be used to calculate forward gammas in a framework with historical volatilities.

**Proposition 6.3 (Forward Gamma Calculation)** *Let the Ornstein-Uhlenbeck model in Chapter 2.2 be given together with an arbitrary market bid stack  $f_{bs}(D_t, \mathbf{S}_t^F)$  defined by (2.1) and a set of calibration instruments given by Definition 1.2.*

*Then, for a given contingent claim  $\Psi(\mathbf{S}_t^F, S_t^P)$  ( $t \in \mathcal{T}$ ) the gamma score of a certain fuel forward  $F_{t_0, T}^i$  ( $i \in I$  and  $T \in \mathcal{T}$  arbitrary but fix) is given by*

$$\text{Score} \left( \frac{\partial^2}{\partial (F_{t_0, T}^i)^2} \right) = \begin{cases} \left( \frac{1}{F_{t_0, T}^i} (\mathbf{Z}^T \mathbf{G}_t^{-1})_i + (\mathbf{Z}^T \mathbf{G}_t^{-1})_{n+1} \frac{\partial}{\partial F_{t_0, T}^i} s^D(T) \right)^2 - \frac{(\Sigma_t^{-1})_{ii}}{(F_{t_0, T}^i)^2} - \left( \frac{\partial}{\partial F_{t_0, T}^i} s^D(T) \right)^2 (\Sigma_t^{-1})_{n+1, n+1} - & \text{if } T = t \\ \frac{(\mathbf{Z}^T \mathbf{G}_t^{-1})_i}{(F_{t_0, T}^i)^2} + (\mathbf{Z}^T \mathbf{G}_t^{-1})_{n+1} \frac{\partial^2}{\partial (F_{t_0, T}^i)^2} s^D(T) & \\ 0 & \text{if } t \in \mathcal{T} \setminus \{T\}. \end{cases} \quad (6.13)$$

In terms of the power forward gamma it holds

$$\text{Score} \left( \frac{\partial^2}{\partial (F_{t_0, T}^P)^2} \right) = \begin{cases} \left( (\mathbf{Z}^T \mathbf{G}_t^{-1})_{n+1} \frac{\partial}{\partial F_{t_0, T}^P} s^D(T) \right)^2 - \left( \frac{\partial}{\partial F_{t_0, T}^P} s^D(T) \right)^2 (\Sigma_t^{-1})_{n+1, n+1} + & \text{if } T = t \\ (\mathbf{Z}^T \mathbf{G}_t^{-1})_{n+1} \frac{\partial^2}{\partial (F_{t_0, T}^P)^2} s^D(T) & \\ 0 & \text{if } t \in \mathcal{T} \setminus \{T\}. \end{cases} \quad (6.14)$$

**Proof.** We have to calculate (6.12). First order derivatives have already been calculated in Proposition 6.2. Therefore, only  $\mathbf{Z}^T \mathbf{G}_t^{-1} \begin{pmatrix} \ddot{\mu}_t^F(f) \\ \ddot{\mu}_t^D(f) \end{pmatrix}$  still remains to be calculated:

$$\begin{aligned}
\frac{\partial^2}{\partial^2 F_{t_0, T}^i} \mu_t^j &= \begin{cases} -\frac{1}{(F_{t_0, T}^i)^2} & \text{if } i = j \text{ and } T = t \\ 0 & \text{else.} \end{cases} \\
\frac{\partial^2}{\partial^2 F_{t_0, T}^P} \mu_t^j &= 0 \\
\frac{\partial^2}{\partial^2 F_{t_0, T}^i} \mu_D &= \begin{cases} \frac{\partial^2}{\partial^2 F_{t_0, T}^i} s^D(t) & \text{if } T = t \\ 0 & \text{else} \end{cases}
\end{aligned}$$

By Inserting everything into (6.12) and being aware that correlation between demand and fuels processes is zero by assumption, we get the result.

■

**Remark 6.4 (Calculation of the Second Derivative)** *Because the first derivative in direction of  $F_{t_0,t}^i$  and  $\mu_t^D$  respectively are already a sum of more than 10 terms, we set the analytical calculation of the second derivative aside. Instead, we used the difference quotient as an approximation in our numerical evaluation (cf. Chapter 6.5).*

### 6.3.3 Vega Calculation

Whereas we propose to use forward contracts to hedge against the payoff of our contingent claim  $\Psi(S_t^F, S_t^P)$  (due at maturity  $T > t_0$ ), we have to use other kind of derivatives  $O_1, \dots, O_K$  (i.e. options) to hedge against volatility changes during the lifetime of the contract. Instead of historical estimation of model parameters (cf. Chapter 4),  $O_1, \dots, O_K$  may be used to calibrate the model volatility against observable option prices. We are less interested in  $\frac{\partial PV_t}{\partial O_i}$  but instead in  $\frac{\partial PV_t}{\partial v}$  for  $v = v_t^{(i)}$   $i = 1, \dots, n, D$  (model volatility, cf. Chapter 2).

Again, we start with a model fulfilling the (log-) normal condition (6.6). We derive how to calculate the parameter sensitivity  $\frac{\partial PV_t}{\partial v}$  for the likelihood ratio method when  $\Sigma_t$  and  $\mu_t$  being dependent on model parameters  $v \in \{v_t^{(1)}, \dots, v_t^{(n)}, v_t^D\}$ . The derivation is similar to [Glassermann, 2003].

In a first step, we calculate the vega score when merely the covariance matrix depends a model volatility  $v$ . We use the lognormal condition in (6.6) together with its Cholesky representation in (6.9) to show the vega score to be

$$\frac{d}{dv} \ln [\phi^{v, \Sigma_t, \mu_t}(\ln(S_t^F), D_t)] = \frac{d}{dv} \ln \left[ \frac{1}{\sqrt{(2\pi)^{n+1} |\Sigma_t|}} \exp \left( -\frac{1}{2} \cdot \right. \right. \quad (6.15)$$

$$\left. \left( \ln(S_t^F) - \mu_t^F, D_t - \mu_t^D \right) \Sigma_t^{-1} \left( \ln(S_t^F) - \mu_t^F, D_t - \mu_t^D \right)^T \right] \quad (6.16)$$

$$\begin{aligned} &= -\frac{1}{2} \frac{\frac{\partial}{\partial v} |\Sigma_t(v)|}{|\Sigma_t(v)|} - \frac{1}{2} \mathbf{Z}^T \mathbf{G}_t^T \frac{\partial}{\partial v} \Sigma_t^{-1} \mathbf{G}_t \mathbf{Z} \\ &= -\frac{1}{2} \text{tr} \left( \Sigma_t^{-1}(v) \frac{\partial}{\partial v} \Sigma_t(v) \right) + \frac{1}{2} \mathbf{Z}^T \mathbf{G}_t^{-1} \frac{\partial}{\partial v} \Sigma_t(v) \mathbf{G}_t^{-T} \mathbf{Z}, \end{aligned} \quad (6.17)$$

where  $\text{tr}(\cdot)$  denotes the trace of a matrix. For the second sum we used the relation  $0 = \frac{\partial}{\partial v} (\Sigma_t \Sigma_t^{-1}) = \frac{\partial \Sigma_t}{\partial v} \Sigma_t^{-1} + \Sigma_t \frac{\partial \Sigma_t^{-1}}{\partial v}$ .

However, the result cannot already be applied for our setup because the seasonalities  $s^{(1)}(t), \dots, s^{(n)}(t), s^D(t)$  depend on model volatility as well (cf. (2.9) and Definition 2.1). Using equation (6.1) yields

$$\frac{\partial}{\partial \sigma_t^i} PV_t = \sum_{k=1}^n \frac{\partial PV_t}{\partial \mu_t^k} \frac{\partial \mu_t^k}{\partial \sigma_t^i} + \frac{\partial PV_t}{\partial \mu_t^D} \frac{\partial \mu_t^D}{\partial \sigma_t^i} + \sum_{k=1}^n \frac{\partial PV_t}{\partial \sigma_t^k} \frac{\partial \sigma_t^k}{\partial \sigma_t^i} + \frac{\partial PV_t}{\partial \sigma_t^D} \frac{\partial \sigma_t^D}{\partial \sigma_t^i}$$

implying that we have to consider not only the covariance matrix  $\Sigma_t$  to be dependent on  $\sigma_t^i$  but also the drift  $\mu_t^F$  and  $\mu_t^D$ . Altogether, this leads to Proposition 6.4. At first, Lemma 6.3 simplifies the score under the assumptions of the structural electricity model in Chapter 2 further.

**Definition 6.1 (Definition of  $\beta_t^{i,j,a}(\mathbf{v})$ )** Let the structural electricity model in Chapter 2 be given. Referring to condition (2.11), it exists for an arbitrary  $\tau \in [t_0, t]$  ( $t > t_0 \geq 0$ ) an index  $a \in \{1, \dots, d(t)\}$  such that  $\tau \in (t_{a-1}, t_a]$ . We define

$$\beta_t^{i,j,a}(\mathbf{v}) := \frac{\nu \rho_{ij}}{\alpha^{i,j,a}} \exp \left( - \sum_{m=a+1}^{d(t)} \alpha^{i,j,m} \Delta t_m \right) [1 - \exp(-\alpha^{i,j,a} \Delta t_a)],$$

where  $\alpha^{i,j,m} := \alpha^{i,m} + \alpha^{j,m}$ ,  $\Delta t_m := t_m - t_{m-1}$ .

**Lemma 6.3** Let the structural electricity model in Chapter 2 be given with constant volatilities  $\mathbf{v}_t^{(i)} \equiv \mathbf{v}^{(i)} > 0$  and  $\mathbf{v}_t^D \equiv \mathbf{v}^D > 0$ . We use the Definition of  $\beta_t^{i,j,a}(\mathbf{v})$  in Definition 6.1. Then, it holds for  $i, j = 1, \dots, n+1$  and  $k = (1), \dots, (n), P$

$$\frac{\partial}{\partial \mathbf{v}^k} (\Sigma_t)_{i,j} = \begin{cases} \sum_{l=1}^{d(t)} \beta_t^{i,j,l}(\mathbf{v}^i) & k = j \\ \sum_{l=1}^{d(t)} \beta_t^{i,j,l}(\mathbf{v}^j) & k = i \\ 2 \sum_{l=1}^{d(t)} \beta_t^{i,j,l}(\mathbf{v}^k) & k = j = i \\ 0 & \text{else,} \end{cases}$$

$$\text{tr} \left( \Sigma_t^{-1} \frac{\partial}{\partial \mathbf{v}^k} \Sigma_t \right) = 2 \sum_{i=1}^{n+1} (\Sigma_t^{-1})_{i,k} \sum_{l=1}^{d(t)} \beta_t^{k,i,l}(\mathbf{v}^i).$$

and

$$\mathbf{Z}^T \mathbf{G}_t^{-1} \frac{\partial}{\partial \mathbf{v}} \Sigma_t \mathbf{G}_t^{-T} \mathbf{Z} = 2 (\mathbf{Z}^T \mathbf{G}_t^{-1})_k \sum_{i=1}^{n+1} \sum_{l=1}^{d(t)} \beta_t^{i,k,l}(\mathbf{v}^i) (\mathbf{Z}^T \mathbf{G}_t^{-1})_i$$

**Proof.** Let  $i, j = 1, \dots, n+1$  and  $k = (1), \dots, (n), D$  be arbitrary. We know from (2.11)  $t_{d(t)} = t$ . We use Lemma 6.1 and define  $\alpha^{i,j,m} := \alpha^{i,m} + \alpha^{j,m}$ ,  $\Delta t_m := t_m - t_{m-1}$ . It holds

$$\begin{aligned} (\Sigma_t)_{i,j} &= \rho_{ij} \int_{t_0}^t \mathbf{v}^{(i)} \mathbf{v}^{(j)} \exp \left( - \int_s^t (\alpha_u^{(i)} + \alpha_u^{(j)}) du \right) ds \\ &= \rho_{ij} \mathbf{v}^{(i)} \mathbf{v}^{(j)} \sum_{l=1}^{d(t)} \int_{t_{l-1}}^{t_l} \exp \left( - \int_s^t (\alpha_u^{(i)} + \alpha_u^{(j)}) du \right) ds \\ &= \rho_{ij} \mathbf{v}^{(i)} \mathbf{v}^{(j)} \sum_{l=1}^{d(t)} \exp \left( - \sum_{m=l+1}^{d(t)} \alpha^{i,j,m} \Delta t_m \right) \int_{t_{l-1}}^{t_l} \exp \left( - \int_s^{t_l} \alpha^{i,j,l} du \right) ds \\ &= \rho_{ij} \mathbf{v}^{(i)} \mathbf{v}^{(j)} \sum_{l=1}^{d(t)} \frac{1}{\alpha^{i,j,l}} \exp \left( - \sum_{m=l+1}^{d(t)} \alpha^{i,j,m} \Delta t_m \right) [1 - \exp(-\alpha^{i,j,l} \Delta t_l)]. \end{aligned}$$

Derivation in direction  $\frac{\partial}{\partial \mathbf{v}^k}$  leads to the first statement of the Lemma.

Next, we have to calculate the trace of  $\Sigma_t^{-1} \frac{\partial}{\partial \mathbf{v}^{k,a}} \Sigma_t$ . We can write

$$\Sigma_t^{-1} \frac{\partial}{\partial \mathbf{v}^k} \Sigma_t = \begin{pmatrix} (\Sigma_t^{-1})_{1,k} \sum_{l=1}^{d(t)} \beta_t^{k,1,l}(\mathbf{v}^{(1)}) & \dots & (\Sigma_t^{-1})_{1,k} \sum_{l=1}^{d(t)} \beta_t^{k,n+1,l}(\mathbf{v}^D) \\ \vdots & \ddots & \vdots \\ (\Sigma_t^{-1})_{n+1,k} \sum_{l=1}^{d(t)} \beta_t^{k,1,l}(\mathbf{v}^1) & \dots & (\Sigma_t^{-1})_{n+1,k} \sum_{l=1}^{d(t)} \beta_t^{k,n+1,l}(\mathbf{v}^D) \end{pmatrix} +$$

$$\begin{pmatrix} 0 & \cdots & \sum_{j=1}^{n+1} (\Sigma_t^{-1})_{1j} \sum_{l=1}^{d(t)} \beta_t^{j,k,l}(\mathbf{v}^{(j)}) & \cdots & 0 \\ \vdots & & \vdots & & \vdots \\ 0 & \cdots & \sum_{j=1}^{n+1} (\Sigma_t^{-1})_{n+1j} \sum_{l=1}^{d(t)} \beta_t^{j,k,l}(\mathbf{v}^{(j)}) & \cdots & 0 \end{pmatrix}$$

and therefore

$$\text{tr} \left( \Sigma_t^{-1} \frac{\partial}{\partial \mathbf{v}^k} \Sigma_t \right) = \sum_{i=1}^{n+1} (\Sigma_t^{-1})_{ik} \sum_{l=1}^{d(t)} \beta_t^{k,i,l}(\mathbf{v}^{(i)}) + \sum_{i=1}^{n+1} (\Sigma_t^{-1})_{ki} \sum_{l=1}^{d(t)} \beta_t^{i,k,l}(\mathbf{v}^{(i)})$$

which implies the assertion because of the symmetry of  $\Sigma_t^{-1}$  and  $\sum_{l=1}^{d(t)} \beta_t^{i,k,l}$ .

It remains to calculate  $\mathbf{Z}^T \mathbf{G}_t^{-1} \frac{\partial}{\partial \mathbf{v}} \Sigma_t \mathbf{G}_t^{-T} \mathbf{Z}$ . It holds for  $\mathbf{x} \in \mathbb{R}^{n+1}$  and  $i = 1, \dots, n+1$

$$\left( \frac{\partial}{\partial \mathbf{v}^k} \Sigma_t \mathbf{x} \right)_i = \begin{cases} \sum_{l=1}^{d(t)} \beta_t^{i,k,l}(\mathbf{v}^i) x_k & \text{if } i \neq k \\ \sum_{l=1}^{d(t)} \beta_t^{k,k,l}(\mathbf{v}^k) x_k + \sum_{j=1}^{n+1} \sum_{l=1}^{d(t)} \beta_t^{k,j,l}(\mathbf{v}^j) x_j & \text{if } i = k \end{cases}$$

and therefore because of the symmetry  $\beta_t^{k,j,l}(\mathbf{v}) = \beta_t^{j,k,l}(\mathbf{v})$

$$\mathbf{x}^T \frac{\partial}{\partial \mathbf{v}^{k,a}} \Sigma_t \mathbf{x} = 2x_k \sum_{j=1}^{n+1} \sum_{l=1}^{d(t)} \beta_t^{k,j,l}(\mathbf{v}^j) x_j.$$

By setting  $x = \mathbf{G}_t^{-T} \mathbf{Z}$  it follows the last statement of the Lemma. ■

**Proposition 6.4 (Vega Calculation)** *Let the structural electricity model in Chapter 2 be given with constant volatilities  $\mathbf{v}_t^{(i)} \equiv \mathbf{v}^{(i)} > 0$  and  $\mathbf{v}_t^D \equiv \mathbf{v}^D > 0$  and a contingent claim  $\Psi(\mathbf{S}_t^F, \mathbf{S}_t^P)$  ( $t > t_0 \geq 0$ ). Given Definition 6.1, the vega score for an arbitrary  $a \in \{1, \dots, d(t)\}$  and  $k = 1, \dots, n$  is can be expressed as*

$$\begin{aligned} \text{Score} \left( \frac{\partial}{\partial \mathbf{v}^k} \right) &= \sum_{l=1}^{d(t)} \beta_t^{k,k,l}(\mathbf{v}^k) \left( \frac{1}{\sigma_{X_t^k}} (\mathbf{Z}^T \mathbf{G}_t^{-1})_{n+1} \frac{\partial \mu_t^D}{\partial \sigma_{X_t^k}} - (\mathbf{Z}^T \mathbf{G}_t^{-1})_k \right) \\ &\quad - \sum_{i=1}^{n+1} (\Sigma_t^{-1})_{ik} \sum_{l=1}^{d(t)} \beta_t^{k,i,l}(\mathbf{v}^i) + (\mathbf{Z}^T \mathbf{G}_t^{-1})_k \sum_{i=1}^{n+1} \sum_{l=1}^{d(t)} \beta_t^{i,k,l}(\mathbf{v}^i) (\mathbf{Z}^T \mathbf{G}_t^{-1})_i. \end{aligned}$$

For the demand ( $k = n+1 \triangleq D$ ), the score is given by

$$\begin{aligned} \text{Score} \left( \frac{\partial}{\partial \mathbf{v}^{n+1}} \right) &= \sum_{l=1}^{d(t)} \beta_t^{n+1,n+1,l}(\mathbf{v}^{n+1}) \frac{1}{\sigma_{X_t^{n+1}}} (\mathbf{Z}^T \mathbf{G}_t^{-1})_{n+1} \frac{\partial \mu_t^D}{\partial \sigma_{X_t^{n+1}}} \\ &\quad - \sum_{i=1}^{n+1} (\Sigma_t^{-1})_{i,n+1} \sum_{l=1}^{d(t)} \beta_t^{n+1,i,l}(\mathbf{v}^{n+1}) + (\mathbf{Z}^T \mathbf{G}_t^{-1})_k \sum_{i=1}^{n+1} \sum_{l=1}^{d(t)} \beta_t^{n+1,i,l}(\mathbf{v}^{n+1}) (\mathbf{Z}^T \mathbf{G}_t^{-1})_i. \end{aligned}$$

**Proof.** The score is given by the sum of (6.8) and (6.17):

$$\mathbf{Z}^T \mathbf{G}_t^{-1} \begin{pmatrix} \dot{\mu}_t^F(\mathbf{v}^k) \\ \dot{\mu}_t^D(\mathbf{v}^k) \end{pmatrix} - \frac{1}{2} \text{tr} \left( \Sigma_t^{-1}(\mathbf{v}^k) \frac{\partial}{\partial \mathbf{v}^k} \Sigma_t(\mathbf{v}^k) \right) + \frac{1}{2} \mathbf{Z}^T \mathbf{G}_t^{-1} \frac{\partial}{\partial \mathbf{v}^k} \Sigma_t(\mathbf{v}^k) \mathbf{G}_t^{-T} \mathbf{Z}$$

The first row of the assertion comes from the drift derivatives of  $\mu_t^F(\mathbf{v}^k)$  and  $\mu_t^D(\mathbf{v}^k)$  in (6.8) in direction of volatility: Let  $k = 1, \dots, n, D$  be arbitrary. It holds

$$\sigma_{X_t^i}^2 = (\Sigma_t)_{i,i} = \int_{t_0}^t (\mathbf{v}_s^{(i)})^2 \exp \left( -2 \int_s^t \alpha_u^{(i)} du \right) ds$$

for  $j = 1, \dots, n$  because of Lemma 6.1 and 6.4 it holds

$$\begin{aligned} \frac{\partial \mu_t^j}{\partial v^k} &= \frac{\partial \mu_t^j}{\partial \sigma_{X_t^k}} \frac{\partial \sigma_{X_t^k}}{\partial v^k} \stackrel{(2.7)}{=} \frac{\partial}{\partial \sigma_{X_t^k}} \left( \ln(F_t^j) - \exp \left( - \int_{t_0}^t \alpha_s^{(j)} ds \right) \ln(s_j) - \frac{1}{2} (\sigma_{X_t^k})^2 \right) \frac{\partial \sigma_{X_t^k}}{\partial v^k} \\ &= \begin{cases} - \sum_{l=1}^{d(t)} \beta_t^{k,k,l}(v^k) & \text{if } k = j \\ 0 & \text{else} \end{cases} \end{aligned}$$

and

$$\frac{\partial \mu_t^D}{\partial v^k} = \frac{\partial \mu_t^D}{\partial \sigma_{X_t^k}} \frac{\partial \sigma_{X_t^k}}{\partial v^k} = \frac{\partial \mu_t^D}{\partial \sigma_{X_t^k}} \frac{\sum_{l=1}^{d(t)} \beta_t^{k,k,l}(v^k)}{\sigma_{X_t^k}}.$$

Inserting this into (6.8) leads to the first row of the formula. The remaining part directly follows from Lemma 6.4 and equation (6.17).

■

In case of a time-dependent volatility, Lemma 6.4 and Proposition 6.6 provide similar results. The derivations also belong to our research but are presented at the end of this Chapter (Lemma 6.4, p. 140).

### 6.3.4 Sensitivity in Mean-Reversion

In order to underline why a sensitivity of changes in mean-reversion might be important in our model, we take a look again to the estimation procedure in Chapter 4. We found out that we have to estimate the model volatility  $v^D$  to match electricity spot volatility (Appendix B.3); and mean-reversion  $\alpha$  to cope with volatility in the futures/ forwards market respectively. Consequently, mean-reversion sensitivity might be regarded as our main vega in the model of this thesis. The reason is that mean-reversion reflects volatility in our hedging instruments and this is what a practitioner might want to hedge.

However, in the context of this thesis, likelihood ratio method for mean-reversions leads to more complex expressions than the betas in Lemma 6.4. We therefore believe the numerical performance of the vega calculation to be a lower bound for mean-reversion sensitivity calculation using the likelihood ratio method.

## 6.4 Pathwise Derivative Method

The idea to apply the pathwise derivatives method to a structural electricity model is to interpret  $\Psi \circ f_{bs}$  as a payoff function with input  $S_t^F$  and  $S_t^P$ . Although the modified payoff function  $\bar{\Psi} := \Psi \circ f_{bs}$  may - in general - contain jumps at locations where the margin fuel changes, we show that the pathwise derivative approach is still applicable.

Throughout this Chapter, we assume:

1. the fuels' and demand dynamics to be (log-) normally distributed as given in (6.6),
2. additionally independence between fuels and demand dynamics,

3. an exponential bid stack to be given (cf. Chapter 2.1) without negative prices and spikes part ( $b_N = 0$  and  $b_S = 0$ ).

We use the simplified notation  $\phi^F := \phi^{\Sigma^F, \mu_t^F}$  and  $\phi := \phi^{1,0}$  compared to the prior Chapter.

### 6.4.1 Power Forward Delta in a Framework with Historical Volatilities

Let  $f := F_{t_0, t}^P$  be an arbitrary power forward price which the mean  $\mu_t^D$  of the demand  $D_t$  depends on. Then, it holds for a contingent claim  $\Psi(S_t^P(\mathbf{F}))$  (to emphasize the dependence on  $f$  we will shorten the notation to  $\Psi(S_t^P(f))$ ) using the formula of the power spot price in Appendix A.1:

$$\begin{aligned}
\frac{\partial}{\partial f} PV_t(S_t^P(f)) &= \frac{\partial}{\partial f} \mathbb{E}^{\mathbb{Q}} [\Psi(f_{bs}(D_t(f), \mathbf{S}_t^F)) | \mathcal{F}_{t_0}] \\
&= \frac{\partial}{\partial f} \int_{-\infty}^{\infty} \int_{\mathbb{R}^2} \Psi(f_{bs}(D_t(\xi; f), \mathbf{S}_t^F(\mathbf{x}))) \phi^F(\mathbf{x}) \phi\left(\frac{\xi - \mu_t^D}{\sigma_t^D}\right) / \sigma_t^D d\mathbf{x} d\xi \\
&\stackrel{App.A.1}{=} \frac{\partial}{\partial f} \int_{\frac{\xi^- - \mu_t^D}{\sigma_t^D}}^{\frac{\xi^+ - \mu_t^D}{\sigma_t^D}} \int_{\mathbb{R}^2} \Psi(b_{low}(D_t(\xi; f), \mathbf{S}_t^F(\mathbf{x}))) \phi^F(\mathbf{x}) \phi(\xi) d\mathbf{x} d\xi \\
&\quad + \frac{\partial}{\partial f} \int_{\frac{\xi^- - \mu_t^D}{\sigma_t^D}}^{\frac{\xi^+ - \mu_t^D}{\sigma_t^D}} \int_{\mathbb{R}^2} \Psi(b_{mid}(D_t(\xi; f), \mathbf{S}_t^F(\mathbf{x}))) \phi^F(\mathbf{x}) \phi(\xi) d\mathbf{x} d\xi \\
&\quad + \frac{\partial}{\partial f} \int_{\frac{\xi^- - \mu_t^D}{\sigma_t^D}}^{\frac{\xi^+ - \mu_t^D}{\sigma_t^D}} \int_{\mathbb{R}^2} \Psi(b_{high}(D_t(\xi; f), \mathbf{S}_t^F(\mathbf{x}))) \phi^F(\mathbf{x}) \phi(\xi) d\mathbf{x} d\xi. \tag{6.18}
\end{aligned}$$

Because  $b_{low}, b_{mid}$  and  $b_{high}$  are - at least locally - Lipschitz continuous (proved in Appendix A.1, Proposition A.1), we are allowed to interchange integration and differentiation for suitable payoff-functions and fuel/demand dynamics (cf. Proposition 6.1). By keeping track of the integral limits and its derivatives, we get

$$\begin{aligned}
\cdots &= \int_{\frac{\xi^- - \mu_t^D}{\sigma_t^D}}^{\frac{\xi^+ - \mu_t^D}{\sigma_t^D}} \int_{\mathbb{R}^2} \frac{\partial \Psi(b_{low}(D_t(\xi), \mathbf{S}_t^F(\mathbf{x})))}{\partial S_t^P} \frac{\partial b_{low}(D_t(\xi), \mathbf{S}_t^F(\mathbf{x}))}{\partial D_t} \frac{\partial D_t(\xi; f)}{\partial f} \phi^F(\mathbf{x}) \phi(\xi) d\mathbf{x} d\xi \\
&\quad + \int_{\frac{\xi^- - \mu_t^D}{\sigma_t^D}}^{\frac{\xi^+ - \mu_t^D}{\sigma_t^D}} \int_{\mathbb{R}^2} \frac{\partial \Psi(b_{mid}(D_t(\xi), \mathbf{S}_t^F(\mathbf{x})))}{\partial S_t^P} \frac{\partial b_{mid}(D_t(\xi), \mathbf{S}_t^F(\mathbf{x}))}{\partial D_t} \frac{\partial D_t(\xi; f)}{\partial f} \phi^F(\mathbf{x}) \phi(\xi) d\mathbf{x} d\xi \\
&\quad + \int_{\frac{\xi^- - \mu_t^D}{\sigma_t^D}}^{\frac{\xi^+ - \mu_t^D}{\sigma_t^D}} \int_{\mathbb{R}^2} \frac{\partial \Psi(b_{high}(D_t(\xi), \mathbf{S}_t^F(\mathbf{x})))}{\partial S_t^P} \frac{\partial b_{high}(D_t(\xi), \mathbf{S}_t^F(\mathbf{x}))}{\partial D_t} \frac{\partial D_t(\xi; f)}{\partial f} \phi^F(\mathbf{x}) \phi(\xi) d\mathbf{x} d\xi \\
&\quad + \int_{\mathbb{R}^2} \Psi(b_{low}(\bar{\xi}^-, \mathbf{S}_t^F(\mathbf{x}))) \phi^F(\mathbf{x}) d\mathbf{x} \phi\left(\frac{\bar{\xi}^- - \mu_t^D}{\sigma_t^D}\right) \left(-\frac{1}{\sigma_t^D}\right) \frac{\partial \mu_t^D(f)}{\partial f} \\
&\quad + \int_{\mathbb{R}^2} \Psi(b_{mid}(\bar{\xi}^+, \mathbf{S}_t^F(\mathbf{x}))) \phi^F(\mathbf{x}) d\mathbf{x} \phi\left(\frac{\bar{\xi}^+ - \mu_t^D}{\sigma_t^D}\right) \left(-\frac{1}{\sigma_t^D}\right) \frac{\partial \mu_t^D(f)}{\partial f} \\
&\quad - \int_{\mathbb{R}^2} \Psi(b_{mid}(\bar{\xi}^-, \mathbf{S}_t^F(\mathbf{x}))) \phi^F(\mathbf{x}) d\mathbf{x} \phi\left(\frac{\bar{\xi}^- - \mu_t^D}{\sigma_t^D}\right) \left(-\frac{1}{\sigma_t^D}\right) \frac{\partial \mu_t^D(f)}{\partial f}
\end{aligned}$$

$$- \int_{\mathbb{R}^2} \Psi(b_{\text{high}}(\bar{\xi}^{i+}, \mathbf{S}_t^F(\mathbf{x}))) \phi^F(\mathbf{x}) d\mathbf{x} \phi \left( \frac{\bar{\xi}^{i+} - \mu_t^D}{\sigma_t^D} \right) \left( -\frac{1}{\sigma_t^D} \right) \frac{\partial \mu_t^D(f)}{\partial f}. \quad (6.19)$$

Further simplifications are performed in Chapter 6.7 which also belong to our research. Altogether, this leads to the following Proposition.

**Proposition 6.5 (Power Forward Delta)** *Let  $t, T > t_0$  and  $F_{t_0,t}^P \in \mathbb{R}^+$  be given. Furthermore, let*

1. *the fuels and demand dynamics  $S_t^F$  and  $D_t$  as well as the bid stack be as given in Chapter 2,*
2. *model parameters as been derived in Chapter 4,*
3.  *$\Psi(S_t^F, S_t^P)$  be an Lipschitz continuous payoff function with Lipschitz constant  $\kappa_\Psi$  additionally being differentiable almost everywhere.*

*Then, under the exponential bid stack with two marginal fuels in Chapter 2.1, the pathwise derivative method for the power forward delta is given by*

$$\begin{aligned} \frac{\partial PV_t}{\partial F_{t_0,T}^P} = & \int_{\frac{\bar{\xi}^{i-} - \mu_t^D}{\sigma_t^D}}^{\frac{\bar{\xi}^{i+} - \mu_t^D}{\sigma_t^D}} \int_{\mathbb{R}^2} \frac{\partial \Psi(b_{\text{low}}(D_t(\xi), \mathbf{S}_t^F(\mathbf{x})))}{\partial S_t^P} \left( \sum_{j=1}^3 m_{\text{low},j}^{\partial D_t}(\xi, \mathbf{x}) \right) \frac{\partial D_t(\xi; f)}{\partial f} \phi^F(\mathbf{x}) \phi(\xi) d\mathbf{x} d\xi \\ & + \int_{\frac{\bar{\xi}^{i-} - \mu_t^D}{\sigma_t^D}}^{\frac{\bar{\xi}^{i+} - \mu_t^D}{\sigma_t^D}} \int_{\mathbb{R}^2} \frac{\partial \Psi(b_{\text{mid}}(D_t(\xi), \mathbf{S}_t^F(\mathbf{x})))}{\partial S_t^P} \left( \sum_{j=1}^3 m_{\text{mid},j}^{\partial D_t}(\xi, \mathbf{x}) \right) \frac{\partial D_t(\xi; f)}{\partial f} \phi^F(\mathbf{x}) \phi(\xi) d\mathbf{x} d\xi \\ & + \int_{\frac{\bar{\xi}^{i-} - \mu_t^D}{\sigma_t^D}}^{\frac{\bar{\xi}^{i+} - \mu_t^D}{\sigma_t^D}} \int_{\mathbb{R}^2} \frac{\partial \Psi(b_{\text{high}}(D_t(\xi), \mathbf{S}_t^F(\mathbf{x})))}{\partial S_t^P} \left( \sum_{j=1}^3 m_{\text{high},j}^{\partial D_t}(\xi, \mathbf{x}) \right) \frac{\partial D_t(\xi; f)}{\partial f} \phi^F(\mathbf{x}) \phi(\xi) d\mathbf{x} d\xi \\ & + \int_{\mathbb{R}^2} \Psi(b_{\text{low}}(\bar{\xi}^{i-}, \mathbf{S}_t^F(\mathbf{x}))) \phi^F(\mathbf{x}) d\mathbf{x} \phi \left( \frac{\bar{\xi}^{i-} - \mu_t^D}{\sigma_t^D} \right) \left( -\frac{1}{\sigma_t^D} \right) \frac{\partial \mu_t^D(f)}{\partial f} \\ & + \int_{\mathbb{R}^2} \Psi(b_{\text{mid}}(\bar{\xi}^{i+}, \mathbf{S}_t^F(\mathbf{x}))) \phi^F(\mathbf{x}) d\mathbf{x} \phi \left( \frac{\bar{\xi}^{i+} - \mu_t^D}{\sigma_t^D} \right) \left( -\frac{1}{\sigma_t^D} \right) \frac{\partial \mu_t^D(f)}{\partial f} \\ & - \int_{\mathbb{R}^2} \Psi(b_{\text{mid}}(\bar{\xi}^{i-}, \mathbf{S}_t^F(\mathbf{x}))) \phi^F(\mathbf{x}) d\mathbf{x} \phi \left( \frac{\bar{\xi}^{i-} - \mu_t^D}{\sigma_t^D} \right) \left( -\frac{1}{\sigma_t^D} \right) \frac{\partial \mu_t^D(f)}{\partial f} \\ & - \int_{\mathbb{R}^2} \Psi(b_{\text{high}}(\bar{\xi}^{i+}, \mathbf{S}_t^F(\mathbf{x}))) \phi^F(\mathbf{x}) d\mathbf{x} \phi \left( \frac{\bar{\xi}^{i+} - \mu_t^D}{\sigma_t^D} \right) \left( -\frac{1}{\sigma_t^D} \right) \frac{\partial \mu_t^D(f)}{\partial f}, \end{aligned}$$

where  $m_{\text{low},1}^{\partial D_t}$  is defined in (6.22). The other summands are derived similarly by using the power spot price formula in Appendix A.1.

**Proof.** Because differentiation and integration can be interchanged (Proposition 6.1), the Proposition follows from Lemma 6.5 in the derivation in Chapter 6.7. ■

## 6.4.2 Fuel Forward Delta in a Framework with Historical Volatilities

Let  $f := F_t^i$  be an arbitrary fuel future price which the mean  $\mu^i$  of  $S_t^{(i)}$  depends on ( $i = 1, 2$ ). Then, it holds for a contingent claim  $\Psi(S_t^P(\mathbf{F}), \mathbf{S}_t^F(\mathbf{F}))$  (to emphasize the dependence on  $f$  we will shorten the notation to  $\Psi(S_t^P(f), \mathbf{S}_t^F(f))$ ) using the formula of the power spot price in Appendix A.1:



$$\begin{aligned}
\frac{\partial}{\partial f} PV_t(S_t^P(f), \mathbf{S}_t^F(f)) &= \frac{\partial}{\partial f} \mathbb{E}^{\mathbb{Q}} [\Psi(f_{\text{bs}}(D_t(f), \mathbf{S}_t^F), \mathbf{S}_t^F(f)) | \mathcal{F}_{t_0}] \\
&= \frac{\partial}{\partial f} \int_{\frac{-\mu_t^D}{\sigma_t^D}}^{\frac{\xi^{i-} - \mu_t^D}{\sigma_t^D}} \int_{\mathbb{R}^2} \Psi(b_{\text{low}}(D_t(\xi; f), \mathbf{S}_t^F(\mathbf{x}; f)), \mathbf{S}_t^F(\mathbf{x}; f)) \phi^F(\mathbf{x}) \phi(\xi) d\mathbf{x} d\xi \\
&\quad + \frac{\partial}{\partial f} \int_{\frac{-\mu_t^D}{\sigma_t^D}}^{\frac{\xi^{i+} - \mu_t^D}{\sigma_t^D}} \int_{\mathbb{R}^2} \Psi(b_{\text{mid}}(D_t(\xi; f), \mathbf{S}_t^F(\mathbf{x}; f)), \mathbf{S}_t^F(\mathbf{x}; f)) \phi^F(\mathbf{x}) \phi(\xi) d\mathbf{x} d\xi \\
&\quad + \frac{\partial}{\partial f} \int_{\frac{\xi^{i+} - \mu_t^D}{\sigma_t^D}}^{\frac{\xi - \mu_t^D}{\sigma_t^D}} \int_{\mathbb{R}^2} \Psi(b_{\text{high}}(D_t(\xi; f), \mathbf{S}_t^F(\mathbf{x}; f)), \mathbf{S}_t^F(\mathbf{x}; f)) \phi^F(\mathbf{x}) \phi(\xi) d\mathbf{x} d\xi.
\end{aligned} \tag{6.20}$$

By proceeding similar to in the prior section, we get

$$\begin{aligned}
\cdots &= \int_{\frac{-\mu_t^D}{\sigma_t^D}}^{\frac{\xi^{i-} - \mu_t^D}{\sigma_t^D}} \int_{\mathbb{R}^2} \frac{\partial \Psi(b_{\text{low}}(D_t(\xi), \mathbf{S}_t^F(\mathbf{x}; f)), \mathbf{S}_t^F(\mathbf{x}; f))}{\partial S_t^P} \\
&\quad \cdot \left( \frac{\partial b_{\text{low}}(D_t(\xi), \mathbf{S}_t^F(\mathbf{x}; f))}{\partial S_t^i} \frac{\partial S_t^i(\mathbf{x}; f)}{\partial f} + \frac{\partial b_{\text{low}}(D_t(\xi), \mathbf{S}_t^F(\mathbf{x}; f))}{\partial D_t} \frac{\partial D_t(\xi; f)}{\partial f} \right) \phi^F(\mathbf{x}) \phi(\xi) d\mathbf{x} d\xi \\
&\quad + \int_{\frac{-\mu_t^D}{\sigma_t^D}}^{\frac{\xi^{i+} - \mu_t^D}{\sigma_t^D}} \int_{\mathbb{R}^2} \frac{\partial \Psi(b_{\text{low}}(D_t(\xi), \mathbf{S}_t^F(\mathbf{x}; f)), \mathbf{S}_t^F(\mathbf{x}; f))}{\partial S_t^i} \frac{\partial S_t^i(\mathbf{x}; f)}{\partial f} \phi^F(\mathbf{x}) \phi(\xi) d\mathbf{x} d\xi \\
&\quad + \int_{\frac{\xi^{i+} - \mu_t^D}{\sigma_t^D}}^{\frac{\xi - \mu_t^D}{\sigma_t^D}} \int_{\mathbb{R}^2} \frac{\partial \Psi(b_{\text{mid}}(D_t(\xi), \mathbf{S}_t^F(\mathbf{x}; f)), \mathbf{S}_t^F(\mathbf{x}; f))}{\partial S_t^P} \\
&\quad \cdot \left( \frac{\partial b_{\text{mid}}(D_t(\xi), \mathbf{S}_t^F(\mathbf{x}; f))}{\partial S_t^i} \frac{\partial S_t^i(\mathbf{x}; f)}{\partial f} + \frac{\partial b_{\text{mid}}(D_t(\xi), \mathbf{S}_t^F(\mathbf{x}; f))}{\partial D_t} \frac{\partial D_t(\xi; f)}{\partial f} \right) \phi^F(\mathbf{x}) \phi(\xi) d\mathbf{x} d\xi \\
&\quad + \int_{\frac{\xi^{i+} - \mu_t^D}{\sigma_t^D}}^{\frac{\xi - \mu_t^D}{\sigma_t^D}} \int_{\mathbb{R}^2} \frac{\partial \Psi(b_{\text{mid}}(D_t(\xi), \mathbf{S}_t^F(\mathbf{x}; f)), \mathbf{S}_t^F(\mathbf{x}; f))}{\partial S_t^i} \frac{\partial S_t^i(\mathbf{x}; f)}{\partial f} \phi^F(\mathbf{x}) \phi(\xi) d\mathbf{x} d\xi \\
&\quad + \int_{\frac{\xi^{i+} - \mu_t^D}{\sigma_t^D}}^{\frac{\xi - \mu_t^D}{\sigma_t^D}} \int_{\mathbb{R}^2} \frac{\partial \Psi(b_{\text{high}}(D_t(\xi), \mathbf{S}_t^F(\mathbf{x}; f)), \mathbf{S}_t^F(\mathbf{x}; f))}{\partial S_t^P} \\
&\quad \cdot \left( \frac{\partial b_{\text{high}}(D_t(\xi), \mathbf{S}_t^F(\mathbf{x}; f))}{\partial S_t^i} \frac{\partial S_t^i(\mathbf{x}; f)}{\partial f} + \frac{\partial b_{\text{high}}(D_t(\xi), \mathbf{S}_t^F(\mathbf{x}; f))}{\partial D_t} \frac{\partial D_t(\xi; f)}{\partial f} \right) \phi^F(\mathbf{x}) \phi(\xi) d\mathbf{x} d\xi \\
&\quad + \int_{\frac{\xi^{i+} - \mu_t^D}{\sigma_t^D}}^{\frac{\xi - \mu_t^D}{\sigma_t^D}} \int_{\mathbb{R}^2} \frac{\partial \Psi(b_{\text{high}}(D_t(\xi), \mathbf{S}_t^F(\mathbf{x}; f)), \mathbf{S}_t^F(\mathbf{x}; f))}{\partial S_t^i} \frac{\partial S_t^i(\mathbf{x}; f)}{\partial f} \phi^F(\mathbf{x}) \phi(\xi) d\mathbf{x} d\xi \\
&\quad + \int_{\mathbb{R}^2} \Psi(b_{\text{low}}(\xi^{i-}, \mathbf{S}_t^F(\mathbf{x}; f)), \mathbf{S}_t^F(\mathbf{x}; f)) \phi^F(\mathbf{x}) d\mathbf{x} \phi \left( \frac{\xi^{i-} - \mu_t^D}{\sigma_t^D} \right) \left( -\frac{1}{\sigma_t^D} \right) \frac{\partial \mu_t^D(f)}{\partial f} \\
&\quad + \int_{\mathbb{R}^2} \Psi(b_{\text{mid}}(\xi^{i+}, \mathbf{S}_t^F(\mathbf{x}; f)), \mathbf{S}_t^F(\mathbf{x}; f)) \phi^F(\mathbf{x}) d\mathbf{x} \phi \left( \frac{\xi^{i+} - \mu_t^D}{\sigma_t^D} \right) \left( -\frac{1}{\sigma_t^D} \right) \frac{\partial \mu_t^D(f)}{\partial f} \\
&\quad - \int_{\mathbb{R}^2} \Psi(b_{\text{mid}}(\xi^{i-}, \mathbf{S}_t^F(\mathbf{x}; f)), \mathbf{S}_t^F(\mathbf{x}; f)) \phi^F(\mathbf{x}) d\mathbf{x} \phi \left( \frac{\xi^{i-} - \mu_t^D}{\sigma_t^D} \right) \left( -\frac{1}{\sigma_t^D} \right) \frac{\partial \mu_t^D(f)}{\partial f}
\end{aligned}$$

$$-\int_{\mathbb{R}^2} \Psi(b_{\text{high}}(\bar{\xi}^{i+}, \mathbf{S}_t^F(\mathbf{x}; f)), \mathbf{S}_t^F(\mathbf{x}; f)) \phi^F(\mathbf{x}) d\mathbf{x} \phi\left(\frac{\bar{\xi}^{i+} - \mu_t^D}{\sigma_t^D}\right) \left(-\frac{1}{\sigma_t^D}\right) \frac{\partial \mu_t^D(f)}{\partial f}. \quad (6.21)$$

It can be seen that the product rule has to be applied for the payoff function when building the derivative of such a claim. This leads the runtime to evaluate those additional terms to increase or even double respectively. However, this will lead the main merit of the pathwise derivative method - to be numerically faster than the difference quotient method - to decrease or even vanish. This is the reason why we do not investigate this method further in this thesis.

## 6.5 Numerical Comparison of Different Greek Calculation Methods

In this Chapter we compare the performance of the difference quotient, likelihood ratio and pathwise derivative method. We implemented the Ornstein-Uhlenbeck model in Chapter 2.2 together with the structural electricity model in Chapter 2.1. We use the time-dependent model parameters estimated in Chapter 4.

### A first Evaluation of Power Forwards and an ATM-Option

We compare all three methods analyzed in the prior Chapters. We evaluate the convergence for two power forward contracts (maturing at 05/07/2016, 06:00-07:00h and 08:00-09:00h respectively) and an at-the-money power option (maturing at 05/07/2016, hour 08:00-09:00h; Strike: 35 EUR/MWh).

The results are depicted in Figure 6.1. We have plotted the 90% confidence interval over the amount of Monte Carlo paths. It can be seen that the pathwise derivative method and the difference quotient method have the best convergence properties in this setting. Figure C.1 (Appendix C.2) depicts that computational runtime for the difference quotient method to calculate PV and coal, gas and power deltas is roughly double the runtime of the pathwise derivatives method to calculate merely a PV and a power delta (coal and gas deltas are not tractable anymore; cf. Chapter 6.4.2). Therefore, the pathwise derivatives method loses its merit to be faster than the difference quotient method for our structural electricity model.

Regarding the likelihood ratio method, it can be observed a high volatility / slow convergence which is indicated by the slowly narrowing confidence interval (90%) for increasing Monte Carlo paths. However, Figure C.1 underlines that the method is really fast: in case of 10 million Monte Carlo paths the likelihood ratio method takes roughly 170 seconds to calculate PV and gas, coal and power deltas whereas the difference quotient method takes 850 seconds to calculate gas, coal and power deltas. Compared to the individual runtime of 120 seconds for a raw valuation (calculation of PV; Figure C.2), it takes only additional 50 seconds to get coal, gas and power forward deltas when using the likelihood ratio method. Altogether, the difference quotient method turns out to be the most effective method in terms of runtime and convergence to calculate according deltas for a forward contract. In order to get an accuracy of  $10^{-2}$

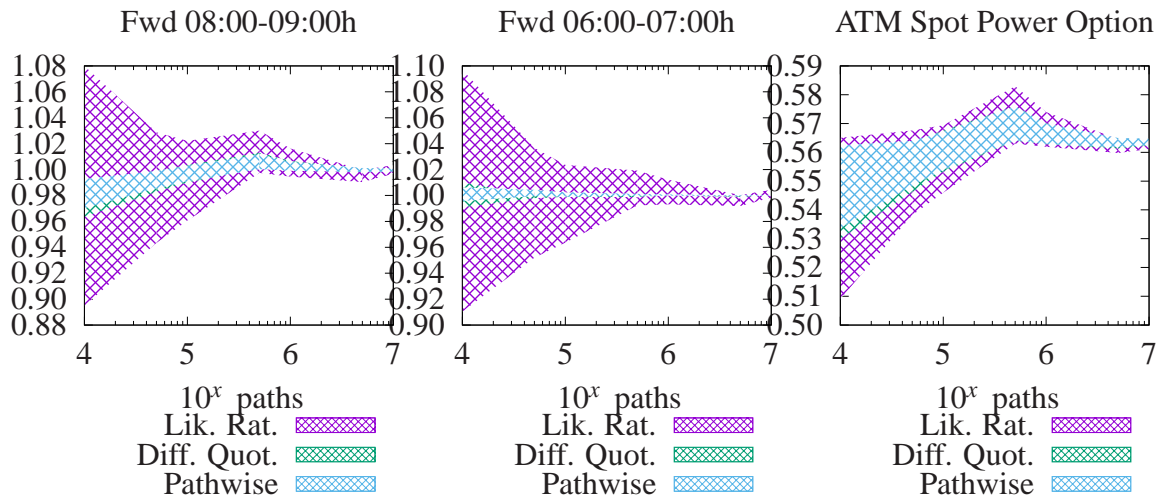


Figure 6.1: Power forward delta for three different kind of contracts for  $T \geq t_{PLTD}$ ; it is depicted the 90 percent confidence interval; convergence of difference quotient and pathwise is quite similar as expected.

in terms of power delta, we need 10.000 paths with a runtime of 12 seconds using the difference quotient method (most of the runtime belongs to the calculation of implied expected demand; cf. Definition 2.1). For the likelihood ratio method we would need 5.000.000 paths with a runtime of 83 seconds.

As a benchmark, we have performed a runtime analysis for a pure fair value calculation (cf. Figure C.2). It verifies that the runtime of the difference quotient method should overall need the sixfold runtime of a PV calculation (plus runtime to recalculate implied expected demand) to calculate delta and vega respectively (two calculations for each: power, coal and gas). For 10 million paths we get: 850 seconds divided by 6 equals 141 seconds which we have to compare against 120 seconds to calculate the according PV.

### Power Forwards: More Greeks and the Impact of the Liquidity Threshold Date

The results are depicted in Figures 6.2 to 6.5. Before we commend on the convergence speed itself, we verify the results. The results for the delta calculations are depicted in Figure 6.2. We assume power forwards to be liquid ( $T < t_{PLTD}$ ). Consequently, the delta for each fuel has to converge against zero. Instead of using fuels for hedging, a back to back power forward hedge is performed with a delta of 1. In comparison, we have performed similar calculations under the assumption  $T \geq t_{PLTD}$ . In this case the fuels converge towards deltas greater than zero. The power delta is still unequal to 0. However, power outright cannot be bought by assumption due to illiquid power futures ( $T < t_{PLTD}$ ). A comprehensive analysis of the delta values for coal and gas is conducted in Chapter 7.2.

We have performed similar calculations for gamma and vega (Figure 6.4 and 6.5). Because we are dealing with a linear payoff function, gamma has always to converge towards zero (for  $T < t_{PLTD}$ ). Vega also converges towards zero as we are dealing with a back to back hedge for  $T < t_{PLTD}$ .

The main conclusion on the convergence speed is that the difference quotient method outperforms

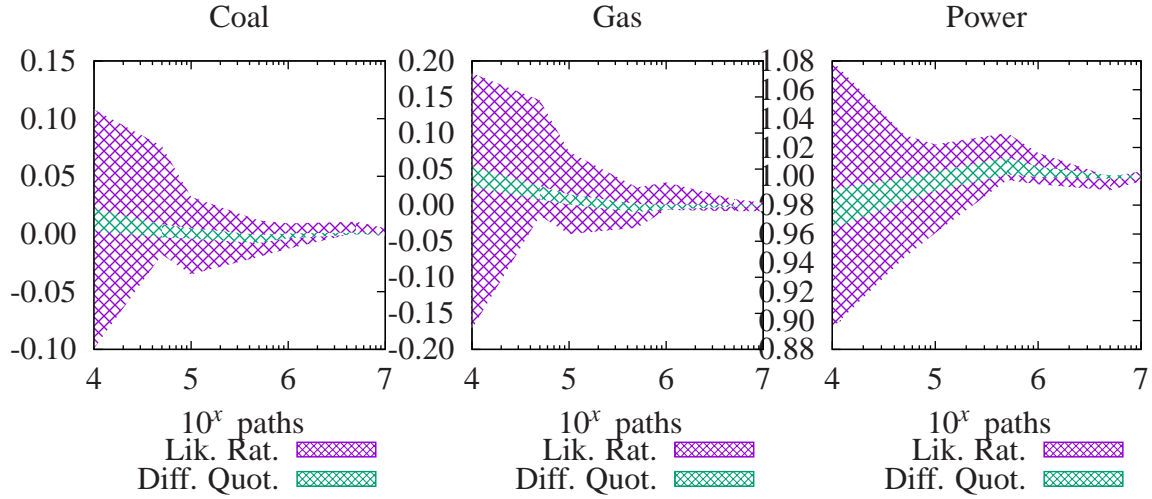


Figure 6.2: Forward delta over simulation paths for a power forward contract and  $T < t_{PLTD}$ ; it is depicted the 90 percent confidence interval of the according deltas; convergence of difference quotient and pathwise is quite similar as expected.

the likelihood ratio method for all Greek types except gamma. We think this to be surprising because the forward electricity payoff function can be interpreted as a non-linear payoff  $\Psi(S_t^P) = S_t^P = f_{BS}(S_t^{(1)}, \dots, S_t^{(n)}, D_t)$  with possible jumps for some  $\omega \in \Omega$  depending on fuel prices and demand. In case of digital options for example, the difference quotient method has difficulties to converge due to the jump in the payoff function. Because  $\bar{\Psi} := \Psi \circ f_{bs}$  can be interpreted as a modified payoff function depending on fuels and demand, we would have expected similar difficulties for the difference quotient method.

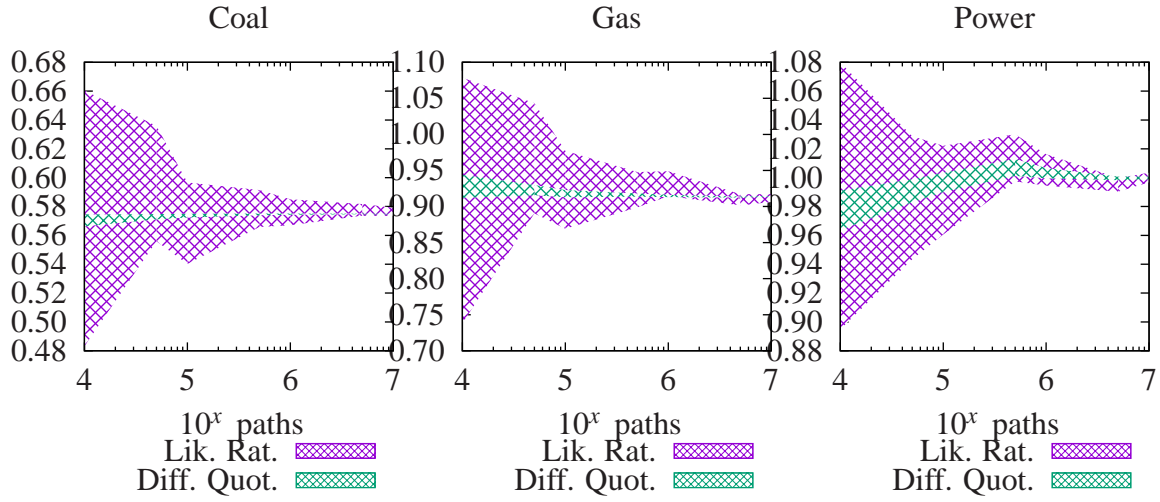


Figure 6.3: Forward delta over simulation paths for a power forward contract and  $T \geq t_{PLTD}$ ; it is depicted the 90 percent confidence interval of the according deltas; convergence of difference quotient and pathwise is quite similar as expected.

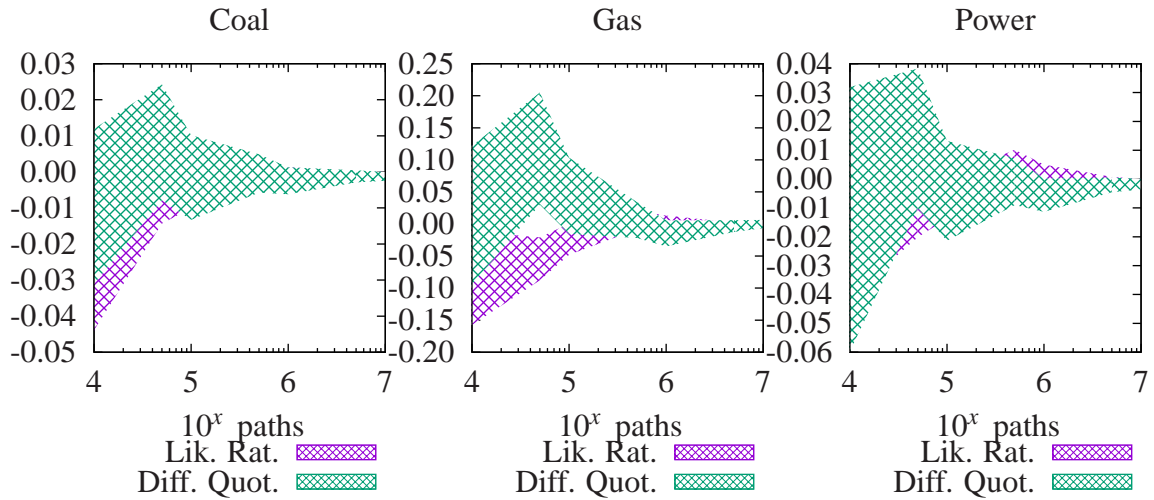


Figure 6.4: Forward gamma over simulation paths for a power forward contract and  $T < t_{PLTD}$ ; it is depicted the 90 percent confidence interval of the according deltas; convergence of difference quotient and pathwise is quite similar as expected.

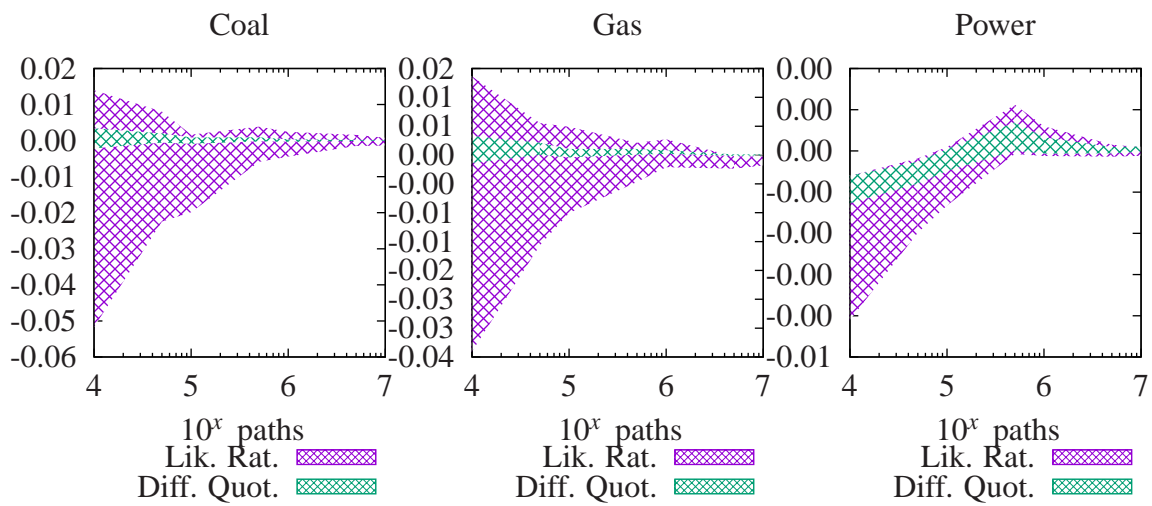


Figure 6.5: Vega over simulation paths for a power forward contract and  $T < t_{PLTD}$ ; it is depicted the 90 percent confidence interval of the according deltas; convergence of difference quotient and pathwise is quite similar as expected

### **An evaluation of Spot ATM Options**

We perform similar calculations for an at-the-money option. The results are depicted in Figures 6.6 to 6.8. It can be observed that the convergence speed of the difference quotient method becomes slower compared to the Greek calculation of forward contracts. However, the convergence rate is still slightly better than the rate of the likelihood ratio method; at least for delta and vega calculations. In terms of gamma, the likelihood ratio method turns out to converge faster than the difference quotient method in our setting (cf. Figure 6.7).

Bringing the results of convergence rate and the runtime together, the likelihood ratio method and the difference quotient method have similar performances. Whereas convergence rates become similar the ATM option, the runtime of the likelihood ratio method is slightly faster: in order to get an accuracy of  $10^{-2}$  for gas, coal and power forwards the difference quotient method needs 1 million paths and the likelihood ratio method needs 5 million paths. This translates into a runtime of 90 seconds for the difference quotient method 80 seconds for the likelihood ratio method.

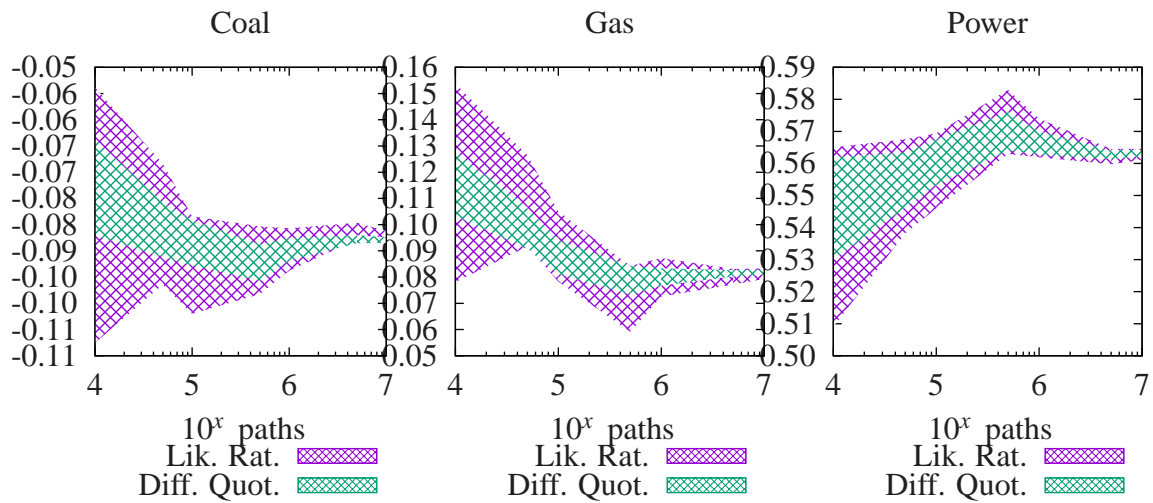


Figure 6.6: Forward delta over simulation paths for a power ATM option contract and  $T < t_{PLTD}$ ; it is depicted the 90 percent confidence interval of the according deltas; convergence of difference quotient and pathwise is quite similar as expected

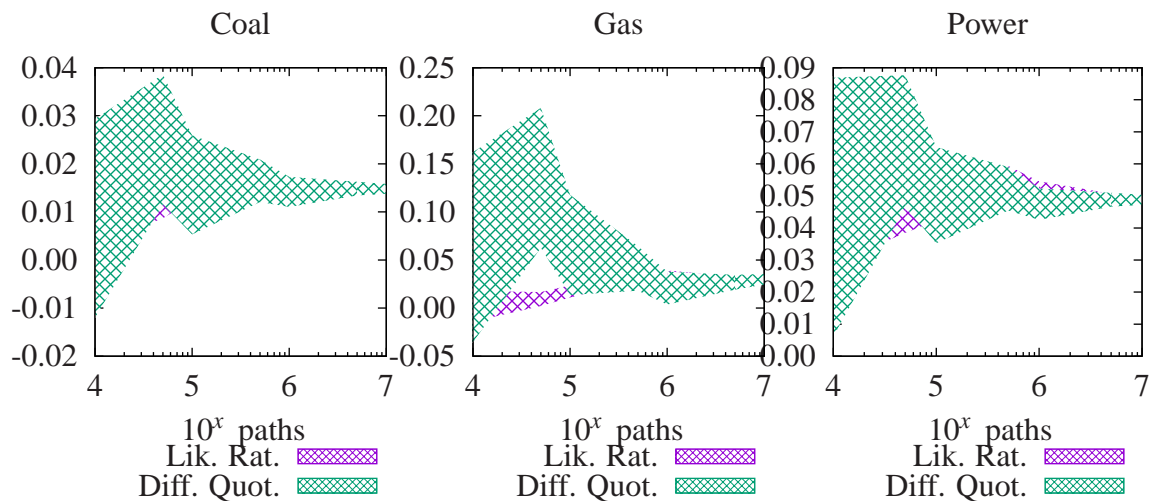


Figure 6.7: Forward gamma over simulation paths for a power ATM option contract and  $T < t_{PLTD}$ ; it is depicted the 90 percent confidence interval of the according deltas; convergence of difference quotient and pathwise is quite similar as expected



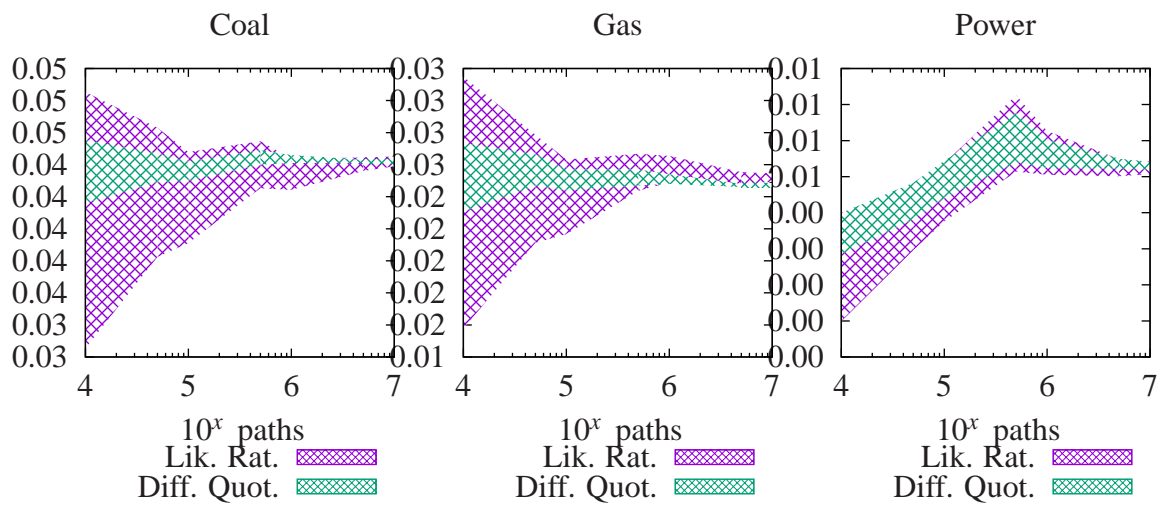


Figure 6.8: Vega over simulation paths for a power ATM option contract and  $T < t_{PLTD}$ ; it is depicted the 90 percent confidence interval of the according deltas; convergence of difference quotient and pathwise is quite similar as expected

## 6.6 Additional Lemma: Likelihood Ratio Method

The following Lemma has been derived under the assumption that the process  $v_t^i$  ( $i \in I \cup \{P\}$ ) is a stepwise constant function over time. In comparison, Lemma 6.3 assumes the according processes to be constant over time.

**Lemma 6.4** *Let the structural electricity model in Chapter 2 be given. Referring to condition (2.11) (p. 21), it exists for an arbitrary  $\tau \in [t_0, t]$  ( $t > t_0 \geq 0$ ) two indices  $a \in \{1, \dots, d(t)\}$  such that  $\tau \in (t_{a-1}, t_a]$ . We define*

$$\beta_t^{i,j,a}(v) := \frac{v \cdot \rho_{ij}}{\alpha^{i,j,a}} \exp \left( - \sum_{m=a+1}^{d(t)} \alpha^{i,j,m} \Delta t_m \right) [1 - \exp(-\alpha^{i,j,a} \Delta t_a)]$$

, where  $\alpha^{i,j,m} := \alpha^{i,m} + \alpha^{j,m}$ ,  $\Delta t_m := t_m - t_{m-1}$ . Then, it holds for  $i, j = 1, \dots, n+1$  and  $v^{k,a}$  ( $v^{k,a}$  defined in (2.11), p. 21) with  $k = (1), \dots, (n), P$

$$\frac{\partial}{\partial v^{k,a}} (\Sigma_t)_{i,j} = \begin{cases} \beta_t^{i,j,a}(v^{i,a}) & k = j \\ \beta_t^{i,j,a}(v^{j,a}) & k = i \\ 2 \cdot \beta_t^{i,j,a}(v^{i,a}) & k = j = i \\ 0 & \text{else,} \end{cases}$$

$$\text{tr} \left( \Sigma_t^{-1} \frac{\partial}{\partial v^{k,a}} \Sigma_t \right) = 2 \cdot \sum_{i=1}^{n+1} (\Sigma_t^{-1})_{i_k} \beta_t^{k,i,a}(v^{i,a}).$$

and

$$\mathbf{Z}^T \mathbf{G}_t^{-1} \frac{\partial}{\partial v} \Sigma_t \mathbf{G}_t^{-T} \mathbf{Z} = 2 (\mathbf{Z}^T \mathbf{G}_t^{-1})_k \sum_{i=1}^{n+1} \beta_t^{i,k,a}(v^{i,a}) (\mathbf{Z}^T \mathbf{G}_t^{-1})_i$$

**Proof.** Let  $i, j = 1, \dots, n+1$  and  $k = (1), \dots, (n), P$  be arbitrary. We know from (2.11) (p. 21)  $t_{d(t)} = t$ . We use Lemma 6.1 (p. 117) and define  $\alpha^{i,j,m} := \alpha^{i,m} + \alpha^{j,m}$ ,  $\Delta t_m := t_m - t_{m-1}$ . It holds

$$\begin{aligned} (\Sigma_t)_{i,j} &= \rho_{ij} \int_{t_0}^t v_s^{(i)} v_s^{(j)} \exp \left( - \int_s^t (\alpha_u^{(i)} + \alpha_u^{(j)}) du \right) ds \\ &= \rho_{ij} \sum_{l=1}^{d(t)} v^{i,l} v^{j,l} \int_{t_{l-1}}^{t_l} \exp \left( - \int_s^t (\alpha_u^{(i)} + \alpha_u^{(j)}) du \right) ds \\ &= \rho_{ij} \sum_{l=1}^{d(t)} v^{i,l} v^{j,l} \exp \left( - \sum_{m=l+1}^{d(t)} \alpha^{i,j,m} \Delta t_m \right) \int_{t_{l-1}}^{t_l} \exp \left( - \int_s^{t_l} \alpha^{i,j,l} du \right) ds \\ &= \rho_{ij} \sum_{l=1}^{d(t)} \frac{v^{i,l} v^{j,l}}{\alpha^{i,j,l}} \exp \left( - \sum_{m=l+1}^{d(t)} \alpha^{i,j,m} \Delta t_m \right) [1 - \exp(-\alpha^{i,j,l} \Delta t_l)]. \end{aligned}$$

Derivation in direction  $\frac{\partial}{\partial v^{k,a}}$  requires to analyze different cases for  $k$  yielding the first statement in the Lemma.

Next, we have to calculate the trace of  $\Sigma_t^{-1} \frac{\partial}{\partial \mathbf{v}^{k,a}} \Sigma_t$ . We can write

$$\Sigma_t^{-1} \frac{\partial}{\partial \mathbf{v}^{k,a}} \Sigma_t = \begin{pmatrix} (\Sigma_t^{-1})_{1k} \beta_t^{k,1,a}(\mathbf{v}^{1,a}) & \cdots & (\Sigma_t^{-1})_{1k} \beta_t^{k,n+1,a}(\mathbf{v}^{D,a}) \\ \vdots & \ddots & \vdots \\ (\Sigma_t^{-1})_{n+1k} \beta_t^{k,1,a}(\mathbf{v}^{1,a}) & \cdots & (\Sigma_t^{-1})_{n+1k} \beta_t^{k,n+1,a}(\mathbf{v}^{D,a}) \end{pmatrix} +$$

$$\begin{pmatrix} 0 & \cdots & \sum_{j=1}^{n+1} (\Sigma_t^{-1})_{1j} \beta_t^{j,k,a}(\mathbf{v}^{j,a}) & \cdots & 0 \\ \vdots & & \vdots & & \vdots \\ 0 & \cdots & \sum_{j=1}^{n+1} (\Sigma_t^{-1})_{n+1j} \beta_t^{j,k,a}(\mathbf{v}^{j,a}) & \cdots & 0 \end{pmatrix}$$

and therefore

$$\text{tr} \left( \Sigma_t^{-1} \frac{\partial}{\partial \mathbf{v}^{k,a}} \Sigma_t \right) = \sum_{i=1}^{n+1} (\Sigma_t^{-1})_{ik} \beta_t^{k,i,a}(\mathbf{v}^{i,a}) + \sum_{i=1}^{n+1} (\Sigma_t^{-1})_{ki} \beta_t^{i,k,a}(\mathbf{v}^{i,a})$$

which implies the assertion because of the symmetry of  $\Sigma_t^{-1}$  and  $\beta_t^{i,k,a}$ .

It remains to calculate  $\mathbf{Z}^T \mathbf{G}_t^{-1} \frac{\partial}{\partial \mathbf{v}} \Sigma_t \mathbf{G}_t^{-T} \mathbf{Z}$ . It holds for  $\mathbf{x} \in \mathbb{R}^{n+1}$  and  $i = 1, \dots, n+1$

$$\left( \frac{\partial}{\partial \mathbf{v}^{k,a}} \Sigma_t \mathbf{x} \right)_i = \begin{cases} \beta_t^{i,k,a}(\mathbf{v}^{i,a}) x_k & \text{if } i \neq k \\ \beta_t^{k,k,a}(\mathbf{v}^{k,a}) x_k + \sum_{j=1}^{n+1} \beta_t^{k,j,a}(\mathbf{v}^{j,a}) x_j & \text{if } i = k \end{cases}$$

and therefore because of the symmetry  $\beta_t^{k,j,a}(\mathbf{v}) = \beta_t^{j,k,a}(\mathbf{v})$

$$\mathbf{x}^T \frac{\partial}{\partial \mathbf{v}^{k,a}} \Sigma_t \mathbf{x} = 2x_k \sum_{j=1}^{n+1} \beta_t^{k,j,a}(\mathbf{v}^{j,a}) x_j.$$

Setting  $x = \mathbf{G}_t^{-T} \mathbf{Z}$  it follows the last statement of the Lemma. ■

**Proposition 6.6 (Vega Calculation)** *Let the Ornstein- Uhlenbeck model in Chapter 2.2 be given together with a market bid stack  $f_{bs}(D_t, \mathbf{S}_t^F)$  and a contingent claim  $\Psi(\mathbf{S}_t^F, \mathbf{S}_t^P)$  ( $t > t_0 \geq 0$ ). Given Definition 6.1 (p. 126), the Vega score for an arbitrary  $a \in \{1, \dots, d(t)\}$  and  $k = 1, \dots, n$  is given by*

$$\text{Score} \left( \frac{\partial}{\partial \mathbf{v}^{k,a}} \right) = \beta_t^{k,k,a}(\mathbf{v}^{k,a}) \left( \frac{1}{\sigma_{X_t^k}} (\mathbf{Z}^T \mathbf{G}_t^{-1})_{n+1} \frac{\partial \mu_t^D}{\partial \sigma_{X_t^k}} - (\mathbf{Z}^T \mathbf{G}_t^{-1})_k \right) - \sum_{i=1}^{n+1} (\Sigma_t^{-1})_{ik} \beta_t^{k,i,a}(\mathbf{v}^{i,a}) + (\mathbf{Z}^T \mathbf{G}_t^{-1})_k \sum_{i=1}^{n+1} \beta_t^{i,k,a}(\mathbf{v}^{i,a}) (\mathbf{Z}^T \mathbf{G}_t^{-1})_i.$$

For the demand ( $k = n+1 \triangleq D$ ), the score is given by

$$\text{Score} \left( \frac{\partial}{\partial \mathbf{v}^{n+1,a}} \right) = \beta_t^{n+1,n+1,a}(\mathbf{v}^{n+1,a}) \frac{1}{\sigma_{X_t^{n+1}}} (\mathbf{Z}^T \mathbf{G}_t^{-1})_{n+1} \frac{\partial \mu_t^D}{\partial \sigma_{X_t^{n+1}}} - \sum_{i=1}^{n+1} (\Sigma_t^{-1})_{in+1} \beta_t^{n+1,i,a}(\mathbf{v}^{n+1,a}) + (\mathbf{Z}^T \mathbf{G}_t^{-1})_k \sum_{i=1}^{n+1} \beta_t^{n+1,i,a}(\mathbf{v}^{n+1,a}) (\mathbf{Z}^T \mathbf{G}_t^{-1})_i.$$

**Proof.** The first row of the assertion comes from the drift derivatives of  $\mu_t^F(\mathbf{v}^{k,a})$  and  $\mu_t^D(\mathbf{v}^{k,a})$  in (6.8) (p. 118) in direction of volatility: Let  $k = 1, \dots, n, D$  be arbitrary. It holds

$$\sigma_{X_t^i}^2 = (\Sigma_t)_{ii} = \int_{t_0}^t (\mathbf{v}_s^{(i)})^2 \exp \left( -2 \int_s^t \alpha_u^{(i)} du \right) ds$$

for  $j = 1, \dots, n$  because of Lemma 6.1 (p. 117) and 6.4 (p. 140) it holds

$$\begin{aligned} \frac{\partial \mu_t^j}{\partial v^{k,a}} &= \frac{\partial \mu_t^j}{\partial \sigma_{X_t^k}} \cdot \frac{\partial \sigma_{X_t^k}}{\partial v^{k,a}} \stackrel{(2.7)}{=} \frac{\partial}{\partial \sigma_{X_t^k}} \left( \ln(F_t^j) - \exp \left( - \int_{t_0}^t \alpha_s^{(j)} ds \right) \ln(s_j) - \frac{1}{2} (\sigma_{X_t^k})^2 \right) \cdot \frac{\partial \sigma_{X_t^k}}{\partial v^{k,a}} \\ &= \begin{cases} -\beta_t^{k,k,a}(v^{k,a}) & \text{if } k = j \\ 0 & \text{else} \end{cases} \end{aligned}$$

and

$$\frac{\partial \mu_t^D}{\partial v^{k,a}} = \frac{\partial \mu_t^D}{\partial \sigma_{X_t^k}} \cdot \frac{\partial \sigma_{X_t^k}}{\partial v^{k,a}} = \frac{\partial \mu_t^D}{\partial \sigma_{X_t^k}} \frac{\beta_t^{k,k,a}(v^{k,a})}{\sigma_{X_t^k}}.$$

Inserting this into (6.8) (p. 118) leads to the first row of the formula. The remaining part directly follows from Lemma 6.4 and equation (6.17) (p. 125).

■

## 6.7 Additional Simplifications: Pathwise Derivative Method

The following calculations give additional illustrations on how the pathwise derivative method has been derived for a structural electricity model.

We further simplify (6.19) (p. 130).

Technically, the derivatives of  $b_i$  ( $i = \text{low, mid, high}$ ) in (6.19) (p. 130) require to take the derivative of the Heaviside function

$$H(x) := \begin{cases} 1 & x > 0 \\ 0 & x \leq 0 \end{cases}.$$

In [Joshi and Kainth, 2004], a similar problem was observed for an  $n$ th-to-default swap in order to calculate par spread deltas. The Delta distribution  $\delta(x)$  fulfills

$$\int_{-\infty}^{\infty} f(x) \delta(x) dx = f(0)$$

for an arbitrary integrable function  $f$ <sup>3</sup>. For example, the first summand in  $b_{\text{low}}$  (cf. Appendix A.1) becomes for  $\xi \in [0; \bar{\xi}^{i-}]$

$$\begin{aligned} \frac{\partial}{\partial D_t} b_{\text{low}}(\xi, \mathbf{x}) &= \frac{\partial}{\partial D_t} \left( b_c(D_t(\xi), S_t^c(\mathbf{x})) \mathbb{I}_{\{b_c(D_t(\xi), S_t^c(\mathbf{x})) < b_g(0, S_t^g(\mathbf{x}))\}} \right) + \dots \\ &= \frac{\partial}{\partial D_t} b_c(D_t(\xi), S_t^c(\mathbf{x})) \mathbb{I}_{\{b_c(D_t(\xi), S_t^c(\mathbf{x})) < b_g(0, S_t^g(\mathbf{x}))\}} \\ &\quad + b_c(D_t(\xi), S_t^c(\mathbf{x})) \frac{\partial}{\partial D_t} \mathbb{I}_{\{b_c(D_t(\xi), S_t^c(\mathbf{x})) < b_g(0, S_t^g(\mathbf{x}))\}} + \dots \\ &=: m_{\text{low},1}^{\partial D_t}(\xi, \mathbf{x}) + n_{\text{low},1}^{\partial D_t}(\xi, \mathbf{x}) + \dots \end{aligned} \tag{6.22}$$

<sup>3</sup>For further reading in terms of the Delta distribution and its relation to the Heaviside function we refer to [Davies, 2002]

The first term can already be evaluated within a Monte Carlo simulation. Further calculations for the second term lead to

$$\begin{aligned}
n_{\text{low},1}^{\partial D_t}(\xi, \mathbf{x}) &= b_c(D_t(\xi), S_t^c(\mathbf{x})) \frac{\partial}{\partial D_t} H(b_g(0, S_t^g(\mathbf{x})) - b_c(D_t(\xi), S_t^c(\mathbf{x}))) \\
&= b_c(D_t(\xi), S_t^c(\mathbf{x})) \cdot \delta(b_g(0, S_t^g(\mathbf{x})) - b_c(D_t(\xi), S_t^c(\mathbf{x}))) \frac{\partial}{\partial D_t} (-b_c(D_t(\xi), S_t^c(\mathbf{x}))) \\
&= -m_c \cdot b_c^2(D_t(\xi), S_t^c(\mathbf{x})) \cdot \delta(b_g(0, S_t^g(\mathbf{x})) - b_c(D_t(\xi), S_t^c(\mathbf{x}))) \quad (6.23)
\end{aligned}$$

However, the following Lemma derives that the terms  $n_{i,j}^{\partial D_t}(\xi, \mathbf{x})$  for  $i = \text{low}, \text{mid}, \text{high}$  and  $j = 1, 2, 3$  disappear after summing them up appropriately.

**Lemma 6.5** *Under the structural electricity model in Chapter 2  $n_{i,j}^{\partial D_t}(\xi, \mathbf{x})$  for  $i = \text{low}, \text{mid}, \text{high}$  and  $j = 1, 2, 3$  (cf. equation (6.22), p. 142) it holds:*

$$\begin{aligned}
\sum_{j=1}^3 n_{\text{low},j}^{\partial D_t} &= 0 \\
\sum_{j=1}^3 n_{\text{mid},j}^{\partial D_t} &= 0 \\
\sum_{j=1}^3 n_{\text{high},j}^{\partial D_t} &= 0
\end{aligned}$$

**Proof.** By using the relation

$$\mathbb{I}_{\{a \geq b, c \geq d\}} = (1 - \mathbb{I}_{\{a < b\}}) \cdot (1 - \mathbb{I}_{\{c < d\}})$$

for the  $b_{cg}$ -terms, we apply the product rule to get

$$\begin{aligned}
n_{\text{low},3}^{\partial D_t}(\xi, \mathbf{x}) &= m_c \cdot b_{cg}(D_t(\xi), \mathbf{S}_t^F(\mathbf{x})) \cdot b_c(D_t(\xi), S_t^c(\mathbf{x})) \\
&\quad \cdot \delta(b_g(0, S_t^g(\mathbf{x})) - b_c(D_t(\xi), S_t^c(\mathbf{x}))) \cdot \mathbb{I}_{\{b_g(D_t(\xi), S_t^g(\mathbf{x})) \geq b_c(0, S_t^c(\mathbf{x}))\}} \\
&+ m_g \cdot b_{cg}(D_t(\xi), \mathbf{S}_t^F(\mathbf{x})) \cdot b_g(D_t(\xi), S_t^g(\mathbf{x})) \\
&\quad \cdot \delta(b_c(0, S_t^c(\mathbf{x})) - b_g(D_t(\xi), S_t^g(\mathbf{x}))) \cdot \mathbb{I}_{\{b_c(D_t(\xi), S_t^c(\mathbf{x})) \geq b_g(0, S_t^g(\mathbf{x}))\}} \\
n_{\text{mid},3}^{\partial D_t}(\xi, \mathbf{x}) &= m_{i_+} \cdot b_{cg}(D_t(\xi), \mathbf{S}_t^F(\mathbf{x})) \cdot b_{i_+}(D_t(\xi), S_t^{i_+}(\mathbf{x})) \\
&\quad \cdot \delta(b_{i_-}(0, S_t^{i_-}(\mathbf{x})) - b_{i_+}(D_t(\xi), S_t^{i_+}(\mathbf{x}))) \cdot \mathbb{I}_{\{b_{i_+}(D_t(\xi) - \bar{\xi}^{i_-}, S_t^{i_+}(\mathbf{x})) \leq b_{i_-}(\bar{\xi}^{i_-}, S_t^{i_-}(\mathbf{x}))\}} \\
&+ m_{i_+} \cdot b_{cg}(D_t(\xi), \mathbf{S}_t^F(\mathbf{x})) \cdot b_{i_+}(D_t(\xi) - \bar{\xi}^{i_-}, S_t^{i_+}(\mathbf{x})) \\
&\quad \cdot \delta(b_{i_+}(D_t(\xi) - \bar{\xi}^{i_-}, S_t^{i_+}(\mathbf{x})) - b_{i_-}(\bar{\xi}^{i_-}, S_t^{i_-}(\mathbf{x}))) \cdot \mathbb{I}_{\{b_{i_+}(D_t(\xi), S_t^{i_+}(\mathbf{x})) \geq b_{i_-}(0, S_t^{i_-}(\mathbf{x}))\}} \\
n_{\text{high},3}^{\partial D_t}(\xi, \mathbf{x}) &= m_c \cdot b_{cg}(D_t(\xi), \mathbf{S}_t^F(\mathbf{x})) \cdot b_c(D_t(\xi) - \bar{\xi}^g, S_t^c(\mathbf{x})) \\
&\quad \cdot \delta(b_c(D_t(\xi) - \bar{\xi}^g, S_t^c(\mathbf{x})) - b_g(\bar{\xi}^g, S_t^g(\mathbf{x}))) \cdot \mathbb{I}_{\{b_g(D_t(\xi) - \bar{\xi}^c, S_t^g(\mathbf{x})) \leq b_c(\bar{\xi}^c, S_t^c(\mathbf{x}))\}} \\
&+ m_g \cdot b_{cg}(D_t(\xi), \mathbf{S}_t^F(\mathbf{x})) \cdot b_g(D_t(\xi) - \bar{\xi}^c, S_t^g(\mathbf{x}))
\end{aligned}$$

$$\cdot \delta(b_g(D_t(\xi) - \bar{\xi}^c, S_t^g(\mathbf{x})) - b_c(\bar{\xi}^c, S_t^c(\mathbf{x}))) \cdot \mathbb{I}_{\{b_c(D_t(\xi) - \bar{\xi}^g, S_t^c(\mathbf{x})) \leq b_g(\bar{\xi}^g, S_t^g(\mathbf{x}))\}}$$

Straight calculations show that the expressions in the indicator functions are automatically fulfilled when the delta dirac function  $\delta$  is unequal to zero. Therefore, we can distribute  $n_{i,3}^{\partial D_t}$  over  $n_{i,1}^{\partial D_t}$  and  $n_{i,2}^{\partial D_t}$  ( $i = \text{low, mid, high}$ ). We illustrate the result for  $i = \text{low}$  where

$$\begin{aligned} n_{\text{low},1}^{\partial D_t}(\xi, \mathbf{x}) &= -m_c \cdot b_c^2(D_t(\xi), S_t^c(\mathbf{x})) \cdot \delta(b_c(D_t(\xi), S_t^c(\mathbf{x})) - b_g(0, S_t^g(\mathbf{x}))) \\ n_{\text{low},2}^{\partial D_t}(\xi, \mathbf{x}) &= -m_g \cdot b_g^2(D_t(\xi), S_t^g(\mathbf{x})) \cdot \delta(b_g(D_t(\xi), S_t^g(\mathbf{x})) - b_c(0, S_t^c(\mathbf{x}))) \end{aligned}$$

and therefore

$$\begin{aligned} \sum_{j=1}^3 n_{\text{low},j}^{\partial D_t} &= m_c \cdot b_c(D_t(\xi), S_t^c(\mathbf{x})) \cdot \underbrace{(b_{cg}(D_t(\xi), \mathbf{S}_t^F(\mathbf{x})) - b_c(D_t(\xi), S_t^c(\mathbf{x})))}_{=0 \text{ where } \delta \neq 0 \text{ because of Prop. A.1 (p. 160)}} \\ &\quad \cdot \delta(b_c(D_t(\xi), S_t^c(\mathbf{x})) - b_g(0, S_t^g(\mathbf{x}))) \\ &\quad + m_g \cdot b_g(D_t(\xi), S_t^g(\mathbf{x})) \cdot \underbrace{(b_{cg}(D_t(\xi), \mathbf{S}_t^F(\mathbf{x})) - b_g(D_t(\xi), S_t^g(\mathbf{x})))}_{=0 \text{ where } \delta \neq 0 \text{ because of Prop. A.1}} \\ &\quad \cdot \delta(b_g(D_t(\xi), S_t^g(\mathbf{x})) - b_c(0, S_t^c(\mathbf{x}))) \\ &\equiv 0 \quad \forall \mathbf{x} \in \mathbb{R}^2, D_t(\xi) \in [0, \bar{\xi}^{i-}]. \end{aligned}$$

The derivation for  $i = \text{mid, high}$  is quite similar. ■

## CHAPTER 7.

# Delta Hedging - A Practical Analysis for a Virtual Power Plant

In the prior Chapters, we have shown that delta hedging can be applied for structural electricity models under certain conditions (cf. Chapter 3). Furthermore, we estimated model parameters (cf. Chapter 4) and compared different methods for Greek calculation (cf. Chapter 6). Consequently, we are finally able to analyze the hedging behavior of a virtual power plant under delta hedging<sup>1</sup>.

In the following, we use a Monte Carlo method to calculate the present value and the difference quotient method to calculate the deltas for fuels and power.

## 7.1 An Example based on Realistic Price Forward Curves

We quantify the deltas of hourly power, gas and coal forward contracts to hedge a simplified coal virtual power plant as of year end 2015 for a time horizon of 0.5 years (cf. equation (1.1) for the according payoff function). Afterwards, we use Proposition 3.3 to come from hourly deltas to futures deltas.

Figure 7.1 depicts the intrinsic<sup>2</sup> dark spread over 2016 for hour 06:00-07:00h and 08:00-09:00h based on the daily forward curves in Figure 2.1. We used  $h_R = 0.3$  kg/MWh. In order to reflect variable costs of a power plant (emission cost, transport costs), we consider a strike of 15 EUR/MWh.

We start to analyze the hedging behaviour for a typical Thursday in June 2016 (30/06/2016). For additional illustrations we depict the hedging strategy for a dark spread (parameters as been given above) as well as a spark spread option ( $h_R = 2$  MWh[gas]/MWh[power],  $K = 3.5$  EUR/MWh). Figure 7.2 depicts the hourly forward delta hedging strategy as of year end 2015 using 100.000 Monte Carlo paths. We calculate deltas for a liquid power futures (high  $t_{PLTD} > 1$ ; cf. Definition 3.6) market and an illiquid power futures market (low  $t_{PLTD} = 0$ ). Table 7.1 gives further explanations on how to interpret the Figures. Due the complexity for a low  $t_{PLTD}$ , we perform an additional analysis in Chapter 7.2 where we derive the hedging strategy of an hourly power forward curve using coal and gas forwards.

In order to build Figure 7.3, we calculated hourly deltas and summed them up accordingly to get daily

---

<sup>1</sup>In detail, we are assuming that we are short a virtual power plant as it might be when - from an Energy trader point of view - selling tolling agreements to customers without having the back-to-back physical power plant as a hedge.

<sup>2</sup>A valuation is called in literature to be intrinsic in case forward prices are assumed to be realized with certainty.

deltas (cf. Corrolary 3.1). The coal plant seems to be in the money for roughly 16-18 hours of a day (power delta is roughly at 16-18 for high  $t_{PLTD}$ ). In case of a low  $t_{PLTD}$ , we depict the according coal and gas outright which is used to hedge against changes in the power price. It can be seen that - though we hedge a coal VPP - no short position of coal is built up but the opposite instead. The reason for that is given by the fact that coal plants are marginal most of the hours of a day in our parametrization. Therefore, the long position in coal to hedge against changes in power is higher than the short position to hedge against changes in coal.

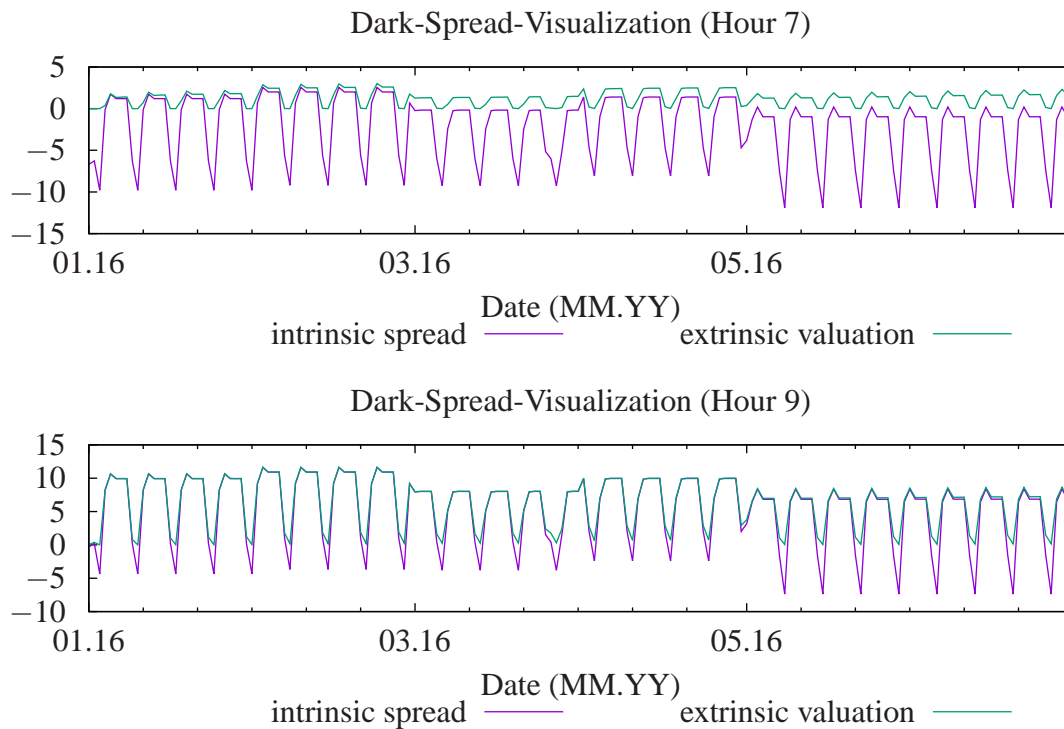


Figure 7.1: VPP (EUR/MWh) daily for hour 6-7 and 8-9 of 2016 based on the hourly forward curves in Figure 2.1.



<p><u>Low <math>t_{PLTD}</math>, Dark Spread:</u></p> <p>We assume power futures to be illiquid. Consequently, we hedge power with fuel futures. Because <math>h_R = 0.3</math> we would roughly expect a coal delta in <math>[-0.3; 0]</math> (cf. high <math>t_{PLTD}</math>). However, coal seems to be marginal for all hours where the VPP is in-the-money, therefore - in order to hedge power - the delta increases to a value between <math>[0; 0.5]</math>. Additionally, it can be seen that gas is marginal in the morning and evening hours. Therefore, the gas delta increases during these hours to hedge against power. It can be seen that the highest gas impact is between 4pm and 8pm.</p>	<p><u>Low <math>t_{PLTD}</math>, Spark Spread:</u></p> <p>The interpretation is similar to the dark spread hourly scheme, however we used <math>h_R = 2</math> for the VPP. Consequently, we would expect the gas delta to be in <math>[-2; 0]</math> (cf. high <math>t_{PLTD}</math>, we get up to -1.5). However, for the evening hours (in-the-money), we get a gas delta of -0.5 implying that roughly one unit of gas is used to hedge against changes in power prices. Because coal is marginal in the evening hours as well, we also need to buy coal futures to hedge against power. Consistent to the low <math>t_{PLTD}</math> case of the dark spread, it can be seen that the highest gas impact is between 4pm and 8pm.</p>
<p><u>High <math>t_{PLTD}</math>, Dark Spread:</u></p> <p>Because we assume power futures to be liquid, we do not need to apply fuel futures to hedge against changes in power prices. Consequently, we need a short position in coal and a long position in power. The gas position is zero.</p>	<p><u>High <math>t_{PLTD}</math>, Spark Spread:</u></p> <p>Because we assume power futures to be liquid, we do not need fuel futures to hedge against changes in power prices. Consequently, we need a short position in gas and a long position in power. The coal position is zero. It can be seen that our calibration leads the gas plant only to be profitable in the morning and evening hours.</p>

Table 7.1: Explanations for Figure 7.2

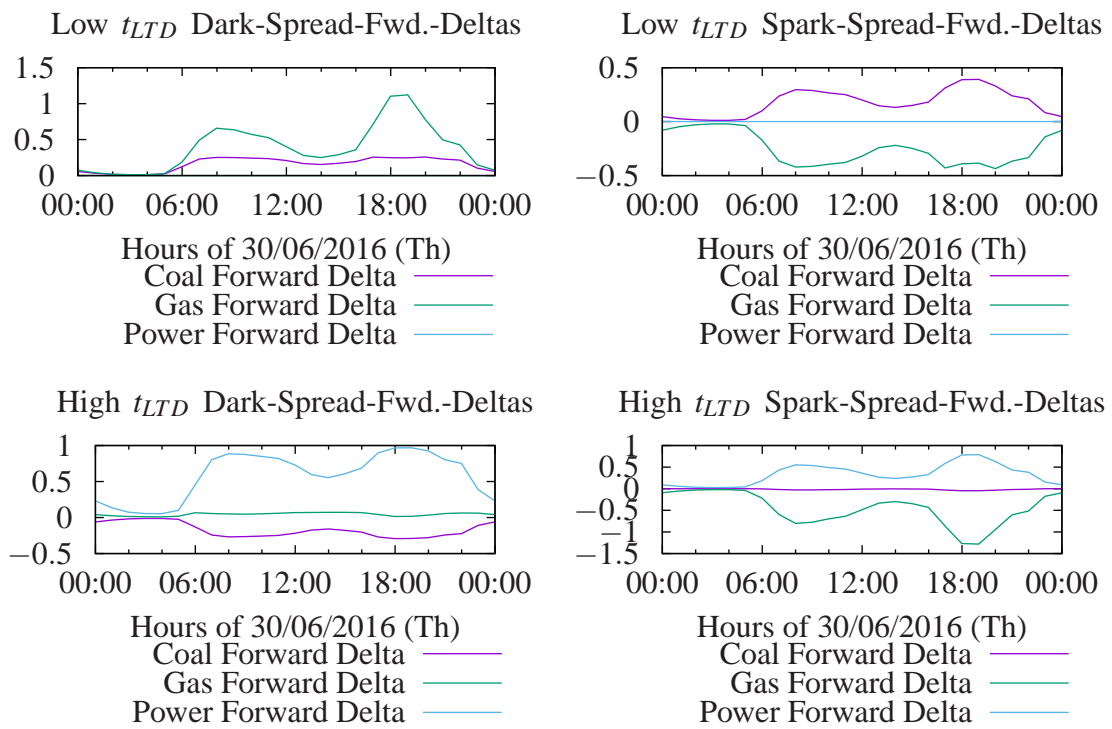


Figure 7.2: Spark (right) and Dark (left) spread option deltas for one weekday of 2016 (30/06/2016, Thursday) when no liquid power forwards available (on top) and when liquid ones available (on bottom).

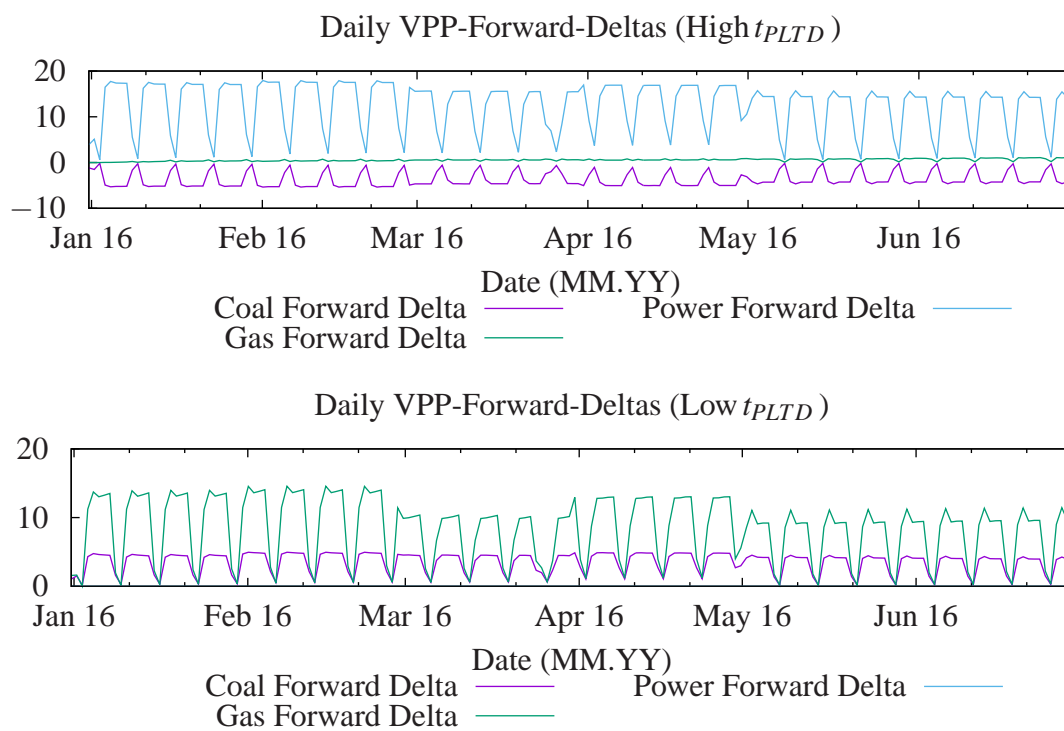


Figure 7.3: Daily VPP forward deltas for 2016 with high  $t_{PLTD}$  based on hourly forward curves in Figure 2.1 (daily deltas are calculated by adding the hourly deltas of a certain day, cf. Corollary 3.1)

## 7.2 Illustrations in case of an Illiquid Power Futures Market

In Chapter 7.1 we have analyzed the hourly deltas to hedge a (simplified) virtual power plant. In detail, we compared two different scenarios: (1) low power forwards liquidity  $t_{PLTD} = 0$  and (2) high power forwards liquidity  $t_{PLTD} > 1$ .

To get a better understanding of the hedging behavior in case of  $t_{PLTD} = 0$ , we calculate deltas for an hourly power forwards profile for January 2016 which is consequently hedged by coal and gas forwards<sup>3</sup>. Again, we use the hourly forward curve of the prior Chapters and the calibration of the structural model in Chapter 4 (i.e. Table 4.2 for estimated bid stack parameters).

As of year end 2015, prices for coal and gas were  $S_0^c = 40$  and  $S_0^g = 14.9$ . Bringing the bid stack parameters into play, we know coal starts to be marginal at a price larger than  $40 \exp(-\log(40) + \log(8.99)) = 8.99$  and gas at a price larger  $14.9 \exp(-\log(14.9) + \log(30.43)) = 30.43$  (using the estimation results in Table 4.2).

The delta hedging strategy of the hourly power forwards of January 2016 over the power forward price is depicted in Figure 7.4.

**Conclusion 7.1 (Gas)** *In case of zero volatility (purple plus-dots), we use gas for delta hedging as soon as the power forward price exceeds 30 EUR/MWh. By increasing volatility, the hedging strategy is becoming smoother (green cross-dots). Therefore, the hedging behavior is as expected.*

**Conclusion 7.2 (Coal)** *Coal forward deltas drop as soon as the electricity price reaches a price of 30 which is the price where gas plants start to produce electricity. Coal deltas do not drop to zero which implies that both fuels are marginal at the same time.*

*However, the model will yield deltas unequal to zero even if coal is not producing electricity (i.e. purple plus-dots and green cross-dots should intuitively drop to zero below a price of 9). The reason is the modeling of negative demand: in order to get a smooth transition from positive to negative demand,  $b_c(0, \mathbf{S}_t^F)$  is used to define  $b_N$  (cf. Appendix A.1):*

$$b_N(D_t, S_t) = \underbrace{\min_{i \in I} b_i(0, S_t^{(i)})}_{=b_c(0, S_t^{(i)})} - \exp(-m_N D_t) + 1. \quad (7.1)$$

*The constant coal forward delta for  $\Pr^Q[D_t < 0] = 1$  is therefore  $\exp(k_c)$  instead of zero. We also get gas deltas unequal to zero for  $\Pr^Q[D_t > \bar{\xi}] = 1$  (spikes).*

---

<sup>3</sup>In case of a high  $t_{PLTD}$ , power futures contracts for January 2016 could be bought to hedge against changes in power prices.

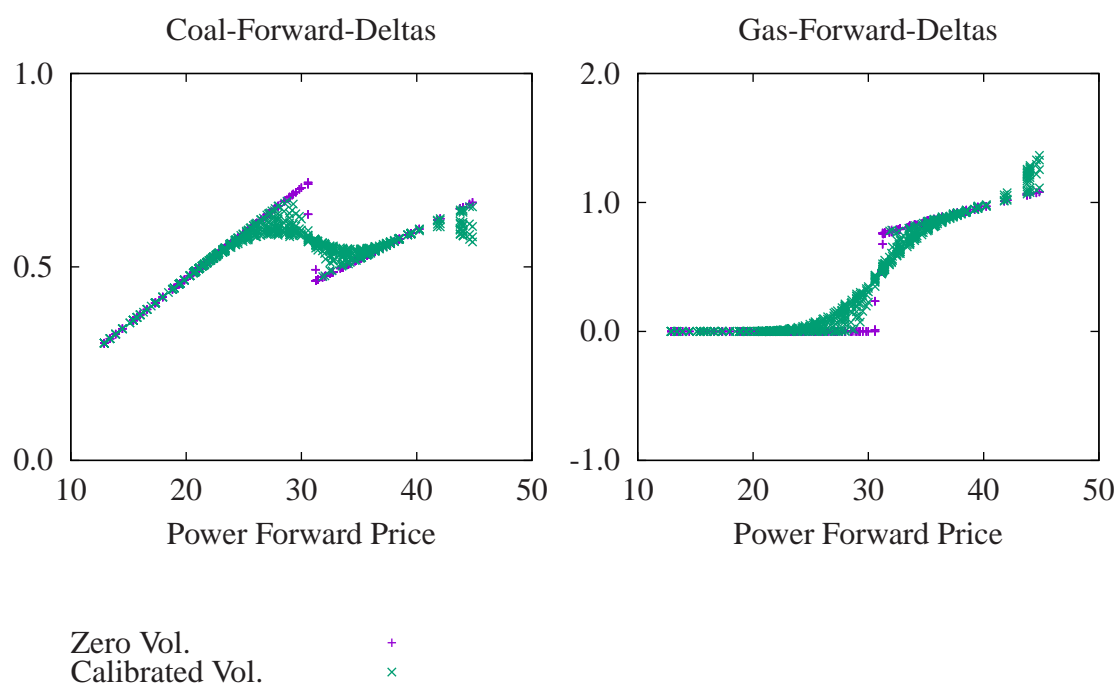


Figure 7.4: Gas and coal forward delta over power forward price for low power forwards liquidity in January 2016



## CHAPTER 8.

# Conclusion

In order to use structural electricity models for dynamic hedging in practice, we - at first - needed to analyze how replication portfolios under this kind of model can be derived. We have shown that delta hedging can be used for that purpose (cf. Chapter 3), at least in case fuels and demand fulfill the Markovian property and the bid stack function is integrable and enables to apply the Itô Lemma. In detail, we concluded electricity forwards to be martingales under  $\mathbb{Q}$ . Furthermore, electricity and fuel forwards behave close to a cointegrated forwards model. In detail, the interconnection of electricity and fuels' forwards is directly implied by the merit order of the market. We believe this to be a relevant result for research. For instance, in [de Jong and Schneider, 2009] a cointegration model for gas and electricity spot prices was investigated. However, they found out cointegration to be mainly observable in forward instead of spot prices. By implying the forwards model directly from the merit order of the market, the model comes close to that observation.

We found that the model delivers two different hedging strategies: one strategy involves to trade power futures contracts and the other does not. In the second case, the uncertainty in power prices is partly hedged by trading in the marginal fuel. However, residual demand remains to be a non-hedgeable risk factor in that case.

Furthermore, we investigated how hedging strategies using futures contracts instead of hourly forwards can be derived (cf. Chapter 3.5). We found out that in our setting we can calculate the hedging strategy in two steps: (i) calculate hourly deltas and (ii) perform an optimization procedure to cover the hourly delta profile with futures contracts. In case of non-overlapping futures contracts, we just sum up the hourly deltas.

In the next step we estimated model parameters based on historical data (cf. Chapter 4). Due to our hedging point of view, we believe that the demand dynamic has to be calibrated directly against electricity forwards data. Consequently, we reflect the volatility of our hedging instruments in the model. In order to realize that idea, we started with observable electricity forwards data and calculated an implied expected demand time series. The estimation procedure turned out to be complex because the expected demand time series itself depends on model parameters as well.

Additionally, we underline the estimation procedure of the bid stack parameters. We started with the idea of [Coulon et al., 2014] to use a mixture density model for that purpose. However, it was - based on our knowledge - the first time that the density function was directly implied by the exponential bid stack model. The density can be derived analytically. Instead of estimating this density directly, we

performed an intermediate step and used a normal density network. Afterward, we used a modification of the Wasserstein distance to link the implied densities and the normal density network to each other. We are even able to calculate the asymptotic covariance matrix of the estimators.

Using the idea of [Bannör and Scherer, 2013], we proceeded to quantify parameter risk in our model (cf. Chapter 4.3 and 4.4). We decided to quantify parameter risk for an hourly price forward curve and a virtual power plant respectively. We found that parameter risk in the bid stack parameters as well as the implied demand volatility are significant risk factors in our model. On the one hand, it might be argued that structural electricity models face too high parameter risk to be applicable for practitioners. On the other hand, based on the value approach for model risk in [Morini, 2011], there are reasons to be cautious in neglecting model parameters which have a strong impact on the derivatives value like the bid stack parameters in our analysis.

After the estimation of model parameters, we observed a high power price volatility for maturities beyond 6 months and hours with high demand (i.e. the option to buy electricity at the regulatory price threshold increases significantly; cf. Figure A.1). We investigated whether approximation methods may compete with ordinary Monte Carlo methods in order to reduce computational runtime. We decided to generalize the common known Kirk formula (cf. Chapter 5). For that purpose we have derived the option price formula for the exponential bid stack model (Chapter 5.4). Based on our knowledge this is the first time that the formula is derived. The formula can also be used to incorporate regulatory price thresholds into a structural model (cf. Appendix A.3). Within a numerical analysis we found out that the Kirk approach can compete with Monte Carlo methods. Even the accuracy of the formula seems to be acceptable for maturities up to two years (below one percent).

Before we tested the model in practice, we analyzed different methods for Greek calculation (cf. Chapter 6). In detail, we compared the difference quotient method to the likelihood ratio method and pathwise derivatives method. For all three methods, we derived algorithms to calculate delta, gamma and vega. We concluded to use the difference quotient method as it combines numerical performance and good convergence speed. However, we found that the likelihood ratio method is a serious competitor for the difference quotient method. Especially, for the calculation of gamma, the likelihood ratio method turns out to have similar convergence speeds but has faster numerical runtimes.



## CHAPTER 9.

# Outlook

Altogether, we believe our research to be relevant likewise for practitioners as well as for researchers. Based on the results, we find the information of the bid stack to be a significant risk factor. Therefore, structural electricity models can deal as an important framework to calculate alternative hedging strategies in practice.

Several topics remain for future research. For example, it may be analyzed how hedging strategies change as soon as interconnection between markets is considered (i.e. Germany and France). Recent progress has been for instance achieved in [Füss et al., 2015].

After the inclusion of interconnectors it would be interesting to further improve the estimator of the bid stack parameters. In Remark 4.7, we propose for instance to refine the optimization procedure on how to come from a normal mixed density function to the bid stack parameters. On the one hand, such an inclusion can lead to more robust estimators (due to a narrowed choice of parameter  $k_i$ ,  $i \in I$ ). On the other hand, the approach introduces a new parameter  $\beta$  which has to be chosen manually before starting the optimization procedure.

Another open issue is the change of merit order during the day. In order to derive a replication portfolio (Chapter 3.3), we need to apply Itô's Lemma. Therefore, if we assume different hours to have different bid stack parameters, we have to ensure the transition from hour to hour to be smooth. It might be interesting to interpret this function to be a stochastic differential equation in order to introduce uncertainty in the bid stack parameters. However, the close form formula for forward prices (Appendix A.2) would have to be extended for that purpose.



# Appendices



## APPENDIX A.

# Additional Results for the Structural Model

In this Chapter we summarize selective results from [Carmona et al., 2013]. Additionally, we give further Propositions on this structural electricity model. We will explicitly underline when proofs have been derived individually within our research and were not taken from other research.

## A.1 Spot Price Formula

It is shown that the spot price formula in [Carmona et al., 2013] has the form

$$S_t^P = b_{\text{low}}(D_t, S_t) \mathbb{I}_{[0; \bar{\xi}^-]}(D_t) + b_{\text{mid}}(D_t, S_t) \mathbb{I}_{(\bar{\xi}^-; \bar{\xi}^+]}(D_t) + b_{\text{high}}(D_t, S_t) \mathbb{I}_{(\bar{\xi}^+; \bar{\xi}]}(D_t),$$

where  $i^- := \operatorname{argmin} \{ \bar{\xi}^c, \bar{\xi}^g \}$ ,  $i^+ := \operatorname{argmax} \{ \bar{\xi}^c, \bar{\xi}^g \}$  and for  $(\xi, \mathbf{s}) \in [0; \bar{\xi}] \times \mathbb{R}_+^2$

$$\begin{aligned} b_{\text{low}}(\xi, \mathbf{s}) &:= b_c(\xi, s^c) \mathbb{I}_{\{b_c(\xi, s^c) < b_g(0, s^g)\}} + b_g(\xi, s^g) \mathbb{I}_{\{b_g(\xi, s^g) < b_c(0, s^c)\}} \\ &\quad + b_{cg}(\xi, \mathbf{s}) \mathbb{I}_{\{b_c(\xi, s^c) \geq b_g(0, s^g), b_g(\xi, s^g) \geq b_c(0, s^c)\}} \\ b_{\text{mid}}(\xi, \mathbf{s}) &:= b_{i^+}(\xi, s^{i^+}) \mathbb{I}_{\{b_{i^+}(\xi, s^{i^+}) < b_{i^-}(0, s^{i^-})\}} + b_{i^+}(\xi - \bar{\xi}^{i^-}, s^{i^+}) \mathbb{I}_{\{b_{i^+}(\xi - \bar{\xi}^{i^-}, s^{i^+}) > b_{i^-}(\bar{\xi}^{i^-}, s^{i^-})\}} \\ &\quad + b_{cg}(\xi, \mathbf{s}) \mathbb{I}_{\{b_{i^+}(\xi, s^{i^+}) \geq b_{i^-}(0, s^{i^-}), b_{i^+}(\xi - \bar{\xi}^{i^-}, s^{i^+}) \leq b_{i^-}(\bar{\xi}^{i^-}, s^{i^-})\}} \\ b_{\text{high}}(\xi, \mathbf{s}) &:= b_c(\xi - \bar{\xi}^g, s^c) \mathbb{I}_{\{b_c(\xi - \bar{\xi}^g, s^c) > b_g(\bar{\xi}^g, s^g)\}} + b_g(\xi - \bar{\xi}^c, s^g) \mathbb{I}_{\{b_g(\xi - \bar{\xi}^c, s^g) > b_c(\bar{\xi}^c, s^c)\}} \\ &\quad + b_{cg}(\xi, \mathbf{s}) \mathbb{I}_{\{b_c(\xi - \bar{\xi}^g, s^c) \leq b_g(\bar{\xi}^g, s^g), b_g(\xi - \bar{\xi}^c, s^g) \leq b_c(\bar{\xi}^c, s^c)\}}, \end{aligned}$$

and

- $b_{cg}((s_g, s_c), \xi) := s_c^{\alpha_c} s_g^{\alpha_g} \exp(\beta + \gamma \xi)$
- $\alpha_i = \frac{m_i}{m_c + m_g}$
- $\beta = \frac{k_c m_g + k_g m_c}{m_c + m_g}$
- $\gamma = \frac{m_c m_g}{m_c + m_g}$
- $b_i, \bar{\xi}_i$  as defined in Chapter 2.1.

In order to define the power spot price for negative demand and demand higher than market capacity, the spot formula is extended as follows:

1.  $D_t < 0$ :

$$b_N(D_t, S_t) = b(0, S_t) - \exp(-m_N D_t) + 1$$

2.  $D_t > \bar{\xi}^c + \bar{\xi}^g$ :

$$b_S(D_t, S_t) = b(\bar{\xi}^c + \bar{\xi}^g, S_t) + \exp(m_S(D_t - \bar{\xi}^c - \bar{\xi}^g)) - 1.$$

The next Proposition was derived during our research and was not taken from other literature.

**Proposition A.1 (Continuity of the Exponential Bid Stack)**  $b_{low}, b_{mid}$  and  $b_{high}$  are continuous functions.

**Proof.** We show the proof for  $b_{low}$ .  $b_{low}$  consists of three different kind of exponential (and continuous) functions  $b_c, b_g, b_{cg}$  which are connected via indicator functions. We have to proof  $b_{low}$  to be continuous on  $\{\xi \in [0, \bar{\xi}^{i-}], s_c, s_g \in \mathbb{R}^+ : b_i(\xi, s^i) = b_j(0, s^j)\}$  for  $i, j \in \{c, g\}$  and  $i \neq j$  being the sets where transitions of those three functions take place. It leads us to proof for  $i, j \in \{c, g\}$  and  $i \neq j$  the implication

$$b_i(\xi, s^i) = b_j(0, s^j) \text{ for some } \xi, s^i, s^j \in \mathbb{R} \Rightarrow b_i(\xi, s^i) = b_{cg}(\xi, \mathbf{s}).$$

Therefore, let  $\xi, s^i, s^j \in \mathbb{R}$  be such that  $b_i(\xi, s^i) = b_j(0, s^j)$ . It holds  $\xi = (\ln(s^j/s^i) + k_j - k_i)/m_i$  and

$$\begin{aligned} b_{cg}(\xi, \mathbf{s}) &\stackrel{\text{Def.}}{=} s_c^{\frac{m_g}{m_g+m_c}} s_g^{\frac{m_c}{m_g+m_c}} \exp\left(\frac{k_c m_g + k_g m_c}{m_c + m_g} + \frac{m_c m_g}{m_c + m_g} \xi\right) \\ &= s_i^{\frac{m_j - m_c m_g / m_i}{m_g + m_c}} s_j^{\frac{m_i + m_c m_g / m_i}{m_g + m_c}} \exp\left(\frac{k_c m_g + k_g m_c}{m_c + m_g} + \frac{m_c m_g (k_j - k_i)}{(m_c + m_g) m_i}\right) \\ &= b_j(0, s^j) = b_i(\xi, s^i). \end{aligned}$$

■

**Proposition A.2 (Lipschitz Continuity)**  $b_{low}, b_{mid}$  and  $b_{high}$  are Lipschitz continuous on  $[0, \bar{\xi}^{i-}] \times [a, b]^2$ ,  $[\bar{\xi}^{i-}, \bar{\xi}^{i+}] \times [a, b]^2$  and  $[\bar{\xi}^{i+}, \bar{\xi}] \times [a, b]^2$  respectively for  $[a, b] \subset \mathbb{R}^+$  arbitrary but fix.

**Proof.** From Proposition A.1, we know each of the functions to be continuous. For  $\xi_1, \xi_2 \in [0, \bar{\xi}^{i-}]$  and  $\mathbf{s}_1, \mathbf{s}_2 \in \mathbb{R}^2$ , we proof the Proposition for  $b_{low}$ . Let  $[a, b] \subset \mathbb{R}^+$  be given. We define

$$A_i := \{\xi \in [0, \bar{\xi}^{i-}], s_c, s_g \in [a, b] : b_i(\xi, s^i) < b_j(0, s^j)\} \text{ for } i, j \in \{c, g\}$$

and

$$B := \{\xi \in [0, \bar{\xi}^{i-}], s_c, s_g \in [a, b] : b_i(\xi, s^i) \geq b_j(0, s^j) \forall i, j \in \{c, g\}\}.$$

Due to continuity, it holds

$$|b_{low}(\xi_1, \mathbf{s}_1) - b_{low}(\xi_2, \mathbf{s}_2)| \leq \max \left\{ \sup_{(d, \mathbf{s}) \in A_i, i \in I} \{\|Db_i(d, \mathbf{s})\|_\infty\}, \sup_{(d, \mathbf{s}) \in B} \{\|Db_{cg}(d, \mathbf{s})\|_\infty\} \right\}$$

$$\left\| \begin{pmatrix} \xi_1 - \xi_2 \\ \mathbf{s}_1 - \mathbf{s}_2 \end{pmatrix} \right\|.$$

The overall maximum is smaller than infinity on  $[0, \bar{\xi}^{i-}] \times [a, b]^2$  due to

$$\begin{aligned} Db_c(d, \mathbf{s}) &= \begin{pmatrix} m_c b_c(d, \mathbf{s}) & \exp(k_c + m_c d) & 0 \end{pmatrix}, \\ Db_g(d, \mathbf{s}) &= \begin{pmatrix} m_g b_g(d, \mathbf{s}) & 0 & \exp(k_g + m_g d) \end{pmatrix}, \\ Db_{cg}(d, \mathbf{s}) &= \begin{pmatrix} \gamma b_{cg}(d, \mathbf{s}) & \frac{\alpha_c b_{cg}(d, \mathbf{s})}{s_c} & \frac{\alpha_g b_{cg}(d, \mathbf{s})}{s_g} \end{pmatrix} \end{aligned}$$

being less than infinity for each component on  $[0, \bar{\xi}^{i-}] \times [a, b]^2$ . ■

## A.2 Forward Price Formula

We present the closed form forward price formula derived in [Carmona et al., 2013] for the case of two fuels (i.e. coal and gas).

Let  $\Phi_1(\cdot)$  be the univariate cumulative standard normal distribution and  $\Phi_2(\cdot, \cdot; \rho)$  the bivariate cumulative standard distribution. We define

$$\Phi_2^{2 \times 1} \left( \begin{bmatrix} x_1 \\ x_2 \end{bmatrix}, y; \rho \right) := \Phi_2(x_1, y, \rho) - \Phi_2(x_2, y, \rho). \quad (\text{A.1})$$

Furthermore, we assume the log-prices of both fuels (gas and coal) as well as the residual demand to be normally distributed with mean  $\mu_i$  and variance  $\sigma_i$  ( $i = c, g, d$ ). In detail, it is assumed that

$$D_t = \min(\bar{\xi}, \max(0, X_t)), \text{ where } X_t \stackrel{\mathcal{D}}{=} \mathcal{N}(\mu_d, \sigma_d^2), \quad (\text{A.2})$$

where  $\{X_t \geq \bar{\xi}\}$  and  $\{X_t \leq 0\}$  may be used to implement spikes for  $X_t \geq \bar{\xi}$  and negative prices for  $X_t \leq 0$ . The fuels are assumed to be correlated with a factor  $\rho$  whereas the demand is assumed to behave independently of the fuel prices.

The power forward price is then

$$\begin{aligned} F_t^P &= \sum_{i \in I} \exp\left(\frac{m_i^2 \sigma_d^2}{2}\right) \left\{ b_i(\mu_d, F_t^i) \Phi_2^{2 \times 1} \left( \begin{bmatrix} \frac{\bar{\xi}^i - \mu_d}{\sigma_d} - m_i \sigma_d \\ \frac{-\mu_d}{\sigma_d} - m_i \sigma_d \end{bmatrix}, \frac{R_i(\mu_d, 0) - m_i^2 \sigma_d^2}{\sigma_{i,d}}, \frac{m_i \sigma_d}{\sigma_{i,d}} \right) \right. \\ &\quad \left. + b_i(\mu_d - \bar{\xi}^j, F_t^i) \Phi_2^{2 \times 1} \left( \begin{bmatrix} \frac{\bar{\xi}^i - \mu_d}{\sigma_d} - m_i \sigma_d \\ \frac{\bar{\xi}^j - \mu_d}{\sigma_d} - m_i \sigma_d \end{bmatrix}, \frac{-R_i(\mu_d - \bar{\xi}^j, \bar{\xi}^j) + m_i^2 \sigma_d^2}{\sigma_{i,d}}, \frac{-m_i \sigma_d}{\sigma_{i,d}} \right) \right\} \\ &\quad + \sum_{i \in I} \delta_i \exp(\eta) b_{cg}(\mu_d, \mathbf{F}_t) \left\{ -\Phi_2^{2 \times 1} \left( \begin{bmatrix} \frac{\bar{\xi}^i - \mu_d}{\sigma_d} - \gamma \sigma_d \\ \frac{-\mu_d}{\sigma_d} - \gamma \sigma_d \end{bmatrix}, \frac{R_i(\mu_d, 0) + \alpha_j \sigma^2 - \gamma m_i \sigma_d^2}{\delta_i \sigma_{i,d}}, \frac{m_i \sigma_d}{\delta_i \sigma_{i,d}} \right) \right. \\ &\quad \left. + \Phi_2^{2 \times 1} \left( \begin{bmatrix} \frac{\bar{\xi}^i - \mu_d}{\sigma_d} - \gamma \sigma_d \\ \frac{\bar{\xi}^j - \mu_d}{\sigma_d} - \gamma \sigma_d \end{bmatrix}, \frac{R_i(\mu_d - \bar{\xi}^j, \bar{\xi}^j) + \alpha_j \sigma^2 - \gamma m_i \sigma_d^2}{\delta_i \sigma_{i,d}}, \frac{m_i \sigma_d}{\delta_i \sigma_{i,d}} \right) \right\} \\ &\quad + \Phi_1\left(\frac{-\mu_d}{\sigma_d}\right) \sum_{i \in I} b_i(0, F_t^i) \Phi_1\left(\frac{R_i(0, 0)}{\sigma}\right) + \Phi_1\left(\frac{\mu_d - \bar{\xi}}{\sigma_d}\right) \sum_{i \in I} b_i(\bar{\xi}^i, F_t^i) \Phi_1\left(\frac{-R_i(\bar{\xi}^i, \bar{\xi}^j)}{\sigma}\right), \end{aligned}$$

$$=: F_{BS}(t, F_{t,T}^{(1)}, \dots, F_{t,T}^{(n)}, \mu_{t,T}^D) \quad (\text{A.3})$$

where

- $\mathbf{F}_t = (F_t^g, F_t^c)$  : Forward Prices of the fuels for the given maturity
- $j = I \setminus \{i\}$
- $\sigma^2 = \sigma_c^2 - 2\rho\sigma_c\sigma_g + \sigma_g^2$
- $R_i(\xi_i, \xi_j) := k_j + m_j\xi_j - k_i - m_i\xi_i + \ln(F_t^j) - \ln(F_t^i) - \frac{1}{2}\sigma^2$
- $\eta = \frac{\gamma^2\sigma_d^2 - \alpha_c\alpha_g\sigma^2}{2}$
- $\sigma_{i,d}^2 = m_i^2\sigma_d^2 + \sigma^2$
- $\delta_i = \begin{cases} 1 & \text{for } i = c \\ -1 & \text{else} \end{cases}$

In case price spikes (for  $D_t > \bar{\xi}$ ) and negative demand shall be included the following terms have to be added

$$\begin{aligned} & \exp\left(m_S(\mu_d - \bar{\xi}) + \frac{1}{2}m_S^2\sigma_d^2\right) \Phi_1\left(\frac{\mu_d - \bar{\xi}}{\sigma_d} + m_S\sigma_d\right) - \Phi_1\left(\frac{\mu_d - \bar{\xi}}{\sigma_d}\right) \\ & - \exp\left(-m_N\mu_d + \frac{1}{2}m_N^2\sigma_d^2\right) \Phi_1\left(m_N\sigma_d - \frac{\mu_d}{\sigma_d}\right) + \Phi_1\left(\frac{-\mu_d}{\sigma_d}\right). \end{aligned}$$

The next Proposition was derived during our research and was not taken from other literature.

**Lemma A.1 (Strong Monotony)** *Let the fuels and demand dynamics in Section 2.2 be given. If  $m_c, m_g, m_N, m_S > 0$ , it holds for the exponential bid stack:*

1.  $\forall d_1, d_2 \in \mathbb{R} : d_1 < d_2 \Rightarrow f_{BS}(d_1, \mathbf{s}) < f_{BS}(d_2, \mathbf{s}) \quad \forall \mathbf{s} \in \mathbb{R}^2,$
2.  $\forall \mu_d^1, \mu_d^2 : \mu_d^1 < \mu_d^2 \Rightarrow F_{BS}(T-t, F_{t,T}^{(1)}, F_{t,T}^{(2)}, \mu_d^1) < F_{BS}(t, F_{t,T}^{(1)}, F_{t,T}^{(2)}, \mu_d^2), \quad \forall T > t,$   
 $\forall F_{t,T}^{(1)}, F_{t,T}^{(2)} > 0.$

**Proof.** Let  $d \in [0, \bar{\xi}]$  be given. Due to  $m_c, m_g > 0$ ,  $b_c, b_g$  and  $b_c^{-1}, b_g^{-1}$  are strongly monotonically increasing on their defined intervals. In [Carmona et al., 2013], it is shown

$$f_{bs}(d, \mathbf{s}) = \min_{i \in I} b_i(0, s^i) \vee \sup \left\{ p \in \mathbb{R} : \sum_{i \in I} b_i^{-1}(\cdot, s^i)(p) < d \right\}$$

leading the supremum to increase strongly monotonically after an increase of  $d$ . Strong monotony also holds for  $d \in \mathbb{R} \setminus [0, \bar{\xi}]$  due to the continuous transition by construction and  $m_N, m_S > 0$ .

We use the first statement to prove the second. Let  $\mu_d^1, \mu_d^2 > 0$  with  $\mu_d^1 < \mu_d^2$  as well as  $\mathbf{s} \in \mathbb{R}^2$  and  $F_{t,T}^{(1)}, F_{t,T}^{(2)} > 0$  be arbitrary but fix. It holds due to the risk-neutral valuation and the tower property:



$$\begin{aligned}
F_{BS}(t, F_{t,T}^{(1)} F_{t,T}^{(2)}, \mu_d^2) &= \mathbb{E}^{\mathbb{Q}} [f_{bs}(D_T, \mathbf{S}_T^F) | \mathcal{F}_t] \\
&= \mathbb{E}^{\mathbb{Q}} \left[ \mathbb{E}^{\mathbb{Q}} [f_{bs}(D_T, \mathbf{S}_T^F) | \mathcal{F}_T^{\mathbf{W}} \vee \mathcal{F}_t^D] | \mathcal{F}_t^{\mathbf{W}} \vee \mathcal{F}_t^D \right]
\end{aligned}$$

which is why we prefer to analyze further with a fix  $\mathbf{s} \in \mathbb{R}^2$  and integrate over demand first. By taking a look at the difference and use the demand to be normally distributed with mean  $\mu_d^1$  and  $\mu_d^2$  respectively as well as variance  $\sigma_d^2 > 0$ , we get

$$\begin{aligned}
&\int_{\mathbb{R}} f_{bs}(x, \mathbf{s}) \phi^{0,1} \left( \frac{x - \mu_d^2}{\sigma_d} \right) \frac{1}{\sigma_d} dx - \int_{\mathbb{R}} f_{bs}(x, \mathbf{s}) \phi^{0,1} \left( \frac{x - \mu_d^1}{\sigma_d} \right) \frac{1}{\sigma_d} dx \\
&= \int_{\mathbb{R}} (f_{bs}(\sigma_d x + \mu_d^2, \mathbf{s}) - f_{bs}(\sigma_d x + \mu_d^1, \mathbf{s})) \phi^{0,1}(x) dx
\end{aligned}$$

being greater than zero for all  $x \in \mathbb{R}$  due to the strong monotony of  $f_{BS}$ . The sum remains to be positive after integrating over the fuels leading to the second statement in the Lemma. ■

### A.3 Extension of the Forward Price Formula to Price Thresholds

The insights and considerations within this Chapter are based on our research. We believe it to be the first time that price thresholds are considered for the exponential bid stack in Chapter A.1.

Based on the estimation of the demand dynamic in Chapter 4.2.3, we observe an European electricity call option with strike 3.000 EUR/MWh to have a positive value for maturities beyond 9 months (cf. Figure A.1). Of course, price thresholds in the Western European market expose the option price to have a value of zero (price threshold at 3.000 EUR/MWh) which is why we extended the exponential bid stack with two marginal fuels (cf. Chapter 2.1) to capture that behavior.

We concentrate on positive thresholds in the electricity day ahead (spot) market in this Chapter. However, similar calculations may be performed to deal with negative price thresholds (i.e. -500 EUR/MWh at EEX Spot).

By considering a positive regulatory price threshold  $K_{Up} > 0$ , the risk-neutral payoff of a power forward contract becomes

$$\begin{aligned}
F_{t,T}^P &= \mathbb{E}^{\mathbb{Q}} [S_T^P | \mathcal{F}_t] = \mathbb{E}^{\mathbb{Q}} [\min \{f_{bs}(D_t, \mathbf{S}_t^F), K_{Up}\} | \mathcal{F}_t] \\
&= \mathbb{E}^{\mathbb{Q}} [f_{bs}(D_t, \mathbf{S}_t^F) | \mathcal{F}_t] - \mathbb{E}^{\mathbb{Q}} [\max \{f_{bs}(D_t, \mathbf{S}_t^F) - K_{Up}, 0\} | \mathcal{F}_t]
\end{aligned}$$

being the forward price without threshold minus a call option with strike  $K_{Up}$ . In Chapter 5.4, a close form formula for European Call Options under the exponential bid stack with two marginal fuels (cf. Chapter 2.1) is derived. However, for a positive spike regime  $m_S > 0$ , the formula gets semi-analytic leading the formula to be too time-consuming to be useable for our calibration purposes (calculation of implied demand seasonality; cf. Definition 2.1). Therefore, we use the following simplification when calculating the implied demand seasonality:

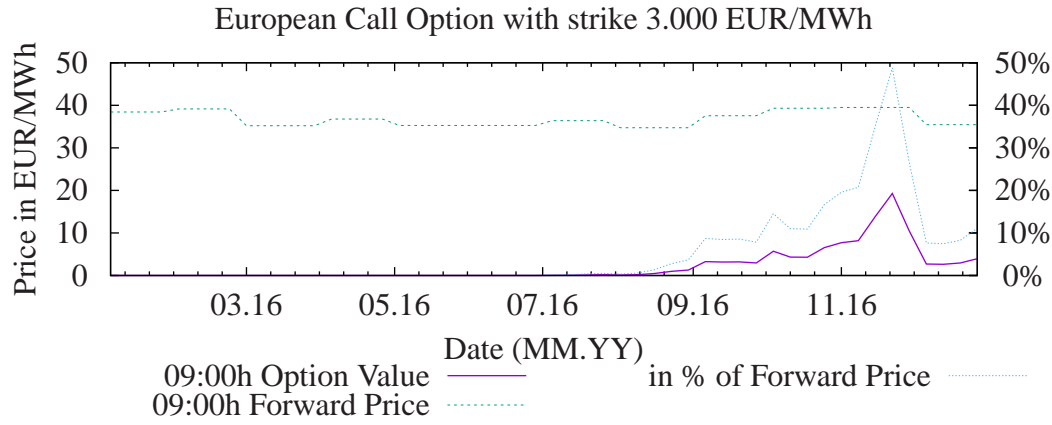


Figure A.1: European Call Option value for each Tuesday of 2016 at 9.00h am. The valuation was done after a complete historical estimation of all model parameters of the structural electricity model in Chapter 2 as been described in Chapter 4.

The payoff for  $D_t > \bar{\xi}$  leads to

$$\mathbb{E}^{\mathbb{Q}} \left[ \max \left\{ b(\bar{\xi}^c + \bar{\xi}^g, S_t) + \exp(m_S(D_t - \bar{\xi}^c - \bar{\xi}^g)) - 1 - K_{Up}; 0 \right\} \middle| \mathcal{F}_t \right].$$

Because we deal with a high  $K_{Up} = 3.000$  the bid stack is quite steep in that area. It follows that the probability for a positive payoff is mainly caused by  $D_t$  instead of the fuels  $S_t^F$ . We therefore focus on the case of high demand such that

$$\exp(m_S(D_t - \bar{\xi}^c - \bar{\xi}^g)) - 1 - K_{Up} > 0.$$

Consequently, the maximum vanishes and integration can be performed analytically similarly to the forward price formula.

## APPENDIX B.

# Additional Insights on Calibration and Parameter Risk

## B.1 Selective Results from Asymptotic Statistics

The following Propositions are from [van der Vaart, 2000].

**Proposition B.1 (General Delta- Method)** *Let  $\phi : \mathbb{D}_\phi \subset \mathbb{R}^k \mapsto \mathbb{R}^m$  be a map defined on a subset of  $\mathbb{R}^k$  and differentiable at  $\theta$ . Let  $\phi'$  be the according Jacobian matrix. Let  $T_n$  be random vectors taking their values in the domain of  $\phi$ . If  $r_n(T_n - \theta) \xrightarrow{\mathcal{D}} T$  for numbers  $r_n \rightarrow \infty$ , then  $r_n(\phi(T_n) - \phi(T)) \xrightarrow{\mathcal{D}} \phi'_\theta(T)$ . Moreover, the difference between  $r_n(\phi(T_n) - \phi(T))$  and  $\phi'_\theta(r_n(T_n - \theta))$  converges to zero in probability.*

**Corollary B.1 (Delta- Method)** *For  $r_n = \sqrt{n}$  in Proposition B.1,  $\sqrt{n}(T_n - \theta)$  converges to a multivariate normal distribution  $\mathcal{N}_k(\mu, \Sigma)$ . Then the sequence  $\sqrt{n}(\phi(T_n) - \phi(T))$  converges in law to the  $\mathcal{N}_m(\phi'_\theta \mu, \phi'_\theta \Sigma (\phi'_\theta)^T)$  distribution.*

**Proposition B.2 (Asymptotical Properties of the Z-Estimator)** *For each  $\theta$  in an open subset of Euclidean space, let  $x \mapsto \Psi_\theta(x)$  be a measurable vector-valued function such that, for every  $\theta_1$  and  $\theta_2$  in a neighborhood of  $\theta_0$  and a measurable function  $\dot{\Psi}$  with  $\mathbb{P}\dot{\Psi}^2 < \infty$ ,*

$$\|\Psi_{\theta_1}(x) - \Psi_{\theta_2}(x)\| \leq \dot{\Psi}(x) \|\theta_1 - \theta_2\|.$$

*Assume that  $\mathbb{P}\|\Psi_{\theta_0}\|^2 < \infty$  and that the map  $\theta \mapsto \mathbb{P}\Psi_\theta$  is differentiable at a zero  $\theta_0$ , with nonsingular derivative matrix  $V_{\theta_0}$ . If  $\mathbb{P}_n \Psi_{\hat{\theta}_n} = o_P(n^{-1/2})$ , and  $\hat{\theta}_n \xrightarrow{\mathbb{P}} \theta_0$ , then*

$$\sqrt{n}(\hat{\theta}_n - \theta_0) = -V_{\theta_0}^{-1} \frac{1}{\sqrt{n}} \sum_{i=1}^n \Psi_{\theta_0}(X_i) + o_P(1),$$

*In particular, the sequence  $\sqrt{n}(\hat{\theta}_n - \theta_0)$  is asymptotically normal with mean zero and covariance matrix*

$$V_{\theta_0}^{-1} \mathbb{P}(\Psi_{\theta_0} \Psi_{\theta_0}^T) V_{\theta_0}^{-T}.$$

## B.2 Selective Results from Multiple Time Series Analysis

The following Proposition is from [Lütkepohl, 2007] (ML=Maximum Likelihood). For the purpose of the Proposition, we need the following notations.

**Notation B.1** Let  $\mathbf{A} = (\mathbf{a}_1, \dots, \mathbf{a}_n) \in \mathbb{R}^{m \times n}$ . The *vec*-operator transforms  $\mathbf{A}$  into an  $(mn \times 1)$  vector by stacking the columns, that is,

$$\text{vec}(\mathbf{A}) := \begin{bmatrix} \mathbf{a}_1 \\ \vdots \\ \mathbf{a}_n \end{bmatrix} \in \mathbb{R}^{mn}.$$

**Notation B.2** Let  $\mathbf{A} = (a_{ij}) \in \mathbb{R}^{m \times n}$  and  $\mathbf{B} = (b_{ij}) \in \mathbb{R}^{p \times q}$ . We denote

$$\mathbf{A} \otimes \mathbf{B} := \begin{bmatrix} a_{11}\mathbf{B} & \cdots & a_{1n}\mathbf{B} \\ \vdots & & \vdots \\ a_{m1}\mathbf{B} & \cdots & a_{mn}\mathbf{B} \end{bmatrix} \in \mathbb{R}^{mp \times nq}.$$

**Notation B.3** Let  $\mathbf{A} = (a_{ij}) \in \mathbb{R}^{m \times m}$ . The *vech*-operator stacks the elements on and below the main diagonal of a symmetric square matrix. We denote

$$\text{vech}(\mathbf{A}) := [a_{11}, \dots, a_{m1}, a_{22}, \dots, a_{m2}, \dots, a_{mm}]^T \in \mathbb{R}^{m(m+1)/2}.$$

**Definition B.1 (Duplication Matrix)** The duplication matrix  $\mathbf{D}_m$  is defined so that, for any symmetric  $\mathbf{A} = (a_{ij}) \in \mathbb{R}^{m \times m}$ ,

$$\text{vec}(\mathbf{A}) = \mathbf{D}_m \text{vech}(\mathbf{A}).$$

**Proposition B.3 (Asymptotic Properties of the Restricted ML Estimators)** Let a VAR( $p$ ) process be given by Definition 4.2. Suppose that linear constraints are given in the form

$$\boldsymbol{\beta} := \text{vec}(\mathbf{B}) = \mathbf{R}\boldsymbol{\gamma} + \mathbf{r},$$

where  $\boldsymbol{\beta} \in \mathbb{R}^{K(Kp+1)}$ ,  $\mathbf{R} \in \mathbb{R}^{K(Kp+1) \times M}$ ,  $\boldsymbol{\gamma} \in \mathbb{R}^M$  and  $\mathbf{r} \in \mathbb{R}^{K(Kp+1)}$ .

Then, the ML estimators  $\tilde{\boldsymbol{\beta}}$  and  $\tilde{\boldsymbol{\sigma}} = \text{vech}(\tilde{\boldsymbol{\Sigma}}_u)$  are given by ( $\mathbf{I}_K := \text{diag}(1, \dots, 1) \in \mathbb{R}^{K \times K}$ )

$$\begin{aligned} \tilde{\boldsymbol{\gamma}} &= \left[ \mathbf{R}^T (\mathbf{Z}\mathbf{Z}^T \otimes \tilde{\boldsymbol{\Sigma}}_u^{-1}) \mathbf{R} \right]^{-1} \mathbf{R}^T (\mathbf{Z} \otimes \tilde{\boldsymbol{\Sigma}}_u^{-1}) \mathbf{z}, \\ \tilde{\boldsymbol{\Sigma}}_u &= \frac{1}{T} (\mathbf{Y} - \tilde{\mathbf{B}}\mathbf{Z})(\mathbf{Y} - \tilde{\mathbf{B}}\mathbf{Z})^T, \\ \mathbf{z} &= \text{vec}(\mathbf{Y}) - (\mathbf{Z}^T \otimes \mathbf{I}_K) \mathbf{r}. \end{aligned}$$

They are consistent and asymptotically normally distributed,

$$\sqrt{T} \begin{bmatrix} \tilde{\boldsymbol{\beta}} - \boldsymbol{\beta} \\ \tilde{\boldsymbol{\sigma}} - \boldsymbol{\sigma} \end{bmatrix} \xrightarrow{\mathcal{D}} \mathcal{N} \left( 0, \begin{bmatrix} \mathbf{R}[\mathbf{R}^T (\Gamma \otimes \boldsymbol{\Sigma}_u^{-1}) \mathbf{R}]^{-1} \mathbf{R}^T & 0 \\ 0 & 2\mathbf{D}_K^+(\boldsymbol{\Sigma}_u \otimes \boldsymbol{\Sigma}_u)(\mathbf{D}_K^+)^T \end{bmatrix} \right),$$

where  $\mathbf{D}_K^+ = (\mathbf{D}_K^T \mathbf{D}_K)^{-1} \mathbf{D}_K^T$  is the Moore-Penrose inverse of the duplication matrix  $\mathbf{D}_K \in \mathbb{R}^{K^2 \times K(K+1)/2}$  and

$$\Gamma := \mathbb{E} [\mathbf{Z}_t \mathbf{Z}_t^T].$$

## B.3 Choice of Model Volatility for Expected Demand

The analysis below is based on the historical estimation given by Proposition 4.4. The following investigations belong to our research and are not cited from other literature.

Proposition 4.4 assumes  $v^D$  to be known which is why it is worth to analyse the impact in the choice of this parameter. For that purpose Figure B.1 depicts the implied expected demand volatility over  $\tau$  as well as the implied demand spot volatility over  $t > t_0$ . The implied spot volatility increases by increasing  $v$ . Consequently, get larger PVs for a larger choice of  $v$ , even if we estimate mean-reversion speed from historical data afterwards (cf. Figure B.2).

Additionally, Figure B.1 (left) reveals that the implied expected demand forwards volatility gets close to  $v^D$  for small  $\tau$ . Because of  $D_t = \lim_{T \searrow t} \mu_{t,T}$ , we should therefore choose  $v^D$  such that we match power spot volatility. To proof that, we calculate the implied expected demand variance for small  $\tau$  and  $\Delta t$  ( $t_0 = 0$ ) and apply Taylor expansion in  $t = 0$ :

$$\begin{aligned} \int_{t_0}^{t_0+\Delta t} (v_s^D)^2 \exp\left(-2 \int_s^{t_0+\tau} \alpha_u^D du\right) ds &= (v^D)^2 \int_{t_0}^{t_0+\Delta t} \exp(-2(t_0 + \tau - s)\alpha_1^D) ds \\ &= \frac{(v^D)^2}{2\alpha_1^D} [\exp(-2(\tau - \Delta t)\alpha_1^D) - \exp(-2\tau\alpha_1^D)] \\ &\approx \frac{(v^D)^2}{2\alpha_1^D} [-2(\tau - \Delta t)\alpha_1^D + 2\tau\alpha_1^D] \\ &= (v^D)^2 \Delta t. \end{aligned}$$

For the annualized volatility we therefore get  $v^D$ .

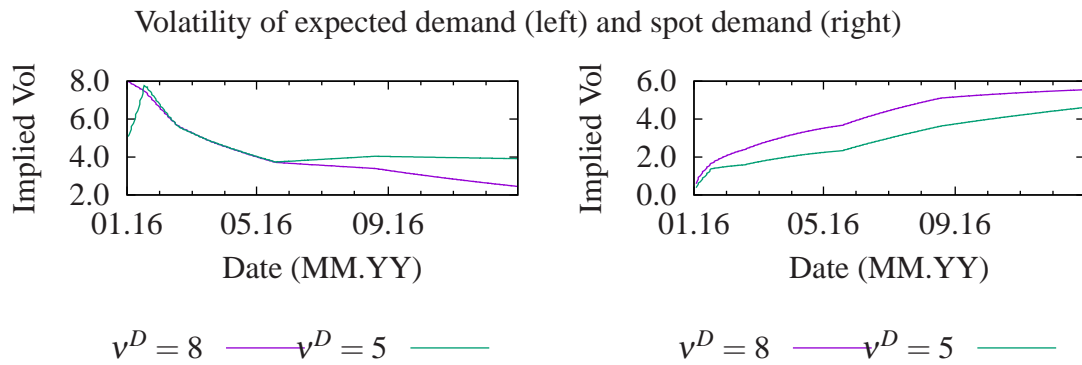


Figure B.1: Implied expected demand forwards volatility over  $\tau$  (left) and implied demand spot volatility over  $t > t_0$  (right) for different choices of  $v^D$  and calibrated bid stack parameters in Table 4.2; we used Proposition 4.4 to estimate mean-reversion speed.

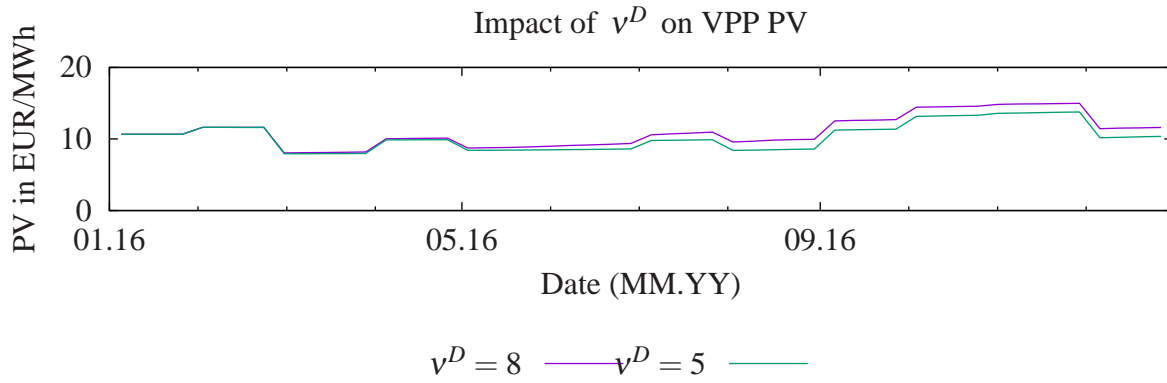


Figure B.2: PV of a coal VPP over time for different choices of  $v^D$ ; we used Proposition 4.4 to estimate mean-reversion speed. We used 10 million paths for a Monte Carlo method.

## B.4 Additional Visualizations

This Chapter gives further visualizations in the context of the calculation of parameter risk for a structural model. We depict sensitivities as well as parameter risk for each payoff of a coal VPP separately.

### B.4.1 Daily VPP Sensitivities

This Chapter depicts the parameter sensitivities (first order derivatives) of a coal VPP for the first 6 months of 2016 as of year-end 2015.

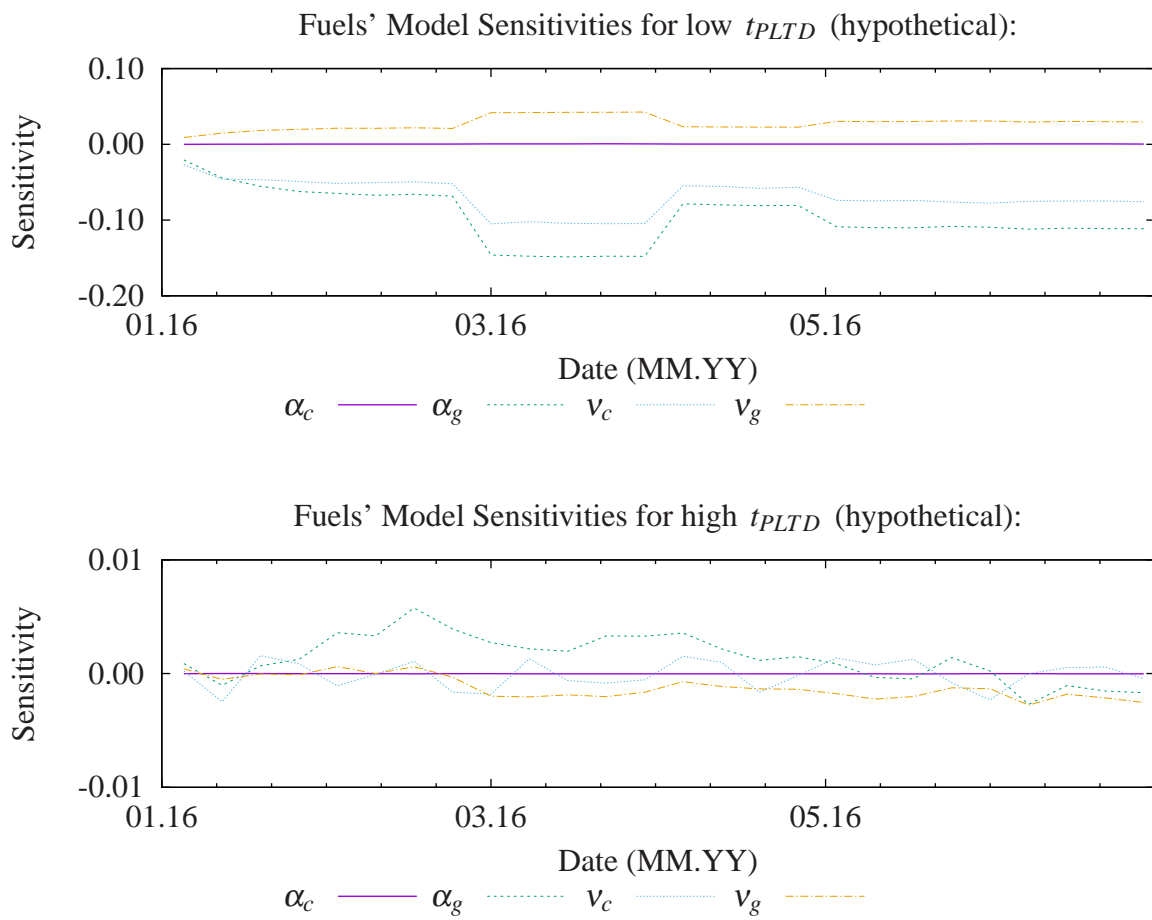


Figure B.3: Sensitivity of model parameters for one hour of a coal VPP in 2016 (08:00h-9:00h) based on historical spot estimation. The graphic on top depicts the sensitivity in case of a low power forwards liquidity and the graphic below for a high power forwards liquidity.

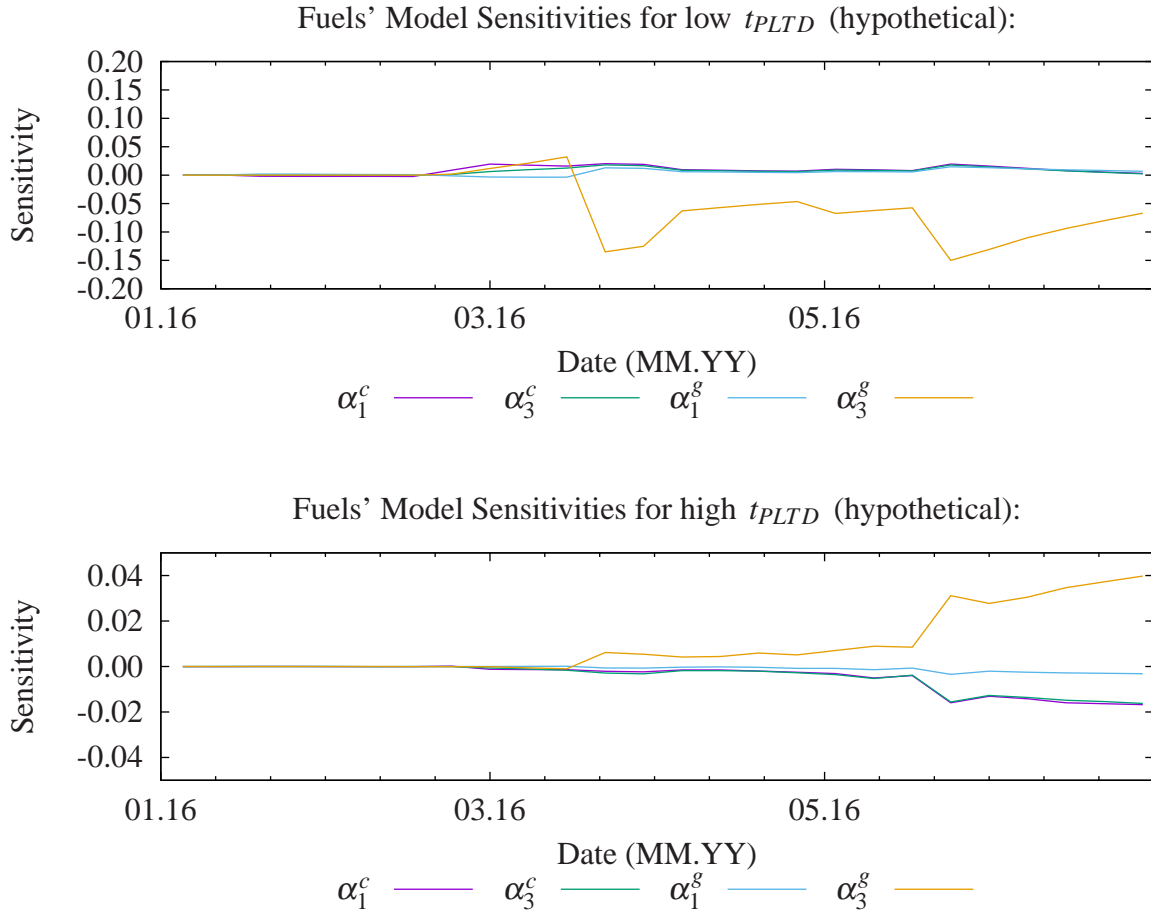
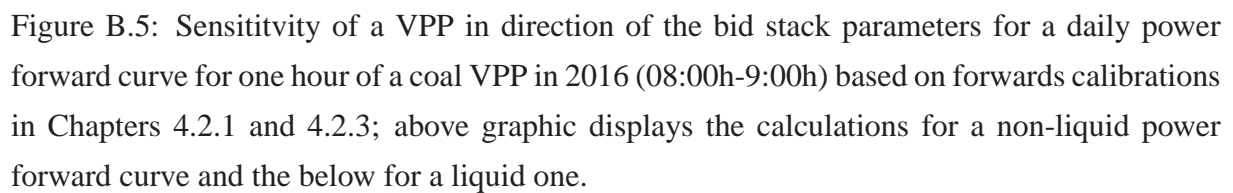


Figure B.4: Sensitivity of model parameters (only the first and the last entry of  $\alpha_t^{(i)}$  and  $v_t^{(i)}$  for  $i = c, g$ ) being an input to calculate model risk for one hour of a coal VPP in 2016 (08:00h-9:00h) based on historical forwards estimation. The graphic on top depicts the sensitivity in case of a low power forwards liquidity and the graphic below for a high power forwards liquidity.





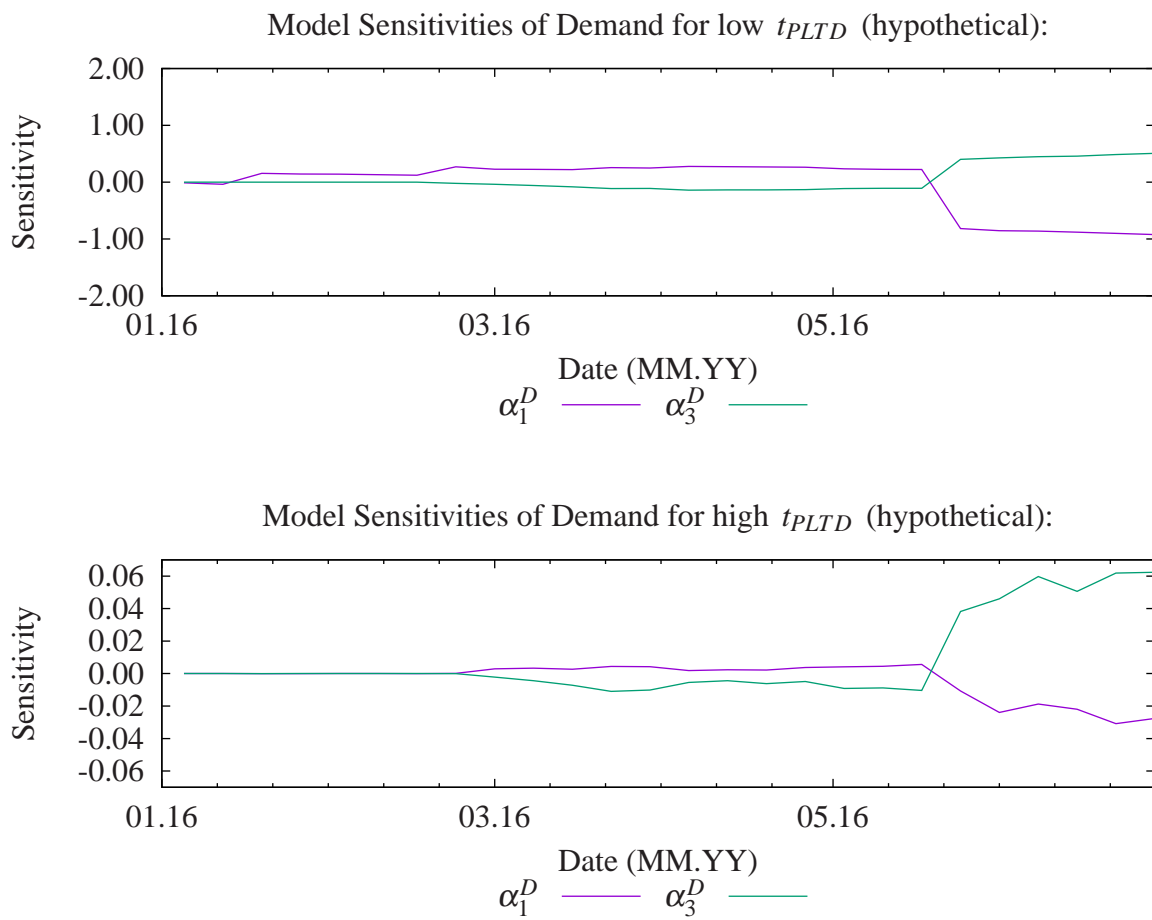


Figure B.6: Sensitivity of model parameters (only the first and the last entry of  $\alpha_t^D$ ) in direction of the demand parameters for one hour of a coal VPP in 2016 (08:00h-9:00h) based on historical forwards estimation. The graphic on top depicts the sensitivity in case of a low power forwards liquidity and the graphic below for a high power forwards liquidity.

### B.4.2 Daily VPP Parameter Risk

This Chapter depicts parameter risk of a coal VPP for the first 6 months of 2016 as of year-end 2015. Parameter risk is calculated for each payoff of the VPP separately.

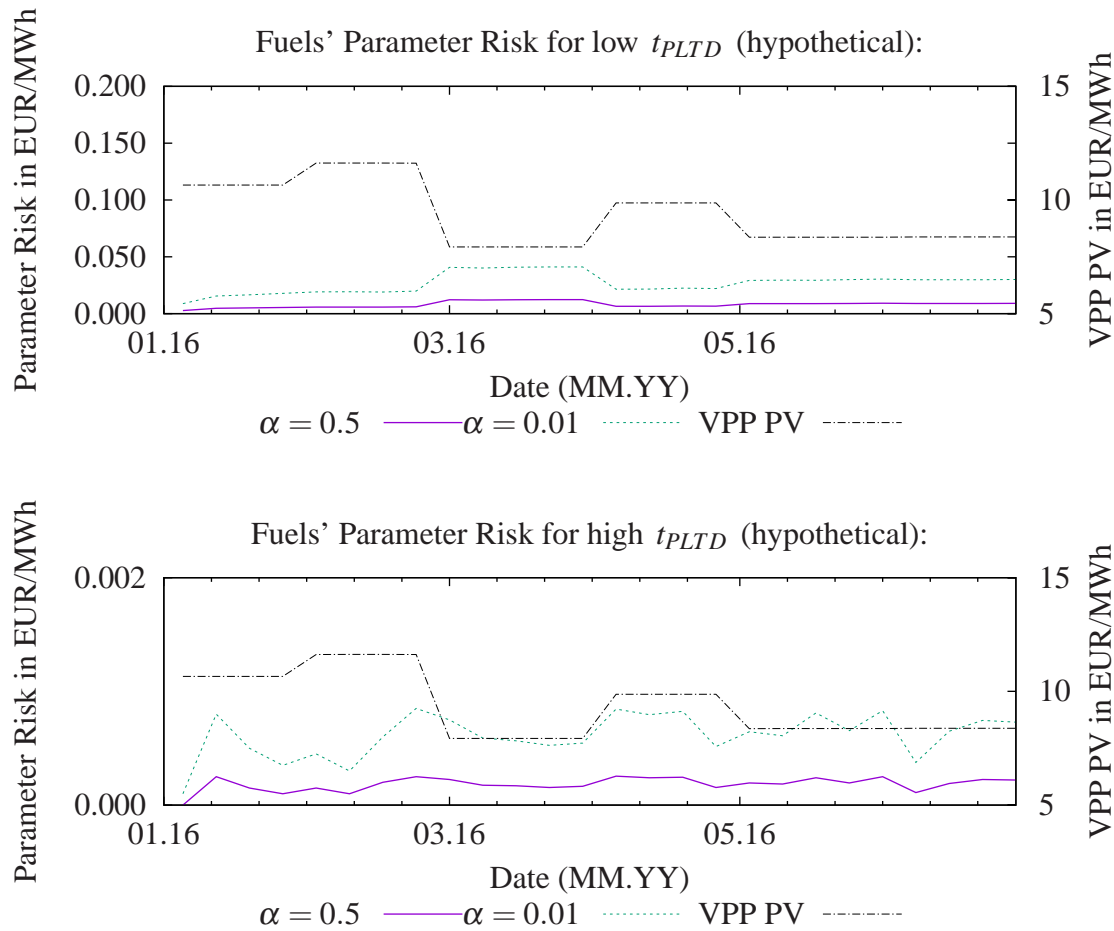


Figure B.7: Parameter risk in fuels based on historical spot estimation for one hour of a coal VPP in 2016 (08:00h-9:00h). The grafic on top depicts the parameter risk in case of a low power forwards liquidity and the grafic below for a high power forwards liquidity.

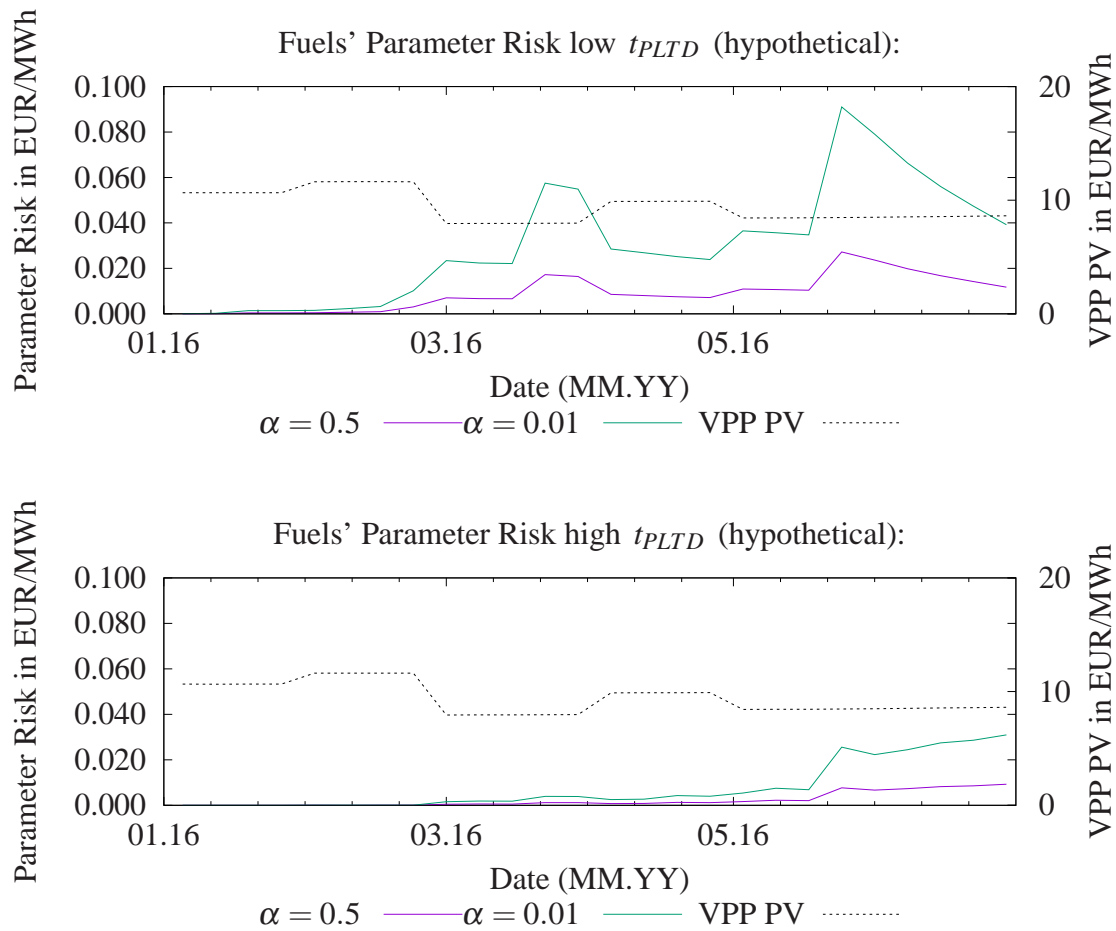


Figure B.8: Parameter risk in fuels based on historical forwards estimation for a daily coal VPP in 2016. The graphic on top depicts the parameter risk in case of a low power forwards liquidity and the graphic below for a high power forwards liquidity.

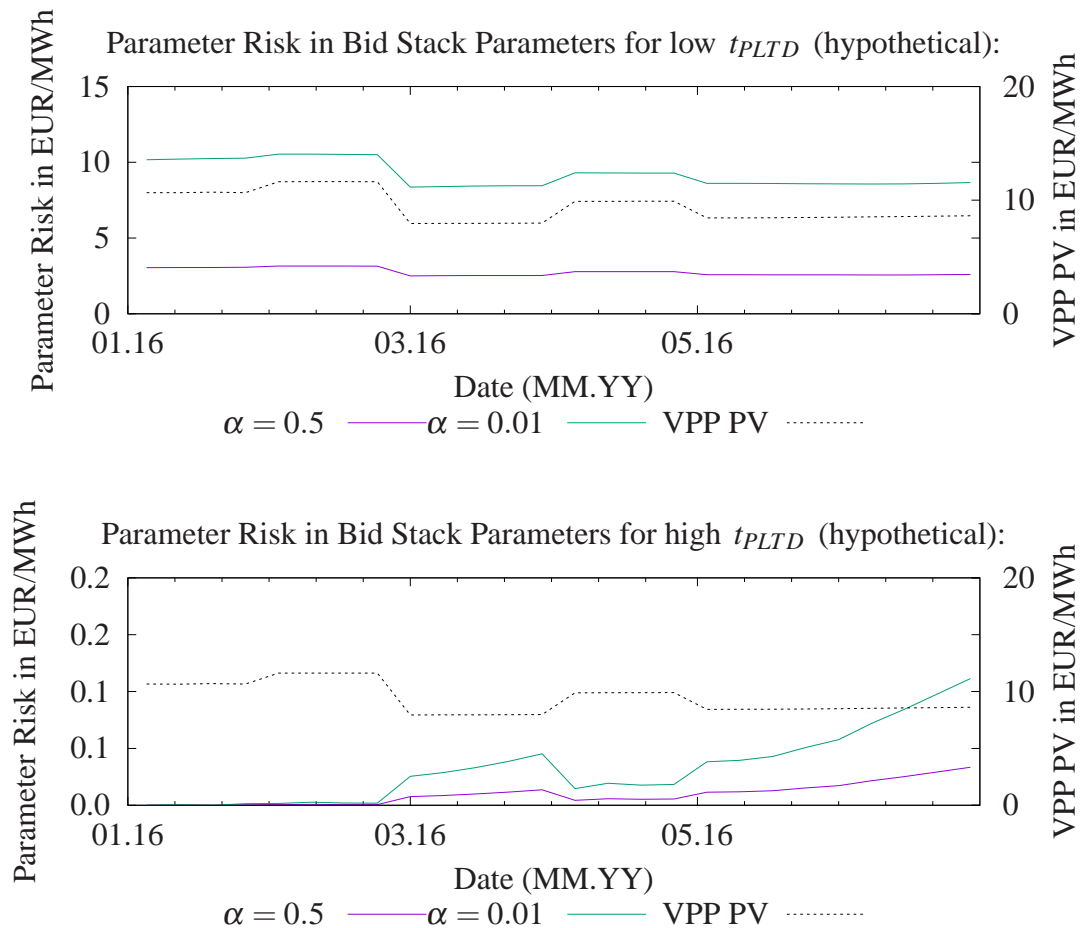


Figure B.9: Parameter risk in bid stack parameters based on historical forwards estimation in Chapter 4.2.1 and 4.2.3 for one hour of a coal VPP in 2016 (08:00h-09:00h). The graphic on top depicts the parameter risk in case of a low power forwards liquidity and the graphic below for a high power forwards liquidity.

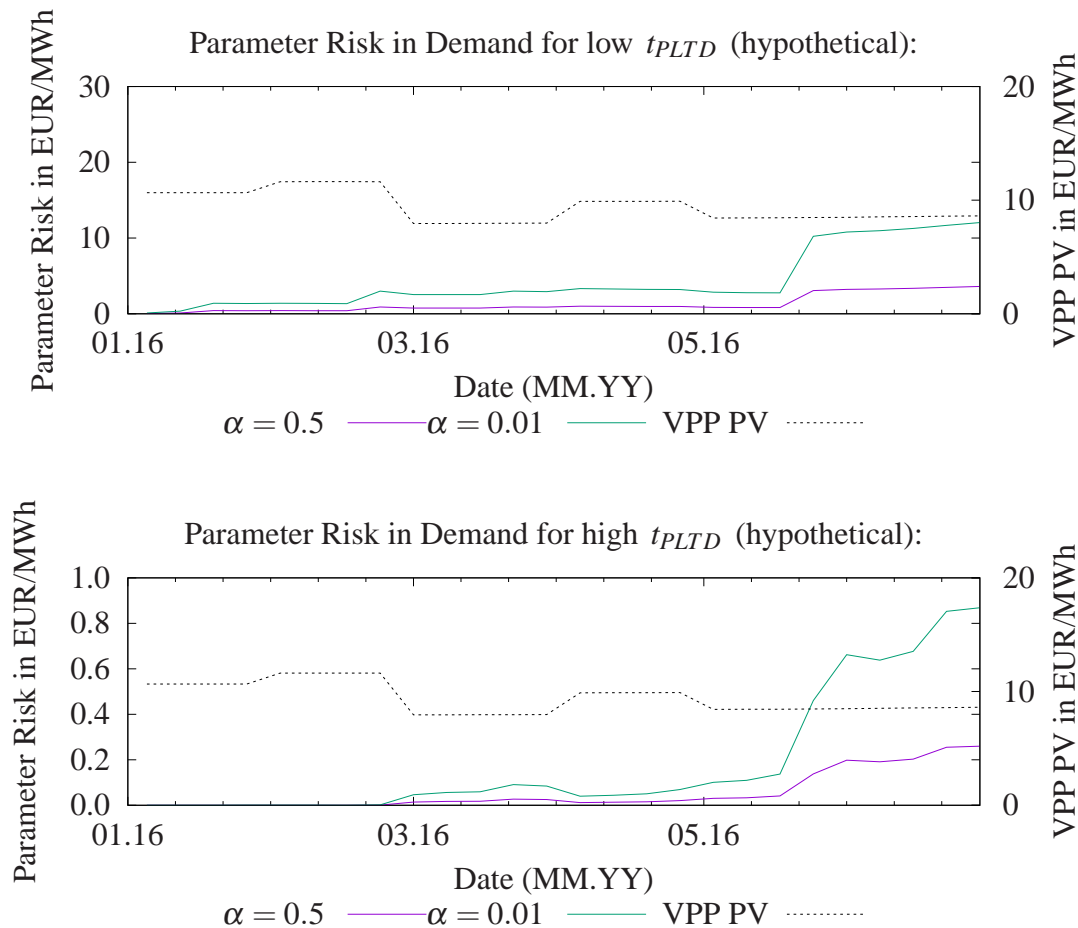


Figure B.10: Parameter risk in the demand dynamic based on historical forwards estimation for one hour of a coal VPP in 2016 (08:00h-9:00h). The graphic on top depicts the parameter risk in case of a low power forwards liquidity and the graphic below for a high power forwards liquidity.

## Additional Insights regarding Greek Calculation

### C.1 Interchange of Integration and Differentiation

In order to apply the pathwise derivatives method and the likelihood ratio method respectively, differentiation and integration has to be interchanged. By applying the Leibniz rule (cf. [Forster, 2011]) it would be sufficient to have a continuous differentiable integrand. However, as the typical payoff functions (i.e. put/call) do not fulfill this condition, the following weaker requirements are derived in [Glassermann, 2003]. Let  $\mathbf{X}(\theta) = (X_1(\theta), \dots, X_m(\theta))$  be a vector of random variables with  $\theta \in \Theta \subset \mathbb{R}$  being the parameter of interest and let  $\Psi(\mathbf{X})$  be a payoff function. Then, the requirements to interchange differentiation and integration are:

A1 At each  $\theta \in \Theta$ ,  $X_i(\theta)$  exists with probability 1, for all  $i = 1, \dots, m$ ,

A2 let  $D_\Psi \subset \mathbb{R}^m$  denote the set of points at which  $\Psi$  is differentiable. Then,

$$P(\mathbf{X}(\theta) \in D_\Psi) = 1$$

for all  $\theta \in \Theta$ ,

A3 there exist a constant  $\kappa_\Psi$ ,  $i = 1, \dots, m$  such that for all  $x, y \in \mathbb{R}^m$ ,

$$|\Psi(y) - \Psi(x)| \leq \kappa_\Psi \|y - x\|,$$

i.e.  $\Psi$  is Lipschitz continuous,

A4 there exist random variables  $\kappa_i$ ,  $i = 1, \dots, m$  such that for all  $\theta_1, \theta_2 \in \Theta$ ,

$$|X_i(\theta_2) - X_i(\theta_1)| \leq \kappa_i |\theta_2 - \theta_1|$$

and  $\mathbb{E}[\kappa_i] < \infty, i = 1, \dots, m$

### C.2 Additional Numerical Evaluations and Figures

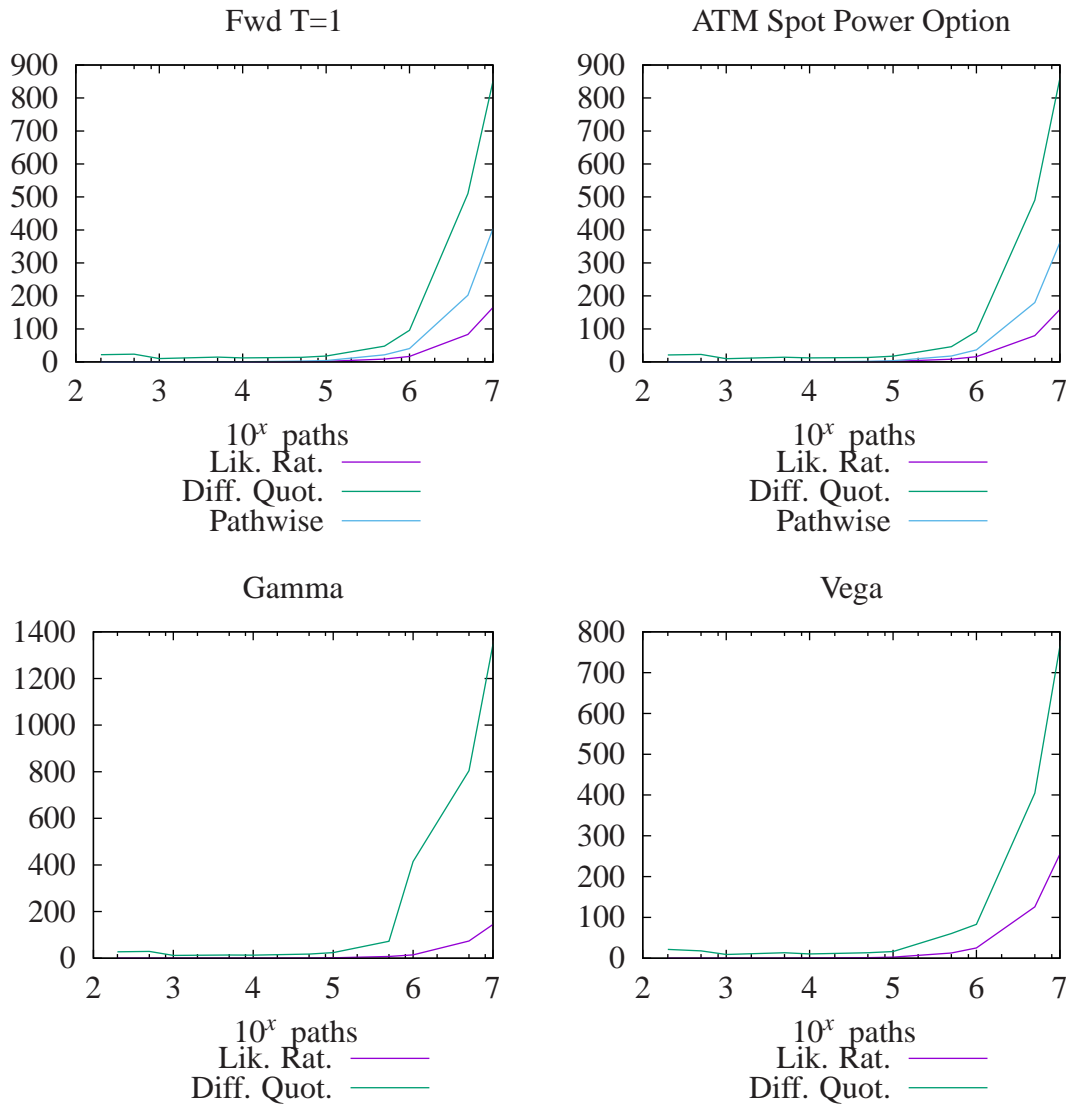


Figure C.1: Runtime in seconds for the corresponding evaluations in Chapter 6.5; it is measured the overall runtime to calculate the sensitivity for coal, gas and power (difference quotient method and likelihood ratio method) and power respectively (pathwise derivatives method); calculations done with an Intel i3 4010-U, 1.7GHz, RAM 4GB, 64bit operating system



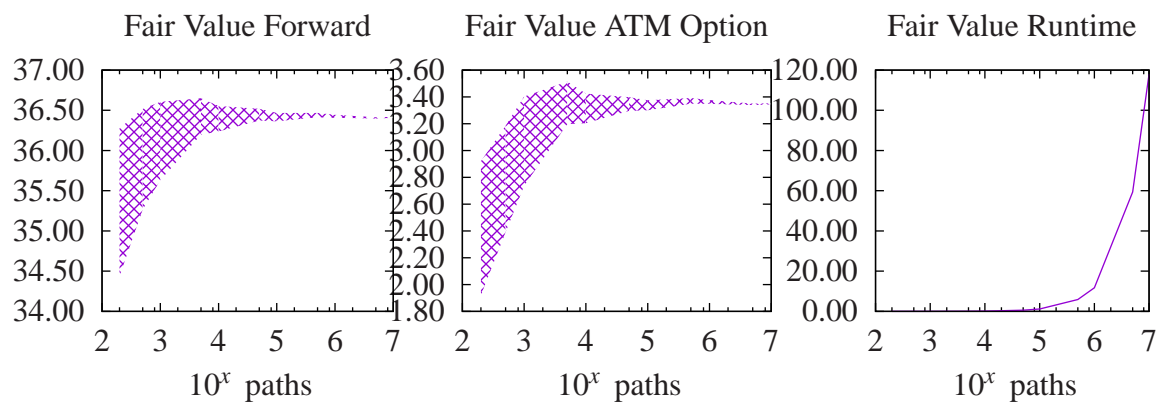


Figure C.2: Fair Value as a Benchmark to the corresponding evaluations in Chapter 6.5; Calculations done with an Intel i3 4010-U, 1.7GHz, RAM 4GB, 64bit operating system



# Bibliography

- [Aïd et al., 2013] Aïd, R., Campi, L., and Langrene, N. (2013). A structural risk-neutral model for pricing and hedging power derivatives. *Mathematical Finance*, 23(3):387–438.
- [Alexandrovich, 2014] Alexandrovich, G. (2014). *An exact Newtons method for ML estimation of a Gaussian mixture*.
- [Alos et al., 2011] Alos, E., Eydeland, A., and Laurence, P. (2011). A Kirk’s and a Bachelier’s formula for three-asset spread options. Risk.net, Cutting Edge.
- [Ankirchner et al., 2013] Ankirchner, S., Pigorsch, C., and Schweizer, N. (2013). Estimating residual hedging risk with least-squares Monte Carlo.
- [Bannör et al., 2013] Bannör, K., Kiesel, R., Nazarova, A., and Scherer, M. (2013). Parametric model risk and power plant valuation.
- [Bannör and Scherer, 2013] Bannör, K. F. and Scherer, M. (2013). Capturing parameter risk with convex risk measures.
- [Barlow, 2002] Barlow, M. (2002). A diffusion model for electricity prices. *Mathematics Finance*, 12:287–298.
- [Benth and Paraschiv, 2016] Benth, F. and Paraschiv, F. (2016). A structural model for electricity forward prices. *Under review in: Journal of Banking and Finance*.
- [Bianchetti et al., 2016] Bianchetti, M., Kucherenko, S., and Scoreli, S. (2016). Pricing and hedging multi asset options with high dimensional quasi Monte Carlo: Finite difference vs adjoint methods greeks. *Argo - New Frontiers in Practical Risk Management*, 10:7–28.
- [Bishop, 1994] Bishop, C. M. (1994). Mixture density networks. Technical report.
- [Breslin et al., 2008] Breslin, J., Clewlow, L., Elbert, T., Kwok, C., and Strickland, C. (2008). Gas storage: overview and static valuation. EnergyRisk.
- [Brigo and Mercurio, 2006] Brigo, D. and Mercurio, F. (2006). *Interest Rate Models - Theory and Practice - With Smile*. Springer.
- [Brigo et al., 2013] Brigo, D., Morini, M., and Pallavicini, A. (2013). *Counterparty Credit Risk, Collateral and Funding: With Pricing Cases For All Asset Classes*. John Wiley and Sons.

- [Burger et al., 2014] Burger, M., Graeber, B., and Schindlmayr, G. (2014). *Managing Energy Risk*. John Wiley and Sons.
- [Carmona and Coulon, 2014] Carmona, R. and Coulon, M. (2014). A survey of commodity markets and structural models for electricity prices. In Benth, F. E., Kholodnyi, V. A., and Laurence, P., editors, *Quantitative Energy Finance*, pages 41–83. Springer Verlag.
- [Carmona et al., 2012] Carmona, R., Coulon, M., and Schwarz, D. (2012). The valuation of clean spread options: Linking electricity, emissions and fuels. *Quantitative Finance*, 12(12):1951–1965.
- [Carmona et al., 2013] Carmona, R., Coulon, M., and Schwarz, D. (2013). Electricity price modelling and asset valuation: A multi-fuel structural approach. *Mathematics and Financial Economics*, 7(2):167–202.
- [Cartea et al., 2012] Cartea, A., Jaimungal, S., and Qin, Z. (2012). Model uncertainty in commodity markets. Forthcoming: *SIAM Journal of Financial Mathematics*. Available at SSRN: <http://ssrn.com/abstract=2606679> or <http://dx.doi.org/10.2139/ssrn.2606679>.
- [Černý, 2009] Černý, A. (2009). *Mathematical Techniques in Finance: Tools for Incomplete Markets, Second Edition*. Princeton University Press.
- [Clewlow and Strickland, 2000] Clewlow, L. and Strickland, C. (2000). *Energy Derivatives: Pricing and Risk Management*. Lacima Group.
- [Cont, 2006] Cont, R. (2006). Model uncertainty and its impact on the pricing of derivative instruments. *Mathematical Finance*, 16:519–547.
- [Cotter and Hanly, 2015] Cotter, J. and Hanly, J. (2015). Performance of utility based hedges. *Energy Economics*, 49:718–726.
- [Coulon and Howison, 2009] Coulon, M. and Howison, S. (2009). Stochastic behaviour of the electricity bid stack: from fundamental drivers to power prices. *The Journal of Energy Markets*, 2:29–69.
- [Coulon et al., 2014] Coulon, M., Jacobsson, C., and Ströjby, J. (2014). Hourly resolution forward curves for power: statistical modeling meets market fundamentals. In Prokopczuk, M., editor, *Energy Pricing Models: Recent Advances*, pages 147–194. Palgrave Macmillan.
- [Davies, 2002] Davies, B. (2002). *Integral Transforms and their Applications, 3rd Edition*. Springer Verlag.
- [de Jong and Schneider, 2009] de Jong, C. and Schneider, S. (2009). Cointegration between gas and power spot prices. *Journal of Energy Markets*, 2(3):27–46.
- [Eydeland and Wolyniec, 2003] Eydeland, A. and Wolyniec, K. (2003). *Energy and Power Risk Management - New Developments in Modeling, Pricing and Hedging*. John Wiley and Sons.

- [Fiorenzani et al., 2012] Fiorenzani, S., Ravelli, S., and Edoli, E. (2012). *The Handbook of Energy Trading*. John Wiley and Sons.
- [Forster, 2011] Forster, O. (2011). *Analysis 2*. Springer Verlag.
- [Fries, 2007] Fries, C. P. (2007). *Mathematical Finance - Theory, Modelling, Implementation*. John Wiley and Sons.
- [Füss et al., 2015] Füss, R., Mahringer, S., and Prokopczuk, M. (2015). Electricity spot and derivatives pricing when markets are interconnected.
- [Genz and Bretz, 2009] Genz, A. and Bretz, F. (2009). *Calculation of Multivariate Normal and t Probabilities*. Springer Verlag.
- [Giles and Glassermann, 2006] Giles, M. and Glassermann, P. (2006). Smoking adjoints: Fast Monte Carlo greeks. *Risk*, 19:88–92.
- [Glassermann, 2003] Glassermann, P. (2003). *Monte Carlo Methods In Financial Engineering*. Springer Verlag.
- [Gupta, 1963] Gupta, S. S. (1963). Probability integrals of multivariate normal and multivariate t. *The Annals of Mathematical Statistics*, 34(3):792–828.
- [Hamilton, 1994] Hamilton, J. D. (1994). *Time Series Analysis*. Princeton University Press.
- [Harms and Kiesel, 2017] Harms, C. and Kiesel, R. (2017). The application of structural electricity models for dynamic hedging. *Journal of Energy Markets*, 10(1):1–29.
- [Joshi and Kainth, 2004] Joshi, M. S. and Kainth, D. (2004). *Rapid Computation of Prices and Deltas of Nth to Default Swaps in the Li Model*.
- [Kirk, 1995] Kirk, E. (1995). Correlation in the energy markets. *Managing Energy Price Risk*, pages 71–78.
- [Knight, 1921] Knight, F. H. (1921). *Risk, Uncertainty, and Profit*. Hart, Schaffner & Marx.
- [Li, 1999] Li, A. (1999). *Model Calibration, Risk Measurement, and the Hedging of Derivatives*.
- [Lütkepohl, 2007] Lütkepohl, H. (2007). *New Introduction to Multiple Time Series Analysis, 2nd Printing*. Springer.
- [McLachlan and Krishnan, 2008] McLachlan, G. J. and Krishnan, T. (2008). *The EM Algorithm and Extensions*. Wiley Series in Probability and Statistics.
- [McNeal et al., 2005] McNeal, A., Frey, R., and Embrechts, P. (2005). *Quantitative Risk Management*. Princeton University Press.
- [Morini, 2011] Morini, M. (2011). *Understanding and Managing Model Risk*. John Wiley and Sons.

- [Rebonato, 2010] Rebonato, R. (2010). *Coherent stress testing: A Bayesian approach to the analysis of financial stress*. John Wiley and Sons.
- [RWE Supply & Trading GmbH, 2015] RWE Supply & Trading GmbH (2015). Volatility, risk and risk premium in german and continental power markets.
- [Samuelson, 1965] Samuelson, P. A. (1965). Proof that properly anticipated prices fluctuate randomly. *Industrial Management Review*, 6:41–49.
- [Scott, 2002] Scott, W. A. (2002). Maximum likelihood estimation using the empirical fisher information matrix. *Journal of Statistical Computation and Simulation*, 72(8):599–611.
- [van der Vaart, 2000] van der Vaart, A. (2000). *Asymptotic Statistics, First Paperback Edition*. Cambridge University Press.
- [Wooldridge, 2010] Wooldridge, J. M. (2010). *Econometric Analysis of Cross Section and Panel Data, Second Edition*. MIT Press.

# List of Propositions and Definitions

1.1	Definition (Futures Data) . . . . .	2
1.2	Definition (Forwards Data) . . . . .	2
1.3	Definition (Bid Stack, Merit Order and Marginal Fuel) . . . . .	5
1.4	Definition (Hedging) . . . . .	9
1.5	Definition (delta) . . . . .	9
1.6	Definition (gamma) . . . . .	10
1.7	Definition (vega) . . . . .	10
1.8	Definition (Model Uncertainty) . . . . .	13
1.9	Definition (Parameter Uncertainty) . . . . .	13
1.10	Definition (Model Risk) . . . . .	13
1.11	Definition (Parameter Risk) . . . . .	13
2.1	Definition (Implied Demand Seasonality) . . . . .	21
3.1	Proposition (Forward Dynamics) . . . . .	25
3.1	Definition (Integration of Order 0) . . . . .	27
3.2	Definition (Covariance-Stationary) . . . . .	27
3.3	Definition (Lag Operator) . . . . .	28
3.4	Definition (Integration of order $d$ ) . . . . .	28
3.5	Definition (Cointegration) . . . . .	28
3.2	Proposition (Delta Hedging for Structural Models) . . . . .	31
3.6	Definition (Power Liquidity Threshold Date (PLTD)) . . . . .	33
3.3	Proposition (From Forward Deltas to Futures Deltas) . . . . .	35
4.1	Definition (Convex Risk Measure and Model Risk ([Bannör and Scherer, 2013])) . . . . .	40
4.2	Definition (VAR( $p$ ) Process) . . . . .	42
4.1	Proposition (Asymptotic Covariance Matrix: Fuels Spot Estimation) . . . . .	44
4.3	Definition (Empirical Probability Measure) . . . . .	47
4.2	Proposition (Asymptotic Covariance Matrix: Fuel Forwards Estimation) . . . . .	48
4.3	Proposition (Asymptotic Covariance Matrix: Bid Stack Parameters) . . . . .	58
4.4	Proposition (Asymptotic Covariance Matrix: Demand Forwards Estimation) . . . . .	60
5.1	Proposition (Close Form Formulas for Bid Stack with one Fuel) . . . . .	75

5.2	Proposition (Power Call Option Formula for an Arbitrary Demand Density) . . . . .	85
5.1	Definition (Expressions for the Option Price Formula) . . . . .	85
5.3	Proposition (Extension of Proposition 5.2 to Negative Prices and Price Spikes) . . . . .	88
6.1	Proposition (Interchange of Differentiation and Integration) . . . . .	120
6.2	Proposition (Forward Delta Calculation) . . . . .	122
6.3	Proposition (Forward Gamma Calculation) . . . . .	124
6.1	Definition (Definition of $\beta_t^{i,j,a}(\nu)$ ) . . . . .	126
6.4	Proposition (Vega Calculation) . . . . .	127
6.5	Proposition (Power Forward Delta) . . . . .	130
6.6	Proposition (Vega Calculation) . . . . .	141
A.1	Proposition (Continuity of the Exponential Bid Stack) . . . . .	160
A.2	Proposition (Lipschitz Continuity) . . . . .	160
B.1	Proposition (General Delta- Method) . . . . .	165
B.2	Proposition (Asymptotical Properties of the Z-Estimator) . . . . .	165
B.1	Definition (Duplication Matrix) . . . . .	166
B.3	Proposition (Asymptotic Properties of the Restricted ML Estimators) . . . . .	166



# List of Figures

1.1	Typical Demand and Offer curve for a certain hour of a certain day at EPEX Spot (source: <a href="http://www.epexspot.com">www.epexspot.com</a> ) . . . . .	3
1.2	Merit order in the German Electricity as of 2015; source: [RWE Supply & Trading GmbH, 2015] . . . . .	6
1.3	Peak clean spark spread (blue dots) in Germany (left) and France (right) from 2012 until September 2015 in EUR/MWh (effectiveness was assumed to be 50% and CO <sub>2</sub> -conversion factor 0.4; data source: Bloomberg). . . . .	11
2.1	Daily price forward curves in EUR/MWh calculated as of year-end 2015. . . . .	24
2.2	Hourly weights for electricity prices . . . . .	24
3.1	Trading Volumes of a 1Y Baseload contract Phelix at Bloomberg measured in total number of shares traded on a security on the current day. . . . .	34
4.1	Left: Coal, right: Gas; Calibration of mean-reversion speed parameter $\alpha_t^{(i)}$ for $i = c, g$ using a stepwise function (Remark 4.3; left axis); Volatility was taken from Table 4.1; estimated future volatility on right axis. . . . .	50
4.2	Left: Coal, right: Gas; Implied volatility function based on the estimation results in Figure 4.1 . . . . .	50
4.3	Example of a bid and offer curve at Epex Spot as of December, 8th 2015 (09:00h; German market) (left), its transformation into a price curve with inelastic demand (mid) and the implied density function . . . . .	52
4.4	Normal MDN results together with the final calibrated exponential bid stack for the same day as being used in Figure 4.3 (left: fit of density; right: fit of price curve). . . . .	57
4.5	left: Calibration of mean-reversion speed parameter $\alpha_t^D$ using a stepwise function (Remark 4.3) and the calibration results for the fuels in Figure 4.1(left axis); estimated future volatility on right axis. We used the following generic power futures prices from Bloomberg for estimation: 1st, 2nd, 3rd Month; 2nd, 3rd, 4th Quarter; historical daily data of 2015; Volatility was assumed to be 5 MWh. right: result for the corresponding demand time series for 2015 (orange: in MWh/h), we picked the front month futures as an example (in EUR/MWh). . . . .	61
4.6	Implied volatility function of demand based on the estimation results in Figure 4.5 . . . . .	62

4.7	Implied demand by the price forward curves of Figure 2.1. . . . .	63
4.8	Bid Stack Parameter Risk of the power forward curve in Figure 2.1 for hour 7 and 9; green and purple lines are measured on left axis; black dashed line is measured on right axis. . . . .	65
4.9	Estimation of a bid stack based on 5 different Tuesdays in November and December 2015. . . . .	70
4.10	Parameter Risk in Bid Stack to measure risk in power forward curve. Estimation of bid stack was done using several bid and offer curves of different Tuesdays in winter 2015 (cf. Figure 4.9). . . . .	71
5.1	Monte Carlo pricing uncertainty (90% confidence interval as percentage of PV; 1 million paths) over maturity for a VPP delivering electricity in hour 06:00-07:00 and 08:00-09:00 respectively on each Tuesday of 2016. . . . .	76
5.2	Three different bid stacks to be compared when applying the Kirk formula for structural electricity models as of $t_0 = 31/12/2016$ ; 'raw data' depicts the bid stack of 08/12/2016 as it has been observed for hour 08:00-09:00 at EPEX Spot. . . . .	82
5.3	Relative error of General Kirk formula over delivery applied to an exponential bid stack with and without using a fuel in the bid stack model; left: hour 08:00-09:00, middle: hour 06:00-07:00, right: hour 08:00-09:00. . . . .	83
5.4	Relative error of General Kirk formula over delivery applied to an exponential bid stack with two marginal fuels and three different fuel correlations for hour 08:00-09:00 . . . .	83
5.5	Relative error of General Kirk formula over delivery applied to an exponential bid stack with two marginal fuels and three different fuel correlations for hour 06:00-07:00 . . . .	84
6.1	Power forward delta for three different kind of contracts for $T \geq t_{PLTD}$ ; it is depicted the 90 percent confidence interval; convergence of difference quotient and pathwise is quite similar as expected. . . . .	133
6.2	Forward delta over simulation paths for a power forward contract and $T < t_{PLTD}$ ; it is depicted the 90 percent confidence interval of the according deltas; convergence of difference quotient and pathwise is quite similar as expected. . . . .	134
6.3	Forward delta over simulation paths for a power forward contract and $T \geq t_{PLTD}$ ; it is depicted the 90 percent confidence interval of the according deltas; convergence of difference quotient and pathwise is quite similar as expected. . . . .	135
6.4	Forward gamma over simulation paths for a power forward contract and $T < t_{PLTD}$ ; it is depicted the 90 percent confidence interval of the according deltas; convergence of difference quotient and pathwise is quite similar as expected. . . . .	135
6.5	Vega over simulation paths for a power forward contract and $T < t_{PLTD}$ ; it is depicted the 90 percent confidence interval of the according deltas; convergence of difference quotient and pathwise is quite similar as expected . . . . .	136

6.6	Forward delta over simulation paths for a power ATM option contract and $T < t_{PLTD}$ ; it is depicted the 90 percent confidence interval of the according deltas; convergence of difference quotient and pathwise is quite similar as expected . . . . .	138
6.7	Forward gamma over simulation paths for a power ATM option contract and $T < t_{PLTD}$ ; it is depicted the 90 percent confidence interval of the according deltas; convergence of difference quotient and pathwise is quite similar as expected . . . . .	138
6.8	Vega over simulation paths for a power ATM option contract and $T < t_{PLTD}$ ; it is depicted the 90 percent confidence interval of the according deltas; convergence of difference quotient and pathwise is quite similar as expected . . . . .	139
7.1	VPP (EUR/MWh) daily for hour 6-7 and 8-9 of 2016 based on the hourly forward curves in Figure 2.1. . . . .	146
7.2	Spark (right) and Dark (left) spread option deltas for one weekday of 2016 (30/06/2016, Thursday) when no liquid power forwards available (on top) and when liquid ones available (on bottom). . . . .	148
7.3	Daily VPP forward deltas for 2016 with high $t_{PLTD}$ based on hourly forward curves in Figure 2.1 (daily deltas are calculated by adding the hourly deltas of a certain day, cf. Corollary 3.1) . . . . .	149
7.4	Gas and coal forward delta over power forward price for low power forwards liquidity in January 2016 . . . . .	151
A.1	European Call Option value for each Tuesday of 2016 at 9.00h am. The valuation was done after a complete historical estimation of all model parameters of the structural electricity model in Chapter 2 as been described in Chapter 4. . . . .	164
B.1	Implied expected demand forwards volatility over $\tau$ (left) and implied demand spot volatility over $t > t_0$ (right) for different choices of $v^D$ and calibrated bid stack parameters in Table 4.2; we used Proposition 4.4 to estimate mean-reversion speed. . . . .	167
B.2	PV of a coal VPP over time for different choices of $v^D$ ; we used Proposition 4.4 to estimate mean-reversion speed. We used 10 million paths for a Monte Carlo method. . . . .	168
B.3	Sensitivity of model parameters for one hour of a coal VPP in 2016 (08:00h-9:00h) based on historical spot estimation. The grafic on top depicts the sensitivity in case of a low power forwards liquidity and the grafic below for a high power forwards liquidity. . . . .	169
B.4	Sensitivity of model parameters (only the first and the last entry of $\alpha_t^{(i)}$ and $v_t^{(i)}$ for $i = c, g$ ) being an input to calculate model risk for one hour of a coal VPP in 2016 (08:00h-9:00h) based on historical forwards estimation. The graphic on top depicts the sensitivity in case of a low power forwards liquidity and the graphic below for a high power forwards liquidity. . . . .	170

B.5	Sensitivity of a VPP in direction of the bid stack parameters for a daily power forward curve for one hour of a coal VPP in 2016 (08:00h-9:00h) based on forwards calibrations in Chapters 4.2.1 and 4.2.3; above graphic displays the calculations for a non-liquid power forward curve and the below for a liquid one. . . . .	171
B.6	Sensitivity of model parameters (only the first and the last entry of $\alpha_t^D$ ) in direction of the demand parameters for one hour of a coal VPP in 2016 (08:00h-9:00h) based on historical forwards estimation. The graphic on top depicts the sensitivity in case of a low power forwards liquidity and the graphic below for a high power forwards liquidity. . . .	172
B.7	Parameter risk in fuels based on historical spot estimation for one hour of a coal VPP in 2016 (08:00h-9:00h). The grafic on top depicts the parameter risk in case of a low power forwards liquidity and the grafic below for a high power forwards liquidity. . . . .	173
B.8	Parameter risk in fuels based on historical forwards estimation for a daily coal VPP in 2016. The grafic on top depicts the parameter risk in case of a low power forwards liquidity and the grafic below for a high power forwards liquidity. . . . .	174
B.9	Parameter risk in bid stack parameters based on historical forwards estimation in Chapter 4.2.1 and 4.2.3 for one hour of a coal VPP in 2016 (08:00h-09:00h). The grafic on top depicts the parameter risk in case of a low power forwards liquidity and the grafic below for a high power forwards liquidity. . . . .	175
B.10	Parameter risk in the demand dynamic based on historical forwards estimation for one hour of a coal VPP in 2016 (08:00h-9:00h). The graphic on top depicts the parameter risk in case of a low power forwards liquidity and the graphic below for a high power forwards liquidity. . . . .	176
C.1	Runtime in seconds for the corresponding evaluations in Chapter 6.5; it is measured the overall runtime to calculate the sensitivity for coal, gas and power (difference quotient method and likelihood ratio method) and power respectively (pathwise derivatives method); calculations done with an Intel i3 4010-U, 1.7GHz, RAM 4GB, 64bit operating system . . . . .	178
C.2	Fair Value as a Benchmark to the corresponding evaluations in Chapter 6.5; Calculations done with an Intel i3 4010-U, 1.7GHz, RAM 4GB, 64bit operating system . . . . .	179

# List of Tables

2.1	Bid Stack Parameters . . . . .	18
2.2	Available Capacity (ex ante, day ahead) published by EEX Transparency website throughout the year 2015 (yearly average) . . . . .	19
2.3	Summary of market data used for the thesis. . . . .	22
4.1	Historical Estimation of a joint fuels' process (time series: 1 year) . . . . .	45
4.2	Estimated Bid Stack Parameters based on an estimation on 08/12/2015, hour 9 using data from EPEX Spot. . . . .	57
4.3	Quantification of Monte Carlo pricing risk (risk in bid stack parameters) for hour 7 and hour 9 of a Tuesday in 2016. . . . .	64
4.4	Summary of the quantification of parameter risk in fuel dynamics for a coal VPP using the approach in [Bannör et al., 2013] (cf. Chapter 4.1) and historical spot estimation. . .	66
4.5	Summary of the quantification of parameter risk in fuel dynamics for a coal VPP using the approach in [Bannör et al., 2013] (cf. Chapter 4.1) and historical forwards estimation. .	66
4.6	Summary of the quantification of parameter risk in bid stack parameters for a coal VPP using the approach in [Bannör et al., 2013] (cf. Chapter 4.1; hour 08:00-09:00). . . . .	67
4.7	Summary of the quantification of parameter risk in bid stack parameters for a coal VPP using the approach in [Bannör et al., 2013] (cf. Chapter 4.1) and historical forwards estimation in Chapter 4.2.1 and 4.2.3. However, we price a VPP for Tuesday, hour 06:00-07:00 (instead of hour 08:00-09:00). . . . .	68
4.8	Summary of the quantification of parameter risk in demand for a coal VPP using the approach in [Bannör et al., 2013] (cf. Chapter 4.1) and historical forwards estimation (hour 08:00-09:00). . . . .	68
4.9	Summary of the quantification of parameter risk in demand and historical forwards estimation (hour 06:00-07:00 instead of hour 08:00-09:00). . . . .	69
4.10	Estimated Bid Stack Parameters based on an estimation from 17th November until 15th December 2015, hour 9 using data from EPEX Spot. . . . .	70
5.1	Average numerical Effort in ms to perform one valuation for Figure 5.3 to 5.5 . . . . .	84
7.1	Explanations for Figure 7.2 . . . . .	147



# **Ehrenwörtliche Erklärung**

Ich versichere an Eides statt durch meine Unterschrift, dass ich die vorstehende Arbeit selbständig und ohne fremde Hilfe angefertigt und alle Stellen, die ich wörtlich oder annähernd wörtlich aus Veröffentlichungen entnommen habe, als solche kenntlich gemacht habe, mich auch keiner anderen als der angegebenen Literatur oder sonstiger Hilfsmittel bedient habe. Die Arbeit hat in dieser oder ähnlicher Form noch keiner anderen Prüfungsbehörde vorgelegen.

Cord Harms

Essen, 13. März 2017